SYSTEMATICS OF THE GENUS *HYPOPTOPOMA* GÜNTHER, 1868 (SILURIFORMES, LORICARIIDAE)

ADRIANA E. AQUINO

Division of Vertebrate Zoology
American Museum of Natural History
(aaquino@amnh.org)

SCOTT A. SCHAEFER

Division of Vertebrate Zoology
American Museum of Natural History
(schaefer@amnh.org)

BULLETIN OF THE AMERICAN MUSEUM OF NATURAL HISTORY
Number 336, 110 pp., 45 figures, 18 tables
Issued June 3, 2010

Copyright © American Museum of Natural History 2010 ISSN 0003-0090

CONTENTS

Abstract . . . 3
Introduction . . . 3
Methods . . . 4
  Meristics . . . 4
    Fin-rays . . . 4
    Teeth . . . 5
    Plates . . . 5
  Morphometrics . . . 5
  Anatomy . . . 5
  Phylogenetic Analysis . . . 6
  Scope and Organization . . . 6
  Abbreviations . . . 7
Systematics . . . 7
  Hypoptopoma Günther, 1868a . . . 7
  General Morphology . . . 14
    Neurocranium . . . 16
    Infraorbital series and laterosensory canals . . . 17
    Suspensorium and mandibular arch . . . 17
    Opercular series . . . 17
    Weberian apparatus and axial skeleton . . . 18
    Median fins . . . 20
    Paired fins . . . 21
  Key to the species of *Hypoptopoma* . . . 22
  Hypoptopoma baileyi, new species . . . 23
  Hypoptopoma guianense Boeseman, 1974 . . . 28
  Hypoptopoma psilogaster Fowler, 1915 . . . 32
  Hypoptopoma thoracatum Günther, 1868a . . . 38
  Hypoptopoma brevirostratum, new species . . . 43
  Hypoptopoma muzuspi, new species . . . 48
  Hypoptopoma spectabile (Eigenmann, 1914) . . . 52
  Hypoptopoma sternoptychum (Schaefer, 1996) . . . 55
  Hypoptopoma bianale, new species . . . 59
  Hypoptopoma inexspectatum (Holmberg, 1893) . . . 60
  Hypoptopoma elongatum, new species . . . 67
  Hypoptopoma incognitum, new species . . . 72
  Hypoptopoma steindachneri Boulenger, 1895 . . . 77
  Hypoptopoma gulare Cope, 1878 . . . 85
  Hypoptopoma machadoi, new species . . . 91
Phylogenetic Analysis . . . 94
  Character Descriptions and Coding . . . 94
  Topology and Character Support . . . 99
  Biogeographical Implications . . . 101
References . . . 104
Appendix . . . 109

ABSTRACT

The systematics of *Hypoptopoma* Günther (1868a) is revised based on comprehensive evaluation of specimen collections and a phylogenetic analysis of the species. The genus *Hypoptopoma* comprises a distinctive assemblage of loricariid catfishes distributed in the lowland drainages of tropical, subtropical, and temperate latitudes of South America to the east of the Andes. *Hypoptopoma* is uniquely diagnosed among genera of the Loricariidae on the basis of the presence of a laterally expanded nuchal plate. Members of the genus can be further distinguished from all other loricariids, except the hypoptopomatin genus *Oxyropsis*, by the depressed head with eyes placed ventrolateral and visible from below. *Hypoptopoma* is further distinguished from all other Hypoptopomatini, including *Oxyropsis*, by the caudal peduncle posterior to the base of the anal fin ovoid in cross section and deeper in the dorsoventral axis. All species of *Hypoptopoma*, except *H. spectabile*, can be further distinguished among loricariids by the presence in adult stages of a column of variably enlarged and flattened odontodes positioned along the posterior margin of the trunk plates. Individuals of several *Hypoptopoma* species attain the largest body size for the subfamily Hypoptopomatinae, with standard length reaching 105 mm. Species of *Hypoptopoma* typically occur in streams of slow to moderate current and muddy to sandy bottom with marginal emergent vegetation. Based on verified specimen records, the species is distributed in the Río Amazonas basin, including the Ucayali, Madeira, and Tapajos rivers, as well as in the rivers east to the Ilha Marajo drainage (Para, Brazil), in the Tocantins and smaller coastal river drainages in northeastern Brazil (Mearim), the upper Río Orinoco basin, the Essequibo and Nickerie river basins of the Guiana Shield, and in the ríos Paraguay and lower Paraná. There are no records of *Hypoptopoma* in the Río Uruguay, the Atlantic coastal drainages of Uruguay and Brazil south of Rio Mearim (Maranão), the upper Paraná, and Rio São Francisco systems. Fifteen species are recognized in *Hypoptopoma*, seven of which are newly described herein. Phylogenetic analysis of *Hypoptopoma* species, based on analysis of 26 characters drawn from aspects of external morphology and internal osteology, recovered a well-supported but incompletely resolved nested set of clade relationships that suggests a widespread ancestral distribution for the group in central Amazonia, plus at least four instances of divergence of a species having a peripheral distribution from an Amazonian sister group. Relationships at the basal node were unresolved. There was insufficient evidence to resolve the relationships among *H. baileyi*, n. sp., of the Madeira river basin, an unresolved clade comprised of *H. guianense* Boesemann, 1974, of the Essequibo and Nickerie basins in Guyana and Surinam; *H. psilogaster* Fowler, 1915, of the upper Amazon basin in Brazil and Peru; and *H. thoracatum* Günther, 1868a, of the upper and middle Amazon basin; and a well-supported clade that includes all other *Hypoptopoma* species. The latter clade was supported by four synapomorphies and includes *H. brevirostratum*, n. sp., of the upper Amazon basin in Brazil and Peru, *H. muzuspi*, n. sp., of the Tocantins basin, and a more restricted clade supported by six character-state changes comprising the remainder of the subfamily. Two species, *H. spectabile* (Eigenmann, 1914) of the upland Amazon and upper Orinoco river basins of Venezuela, Colombia, Ecuador, and Peru and *H. sternoptychum* (Schaefer, 1996a) of the lowland reaches of the Amazon river, formerly placed in the genus *Nannoptopoma* Schaefer, 1996, represent a clade most closely related to a nested subset of *Hypoptopoma* species. These former *Nannoptopoma* species are reassigned to *Hypoptopoma*, thus rendering the former generic name a subjective junior synonym of *Hypoptopoma*. *Hypoptopoma bianale*, n. sp., of the upper Amazon River basin in Brazil and Peru represents the sister group to a largely unresolved clade comprised of *H. inexspectatum* (Holmberg, 1893a) of the Paraguay-Paraná basin, *H. steindachneri* Boulenger, 1895, of the upper Amazon basin in Brazil and Peru, *H. gulare* Cope, 1878, of the upper Amazon basin, *H. machadoi*, n. sp., of the Orinoco basin, and a clade comprised of *H. elongatum*, n. sp., of the lower Tapajos and lower Trombetas rivers plus *H. incognitum*, n. sp., of the middle Amazon basin, Tocantins, and Mearim rivers. A key to the species of *Hypoptopoma* is provided.

INTRODUCTION

Species of the genus *Hypoptopoma* compose a distinctive group of loricariid catfishes distributed throughout the lowland drainages of tropical South America to the east of the Andes. Among the 716 recognized species of armored catfishes (Ferraris, 2007), representatives of *Hypoptopoma* are easily recognized by their seemingly incongruous combination

of a robust trunk, greatly depressed head and pointed snout, yielding a spatulate form to the anterior third of the body. A further consequence of the extreme depresssion of the head and snout in these species is the ventrolateral displacement of the eyes, which typically occupy a more dorsal position on the head in other loricariid catfishes, the ventrolateral position of the opercle, and ventral position of the canal-bearing plate. Günther (1868a, b) erroneously interpreted these two latter as a two-bone gill cover, hence the name of the genus (*hypo-* [Gr. meaning "under, beneath"] plus *opto* [Gr. meaning "visible"] plus *poma* [Gr. meaning "cover, lid"]). The species of *Hypoptopoma* are distributed broadly in lowland freshwaters of the Neotropics, with specimen records known for the Amazon, Essequibo, Nickerie, Orinoco, and Paraná-Paraguay river systems (Schaefer, 2003). Individuals of several *Hypoptopoma* species attain the largest body size for the subfamily, with standard length reaching 105 mm. Species of *Hypoptopoma* are entirely herbivorous, rather sedentary in habit, and typically occur in streams of slow to moderate current and muddy to sandy bottom with marginal emergent vegetation.

The history of discovery and description of species having been assigned to *Hypoptopoma* at one time or another is long temporally, beginning in the late 19th century with *Hypoptopoma thoracatum* Günther, 1868, but relatively shallow in terms of numbers of species. Of the 12 nominal species assigned to *Hypoptopoma* prior to this study, nine were described prior to 1900 and all but two before 1950. In contrast with the tremendous diversity of the Loricariidae and the accelerated pace of discovery and description of catfish species that has occurred in the last five years (Ferraris and Reis, 2005; Ferraris, 2007), representatives of *Hypoptopoma* have not been the subject of recent discoveries involving new neotropical catfishes. The most recent description of a species of *Hypoptopoma* was published in 1974 (*H. guianense* Bosemann, 1974). Representatives of the genus have been included in various recent generic-level and higher phylogenetic studies of loricariid and other catfishes (Schaefer, 1991; Montoya-Burgos, 2003; Armbruster, 2004, 2008; Chiachio et al., 2008), but members of the group have not been the subject of investigation at the species level. Moreover, very few of the more speciose genera of the Loricariidae have been the subject of taxonomic revisionary studies involving comprehensive examination of material, and even fewer involve taxa with species having a geographic distribution on a continentwide or international scale (e.g., *Parotocinclus*—Garavello, 1977; *Pterygoplichthys*—Weber, 1992; *Panaque dentex* clade—Schaefer and Stewart, 1993; *Otocinclus*—Schaefer, 1997; *Oxyropsis*—Aquino and Schaefer, 2002; *Hypostomus cochliodon* group—Armbruster, 2003; *Peckoltia*—Armbruster, 2008).

We present herein a revision of the taxonomy and a phylogenetic analysis of the species of *Hypoptopoma*, the first comprehensive treatment of the genus since the pioneering work on the systematics of the Loricariidae by Regan (1904), and the first phylogenetic analysis of the group that includes all recognized species-level taxa. We recognize a total of 15 species of *Hypoptopoma*, seven of which are newly described herein and two of which were previously assigned to the genus *Nannoptopoma* Schaefer, 1996a. Following upon the previously published tretaments of *Otocinclus* (Schaefer, 1997), *Acestridium* (Reis and Lehman, 2009), and *Oxyropsis* (Aquino and Schaefer, 2002), this work on *Hypoptopoma* serves to complete efforts to address the systematics and biogeography of the fishes of the loricariid subfamily Hypoptopomatinae, tribe Hypoptopomatini.

METHODS

Meristics

Meristic information throughout the text (e.g., species descriptions) is presented as the range followed by the mean in parentheses, unless otherwise indicated. Student's t-test was performed to infer the significance of the difference between the means of pair of species (SPSS Statistics Student Version 17.0, Inc.).

FIN-RAYS: Fin-ray counts do not vary within or among species of *Hypoptopoma*, and therefore fin-ray formulae are presented

only in the generic account. A Roman numeral designates the thickened and consolidated spinelike first unbranched ray, whereas numbers of branched rays are denoted by Arabic numerals. Hereafter and throughout the text, the first unbranched ray of the fin is referred to as "spine" in accord with convention, although we recognize that siluriforms lack true acanthomorph-like fin spines.

TEETH: Tooth counts were obtained separately for each jaw ramus and determined for the functional row (i.e., subdermal preemergent replacement teeth not included). Gaps in the tooth row resulting from loss of teeth were counted as one or more teeth present depending on the size of the gap relative to the average tooth width. Given the lack of significant differences between left and right counts, only the right-side tooth count of the premaxilla and dentary are included in the tables.

PLATES: Bilateral counts of dermal plates follow Schaefer (1997). Loricariids have five overlapping rows of plates along the trunk (fig. 1). These rows are serially homologous and individual rows are distinguished based on positional relationships to one another and to the trunk lateral-line canal. The medial series, like that in most other hypoptopomines, bears the lateral-line canal; the first medial-series plate is the anteriormost plate in contact with the second midventral plate. Lanceolate plates at the base of the caudal-fin rays were not included in the counts. Given the lack of significant differences between right- and left-side counts, only the right-side series of plate counts are included in the tables.

Morphometrics

Measurements were taken using a digital caliper to the nearest 0.1 mm, following Buckup (1981). In the species descriptions, subunits of the head are presented as a percentage of head length (HL). Head length itself and measurements of body parts are given as a percentage of standard length (SL). Dorsal interorbital distance refers to the minimum distance between bony orbit margins measured across the dorsum; likewise, ventral interorbital distance represents the minimum distance between bony orbit margins measured across the ventrum. Least orbit-naris distance was taken as the minimum distance between the bony orbit and posterolateral bony naris margin. Interpelvic distance was taken as the minimum distance between left and right pelvic spines. Caudal-fin base depth was taken at the vertical through the intersection between unbranched ray, branched rays, and basal plates of caudal fin. When included in species diagnoses and descriptions, morphometric and meristic data are presented as the range followed by the mean in parentheses. Sheared principal component analysis (Humphries et al., 1981) based on $\log_{10}$-transformed linear measures of head and body features was performed in order to examine patterns of shape contrasts among species.

Anatomy

Osteological observations were made on specimens cleared and differentially stained ("cs") for bone and cartilage following Taylor and Van Dyke (1985). A few specimens had been previously cleared and stained for bone only. Terminology of osteological and soft anatomical features follows Schaefer (1990). The presence or absence of a laterosensory canal in the preopercle in alcohol preserved specimens (the preopercle, if present, is not externally visible) was assessed by examination of the distribution pattern of pores (skin-surface branch apertures) of the preoperculo-mandibular laterosensory canal. Vertebral count includes five for the compound centra of the Weberian complex and one for the compound ural centrum. Throughout the text, the term *marginal odontodes* refers to the column of enlarged odontodes on the posterior margin of the trunk plates. *Ventral canal-bearing plate* refers to the large triangular dermal plate of the head located ventrally between the cleithrum and infraorbital bones that bears the terminus of the preoperculo-mandibular laterosensory canal. *Compound pterotic* is the term applied to the complex of bones located in the temporal region of the head composed of posttemporal, supracleithrum, pterotic, and ossified Baudelot's ligament. The expression *thoracic plates* refers to the dermal plates

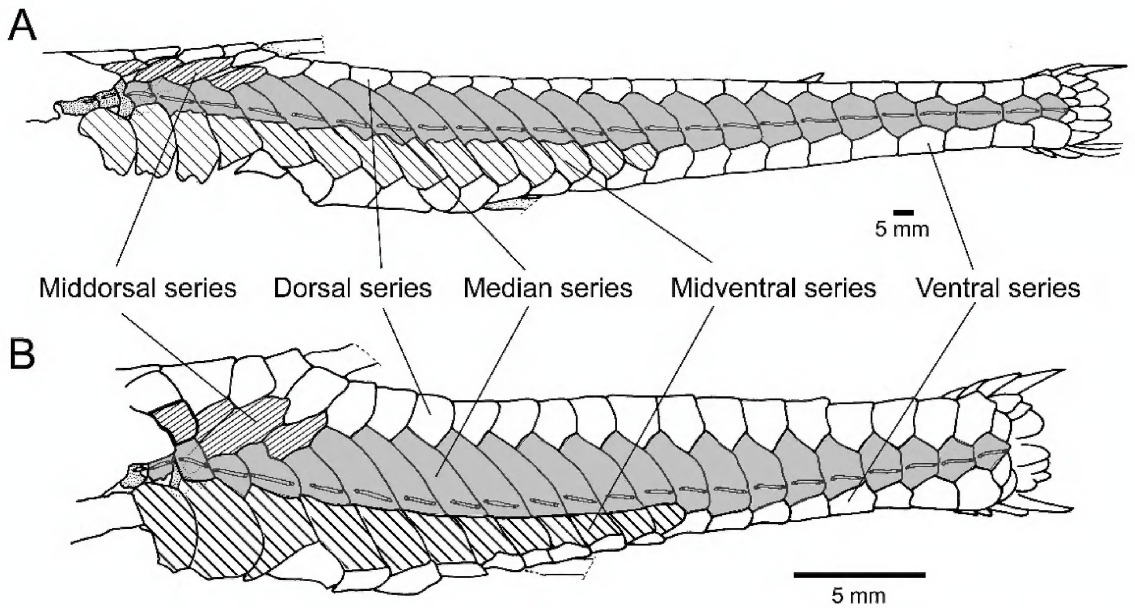

Fig. 1. Dermal plates of the lateral trunk and serial plate homology. **A,** *Hypoptopoma psilogaster* ANSP 138871; **B,** *H. inexspectatum* ILPLA 269.

anterior to the paired cleithra. *Abdominal plates* refer to the ventral shield of dermal plates between the pectoral and pelvic fins; the *anal plate* forms the shield between the anus, abdominal plates, and pelvic fins. The term *preorbital plate* refers to the plate lateral to the lateral ethmoid lateral process, which forms the anterodorsal rim of the orbit. The *paranasal plate* refers to one or more dermal plates, irregular in shape and size, positioned anterior to the naris and the lateral process of the lateral ethmoid. The *pararostral plates* are the series of small and irregularly shaped plates parallel to the mesethmoid bone. Throughout the text, fully developed individuals (mature specimens) are recognized by having complete development of the abdominal plates, which are the last plates to be developed during ontogeny.

Phylogenetic Analysis

Characters were chosen based on the presence of variation among *Hypoptopoma* species. Multistate characters (numbers 4, 6, 22) were unordered (state changes nonadditive) and all characters were equally weighted. In the description of characters, the derived condition is stated and all terminal taxa having a particular character state are listed in alphabetical order. Parsimony analysis of discrete morphological characters was performed using the programs TNT version 1.1 (Goloboff et al., 2008) and WinClada version 1.00.08 (Nixon, 2002) using implicit enumeration. Following Schaefer (1998) and Gauger and Buckup (2005), *Oxyropsis* (*O. acutirostra*, *O. carinata*, *O. wrightiana*) was included as the outgroup in the analyses. Relationships among outgroup taxa were not considered.

Scope and Organization

This revision of *Hypoptopoma* is organized as follows: generic account and decription of the general morphology of the genus, individual species accounts, a key to the species, character descriptions, and phylogenetic analysis. In the systematic treatment, the species accounts are arranged according to the results of the phylogenetic analysis to facilitate comparison of more closely related species. Species accounts are organized by clade relative to their position in the most parsimonious tree, from most basal to most terminal, and alphabetically within clades. Those anatomical features present in most if

not all congeners within a clade are presented in the description of the genus and are not repeated in the species accounts. Material examined is arranged by country, region (= state, province, or department, depending on the country), cataloged lot, number of specimens of each gender (when gender is available), followed by the size range of specimens (mm) and locality. Standard length (SL) is used throughout. Descriptive locality information associated with specimen lots is given verbatim and in the language of origin, in order to avoid errors in translation and interpretation.

Abbreviations

AMNH	American Museum of Natural History, New York, USA
ANSP	Academy of Natural Sciences of Philadelphia, USA
BMNH	Natural History Museum, London, United Kingdom
CAS	California Academy of Sciences, San Francisco, USA
CBF	Colección Boliviana de Fauna, La Paz, Bolivia
FMNH	Field Museum of Natural History, Chicago, USA
ILPLA	Instituto de Limnología "Dr. Raúl A. Ringuelet," La Plata, Argentina
INHS	Illinois Natural History Survey, Champaign-Urbana, USA
INPA	Instituto Nacional de Pesquisas da Amazonia, Manaus, Brazil
LACM	Los Angeles County Museum, Los Angeles, USA
MACN	Museo de Ciencias Naturales "Bernardino Rivadavia," Buenos Aires, Argentina
MBUCV	Museo Biologia de Universidad Central, Caracas, Venezuela
MCNG	Museo de Ciencias Naturales, Guanare, Venezuela
MFA	Museo de Ciencias Naturales "Florentino Ameghino," Santa Fe, Argentina
MHNG	Musée Histoire Naturelle, Genève, Switzerland
MNHN	Musée Natural de Histoire Naturelle, Paris, France
MNRJ	Museu Nacional, Rio de Janeiro, Brazil
MUSM	Museo Universidad de San Marcos, Lima, Peru
MZUSP	Museu de Zoologia, Universidade de São Paulo, Brazil
NRM	Swedish Museum of Natural History, Stockholm, Sweden
RMNH	Rijksmuseum van Natuurlijke Histoire, Leiden, The Netherlands
SIUC	Southern Illinois University, Carbondale, USA
SU	former Stanford University collections, now housed at CAS, USA
TNHC	Texas Natural History Collection, Texas, USA
UMMZ	Museum of Zoology, University of Michigan, Ann Arbor, USA
USNM	National Museum of Natural History, Smithsonian Institution, Washington D.C., USA
ZSM	Zoologische Staatssammlung, München, Germany

SYSTEMATICS

Hypoptopoma Günther, 1868a
Figure 2

Hypoptopoma (*Hypostomatin.*) Günther, 1868a: 477 (type species: *Hypoptopoma thoracatum* Günther, 1868a, by monotypy).

Hypoptopoma (*Hypostomatinum.*) Günther, 1868b: 234 (description of *H. thoracatum*).

Aristommata Holmberg, 1893: 96. *Aristommata inexspectata* Holmberg, 1893 type species by monotypy.—Isbrücker, 1980: 87.—Aquino and Miquelarena, 2001: 2.—Isbrücker, 2002: 26.—Ferraris, 2007: 249.

Aristomata Eigenmann, 1910: 412 (misspelling).

Hypoptoma Miranda Ribeiro, 1911: 97–99 (misspelling; list of fishes of Brazil).

Otocinclus not of Cope, 1871.—Eigennman, 1914: 229 (description of *O. spectabilis*).

Diapeltoplites Fowler, 1915: 237 (proposed as subgenus of *Hypoptopoma* Günther, 1868a).—Isbrücker, 1980: 87 (placed as synonym of *Hypoptopoma* Günther, 1868a).

Diapaletoplites Jordan, 1920: 556 (misspelling; list of fish genera).

Nannoptopoma Schaefer, 1996a: 915 (type species: *Nannoptopoma spectabilis* (Eigenmann, 1914)).

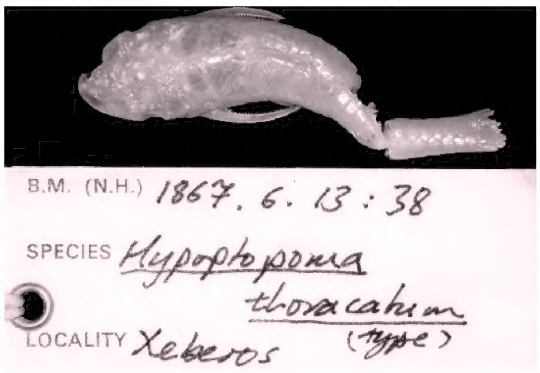

Fig. 2. Holotype and jar label of the type species of the genus *Hypoptopoma*, *H. thoracatum*, BMNH 1867.6.13:38.

DIAGNOSIS: Distinguished from all other loricariids by having the nuchal plate laterally expanded to such an extent that the distance between distal tips is at least twice the width of the base of the dorsal spine at its widest point (fig. 3B–C). In members of the Loricariinae and Hypoptopomatinae except *Niobichthys* and *Acestridium*, the nuchal plate is round to polyhedral, its width equal or slightly surpassing that of the base of the pectoral spine (fig. 3A). In *Niobichthys*, and members of the Ancistrinae and Hypostomatinae, there is a pair of nuchal plates in contact in the midline. Species of *Acestridium* possess 2–4 median unpaired predorsal plates (Reis and Lehman, 2009).

Hypoptopoma can also be distinguished from all other loricariids, except the hypoptopomatin genus *Oxyropsis*, by the shape of the head, which is depressed, and by the ventrolateral placement of the eyes. This typical "*Hypoptopoma*" head shape is further reflected anatomically by a series of uniquely derived osteological characters (shared with *Oxyropsis*): the lateral ethmoid laterally elongated; the T-shaped third infraorbital, with its lateral platelike side positioned ventrally on the head (fig. 4); the canal-bearing plate presenting more than three-fourths of its surface area positioned ventrally on the head, and the fourth infraorbital reduced, smaller than the fifth infraorbital (fig. 5) (except in *H. spectabile*). In other taxa, the position of the eyes is lateral to dorsolateral and not visible from below. Accordingly, the lateral ethmoid is not laterally elongated,

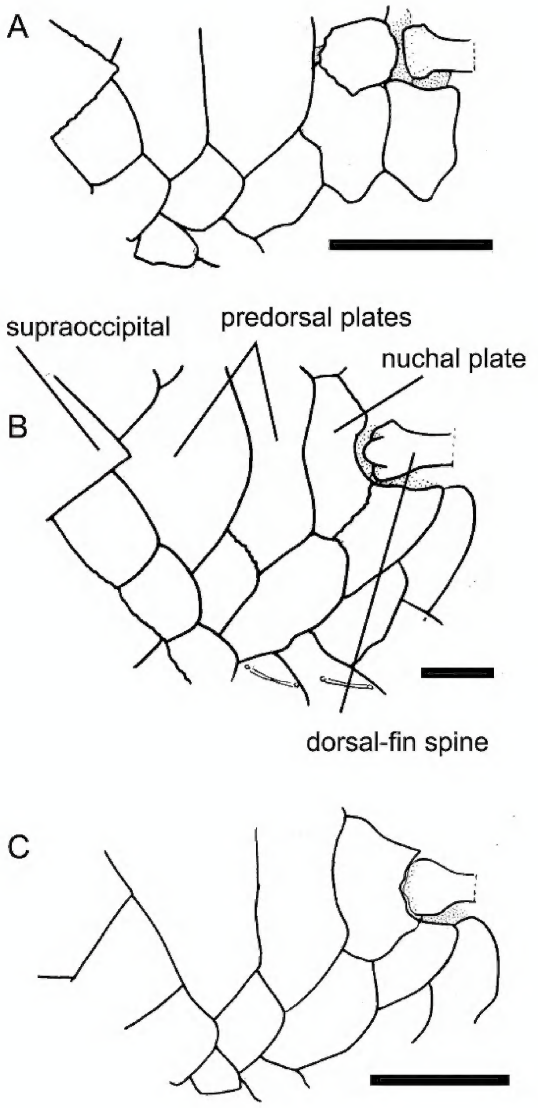

Fig. 3. Schematic diagram of the nuchal plate, dorsal view. **A,** *Oxyropsis acutirostra* ANSP 164280; **B,** *H. machadoi* ANSP 134438; and **C,** *Hypoptopoma baileyi* AMNH 39768. Scale bar = 2 mm.

the third infraorbital is platelike and laterally positioned on the head, the canal-bearing plate presents less than three-fourths of its surface area positioned ventrally on the head, and the fourth infraorbital is larger than the fifth infraorbital.

Hypoptopoma is distinguished from all other Hypoptopomatini, including *Oxyropsis*, by the shape of the caudal peduncle. The

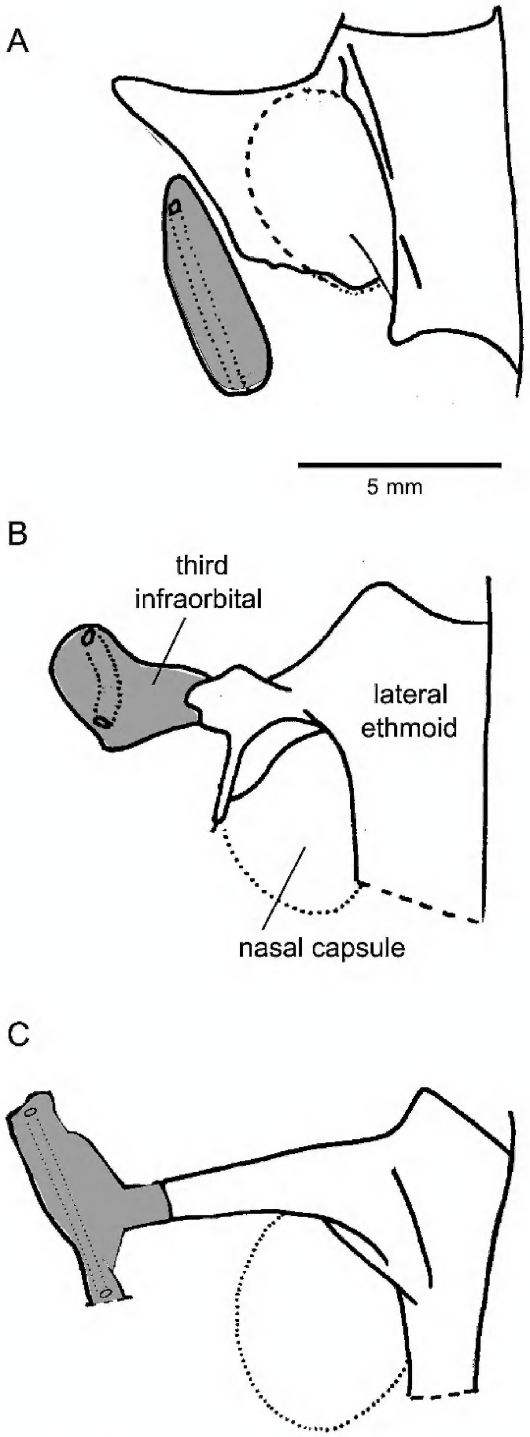

Fig. 4. Schematic diagram of the ventrolateral aspect of the skull, right side, anterior toward bottom, showing relationship of third infraorbital to lateral ethmoid. **A,** *Hypostomus* sp.; **B,** *Hisonotus* sp.; and **C,** *Hypoptopoma* sp.

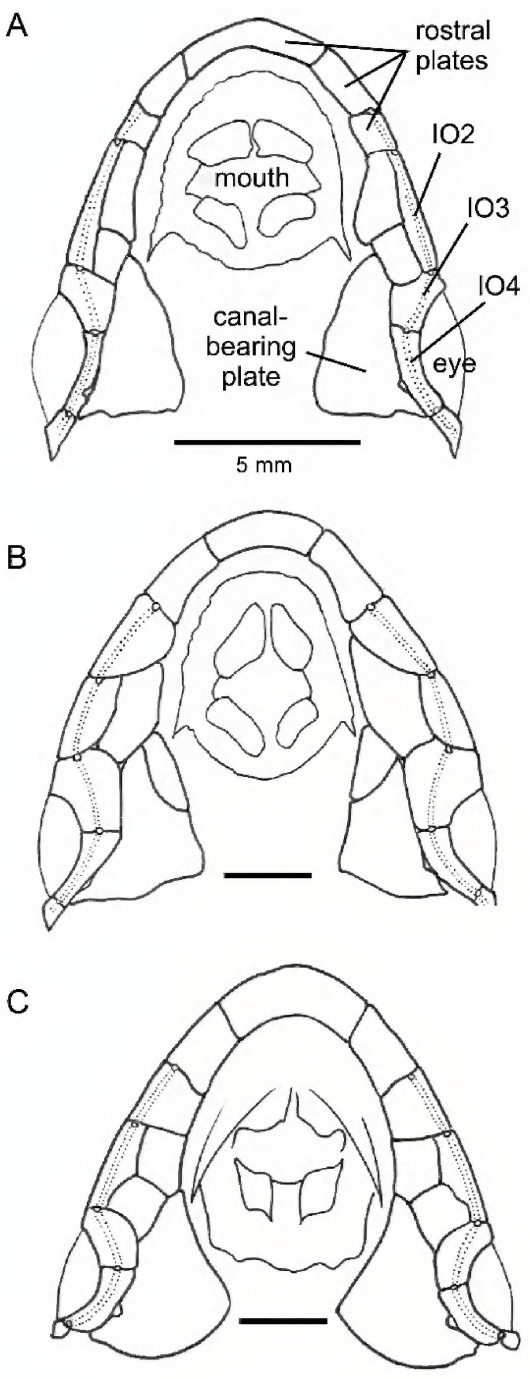

Fig. 5. Dermal plates of the head, ventral view: **A,** *H. inexspectatum* INPA 269; **B,** *H. steindachneri* INHS 40171, and **C,** *H. elongatum* INPA 7240.

cross section of the trunk posterior to the base of the anal fin is distinctly ovoid, with the dorsoventral axis as the longest. The ovoid shape is enhanced by the uniform size of the odontodes in longitudinal rows across the trunk and, in adults of the largest species in average size, by the smoothness of the plates. *Oxyropsis*, *Acestridium*, and *Niobichthys* possess a narrow and depressed caudal peduncle. The trunk cross section posterior to the base of the anal fin is roughly rectangular to oblate spheroidal in shape, with the horizontal axis as the longest. The lateral edges are enhanced by rows of variably enlarged odontodes, which in *Oxyropsis* form a keellike ridge in cross section (Aquino and Schaefer, 2002). In *Otocinclus*, which possess a robust caudal peduncle and the dorsoventral axis the longest, the cross section of the caudal peduncle is progressively rectangular in shape toward the caudal fin (Schaefer, 1997). The rectangular shape is further enhanced by rows of variably enlarged odontodes along the dorsolateral edges of the peduncle.

Hypoptopoma, except for *H. spectabile*, can be further distinguished among loricariids by the presence of a column of odontodes positioned along the posterior margin of the trunk plates (hereafter termed "marginal odontodes"; fig. 6). The marginal odontodes are not visible in the juvenile stages, becoming progressively conspicuous in ontogeny. Their development takes place with a progressive smoothening of the plate surfaces (in the largest specimens, the plates are smooth, the odontodes reduced in number, and their distribution is restricted to the posterior portion of the plate surface). The marginal odontodes are slightly larger and flattened relative to the typical conical odontodes.

DESCRIPTION: Adult body size moderately small relative to most other loricariids; maximum size of *Hypoptopoma* species ranging from 18 to 105 mm SL, attaining greatest body length among genera of Hypoptopomatinae. Head and body almost entirely covered by bony dermal plates, except for area surrounding lips and base of pectoral, pelvic, dorsal, and anal fins. Dermal bones exposed on head and pectoral girdle, and fin rays covered by dermal teeth or odontodes (Bhatti, 1938). Odontodes rather evenly distributed on head, slightly enlarged and variably aligned in dorsal and ventral series on rostral margin of snout, and typically arranged in well-defined longitudinal series on trunk plates. Distinct column of slightly enlarged and flattened marginal odontodes arranged along posterior margin of trunk plates. Anterior surface of pectoral-fin spine and ventral surface of pelvic-fin spine with enlarged odontodes. Series of smaller, irregularly shaped pararostral plates present anterior to each nasal plate between mesethmoid and lateral rostral plates (first to third canal-bearing infraorbitals) and adjacent to naris between nasal plate and lateral rostral plates (fig. 7A). In some species, one or more paranasal plates can be present (one in *H. gulare* and *H. machadoi*; two or more in *H. steindachneri*) (fig. 7B–C).

Dorsal-fin rays I,7; anal-fin rays i,5; pectoral-fin rays I,6; pelvic-fin rays i,5; caudal-fin rays i,7-7,i. Adipose fin variably present. Premaxillary teeth 10–36; dentary teeth 10–37. Oral disk rounded, surface papillose and with scattered unculi.

Dermal plates on trunk arranged in five longitudinal, serially homologous rows (fig. 1). Lateral line complete and continuous; total lateral plates (medial series) 20–26; dorsal series 17–22; middorsal series 3–5; midventral series 11–15; ventral series 17–22. Number of midventral series plates between posterior process of cleithrum and first plate of ventral series (roughly triangular plate at base of pelvic-fin spine) three (*H. bianale*, *H. elongatum*, *H. gulare*, *H. incognitum*, *H. inexspectatum*, *H. machadoi*, *H. spectabile*, *H. sternoptychum*) (figs. 1B, 8B) or four (*H. baileyi*, *H. brevirostratum H. guianense*, *H. muzuspi*, *H. psilogaster*, and *H. thoracatum*) (figs. 1A, 8A), rarely five. Second plate of midventral series contacting a single plate (*H. bianale*, *H. elongatum*, *H. gulare*, *H. incognitum*, *H. inexspectatum*, *H. machadoi*, *H. spectabile*, *H. sternoptychum*) (figs. 1B, 8B) or two plates of medial series (*H. baileyi*, *H. brevirostratum H. guianense*, *H. muzuspi*, *H. psilogaster*, and *H. thoracatum*) (figs. 1A, 8A). Abdominal plates arranged according to three main patterns: (1) plates arranged in paired series of lateral sickle-shaped plates and medial series of roughly squared plates, each series composed of more than three

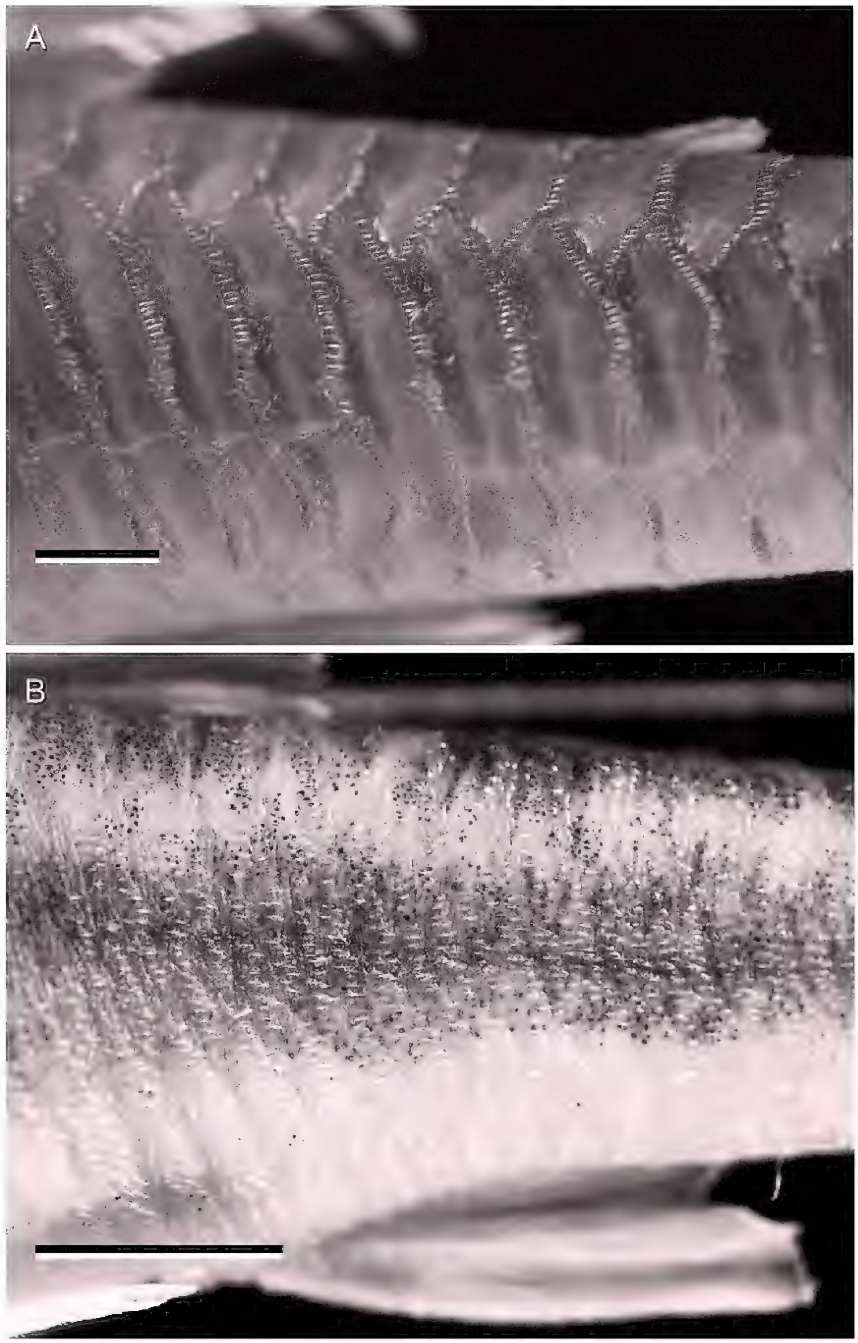

Fig. 6. Photograph of marginal odontodes, left side of trunk between dorsal and adipose fins, anterior toward left. **A,** *H. incognitum*, lamina of trunk plates smooth, marginal odontodes well developed; **B,** *Otocinclus flexilis*, AMNH 79372, lamina of trunk plates with longitudinal lines of small odontodes, marginal odontodes not markedly developed. Scale bar = 2 mm.

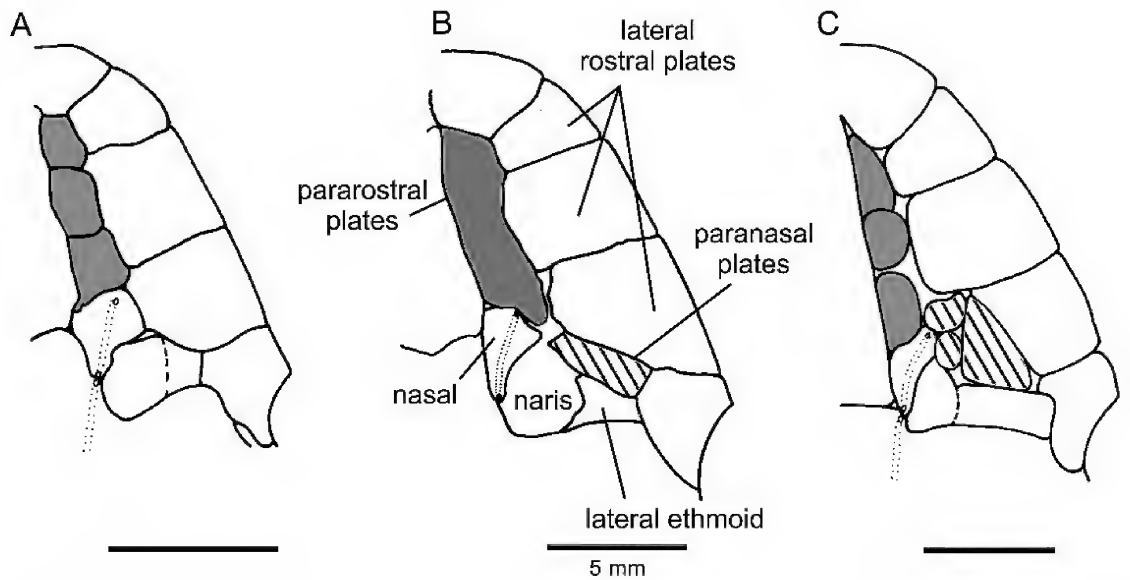

Fig. 7. Schematic drawing of head, showing topology of dermal plates, dorsal view, right side, anterior toward top. **A,** *H. inexspectatum* ILPLA 269; **B,** *H. machadoi* CAS 64283; and **C,** *H. steindachneri* INHS 40171.

plates (*H. baileyi*, *H. brevirostratum*, *H. guianense*, *H. muzuspi*, *H. psilogaster*, and *H. thoracatum*) (fig. 9A); (2) plates arranged in paired series of lateral sickle-shaped plates and only one roughly triangular medial plate between anteriormost pair of lateral plates (all other species, except *H. spectabilis* and *H. sternoptychum*) (fig. 9B–C), and (3) presence of a pair of slender plates posterior to the coracoids, followed by a series of 1–3 unpaired abdominal plates anterior to the anal plate (*H. spectabilis* and *H. sternoptychum*) (Schaefer, 1996a: fig. 1). Thoracic plates present or absent (*H. baileyi*, *H. brevirostratum*, *H. guianense*, *H. muzuspi*, *H. psilogaster*, *H. spectabilis*, and *H. thoracatum*); when present, forming shield between left and right ventral canal-bearing plates (fig. 9B–C). Anal plate composed of single plate (fig. 9A–B), except in *H. bianale*, whose shield is two plates (fig. 9C). Fully developed anal plate shaped as blunt, posteriorly oriented arrowhead.

Complete development of lateral series of trunk plates achieved ontogenetically before full development of abdominal shield and plates anterior to naris (fig. 10). Development of trunk-plate series progresses in rostral direction, with individual plates nearest caudal fin developing first. Plates of medial series and bony canals of lateral line develop asynchronously, with lateralis canal ossifying prior to ossification of surrounding plate lamina. Platelike connecting bone (sensu Schaefer, 1987), counted as second middorsal plate, develops prior to plates lying immediately anterior and posterior to middorsal series. Development of abdominal plates initiates with lateral series in an approximately lateral to medial direction. Fully developed individuals can be recognized by having ventral region between pectoral fins entirely covered by abdominal plates.

Sexual Dimorphism: Male urogenital papilla pointed, short, variably slender, more or less covered by anterior flaplike anus. Males of some species with patch of tightly arranged small odontodes positioned lateral to urogenital papilla and anus, variably developed on plates 1–4 of ventral trunk series. In some species, males with variably developed fringe of soft tissue along posterior margin of pelvic-fin spine, proximal to first branched ray when developed, typically restricted to basal one-third to one-half of spine length. Anus of females tubular, without separate urogenital papilla. In fe-

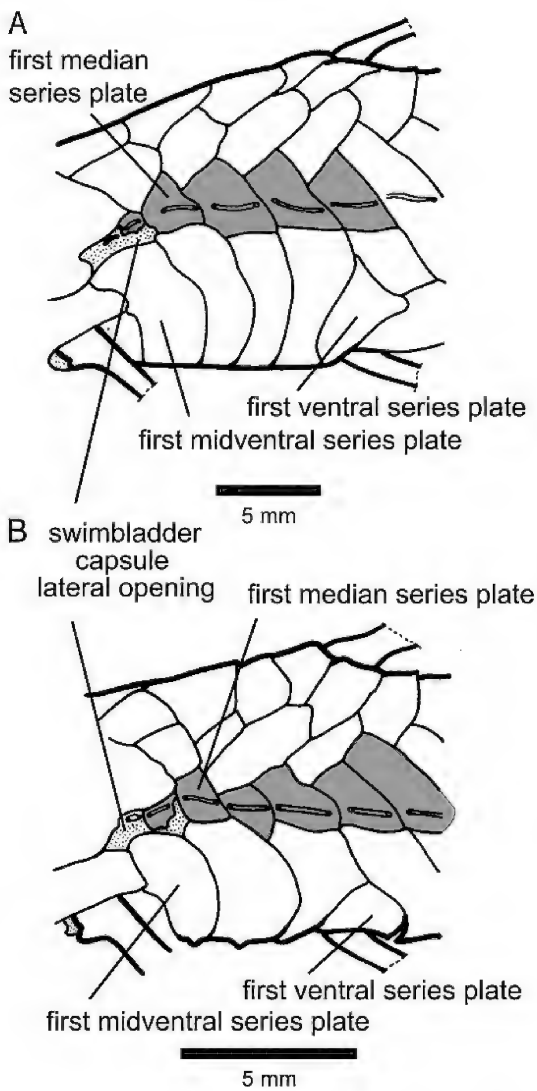

Fig. 8. Anteriormost plates of the canal-bearing medial trunk dermal plate series (shaded), left side, anterior toward left. **A,** *Hypoptopoma thoracatum* INHS 40172; and **B,** *H. inexspectatum* ILPLA 269.

males of all species, size and arrangement of odontodes on plates lateral to anus similar to adjacent plates, without distinct patch of differentially arranged odontodes.

DISTRIBUTION: Widely distributed in lowland cis-Andean South America, with representatives in the major tributaries of the Amazon, Orinoco, Essequibo, Nickerie, Tocantins, and Paraguay/Paraná rivers (fig. 11).

COMPARISONS: The pattern of odontode distribution on the trunk plates changes during ontogeny. In the smallest specimens of each species, odontodes on the plate lamina have a relatively dense and regular distribution in multiple longitudinal rows, a condition observed widely among species of Loricariidae. In larger specimens (actual size of specimen depends on the species), the distribution of odontodes is more uneven and irregular over the plate surface, resulting in one or more relatively open areas lacking odontodes and giving the plate surface a smoother appearance. A pattern of increased irregularity in odontode distribution and greater proportion of the plate surface without odontodes is correlated with increase in the size of specimens. It has not been determined whether trunk-plate smoothing is due to actual loss of odontodes or plate growth in surface area without corresponding increase in number of odontodes, thus expanding the space among odontodes. Observation of open "sockets," or alveoli, would suggest both odontode loss and surface ossification as responsible for plate smoothing during ontogeny. Although odontode loss would not be uncommon among loricariids, progressive plate smoothing has not been reported. Among *Hypoptopoma* species, the greatest degree of plate smoothing is observed mostly among species of the clade at node 7 (see fig. 45) and the largest specimens of *H. thoracatum* and *H. psilogaster*. Among non-loricariid loricarioids, some callichthyids have odontodes arranged along the posterior margin of the trunk plates. However notable differences in morphology of individual odontodes and in arrangement of odontodes suggest nonhomology with the condition observed among *Hypoptopoma* species.

Within the Hypoptopomatinae, *Hypoptopoma* is most similar to *Oxyropsis* in external appearance. Representatives of these two genera share the depressed head and the ventrolateral position of eyes (Schaefer, 1997). In addition to the unique presence of the laterally expanded nuchal plate and marginal trunk-plate odontodes, *Hypoptopoma* can be further distinguished from *Oxyropsis* by having a trunk ovoid in cross section, the ratio of the caudal-peduncle

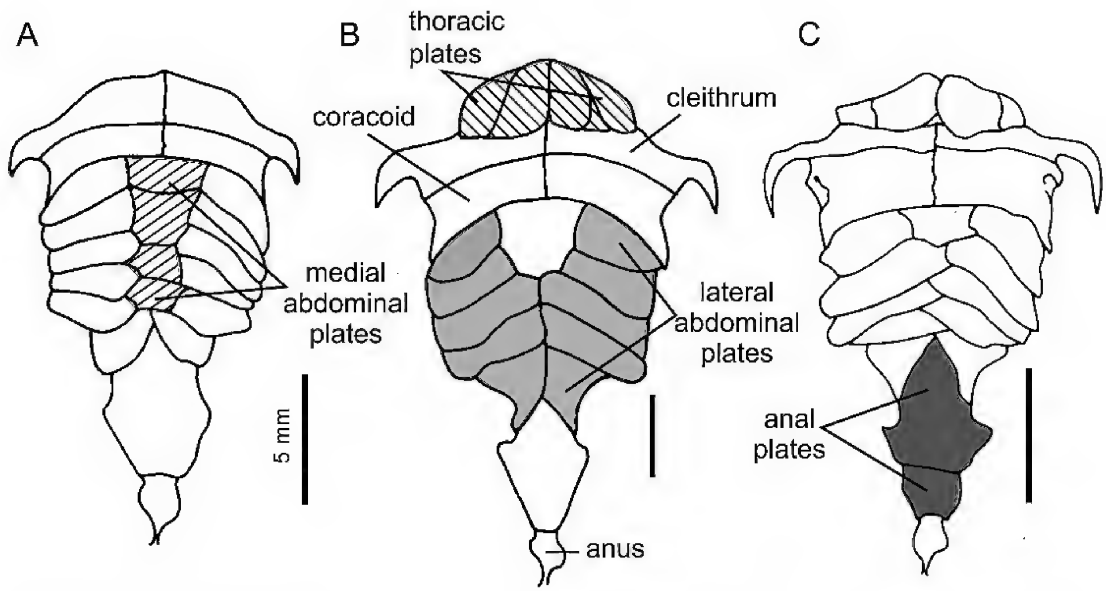

Fig. 9. Ventral view of abdominal region, anterior toward top, showing relationship of abdominal plate series and anal plates. **A,** *H. thoracatum* USNM 308312; **B,** *H. gulare* NRM 16561; and **C,** *H. bianale* FMNH 117745.

depth in the caudal-peduncle width >1 (vs. cross section of trunk depressed, rectangular to oblate spheroid shaped in cross section, ratio of caudal-peduncle depth in caudal-peduncle width <1), and by the absence of the single row of enlarged odontodes along the trunk midline lying adjacent and immediately dorsal to the lateral-line canal, a derived character state unique for *Oxyropsis* (Aquino and Schaefer, 2002).

Taxonomic Remarks: Günther (1868a) distinguished *Hypoptopoma* by characteristics related to the head: head depressed and spatulate, with the eyes located on the lateral margins of the head. Following this diagnosis, Steindachner (1879) assigned his new species *carinatum* to the genus *Hypoptopoma*. Aquino and Schaefer (2002) provided evidence in support of *Oxyropsis* monophyly and demonstrated that the characteristics used by Günther to distinguish *Hypoptopoma* are shared with *Oxyropsis*. A phylogenetic diagnosis of *Hypoptopoma* (Schaefer, 1991) distinguished the genus on the basis of two osteological characters: (1) canal in the preopercle forming a semicircle, and (2) preopercular canal passing through the fifth infraorbital before entering the preopercle. The present study shows that those two characters are not shared by all species of *Hypoptopoma*. In a revised analysis, Schaefer (1998) recognized four derived unreversed characters supporting the *Hypoptopoma* clade (Schaefer, 1998: fig. 3): (1) sphenotic with expanded anterior lamina, (2) preopercle canal semicircular, (3) presence of notch on canal-bearing ventral plate, and (4) trunk plates with enlarged odontodes concentrated along posterior margin (in this paper, marginal odontodes). Likewise, the present study shows that character (1) is shared with other genera of the tribe, and characters (2), (3), and (4) are not shared by all species of *Hypoptopoma*.

General Morphology

The osteology and myology of the Hypoptopomatinae has been treated in relatively few studies (Schaefer, 1991, 1997; Aquino, 1994, 1998; Aquino and Miquelarena, 2000; Aquino and Schaefer, 2002), and only one publication (Aquino and Miquelarena, 2000) dealt exclusively with a species of *Hypoptopoma*. The following account of the anatomy of *Hypoptopoma* is based on examination of

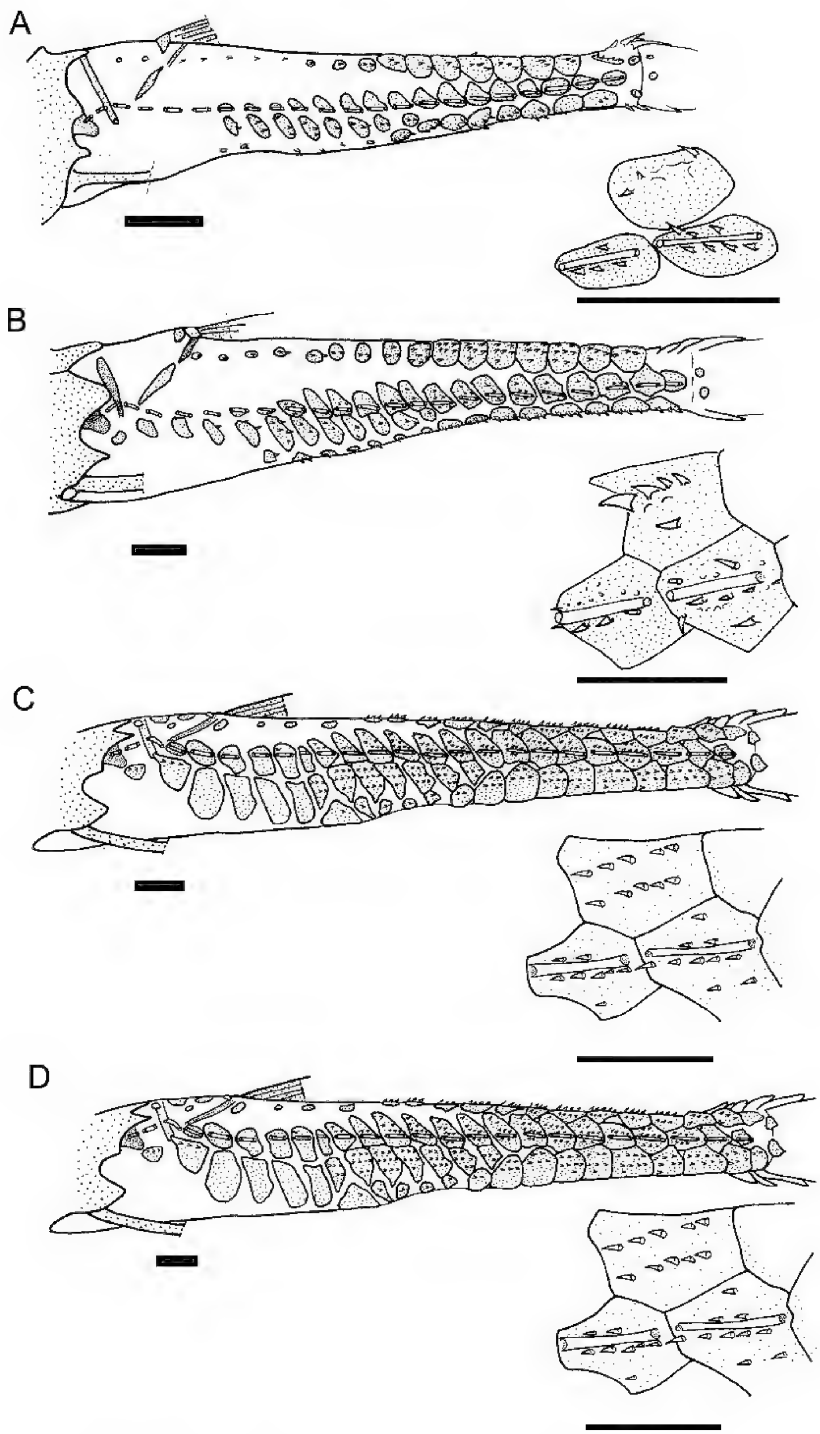

Fig. 10. Ontogeny of the trunk lateral dermal plate series in *Hypoptopoma inexspectatum*, UMMZ 205878, showing changes in the pattern, size, and arrangement of plates with growth. Individual plates shown at right depict size and configuration of odontodes relative to plate margins and laterosensory canal. **A,** 18.6 mm SL; **B,** 24.3 mm SL; **C,** 29.0 mm SL; and **D,** 35.7 mm SL.

Fig. 11. Drainage map of South America and distribution of the genus *Hypoptopoma*. Symbols may represent more than one locality record.

one or more cleared and stained and alcohol-preserved material of all 15 species recognized herein. The following section, although focused on aspects of morphology that have not been treated in previous works, gives an account of the contribution of the aforementioned authors. A description of the dermal plates is included in the taxonomic account for the genus.

NEUROCRANIUM: Mesethmoid long and slender; anterior tip laterally extended (Aquino and Miquelarena, 2000: fig. 5). Ventral process of mesethmoid disk shaped, not terminal (Schaefer, 1991). Nasal approx-

imately triangular in shape (fig. 7). Orbit occupies distinctly lateral position, in correlation with lateral elongation of lateral process of lateral ethmoid. In adults of species of *Hypoptopoma gulare* group, position of orbits slightly lateroventral, so that dorsal interorbital distance can be greater than ventral interorbital distance.

In dorsal view, supraoccipital large and nearly hexagonal in shape; in ventral view, suturing with neural spines of Weberian complex and expanded neural spine of sixth vertebra (Aquino and Miquelarena, 2000: figs. 7, 17). Frontal and sphenotic bones generally forming dorsal wall of orbital chamber. Sphenotic approximately rectangular in shape. Dorsal rim of orbit formed by fifth infraorbital, sphenotic, frontal, and preorbital plate. Species of the clade at node 6 (see fig. 45) with decreasing contribution of frontal and sphenotic to dorsal rim of orbit with increasing size of individuals (fig. 12); only preorbital plate and fifth infraorbital forming dorsal rim of orbit in largest specimens.

Compound pterotic enclosing bony capsule of swimbladder anteriorly and dorsally (Aquino and Miquelarena, 2000: fig. 7), with uniformly circular small pores in dorsal view. Lateral ethmoid with pronounced lateral process; laminar expansion of lateral ethmoid partially encapsulating nasal organ from below; anterior process of lateral ethmoid articulating with palatine (Aquino and Miquelarena, 2000: fig. 6). Lateral processes of parasphenoid approximately rectangular in shape, suturing with prootics anteromedially, and interdigitating with median projection and paired shorter lateral processes of basioccipital posteriorly (Aquino and Miquelarena, 2000: fig. 5). Anterior margin of prootic partially bounding compound foramen for trigeminofacialis and optic nerves. Functional posterior myodome formed by one camera limited by prootics, parasphenoid, and basioccipital (Aquino, 1998; Aquino and Miquelarena, 2000: fig. 8b). Posterior wall of lateral process of lateral ethmoid with ridge that serves as insertion point of obliquus eye muscles (Aquino and Miquelarena, 2000: fig. 8a). Exoccipital forming part of anterior wall of swimbladder.

INFRAORBITAL SERIES AND LATEROSENSORY CANALS: Infraorbital series composed of five elements. First and second infraorbitals platelike, located lateroposterior to snout rostral plate. Third infraorbital T-shaped, with anterior and posterior limbs platelike and mesial strutlike projection articulating with lateral process of lateral ethmoid (fig. 4). In contrast, third infraorbital platelike in other loricariids. Fourth infraorbital narrow, smaller than fifth infraorbital. Fifth infraorbital with infraorbital canal only (*H. baileyi*, *H. guianense*, *H. psilogaster*, and *H. thoracatum*) (fig. 13A), or fifth infraorbital with branches from both preoperculo-mandibular canal and infraorbital canal (fig. 13B).

SUSPENSORIUM AND MANDIBULAR ARCH: Hyomandibula largely enclosing orbit from below, articulating with compound pterotic posteriorly, contacting prootic dorsally, and suturing loosely to metapterygoid via bony interdigitations anterodorsally (Aquino and Miquelarena, 2000: fig. 10a–b). Hyomandibula connecting to quadrate via hyosymplectic cartilage anteriorly. Hyomandibula partially overlapping canal-bearing region of preopercle ventrally in species of the clade at node 6 (fig. 14B).

Metapterygoid approximately trapezoid in shape (Aquino and Miquelarena, 2000: fig. 10a–b). Anterior tip of metapterygoid short and pointed, connecting to three fingerlike processes of palatine that serves as insertion site for *extensor tentaculi*. Depth of metapterygoid canal less than 50% of its length. Canal extended along first third of dorsal margin of metapterygoid in *H. baileyi*, *H. guianense*, *H. psilogaster*, and *H. thoracatum*; extended just beyond anterior first half of dorsal margin in other species. Canal elongate and narrow, shelflike lateral lamina narrower than on opposite side in *H. baileyi*, *H. guianense*, *H. psilogaster*, and *H. thoracatum*; canal widely open, lateral shelflike extension wider than opposite side in other species.

OPERCULAR SERIES: Opercle approximately polygonal in shape (fig. 14), with broad concave area for articulation with hyomandibula. Ridge that serves for insertion of levator operculi largely extending between

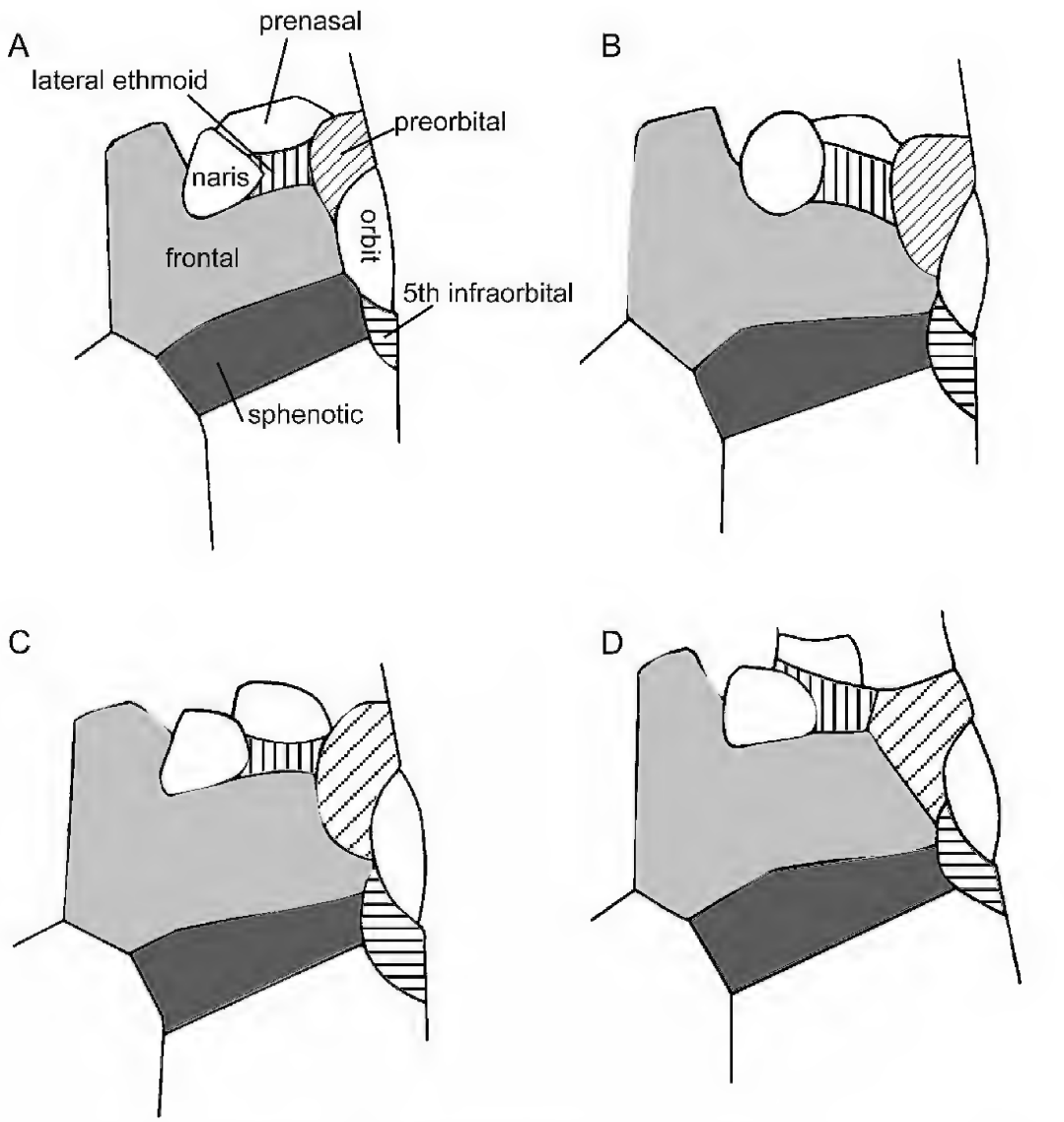

Fig. 12. Schematic diagram of the dorsolateral aspects of the head of *Hypoptopoma* showing ontogenetic changes in the degree of contribution of the bones to the dorsal rim of the orbit, *H. gulare*, INHS 39348. **A,** 52.9 mm SL; **B,** 62.0 mm SL; and **C,** 64.0 mm SL; **D,** 75.0 mm SL.

anteroventral and posterior margins of opercle.

Preopercle not exposed, posterior ramus not reaching hyomandibula adductor crest. Two conditions are recognized: (1) posterior ramus not reaching hyomandibula adductor crest and not reaching to base of opercle condyle, approaching or slightly surpassing tip of opercle (for less than one-third of longest axis of opercle) (fig. 14A) (*H. baileyi*, *H. guianense*, *H. psilogaster*, and *H. thoracatum*; shared with *Otocinclus and Oxyropsis*); (2) posterior ramus of preopercle reaching to or reaching base of opercle condyle (approximately at vertical through one-third of longest axis opercle) (fig. 14B–C). Canal in the preopercle present or absent (fig. 14A–C; when present, canal in preopercle semicircular (nearly U-shaped), receiving branch from fifth infraorbital.

WEBERIAN APPARATUS AND AXIAL SKELETON: Bony swimbladder capsule elongate

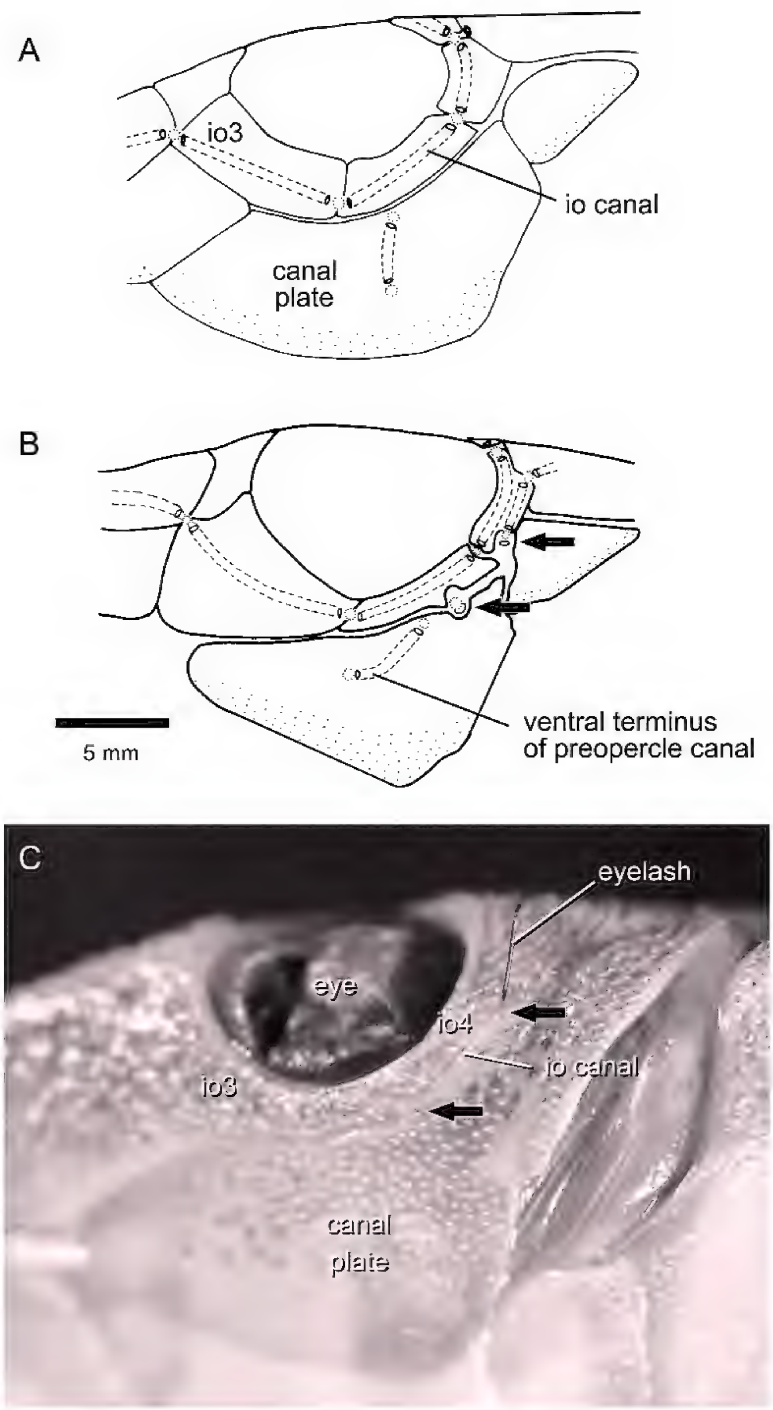

Fig. 13. Third through fifth infraorbital plates, infraorbital canal, canal in preopercle, and ventral canal-bearing plate, left side, anterior toward left. **A,** *Hypoptopoma baileyi* UMMZ 205171; **B,** *H. muzuspi* MZUSP 95186; **C,** photograph showing and eyelash passed through the semicircular preopercular laterosensory canal in *H. gulare*, MCNG 240798. Entrance and exit pores denoted by arrows in B, C. References: io, infraorbital.

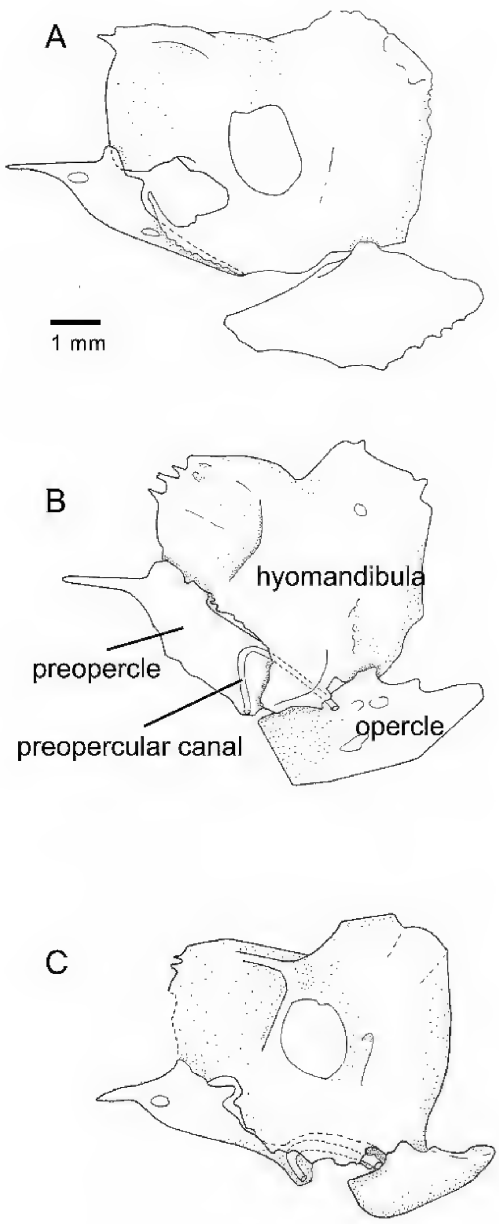

Fig. 14. Preopercle and adjoining bones, right side, lateral view: **A,** *H. baileyi* AMNH 243579; **B,** *H. gulare* USNM 284866; and **C,** *H. muzuspi* 243578.

laterally and slightly tubular in shape, with small lateral openings covered by skin (Aquino and Miquelarena, 2000: figs. 5, 7). Scaphium discoidal, concave mesially; tripus curving at approximately one-third from anterior tip, with small mesial process connecting via connective tissue with dorsoanterior portion of centrum of Weberian complex (Aquino and Miquelarena, 2000: fig. 16a–b).

Total vertebrae 25–28, inclusive of five vertebrae incorporated into Weberian complex and fused with skull, and single centrum incorporated into ural complex. Two bifid hemal spines (three in other loricariids and most Hypoptopomatinae). Neural spine of sixth vertebra expanded dorsally, suturing to supraoccipital (Aquino and Miquelarena, 2000: fig. 17). Rib of sixth vertebra elongate; tip expanded, contacting dermal plates and connecting bone between rib and transverse process of second dorsal-fin pterygiophore. Seventh vertebra with pair of anterior processes; neural spine not expanded dorsally, contacting distal end of first two pterygiophores of dorsal fin. Expanded lamina of single supraneural bone with pair of anterior processes; supraneural bone suturing with anterior margin of first pterygiophore posteriorly. Ossified pleural ribs posterior to rib of sixth centrum present in *H. baileyi*, *H. guianense*, *H. psilogaster*, *H. spectabile*, *H. sternoptychum*, and *H. thoracatum*. Ribs (except for first and, less often, posteriormost one) with single articulation to anteroventral area of centra via strong connective tissue. Anteriormost rib (and, less often, posteriormost one) typically reduced to ossified "floating" segment of rib connected to centrum via connective tissue at exactly same point where more developed ribs articulate with centrum. Development of ribs, thus length, also varies between left and right sides of body.

MEDIAN FINS: Caudal skeleton fused into ural complex (Lundberg and Baskin, 1969; Aquino and Miquelarena, 2000: fig. 18a–b). Basipteryigium fenestrae present, except in *H. spectabile* and *H. sternoptychum* (Schaefer, 1996a). Caudal-fin myology corresponds with condition described for the Loricariidae (Lundberg and Baskin, 1969; Aquino and Miquelarena, 2000: fig. 19a–b). Fossa muscularis of basipterygium with ventral transverse ridge that serves as insertion point for adductor profundus; transverse ridge orthogonal (vs. ridge oblique in most loricariids) to longitudinal axis of girdle (Aquino and Miquelarena, 2000: fig. 23a).

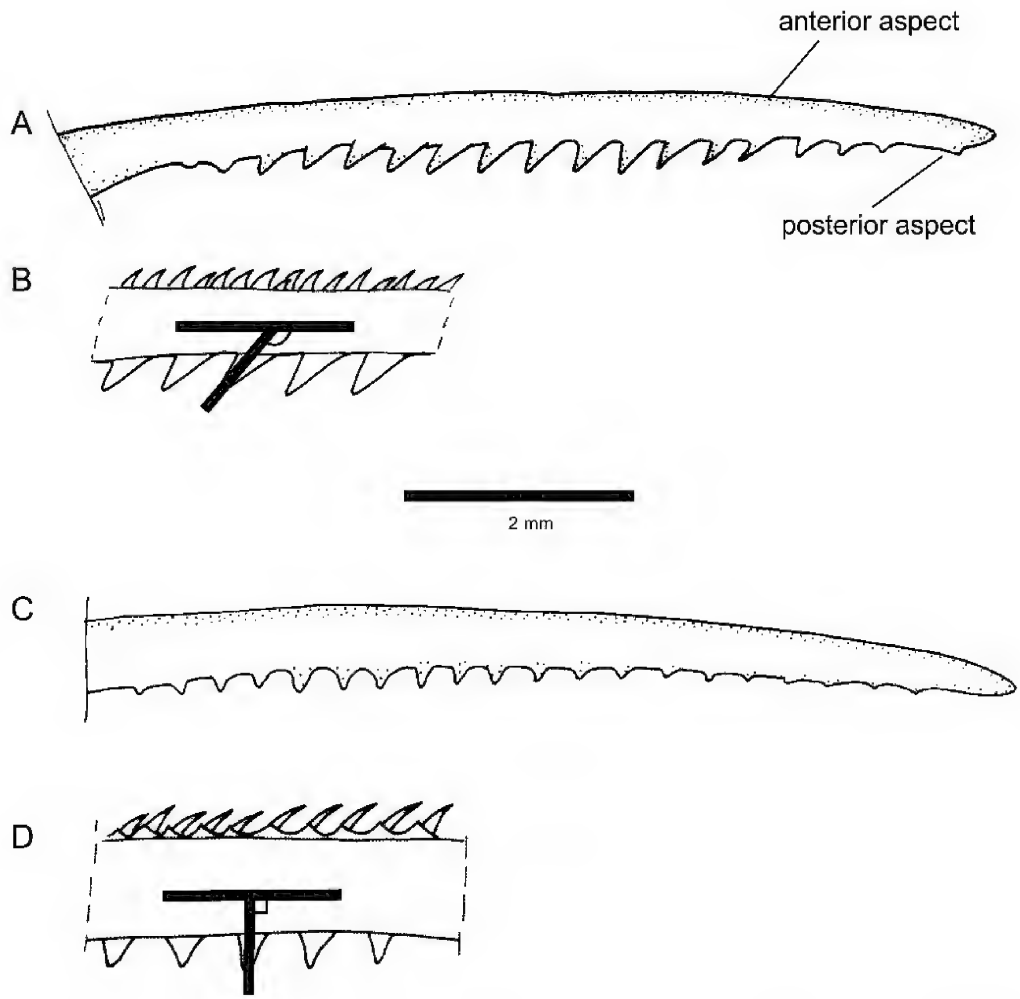

Fig. 15. Pectoral-fin spine, right side dorsal view, anterior toward top. **A, B,** serrae of oblique type, lateral view of whole spine and detail, respectively; **C, D,** serrae of orthogonal type, lateral view of whole spine and detail, respectively.

First dorsal-fin spine (spinelet) and dorsal-fin spine locking mechanism absent. Eight dorsal-fin pterygiophores; transverse processes on second pterygiophore extended, processes of more posterior pterygiophores shorter; last pair of processes forming posterior bifid process. Seven dorsal-fin distal radials, each with short lateral processes. Adipose fin variably present; when present also variable in shape, varying from a patch of odontodes closely arranged to a spiny axis covered by small odontodes supporting a delicate membrane. Six anal-fin pterygiophores; anterior margin of first pterygiophore expanded laterally and connected to anal plate via connective tissue.

PAIRED FINS: Posterior side of pectoral spine serrated, (all species except *H. spectabile* and *H. sternoptychum*). When present, serrae showing either oblique (*H. baileyi*, *H. guianense*, *H. psilogaster*, and *H. thoracatum*) or orthogonal orientation (all other species). Oblique type (fig. 15A–B) characterized by individual serrae oriented at oblique angle relative to pectoral spine axis; tips of individual serrae acute; serrae extend from near distal tip to base of spine, except for short proximal region; serrae well

developed throughout ontogeny. Orthogonal type (fig. 15C–D) characterized by individual serrae oriented orthogonal to pectoral spine axis; tips of individual serrae slightly blunt; serrae most prominent along middle region of spine shaft; serrae poorly developed or absent in largest specimens of species with longest average standard length (i.e., *H. steindachneri*). Two conditions were recognized relative to pectoral-fin radials: (1) three separate radials (*H. baileyi*, *H. guianense*, *H. psilogaster*, and *H. thoracatum*); and (2) first radial separate, second and third radials sutured along longest axis, suture line variably visible (all other species) (Aquino and Miquelarena, 2000: fig. 22c–d).

Key to the species of *Hypoptopoma*

The following key has been designed for identification of fully developed individuals, which can be recognized by presence of a completely developed shield of abdominal plates.

1a. A single pair of slender plates posterior to coracoids, followed by series of 1–3 unpaired abdominal plates anterior to anal plate . . . 2
1b. Four to seven paired lateral abdominal plates posterior to coracoids; medial series of plates present or absent. 3
2a. Thoracic plates absent. Medial series of trunk lateral plates typically 20–22 (20) . . . . . *H. spectabile* (Upper Amazonas and upper Orinoco basins)
2b. Thoracic plates present. Medial series of trunk lateral plates typically 21–22 (21) . . . . . *H. sternoptychum* (Upper and central Amazonas, including upper Madeira basin)
3a. Thoracic plates absent (fig. 9A). Second plate of midventral series of trunk plates contacting one plate of medial series only (fig. 8A). Four midventral plates between cleithral posterior process and first plate of ventral series or triangle-shaped plate above pelvic spine (fig. 8A). 10
3b. Thoracic plates present (fig. 9B–C). Second plate of midventral series of trunk plates relating to two plates of medial series (fig. 8B). Three midventral plates between cleithral posterior process and first plate of ventral series or triangle-shaped plate above pelvic spine (fig. 8B) 4
4a. Anal shield composed of two plates—arranged along body longitudinal axis—between anus and abdominal plates (fig. 9C) . . . . . *H. bianale* (Lower Ucayali and Solimões basins)
4b. Anal shield composed of azygous plate (fig. 9B) 5
5a. Second infraorbital bone laterally contacting with one ventral dermal plate (fig. 5B). Distal tips of unbranched and branched rays of caudal fin dark forming vertical band along posterior margin of fin . . . . . *H. steindachneri* (Lower Ucayali and Solimões basins)
5b. Second infraorbital bone laterally contacting with two ventral dermal plates (fig. 5A–C). Distal tips of unbranched and branched rays of caudal fin light, not forming vertical band along posterior margin of fin 6
6a. Patch of odontodes on anterolateral aspect of cleithrum present (at level of opening to branchial cavity) . . . . . *H. incognitum* (Central Amazonas—including Madeira basin—Tocantins, and NE coastal rivers)
6b. Patch of odontodes on anterolateral aspect of cleithrum absent 7
7a. No paranasal plate (fig. 7A). 8
7b. One or more paranasal plates (figs. 7B–C) . . . 9
8a. Odontodes on rostral margin of snout (rostral plate, first and second infraorbital) arranged in well-aligned dorsal and ventral series; both series separated by odontode-free discontinuity, particularly at level of first and second infraorbital bones (fig. 16). Medial series of trunk plates 20–22 (21) . . . *H. inexspectatum* (Ríos Paraguay and lower Paraná basins)
8b. Odontodes on rostral margin of snout typically not arranged in well-aligned dorsal and ventral series; if present, alignment restricted to rostral plate and series not separated by distinct odontode-free discontinuity. Medial series of trunk lateral plates typically 23. . . *H. elongatum* (Rios Tapajos and Trombetas)
9a. Dorsal fin with dark brown, roughly triangular spot, extended over base of anteriormost 3–4 branched rays, covering around one-third of first branched ray length. Anteriormost caudal-fin "<"-shaped band connected at midpoint to lanceolate plates at base of fin (fig. 17D); upper arm of first band variably developed, typically light brown to absent . . . . . *H. gulare* (Lower Ucayali and Solimões basins)
9b. Dorsal fin without triangular spot at base of branched rays (if present, spot poorly defined). Anteriormost caudal-fin "<"-shaped band not clearly connected at midpoint to lanceolate plates at base of fin (fig. 17G); upper-lobe arm of first band typically complete. . . . . *H. machadoi* (Rio Orinoco basin, including Rio Meta drainage)

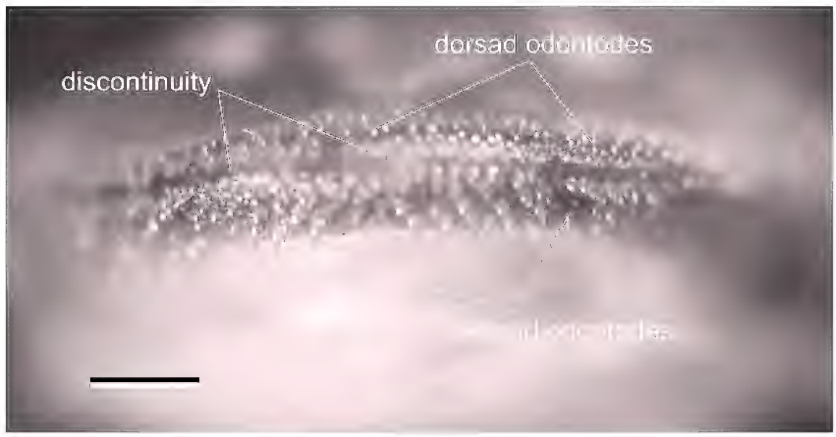

Fig. 16. Rostral dermal plates in *Hypoptopoma inexspectatum* ANSP 175350; frontal view.

10a. Preopercle with canal; pore of canal present, located between fourth infraorbital and canal-bearing plate (fig. 13B); both margin of canal-bearing plate and margin of fourth infraorbital bone with notch for exit of pore of canal in preopercle 11

10b. Preopercle without canal, thus pore of canal between fourth infraorbital and canal-bearing plate absent (fig. 13A); both margin of canal-bearing plate and fourth infraorbital smooth. 12

11a. Cleithral width 23.7%–27.0% of standard length (mean 25.7). Horizontal eye diameter 19.8%–23.3% of head length (mean 21.7). Caudal fin with diamond-shaped basal spot variably developed, followed by 2–3 faint vertical bands . . . . . *H. brevirostratum* (Tributaries of Rio Amazonas between confluence of Ucayali-Marañon)

11b. Cleithral width 19.1%–23.5% of standard length (mean 22.2). Horizontal eye diameter 13.6–20.7 of head length (mean 18.4). Caudal fin with variably shaped basal spot followed by 7–10 vertical bands. . . . . *H. muzuspi* (Rio Tocantins basin)

12a. Caudal fin with 7–10 brown vertical bands; dark spot along medial or lower-lobe branched rays absent. Adipose fin typically absent; if present, membranous. . . . . *H. baileyi* (Upper Madeira basin)

12b. Caudal fin with 5 or fewer variably marked vertical bands; and dark spot along medial branched rays present, variably extended along lower-lobe rays. Adipose fin typically present, composed of bony axis and soft tissue 13

13a. Caudal fin with dark brown spot along medial branched rays slightly more extended over lower lobe, typically covering seventh ray on upper lobe and rays 8–11 on lower lobe (count starts dorsally) (fig. 17A). Cleithral width 20.0%–24.7% of standard length (mean 22.7) . . . . . *H. thoracatum* (Amazonas basin, including Madeira, Purus, Tapajos, Caqueta, and lower Ucayali)

13b. Caudal fin with elongated dark spot along medial branched rays typically symmetrical, typically covering sixth and seventh rays of upper lobe and rays 8–9 of lower lobe (count starts dorsally) (fig. 17B–C). Cleithral width 17.3%–21.4% of standard length. 14

14a. Caudal fin with elongated dark spot along medial branched rays connected to series of lanceolate plates at base of fin (fig. 17C). Head width 17.3%–19.2% of standard length (mean 18.4) . . . . . *H. guianense* (Essequibo and Nickerie basins)

14b. Caudal fin with elongated dark spot along medial branched rays not distinctly connected to series of lanceolate plates at base of fin (fig. 17B). Head width 15.6%–18.1% of standard length (mean 17.1). . . . . *H. psilogaster* (Lower Ucayali and Napo basins)

Hypoptopoma baileyi, new species
Figure 18, table 1

HOLOTYPE: AMNH 39828 (♀, 38.9 mm SL) Bolivia: Beni, backwater, Río Itenez, 10 km SE Costa Marques, Brazil; collected by R.M. Bailey and R. Ramos, 10 September 1964.

PARATYPES (collected with holotype): AMNH 243579 (61 ♀ + 18 ♂, 27.5–44.0 mm SL). UMMZ 205171 (75 ♀ + 32 ♂, 6 cs, 27.7–40.6 mm SL).

OTHER MATERIAL EXAMINED: **BOLIVIA, Beni**: AMNH 39764 (1 ♀, 25.5 mm SL) Río

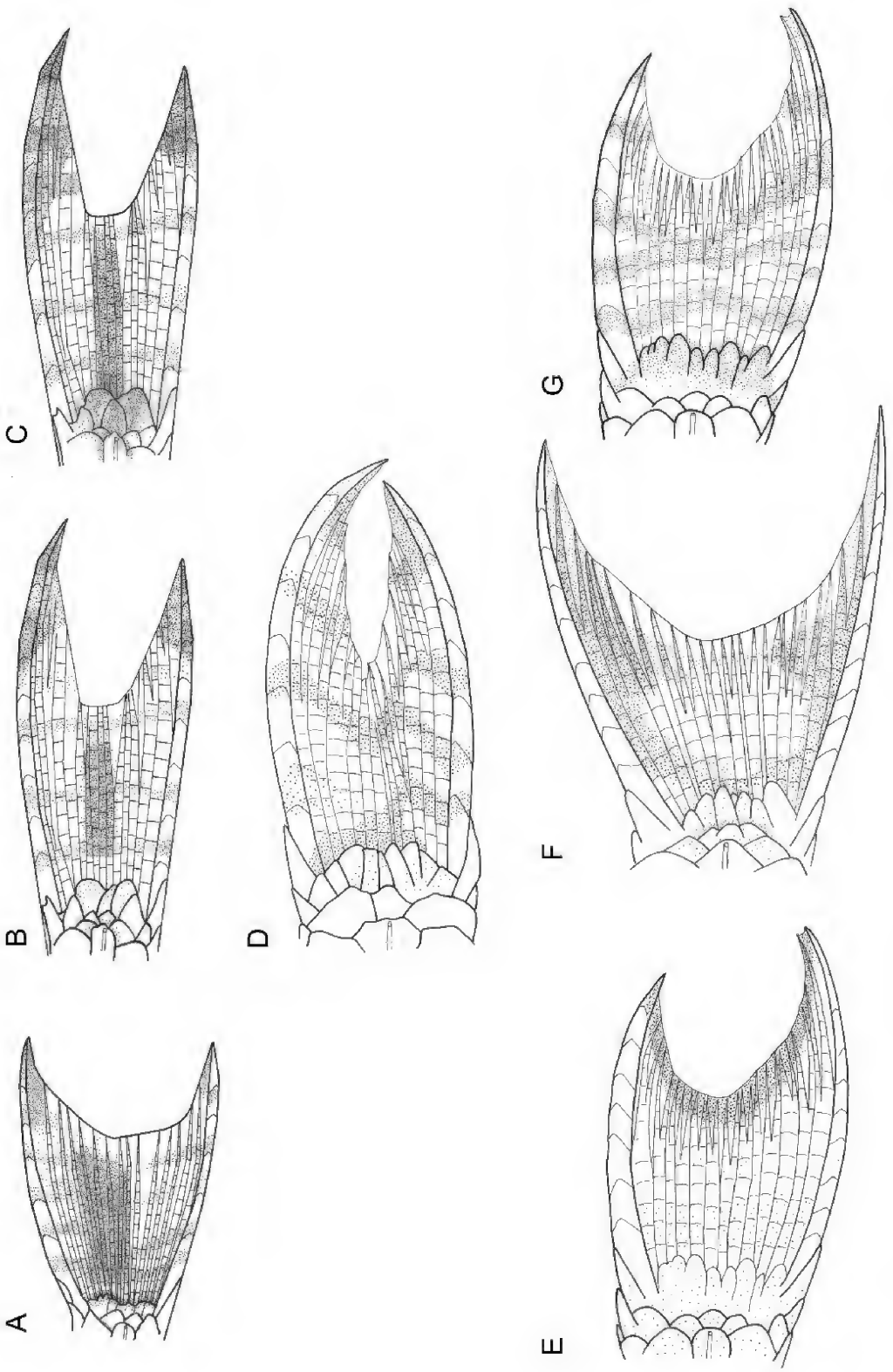

Fig. 17. Pigmentation pattern of the caudal fin: **A**, *H. thoracatum*; **B**, *H. psilogaster*; **C**, *H. guianense*; **D**, *H. gulare*; **E**, *H. steindachneri*; **F**, *H. elongatum*; **G**, *H. machadoi*.

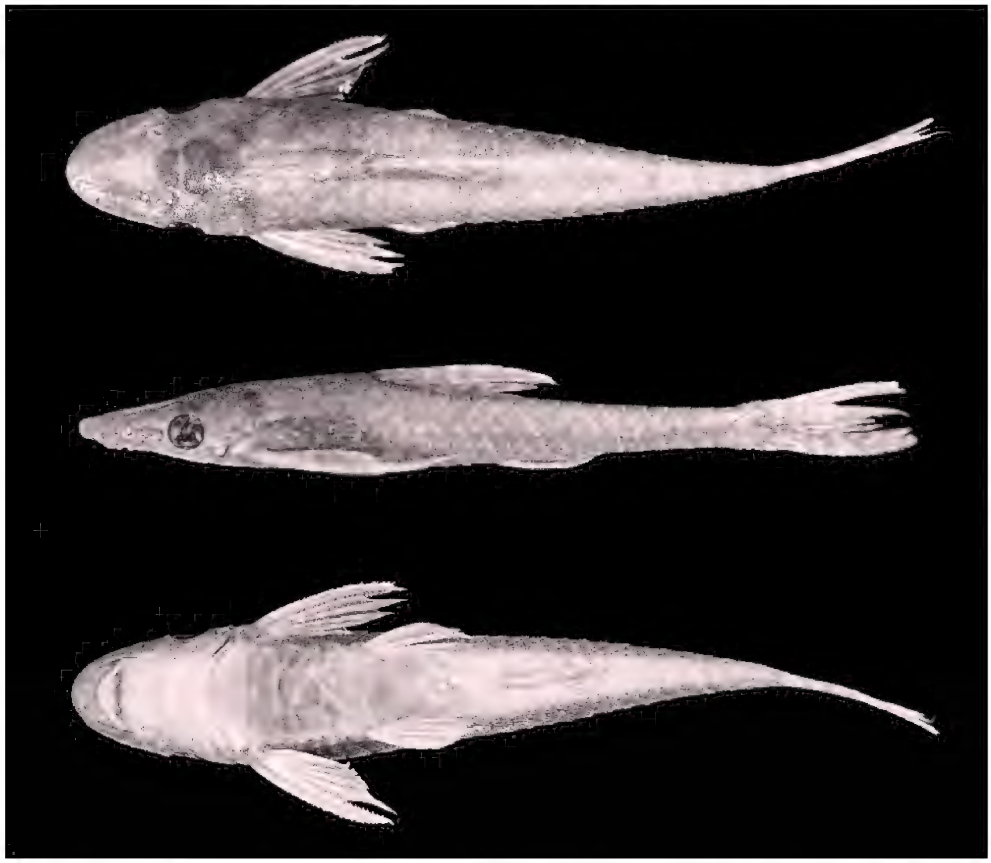

Fig. 18. *Hypoptopoma baileyi*, holotype, AMNH 39828, 38.9 mm SL female, in dorsal, lateral, and ventral views.

Itenez, 3 km SE Costa Marques, Brazil; AMNH 39788 (8 ♀ + 1 ♂, 3 cs, 26.6–33.9 mm SL) Río Itenez, 9 km SE Costa Marques, Brazil; AMNH 39841 (4 ♀, 27.7–32.9 mm SL) Oxbow Río Itenez, 9 km SE Costa Marques, Brazil; AMNH 39861 (27 ♀ + 7 ♂, 24.9–41.5 mm SL) Río Itenez, 9 km SE Costa Marques, Brazil; SIUC 30815 (12 ♀, 29.7–35.4 mm SL) Río Matos in Estación Biológica del Beni (bridge nearest entrance, 6 km E of EBB on road to San Ignacio). **Santa Cruz**: AMNH 229206 (2 ♀, 29.7–31.8 mm SL) Noel Kempff Mercado Nacional Park, Río Paucerna, about 500 m upstream from mouth at Río Itenez; AMNH 229310 (2 ♀, 28.5–33.3 mm SL) Noel Kempff Mercado Nacional Park, Río Itenez, Bahía Piuba at mouth; AMNH 229353 (17 ♀ + 2 ♂, 25.1–37.6 mm SL) Noel Kempff Mercado Nacional Park, Río Itenez, beach about 200 m upstream from Bahía Agua Blanca; CBF 2859 (1 ♀ + 1 ♂, 33.7–43.7 mm SL) Guarayos, Perseverancia, Río Negro.

DIAGNOSIS: *Hypoptopoma baileyi* is distinguished from all congeners except *H. muzuspi* by having trunk pigmentation in the form of a lateral band that is progressively darker along medial, midventral, and ventral series of plates, and a caudal-fin pigmentation pattern formed by 6–8 narrow dark brown bars and a dark spot at the base of the lower lobe. *Hypoptopoma baileyi* is distinguished

TABLE 1
Morphometric and Meristic Data for *Hypoptopoma baileyi*
Holotype: AMNH 39828. Paratype: AMNH 243579.

	Holotype	*N*	Range		Mean	sd
Standard length	38.9	30	29.6	43.2	36.3	4.03
PERCENT OF STANDARD LENGTH						
Predorsal length	42.9	30	41.8	45.2	43.4	0.76
Head length	31.7	30	30.1	33.9	32.3	1.00
Body depth	13.7	30	12.6	14.9	13.9	0.62
Dorsal-fin spine length	28.6	25	23.8	28.4	26.0	1.23
Trunk length	47.8	30	44.3	49.1	46.5	1.14
Pectoral-fin spine length	22.1	30	20.8	24.7	23.2	0.95
Abdominal length	17.1	30	13.7	17.0	15.3	0.91
Caudal-peduncle length	34.9	30	33.7	37.5	35.7	1.00
Caudal-peduncle depth	6.1	30	5.7	6.7	6.2	0.23
Caudal-fin base depth	5.4	29	4.2	6.3	5.3	0.41
Head depth	13.0	30	11.2	13.5	12.8	0.57
Snout length	16.2	30	15.3	17.3	16.3	0.44
Horizontal eye diameter	5.9	30	5.0	6.5	5.9	0.44
Least orbit-naris distance	1.8	30	1.4	2.5	1.9	0.22
Dorsal interobital distance	15.3	30	14.5	16.4	15.6	0.45
Ventral interobital distance	15.7	30	15.8	18.6	17.3	0.63
Cleithral width	20.1	30	18.6	21.6	20.3	0.58
Head width	17.3	30	16.9	19.1	18.2	0.51
Interpelvic distance	10.9	29	9.0	12.1	10.5	0.73
PERCENT OF HEAD LENGTH						
Body depth	43.3	30	38.5	47.5	43.1	1.91
Head depth	41.1	30	35.7	44.0	39.6	2.07
Snout length	51.2	30	47.9	54.1	50.5	1.43
Horizontal eye diameter	18.6	30	16.1	20.4	18.1	1.05
Least orbit-nare distance	5.6	30	4.2	8.2	6.0	0.78
Dorsal interobital distance	48.3	30	45.5	52.7	48.4	1.94
Ventral interobital distance	49.4	30	48.7	56.7	53.6	1.81
Cleithral width	63.6	30	59.4	67.5	62.9	2.15
Head width	54.5	30	53.7	60.9	56.4	1.69
Interpelvic distance	34.3	29	27.7	36.9	32.5	2.20
PERCENT OF CLEITHRAL WIDTH						
Snout	80.6	29	75.5	85.4	80.4	2.38
LATERAL SERIES OF PLATES						
Dorsal series	20	30	19	21	20	0.5
Middorsal series	4	30	3	4	4	0.5
Medial series	23	30	22	23	23	0.3
Midventral series	13	30	12	14	13	0.4
First midventral series plates	4	30	4	4	4	0.0
Ventral series	20	30	19	21	20	0.4
ABDOMINAL SERIES OF PLATES						
Right lateral series	8	29	4	8	6	1.3
Left lateral series	4	29	3	9	5	1.4
Medial lateral series	6	29	3	8	6	1.3
TEETH						
Premaxillary teeth	19	30	14	22	18	2.0
Dentary teeth	16	30	11	18	15	1.9

from *H. muzuspi* by having preopercle reduced, not reaching hyomandibular-opercle condyle (vs. preopercle not reduced, reaching to hyomandibular-opercle condyle) and absence of canal in preopercle (vs. presence of canal in the preopercle) (fig. 14A).

DESCRIPTION: Morphometric and meristic data presented in table 1. Body size relatively small, moderately elongate, and depressed; greatest body depth at dorsal-fin origin. Dorsal profile of head and body from tip of snout to dorsal-fin origin straight, slightly angled dorsally at anterior supraoccipital tip; straight from dorsal-fin origin to anteriormost procurrent caudal-fin ray. Head moderately depressed, almost as wide as cleithral width; lateral process of lateral ethmoid dorsally not visible. Snout slightly rounded in dorsal view, concave at region anterior to naris. Posterior surface of bony pit of nasal organ gradually inclined. Body cross section between pectoral- and pelvic-fin origins ovoid to transversely depressed, progressively compressed posterior to anal-fin base.

Eyes moderately large, positioned slightly closer to posterior tip of compound pterotic than to tip of snout. Ventral margin of orbit located close to ventral surface of head. Dorsal interorbital distance shorter than ventral interorbital distance.

Total plates in lateral medial series 22–23 (23). Dorsal series 19–21 (20); middorsal series 3–4 (4); midventral series 12–14 (13), with four plates anterior of first plate of ventral series; ventral series 19–21 (20). Second plate of midventral series contacting single plate of medial series.

Abdomen covered by paired series of lateral sickle-shaped plates, with unequal number of plates between left and right side series, 3–9 each; medial series of 3–8 (6) roughly squared plates; anterior azygous plate absent; medial series occasionally absent, in which case paired series make contact along midline in fully developed individuals. Single anal plate present. Thoracic plates absent. Preopercular canal absent. Posterolateral margin of canal-bearing plate and lateral margin of fourth infraorbital smooth; pore between canal-bearing ventral plate and fourth infraorbital absent.

Small odontodes evenly distributed on head, roughly arranged in closely spaced longitudinal lines. Odontodes ventral to tip of snout slightly enlarged. Lamina of trunk plates with longitudinal rows of odontodes, becoming progressively smoother ontogenetically; largest specimens maintain longitudinal rows dorsal to lateral-line canal, rows otherwise absent; distinct column of marginal odontodes on posterior plate border in mature adults.

Total vertebrae 27–28; ribs present. Premaxillary teeth 14–22; dentary teeth 11–18. Maxillary barbels short, not reaching to anterior margin of ventral canal-bearing plate.

Dorsal-fin origin located slightly posterior of vertical through pelvic-fin origin. Depressed dorsal fin reaching to vertical through midpoint of anal-fin length. Pectoral fin reaching to vertical through midpoint along pelvic-fin spine. Depressed pelvic fin close or reaching to plate anterior to anal-fin spine. Extension of serrae along length of pectoral-spine margin, except for short basal segment; serrae of oblique type. Pelvic fin short, unbranched slightly shorter than first branched rays. Depressed fin reaching to anus, not reaching to insertion of anal-fin spine. Caudal fin forked. Adipose fin absent.

COLOR IN ALCOHOL: Ground color tan to pale ochre. Melanophores light to dark brown on trunk and particularly clustered at base of plates resulting in mottled appearance. Melanophores slightly more concentrated on compound pterotic dorsal to swimbladder capsule, anterior half of supraoccipital, frontals, plate anterior to naris, lateral rostral plates on snout, on posterior half of lip surface, band on maxillary barbel, anterior half of branchiostegal membrane, and posterior tip of naris flap. Melanophores scattered or absent on dorsal surface of mesethmoid, anterior rostral plate, and narrow band anterior to epiphysial branch of supraorbital canal in frontal. Deep-lying melanophores arranged in narrow transverse bands posterior to dorsal-fin base, noncoincident with posterior margin of plates. Midlateral stripe situtated along medial, midventral, and ventral series of plates, progressively less pigmented toward ventral surface of body, which is mostly unpigmented except for scattered melanophores on posterior portion of trunk, soft tissue along base of pectoral and anal fins, anterolateral

margin of cleithra and posterior tip of cleithral process, ventral canal-bearing plate, and lateral portions of lateral abdominal series. Paired and unpaired fins with relatively numerous narrow dark brown bands. Series of lanceolate plates at base of caudal fin and small posteriormost plate of trunk medial series more densely pigmented with black melanophores. Last 1–2 posteriormost plates of dorsal and ventral trunk series less pigmented, whitish. Upper and lower marginal and branched rays of caudal-fin with 7–10 bands of brown melanophores, with slightly darker area at base of lower lobe.

SEXUAL DIMORPHISM: Male urogenital papilla elongate, slender papilla covered by flap-like anus. Males with patch of tightly arranged small odontodes on second, third, and fourth plates of ventral series, lateral to urogenital papilla. Female anus tubular, without separate urogenital papilla. In females, size and arrangement of odontodes on plates lateral to anus similar to adjacent plates, without distinct patch of differentially arranged odontodes.

DISTRIBUTION: Río Iténez, in the upper Rio Madeira basin, along the border between Bolivia and Brazil (fig. 19).

ETYMOLOGY: The specific epithet *baileyi* is a patronym honoring Reeve M. Bailey (1911–2000), who collected the specimens of the new species in 1964 during an expedition of the AMNH to the Río Itenez.

Hypoptopoma guianense Boeseman, 1974
Figure 20, table 2

Hypoptopoma guianense Boeseman, 1974: 259, 1 fig., 1 pl., tables 1–2 (original description; Surinam: left tributary of the Nickerie river, a few km upstream from the Stondansi Falls).—Isbrücker, 1980: 87 (list of loricariid species).—Nijssen et al., 1982: 54 (catalog of type specimens at Zoölogische Museum Amsterdam).—Ferraris and Vari, 1992: 27 (catalog of type specimens at NMNH).—Eschmeyer and Ferraris, 1998: 688 (catalog of fishes).—Machado Allison et al., 2000: 17 (Venezuela: Río Cuyuní).—Isbrücker, 2002: 28 (list of loricariid species).—Schaefer, 2003: 323 (list of hypoptopomatine species).—Ferraris, 2007: 250 (list of catfish species).—Vari et al., 2009: 38 (list of freshwater fishes of Guiana Shield).

HOLOTYPE: RMNH 26919 (61.5 mm SL) Suriname, left tributary of the Nickerie River, a few kilometers upstream from the Stondansi Falls; collected by H. Boeseman, 30 January 1971 (not seen).

PARATYPES: RMNH 26922 (1 ♀ + 3 ♂, 47.0–56.0 mm SL) Suriname, Nickerie River, below Blanche Marie Falls; collected by H. Boeseman, 11 February 1971. USNM 213484 (2 ♀, 48.9–51.6 mm SL) Surinam, left tributary creek upper Nickerie River; collected by H. Boeseman, 30 January 1971.

OTHER MATERIAL EXAMINED: Guyana, **Cuyuni-Mazaruni**: INHS 49274 (1 ♀, 27.6 mm SL) 1.5 mi. SW Rockstone [Essequibo river]; INHS 49366 (1 juvenile, 29.3 mm SL) 31.9 mi. SSW Rockstone. **Potaro-Siparuni**: INHS 49402 (1 juvenile, 23.3 mm SL) Essequibo River drainage, Tumatumari Cataract, S bank, below old hydroelectric plant. **Upper Demerara-Berbice**: AMNH 13341 (2 ♀, 35.5–40.7 mm SL) Malali; AMNH 13666 (1 ♀ + 1 ♂, 38.5–39.2 mm SL) Rockstone, Essequibo River drainage; AMNH 220509 (2 ♀, 46.3–47.5 mm SL) Essequibo River drainage; INHS 49660 (10 ♀ + 2 juveniles, 25.2–63.4 mm SL) Rockstone. **Upper Takutu–Upper Essequibo**: BMNH 1983.7.26:12–28 (16 ♀ + 1 ♂, 2 cs, 28.5–47.8 mm SL) Rupununi River; BMNH 1983.26:49–54 (6 ♀, 37.2–46.1 mm SL) Rupununi River, Kamarang; FMNH 69962 (3 ♀, 37.3–42.1 mm SL) Moco Moco River.

DIAGNOSIS: *Hypoptopoma guianense* is distinguished from all congeners by the presence of an elongated dark spot along the median caudal-fin branched rays, involving the lanceolate plates at the base of the fin. The spot is typically extended over an equal number of branched rays of both the upper and lower lobes and along more than two-thirds of the ray length (fig. 17C).

DESCRIPTION: Morphometric and meristic data presented in table 2. Body moderately elongate and low. Dorsal profile of head and body slightly convex from tip of snout to dorsal-fin origin; straight from dorsal-fin origin to anteriormost caudal-fin procurrent ray. Head moderately depressed and narrow. Lateral process of lateral ethmoid dorsally not visible. Snout rounded to slightly spatulate in dorsal view; smoothly rounded in dorsal view; dorsally variably concave anterior to naris. Posterior surface of bony pit of nasal organ sharply inclined. Body cross

Fig. 19. Drainage map of South America showing distribution of *H. baileyi* (dots + circle), *H. guianense* (triangles), and *H. psilogaster* (squares). Open symbols designate type localities; some symbols represent more than one locality record.

section between pectoral- and pelvic-fin origins horizontally ovoid, posterior to dorsal fin changing from ovoid to rounded, posterior to adipose-fin base progressively compressed.

Eyes moderately large, positioned closer to posterior tip of compound pterotic than to tip of snout. Ventral margin of orbit located close to ventral surface of head. Dorsal interorbital distance shorter than ventral interorbital distance.

Total plates in lateral medial series 23–24 (23). Dorsal series 20–21 (20); middorsal

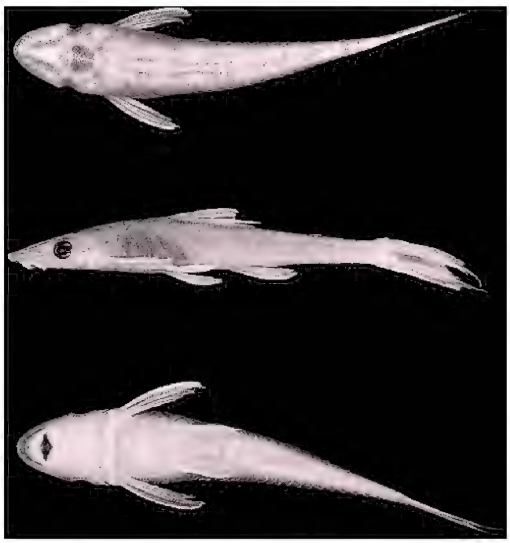

Fig. 20. *Hypoptopoma guianense*, paratype, RMNH 26922, in dorsal, lateral, and ventral views.

series 3–4 (4); midventral series 13–15 (13), with four plates (rarely five) anterior of first plate of ventral series; ventral series 19–21 (20). Second plate of midventral series contacting single plate of medial lateral series.

Abdomen covered by paired series of lateral sickle-shaped plates, with unequal number of plates between left and right series, 4–10 each; medial series of 3–8 (5) roughly squared plates; anterior azygous plate absent. Single anal plate present. Thoracic plates absent. Preopercular canal absent. Posterolateral margin of canal-bearing plate and lateral margin of fourth infraorbital smooth; pore between canal-bearing ventral plate and fourth infraorbital absent.

Small odontodes evenly distributed on trunk and head. Odontodes ventral and dorsal to tip of snout not arranged in aligned series. No odontode-free discontinuity between ventral and dorsal odontodes; odontodes dorsal to tip of snout slightly larger than those on head. Lamina of trunk plates with longitudinal lines of odontodes, becoming progressively smoother ontogenetically; distinct column of marginal odontodes on posterior plate border in mature adults.

Total vertebrae 27. Premaxillary teeth 21–26 (23), dentary teeth 17–24 (20). Maxillary barbels short; reaching to anterior margin of ventral canal-bearing plate in adults.

Dorsal-fin origin located slightly posterior of vertical through pelvic-fin origin. Depressed dorsal fin reaching to vertical through midpoint of anal-fin base length. Pectoral fin reaching to vertical through midpoint of pelvic-fin length. Extension of serrae along pectoral spine margin except for short basal segment; serrae of oblique type. Pelvic fin short, 2–3 longest branched rays slightly longer than spine. Depressed fin reaching to plate anterior to anal-fin spine. Caudal-fin margin forked; upper and lower lobes equal and elongate. Adipose fin variably present; when present, minute.

COLOR IN ALCOHOL: Ground color tan and pale ochre. Melanophores dark brown, on trunk and head clustered resulting in mottled appearance; distinct light spot dorsally on each lateral rostral plate. Melanophores slightly more concentrated on anterior surface of lip, along narrow area among compound pterotic, cleithral process and dorsal tip of opercle, at base of dorsal and pectoral fins. Deep-lying melanophores arranged in narrow transverse bands posterior to dorsal-fin base, noncoincident with posterior margin of plates. Midlateral stripe situated along trunk variably defined. Ventral surface of body mostly unpigmented except for scattered melanophores on posterior portion of trunk, soft tissue along base of pectoral and anal fins, anterolateral margin of cleithra, and lateral portions of lateral abdominal series. Paired and dorsal fins with dark brown bars. Caudal-fin bars variable defined (fig. 17C). Presence of elongated dark spot along middle caudal-fin branched rays; spot typically extending over equal number of upper- and lower-lobe rays and along more than two-thirds of ray length; spot connected to lanceolate plates at base of fin. Tip of upper and lower lobes slightly pigmented with reddish-brown melanophores.

SEXUAL DIMORPHISM: Male urogenital papilla well developed, pointed, joined at base to anterior flaplike anus. Males with patch of tightly arranged small odontodes oriented as a swirl, variably covering first to fourth plates of ventral series, lateral to urogenital papilla. Female anus tubular,

TABLE 2
Morphometric and Meristic Data for *Hypoptopoma guianense*
Paratypes: RMNH 26922. Nontypes: AMNH 13666, 220509; BMNH 1983.7.26:12–28; FMNH 69962; INHS 49960.

	N	Range		Mean	sd
Standard length	40	37.1	56.0	44.7	5.52
PERCENT IN STANDARD LENGTH					
Predorsal length	40	41.0	45.9	43.0	1.13
Head length	40	29.3	33.8	31.8	1.28
Body depth	38	12.9	15.9	14.6	0.67
Dorsal-fin spine length	18	22.6	30.1	27.3	1.79
Trunk length	40	43.7	49.8	47.1	1.34
Pectoral-fin spine length	36	21.4	24.3	22.8	0.70
Abdominal length	40	14.5	17.6	16.1	0.86
Caudal-peduncle length	40	34.3	39.9	37.2	1.21
Caudal-peduncle depth	40	4.8	6.8	6.3	0.37
Caudal-fin base depth	35	5.3	7.1	6.0	0.44
Head depth	37	11.8	14.4	12.8	0.52
Snout length	40	15.6	18.0	17.0	0.58
Horizontal eye diameter	40	4.9	6.4	5.8	0.31
Least orbit-naris distance	40	1.9	3.0	2.4	0.25
Dorsal interobital distance	40	14.2	16.3	15.3	0.58
Ventral interobital distance	40	16.3	18.5	17.3	0.57
Cleithral width	40	19.1	21.4	20.1	0.58
Head width	40	17.3	19.2	18.4	0.52
Interpelvic distance	36	7.9	10.4	9.1	0.68
PERCENT OF HEAD LENGTH					
Body depth	38	39.9	50.9	45.9	2.77
Head depth	37	35.8	47.0	40.3	2.62
Snout length	40	50.6	56.3	53.5	1.72
Horizontal eye diameter	40	16.7	20.4	18.4	0.85
Least orbit-naris distance	40	6.2	9.7	7.5	0.87
Dorsal interobital distance	40	43.7	50.9	48.1	1.96
Ventral interobital distance	40	51.0	56.9	54.3	1.74
Cleithral width	40	59.7	67.5	63.3	1.93
Head width	40	54.2	60.9	57.9	2.21
Interpelvic distance	36	23.8	32.0	28.6	2.33
PERCENT OF CLEITHRAL WIDTH					
Snout	27	81.0	88.9	84.3	2.15
LATERAL SERIES OF PLATES					
Dorsal series	37	20	21	20	0.5
Middorsal series	37	3	4	4	0.2
Medial series	37	23	24	23	0.5
Midventral series	37	13	15	13	0.5
First midventral series plates	37	4	5	4	0.2
Ventral series	37	19	21	20	0.5
ABDOMINAL SERIES OF PLATES					
Right lateral series	11	4	10	6	1.9
Left lateral series	11	5	10	7	1.6
Medial series	9	3	8	5	1.4
TEETH					
Premaxillary teeth	30	21	26	23	1.4
Dentary teeth	30	17	24	20	1.8

without separate urogenital papilla. In females, size and arrangement of odontodes on plates lateral to anus similar to adjacent plates, without distinct patch of differentially arranged odontodes.

DISTRIBUTION: Known from of the basins of the Essequibo (Guyana) and Nickerie (Surinam) rivers (fig. 19).

TAXONOMIC REMARKS: Prior to the present revision, *Hypoptopoma guianense* was the only nominal species of *Hypoptopoma* to be established on the basis of a relatively large number of individuals (approximately 31). The species is most similar to *H. psilogaster* Fowler, 1915, which has been reported from the Ríos Ampiyacu, Itaya, Nanay, Napo, and Yaguas in Amazonian Peru. Valid taxonomic status of both species is supported on the basis of differences in the caudal-fin pigmentation: both species possess an elongate spot along the middle caudal-fin branched rays, but in *H. guianense* the spot is continuous with the dark spot on the lanceolate plates, versus discontinous in *H. psilogaster*. Further differences are shown in an analysis of the overall morphometric variation among *H. guianense*, *H. psilogaster*, and *H. thoracatum*. In a sheared principal component analysis on 18 distance variables (fig. 21; table 3), the scatter plot of the component scores on sheared PC2 and PC3 shows near complete separation among the three species. The second and third components represent 3.1% and 0.9% of the total morphometric variance, respectively. The morphometric variance explained by PC2 reflects differences in the elongation of the body (caudal-peduncle length, trunk length, caudal-peduncle depth); likewise, PC3 appears to reflect differences in head width at the level of the eyes (least distance between orbit and naris).

Hypoptopoma psilogaster Fowler, 1915
Figure 22, table 4

Hypoptopoma psilogaster Fowler, 1915: 235, fig. 9 (original description; Peruvian Amazon).—Fowler, 1915: 237 (assigned to subgenus *Hypoptopoma*).—Fowler, 1939: 286 (Peru: occurrence in Rio Ucayali basin, Nauta).—Fowler, 1945: 100 (list of freshwater fishes of Peru).—Fowler, 1954: 126, fig. 729 (list of freshwater fishes of Peru).—Boeseman, 1974: 264–265 (list of nominal species of *Hypoptopoma*).—Isbrücker, 1980: 88 (list of loricariid species).—Böhlke, 1984:124 (catalog of type specimens at ANSP).—Ortega and Vari, 1986: 17 (list of fishes of Peru; Carachama).—Eschmeyer and Ferraris, 1998: 1390 (catalog of fishes).—Isbrücker, 2002: 28 (list of loricariid species).—Schaefer, 2003: 323 (list of hypoptopomatine species).—Ferraris, 2007: 250 (list of catfish species).

HOLOTYPE: ANSP 21922 (juvenile, 51.0 mm SL) Peruvian Amazon; collected by J. Orton, 1873.

OTHER MATERIAL EXAMINED: PERU, **Loreto**: ANSP 21921 (1 ♀, 45.6 mm SL) Peruvian Amazon; ANSP 138868 (5 ♀, 33.4–66.5 mm SL) Río Nanay, vicinity of Iquitos, well above Morona Coché (coché 9 m. above Río Amazonas); ANSP 138869 (2; 35.5–39.0 mm SL) Río Nanay, vicinity of Iquitos just above Coché Morona (above 9 m. Río Amazonas); ANSP 138871 (1 ♂ + 3 juveniles, 1 cs, 33.4–66.5 mm SL) Río Nanay, vicinity of Iquitos, Morona Coché outlet (about 9 m. above Río Amazonas); ANSP 178335 (2 ♀, 32.6–41.0 mm SL) Río Itaya at bridge on Iquitos-Nauta highway, approx. 25 miles SSW of Iquitos; CAS 134254 (1 ♀, 32.8 mm SL) Río Ampiyacu; CAS 134255 (1 ♀, 38.1 mm SL) Río Ampiyacu; INHS 39826 (6 ♀, 44.0–70.1 mm SL) Río Nanay, Miz Playa, about 1 hr by canoe upstream from Santa Clara; INHS 44076 (9 ♀ + 2 ♂, 38.9–53.9 mm SL) Río Nanay, Pampa Chica, 4.5 km W center of Iquitos; INHS 44125 (2 ♀, 42.8–48.5 mm SL) Río Napo and Quebrada, Mazán, 33.3 km NE Iquitos; MUSM 7655 (1 ♀ + 1 ♂, 49.7–50.8 mm SL) Río Nanay, Maynas, Iquitos; NRM 18000 (1 ♀, 35.6 mm SL) Río Nanay dr., Caño Puñuisiqui; NRM 47511 (5 ♀, 28.9–35.8 mm SL) Río Nanay dr., small tahuampa cocha on left bank, second left bend above Mishana; SIUC 23560 (83 ♀ + 14 ♂, 5 cs, 28.8–55.9 mm SL) Maynas, Río Nanay at Santa Clara, NW of Iquitos; SIUC 28015 (3 ♀ + 1 ♂, 32.8–48.7 mm SL) Río Nanay at Santa Clara; SIUC 28180 (2 ♀, 35.0–40.2 mm SL) Río Nanay, Pamachica Beach in Iquitos; SIUC 28997 (3 ♀, 29.9–44.0 mm SL) Río Nanay, Miz Playa; SIUC 29489 (1 ♀, 46.5 mm SL) Miz Playa just upstream from Santa Clara, 13.9 km from Iquitos; SIUC 29645 (4 ♀ + 2

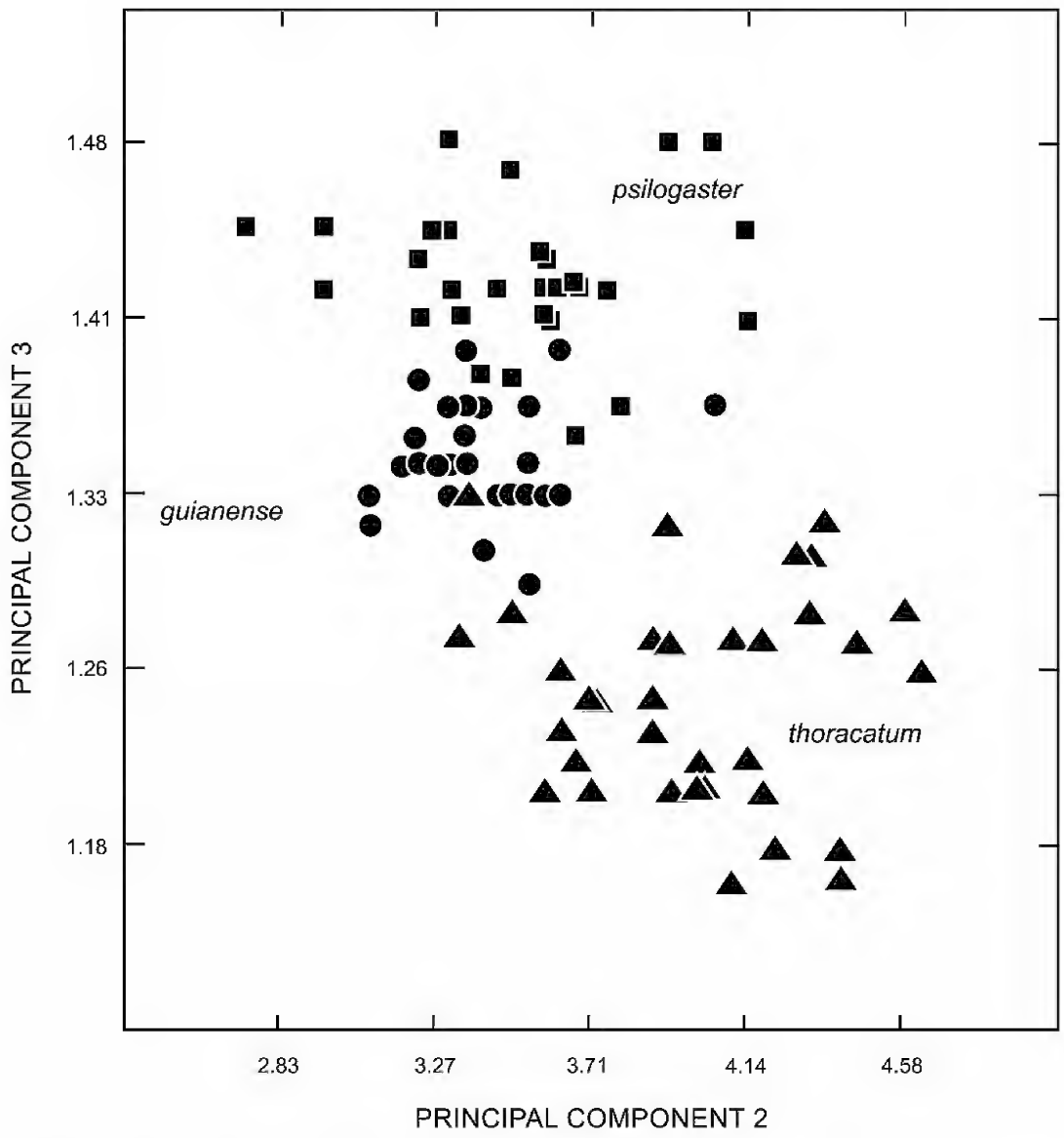

Fig. 21. Plot of scores along sheared second and third principal components from the morphometric analysis of body shape among *H. guianense*, *H. psilogaster*, and *H. thoracatum*.

♂, 38.4–56.3 mm SL) Maynas, Río Nanay, Pampachica Beach 4.5 km from Iquitos center; SIUC 67367 (2 ♀, 44.6–51.9 mm SL) Maynas, Río Itaya and Quebrada Mazana, 11 km from Iquitos center; SU 60557 (1 ♀, 41.3 mm SL) Rio Yaguas Yacu; USNM 284882 (2 ♀, 47.3–47.3 mm SL) Río Nanay at Nanay beach, W of Iquitos; USNM 284876 (1 juvenile, 47.2 mm SL) Río Nanay approximately 20 km upstream of mouth; USNM 284883 (2 ♀, 30.7–30.7 mm SL) Río Nanay approximately 20 km upstream of mouth.

DIAGNOSIS: *Hypoptopoma psilogaster* is distinguished from all congeners by the presence of an elongated dark spot along the middle caudal-fin branched rays, not involving the lanceolate plates at the base of the fin; the spot is typically extended over

TABLE 3
Sheared Principal Component Loadings from the Morphometric Analysis of Head and Trunk of *Hypoptopoma guianense*, *H. psilogaster* and *H. thoracatum*

	PC2	PC3
Standard length	0.294474	−0.059905
Predorsal length	0.112435	0.009817
Head length	0.065723	0.016092
Body length	0.012126	0.024379
Trunk length	0.454835	−0.063438
Pectoral-fin spine length	0.051174	0.059752
Abdominal length	0.156445	−0.005617
Caudal-peduncle length	0.507476	−0.084413
Caudal-peduncle depth	−0.324750	0.214320
Caudal-fin base depth	−0.137501	0.530638
Head depth	−0.052179	0.092752
Snout length	0.059721	0.036302
Horizontal eye diameter	0.097054	−0.069006
Least orbit-naris distance	−0.362217	−0.786168
Dorsal interobital distance	−0.234806	0.070410
Ventral interobital distance	−0.137046	0.062582
Cleithral width	−0.149253	0.053309
Head width	−0.160830	0.093965

equal number of upper- and lower-lobe branched rays and along more than two-thirds of the ray length (figs. 17B, 23).

DESCRIPTION: Morphometric and meristic data presented in table 4. Body elongate, moderately depressed, greatest body depth at dorsal-fin origin, trunk most shallow at caudal peduncle anterior to caudal fin. Dorsal profile of head and body straight from tip of snout to dorsal-fin origin; straight from dorsal-fin origin to anteriormost procurrent caudal-fin ray. Head moderately depressed and narrow; lateral process of lateral ethmoid not visible dorsally. Snout rounded in dorsal view; dorsally smoothly round, slightly concave to flat anterior to naris. Body cross section between pectoral- and pelvic-fin origin horizontally ovoid, vertically ovoid posterior to dorsal fin, progressively compressed posterior to adipose fin.

Eyes moderately large, positioned slightly closer to posterior tip of compound pterotic than to tip of snout. Ventral margin of orbit located close to ventral surface of head. Dorsal interorbital distance shorter than ventral interorbital distance.

Total plates in lateral medial series 24–26 (24); when total plates 25 or 26, posteriormost plate very small, with canal not reaching to posterior border of plate. Dorsal series 20–22 (21); middorsal series 3–4 (4); midventral series 13–14 (13), with 4–5 (4) plates anterior of first plate of ventral series; ventral series 20–22 (21). Second plate of midventral series contacting a single plate of medial lateral series.

Abdomen covered by paired series of lateral sickle-shaped plates, with unequal number of plates between left and right series, 6–10 each; medial series of 6–10 (8) roughly squared plates; anterior azygous plate absent; medial series occasionally absent, in which case paired series make contact along midline in fully developed individuals. Single anal plate present. Thoracic plates absent. Preopercular canal absent. Posterolateral margin of canal-bearing plate and lateral margin of fourth infraorbital smooth; pore between canal-bearing ventral plate and fourth infraorbital absent.

Small odontodes evenly distributed on head. Odontodes ventral and dorsal to tip of snout not arranged in aligned series. No odontode-free discontinuity between ventral and dorsal odontodes; odontodes dorsal to tip of snout slightly larger than those on head. Lamina of trunk plates bearing longitudinal rows of odontodes, plates becoming progressively smoother ontogenetically; distinct column of marginal odontodes on posterior plate border in mature adults.

Total vertebrae 28. Premaxillary teeth 19–26 (22), dentary teeth 16–24 (19). Maxillary barbels short; almost reaching to or slightly surpassing anterior margin of ventral canal-bearing plate in adults.

Dorsal-fin origin located at vertical through pelvic-fin origin. Depressed dorsal fin reaching to vertical through midpoint of anal-fin base. Pectoral fin reaching to vertical through posterior half of pelvic-fin length. Extension of serrae along pectoral spine margin, except for short basal segment; serrae of oblique type; teeth of serrae progressively smaller toward distal end of spine. Pelvic fin short, two longest branched rays slightly longer than spine. Depressed fin reaching to plate anterior to anal-fin spine. Caudal-fin margin forked; upper and lower lobes equal and elongate. Adipose fin present.

Fig. 22. *Hypoptopoma psilogaster*, holotype, ANSP 21922, 51.0 mm SL, juvenile, in dorsal, lateral, and ventral views.

COLOR IN ALCOHOL: Ground color tan and pale ochre. Melanophores dark brown, clustered on trunk and head resulting in mottled appearance. Melanophores slightly more concentrated dorsally on head, narrow area among compound pterotic, cleithral process and opercle, and at base of dorsal fin. Deep-lying melanophores slightly more concentrated along midline posterior to dorsal-fin base. Midlateral stripe situated mostly along medial series of trunk plates. Ventral surface of body mostly unpigmented, except for scattered melanophores on soft tissue along base of pectoral-fin branched rays and anterior surface of lip. Paired and dorsal fins with dark brown bands. Black melanophores slightly more concentrated over lanceolate plates. Caudal-fin bars variable defined. Presence of elongated dark spot along middle caudal-fin branched rays; spot typically extending over equal number of upper- and lower-lobe branched rays and along more than two-thirds of ray length; spot not distinctly connected to lanceolate plates at base of fin (fig. 17B). Tip of upper and lower lobes pigmented with dark melanophores.

SEXUAL DIMORPHISM: Male urogenital papilla short and conical, covered by anterior flaplike anus. Males with patch of tightly arranged small odontodes, variably covering first to fourth plates of ventral series, lateral to urogenital papilla. Males with poorly developed soft-tissue flap along posterior margin of pelvic spine. Female anus tubular,

TABLE 4
Morphometric and Meristic Data for *Hypoptopoma psilogaster*
Holotype: ANSP 21922. Nontypes: ANSP 138868; INHS 39826, 44076, 44125; SIUC 23560, 29645.

	Holotype	*N*	Range		Mean	sd
Standard length	51.1	30	33.4	70.1	50.6	8.65
PERCENT IN STANDARD LENGTH						
Predorsal length	39.8	30	39.1	42.8	40.8	0.95
Head length	30.3	30	26.6	32.0	29.9	1.20
Body depth	14.4	30	12.5	16.4	14.1	0.78
Dorsal-fin spine length	—	26	24.9	28.7	26.6	1.14
Trunk length	50.6	30	47.4	51.0	49.4	1.07
Pectoral-fin spine length	22.1	30	21.0	23.8	22.0	0.64
Abdominal length	15.8	30	14.0	17.4	15.1	0.81
Caudal-peduncle length	40.3	30	37.8	41.1	39.6	0.95
Caudal-peduncle depth	6.2	30	5.0	6.6	5.6	0.40
Caudal-fin base depth	5.8	30	4.7	6.4	5.5	0.41
Head depth	13.6	30	10.8	13.3	11.8	0.62
Snout length	16.6	30	15.0	17.6	16.2	0.63
Horizontal eye diameter	5.4	30	4.9	6.8	5.5	0.41
Least orbit-naris distance	2.8	30	1.8	2.6	2.2	0.23
Dorsal interobital distance	16.0	30	12.7	15.5	14.2	0.62
Ventral interobital distance	17.7	30	14.9	17.1	16.1	0.56
Cleithral width	20.2	30	17.3	20.3	18.7	0.67
Head width	18.4	30	15.6	18.1	17.1	0.57
Interpelvic distance	8.2	30	7.1	9.9	8.8	0.66
PERCENT OF HEAD LENGTH						
Body depth	47.5	30	39.2	55.5	47.1	3.76
Head depth	44.9	30	35.2	47.0	39.8	2.79
Snout length	54.8	30	49.5	56.8	54.4	1.74
Horizontal eye diameter	17.7	30	16.5	21.4	18.4	1.12
Least orbit-naris distance	9.3	30	5.7	8.9	7.3	0.90
Dorsal interobital distance	53.0	30	42.7	54.3	47.9	2.72
Ventral interobital distance	58.5	30	50.3	58.0	54.2	1.71
Cleithral width	66.6	30	58.7	67.3	62.9	2.47
Head width	60.9	30	52.7	61.3	57.3	2.14
Interpelvic distance	27.2	30	22.8	33.8	29.5	2.69
PERCENT OF CLEITHRAL WIDTH						
Snout	82.2	30	80.6	92.4	86.5	3.30
LATERAL SERIES OF PLATES						
Dorsal series	22	30	20	22	21	0.4
Middorsal series	4	30	3	4	4	0.4
Medial series	25	30	24	26	24	0.5
Midventral series	14	30	13	14	13	0.5
First midventral series plates	4	30	4	5	4	0.3
Ventral series	20	30	20	22	21	0.3
ABDOMINAL SERIES OF PLATES						
Right lateral series	—	14	6	10	8	1.4
Left lateral series	—	14	6	10	8	1.2
Medial lateral series	—	13	6	10	8	1.2
TEETH						
Premaxillary teeth	21	30	19	26	22	1.9
Dentary teeth	18	30	16	24	19	2.0

Fig. 23. *Hypoptopoma psilogaster*, ANSP 180654, 59.2 mm SL, female, in dorsal, lateral, and ventral views.

without separate urogenital papilla. In females, size and arrangement of odontodes on plates lateral to anus similar to adjacent plates, without distinct patch of differentially arranged odontodes. Female pelvic spine without flap of soft tissue on posterior surface.

DISTRIBUTION: Ríos Ampiyacu, Itaya, Nanay, Napo, and Yaguas in Western Amazon (fig. 19).

TAXONOMIC REMARKS: Fowler (1915) established the new species *Hypoptopoma psilogaster* on the basis of a single specimen. He compared his new species only with *H. thoracatum*, from which he distinguished the new species by the presence of two rows of abdominal plates separated by an unplated surface (vs. complete cover of the abdominal region with three rows of plates). Our examination of specimens of various size from across an extensive range of the Peruvian Amazon allowed us to confirm that the specimen examined by Fowler possesses the typical arrangement of abdominal plates observed in immature developmental stages in all speces of *Hypoptopoma*. Adults of *H. psilogaster* have the abdominal region completely covered by three rows of plates, similar to the condition observed in *H. thoracatum*. Nevertheless, we provide new evidence supporting the valid taxonomic status of *H. psilogaster* on the basis of the caudal-fin pigmentation, in addition to a combination of morphometric and meristic characteristics. A multivariate analysis of the overall morphometric variation among *H. guianense*, *H. psilogaster*, and *H. thoracatum* is included in the Taxonomic Remarks

section of the systematic account of *H. guianense*.

Hypoptopoma thoracatum Günther, 1868a
Figure 2, table 5

Hypoptopoma thoracatum Günther, 1868a: 477 (original description; Xeberos, Peru).—Günther, 1868b: 234 (descriptions of freshwater fishes from Surinam and Brazil).—Eigenmann and Eigenmann, 1889: 40 (list of catfish species of South America; senior synonym of *H. bilobatum* and *H. joberti*; key).—Eigenmann and Eigenmann, 1890: 388 (list of catfish species of South America).—Boulenger, 1896: 34 (list of fishes from Río Paraguay; key of *Hypoptopoma* species).—Regan, 1904: 263 (senior synonym of *H. bilobatum*; key to *Hypoptopoma* species).—Fowler, 1915: 235, 237 (annotated list of catfish species; assigned to subgenus *Hypoptopoma*).—Eigenmann and Allen, 1942: 200 (list of freshwater fishes of Western South America).—Fowler, 1945: 99 (list of freshwater fishes of Peru).—Gosline, 1945: 98 (list of catfish species of South and Central America).—Fowler, 1954: 127 (list of freshwater fishes of Peru).—Boeseman, 1974: 264–266 (list of nominal species of *Hypoptopoma*).—Isbrücker, 1980: 87 (list of loricariid species); Ortega and Vari, 1986: 17 (list of fishes of Peru; Carachama).—Eschmeyer and Ferraris, 1998: 1674 (catalog of fishes).—Mojica, 1999: 561 (list of freshwater fishes of Colombia).—Isbrücker, 2002: 28 (list of loricariid species).—Schaefer, 2003: 323 (list of hypoptopomatine species).—Mojica et al., 2005: 201 (Colombia: occurrence in the Amazon basin, Leticia).—Bogotá-Gregory and Maldonado-Ocampo, 2006: 76 (list of fishes of the Amazon basin in Colombia).—Ferraris, 2007: 250 (list of catfish species).

Hypoptopoma bilobatum Cope, 1870: 566 (original description; Pebas, Peru).—Cope, 1878: 679 (list of freshwater fishes of Peru).—Steindachner, 1882: 7 (Peru: occurrence at Huallaga).—Isbrücker, 1980: 87 (list of loricariid species).—Ortega and Vari, 1986: 17 (list of fishes of Peru; Carachama).—Schaefer, 2003: 323 (list of hypoptopomatine species).—Ferraris, 2007: 250 (list of catfish species).

Hypoptopoma thoracatus Boulenger, 1895: 527 (misspelling; key to species of *Hypoptopoma*).

HOLOTYPE: BMNH 1867-6:13–38, 76.2 mm SL, Peru, Xeberos.

NON-TYPES: **Bolivia**, **Beni**: INHS 37227 (11 ♀ + 2 ♂ + 1 juvenile, 19.9–42.4 mm SL) Río Apere/Amazonas dr., Río Chevejecure, 41 km E Estación Biológica del Beni on road to San Ignacio; ZSM 28426 (1 ♀, 44.7 mm SL) Espiritu, Río Yacuma. **Pando**: FMNH 107059 (3 ♂, 42.1–47.8 mm SL) Río Madeira dr., Río Nareuda, 7 km río arriba de la desembocadura en el Tahuamanu; FMNH 107060 (19 ♀ + 2 ♂, 30.2–42.0 mm SL) Río Madeira dr., Río Manuripi, +/− 12 km río arriba de Puerto Rico; FMNH 107061 (7 juveniles, 25.0–29.4 mm SL) Río Madeira dr., lago del campamento, +/− 10 km río arriba de Puerto Rico; FMNH 107063 (2 ♀ + 1 ♂ + 9 juveniles, 30.8–47.2 mm SL) Río Madeira dr., Río Manuripi, +/− 13 km río arriba de Puerto Rico; FMNH 107064 (3 ♀, 28.0–33.1 mm SL) Río Madeira dr., Río Manuripi, +/− 13 km río arriba de Puerto Rico; FMNH 107065 (1 ♀ + 14 juveniles, 25.6–47.1 mm SL) Río Madeira dr., lago s/n, +/− 15 km río arriba de Puerto Rico; FMNH 107066 (9 juveniles, 29.1–33.4 mm SL) Río Madeira dr., lago s/n; +/− 13 km río arriba de Puerto Rico; FMNH 107067 (31 ♀ + 2 ♂, 29.5–40.2 mm SL) Río Madeira dr., lago s/n; +/− 12 km río arriba de Puerto Rico; FMNH 107068 (4 ♀, 32.8–36.6 mm SL) Río Madeira dr., Río Orthon, +/− 2 km río abajo de Puerto Rico; FMNH 107069 (1 ♀ + 1 ♂ + 10 juveniles, 24.1–49.3 mm SL) Río Madeira dr., Río Manuripi; +/− 8 km río arriba de Puerto Rico; FMNH 107070 (3 ♀, 32.4–34.1 mm SL) Río Madeira dr., Río Manuripi at playa, 5.78 km from camp, 9.23 from Puerto Rico; FMNH 107071 (54 juveniles, 26.9–31.9 mm SL) Río Madeira dr., lagoon and backwater off Río Manuripi, 1.70 km above Puerto Rico; FMNH 107072 (4 ♀, 30.8–32.3 mm SL) Río Madeira dr., lagoon on SW side of island 3.47 km up river from Puerto Rico on the Río Manuripi. **Brazil**, **Amazonas**: INPA 14036 (8 ♀ + 5 ♂, 41.1–47.4 mm SL) Rio Solimões, Paraná do Rei, Ilha do Careiro; USNM 308312 (1 ♀, 49.9 mm SL) near Manaus, Lago January, Lago Terra Preta; USNM 308336 (1 ♂, 40.3 mm SL) near Manaus, Lago January, Lago Terra Preta; USNM 316539 (7 ♂, 33.3–38.8 mm SL) Rio Purus. **Pará**: FMNH 59620 (1 ♀, 40.20 mm SL) Santarém. **Colombia**, **Amazonas**: CAS 76651 (1 ♀, 46.0 mm SL) Caqueta Dept., Tres Esquinas; CAS 153141 (6 ♀ + 1 ♂, 41.8–73.1 mm SL) Caqueta Dept., Río Orteguaza, tributary of Río Caqueta, within 2 mi. of Tres Esquinas; SU 50479 (4 ♀ + 2 ♂, 36.9–

TABLE 5
Morphometric and Meristic Data for *Hypoptopoma thoracatum*
Syntype of *H. bilobatum*: ANSP 8280. Nontypes: AMNH 78033, 78099; CAS 153141; FMNH 101544, 107058, 107059, 107060, 107063, 107069; INHS 101389; LACM 38608; MUSM 1845, 4413; SIUC 29199; SU 36218.

	N	Range		Mean	sd
Standard length	47	35.6	78.3	53.2	11.06
PERCENT IN STANDARD LENGTH					
Predorsal length	47	41.0	46.4	43.8	1.15
Head length	47	28.4	33.6	31.5	1.20
Body depth	47	14.2	18.8	16.9	1.07
Dorsal-fin spine length	38	24.1	32.5	28.8	1.58
Trunk length	47	44.5	49.8	46.9	1.22
Pectoral-fin spine length	47	21.8	26.7	24.7	1.14
Abdominal length	47	14.8	18.6	16.5	0.93
Caudal-peduncle length	47	33.0	38.8	36.4	1.32
Caudal-peduncle depth	47	6.2	9.2	7.6	0.69
Caudal-fin base depth	34	5.6	7.9	6.9	0.62
Head depth	47	12.5	17.1	14.6	1.00
Snout length	47	15.3	19.2	17.3	0.79
Horizontal eye diameter	47	4.9	6.7	5.8	0.50
Least orbit-naris distance	47	2.3	4.0	3.0	0.45
Dorsal interobital distance	47	16.0	20.4	18.1	1.10
Ventral interobital distance	47	17.0	21.2	19.3	0.98
Cleithral width	47	20.0	24.7	22.7	1.09
Head width	47	18.5	22.9	20.7	1.08
Interpelvic distance	47	8.3	11.6	10.2	0.84
PERCENT OF HEAD LENGTH					
Body depth	47	44.7	62.4	53.7	4.29
Head depth	47	41.2	53.8	46.5	3.23
Snout length	47	50.5	57.8	54.9	1.88
Horizontal eye diameter	47	15.7	21.7	18.3	1.36
Least orbit-naris distance	47	7.1	13.3	9.7	1.62
Dorsal interobital distance	47	51.4	63.6	57.6	3.24
Ventral interobital distance	47	57.6	67.1	61.3	2.42
Cleithral width	47	66.3	76.6	72.0	2.72
Head width	47	60.7	71.0	65.8	2.78
Interpelvic distance	47	26.4	36.9	32.3	2.45
PERCENT OF CLEITHRAL WIDTH					
Snout	47	71.5	83.8	76.4	2.56
LATERAL SERIES OF PLATES					
Dorsal series	47	19	21	20	0.5
Middorsal series	47	3	4	4	0.3
Medial series	47	22	24	23	0.5
Midventral series	47	13	14	13	0.5
First midventral series plates	47	4	5	4	0.1
Ventral series	47	19	21	20	0.5
ABDOMINAL SERIES OF PLATES					
Right lateral series	43	6	11	8	1.2
Left lateral series	43	5	11	8	1.4
Medial lateral series	42	5	13	8	1.7
TEETH					
Premaxillary teeth	38	19	34	24	3.5
Dentary teeth	39	14	28	20	3.5

43.9 mm SL) Caqueta Dept., vecinity of Tres Esquinas, Río Orteguaza near juncture with Río Caqueta; USNM 360864 (1 ♀ + 1 ♂, 68.8–75.8 mm SL) Leticia. **Ecuador**, **Napo**: FMNH 101544 (3 ♂, 53.2–62.2 mm SL) Tributary to Rio Tarapuy. **Peru**, **Loreto**: AMNH 78033 (1 ♀, 55.7 mm SL) Río Tahuayo at Huasi Villeage; AMNH 78099 (9 ♀ + 1 ♂, 1 cs, 45.8–76.9 mm SL) Río Yarapa, tributary of Río Ucayali, several sites along a 10 km stretch of river; AMNH 218005 (1 ♀, 66.4 mm SL) Iquitos, Río Itaya; ANSP 8280/81 (syntypes of *Hypoptopoma bilobatum*) (2, unsexed, 59.5–74.9 mm SL) Pebas; CAS 59599 (3 ♀, 43.03–48.78 mm SL) mouth of Río Pacaya; CAS 134256 (1 ♀, 46.3 mm SL) Río Ampiyacu; CAS 136219 (1 ♀, 56.5 mm SL) Caño del Chancho, near Pebas; INHS 53870 (8 ♀, 33.0–53.7 mm SL) Río Itaya, Ullpa caño, SE of Belem (Iquitos), near confluence with Moena caño; INHS 101388 (1 ♀ + 1 ♂, 52.3–64.8 mm SL) Río Yanashi, Yanashi, 69.8 mi E Iquitos; INHS 101389 (8 ♀ + 2 ♂, 2 cs, 32.1–73.1 mm SL) Río Orosa, mouth of Tonche Caño, Madre Selva II field station 69.4 mi. E Iquitos; INHS 101391 (1 ♀, 68.6 mm SL) Quebrada Mazama, Río Itaya dr., ca. 1 km upstream from confluence with Río Itaya, S of Belem (Iquitos); MUSM 4413 (3 ♀, 49.7–54.5 mm SL) Alto Amazonas, Yurimaguas, Río Shanusi; MUSM 6515 (1♀, 64.3) Maynas, Puesto de Vigilancia Arcadia, Río Napo, Cocha de Conchas; NRM 17992 (3 ♀, 45.8–48.7 mm SL) Río Samiria drainage, Atún caño; NRM 57232 (1 ♀ + 1 ♂, 54.2–60.9 mm SL) Rio Tahuayo dr., caño Huayti; SIUC 29199 (1 ♀ + 1 ♂, 68.3–78.3 mm SL) Maynas, Río Itaya, upriver of Belén, approx. 4.5 km; SIUC 29316 (1 ♀, 66.6 mm SL) Río Napo, Mazan, 33.3 km from center of Iquitos; SIUC 29782 (1, 54.6 mm SL) Maynas, Río Itaya, 11 km from Iquitos center; SIUC 67366 (5 ♀, 44.6–53.1 mm SL) Maynas, Río Itaya and Quebrada Mazana, 11 km from Iquitos center; SU 36218 (2 ♀, 57.4–67.6 mm SL) Río Amazonas, Caño del Chancho, near Pebas. **Ucayali**: LACM 38608 (3 unsexed, 47.0–66.6 mm SL) Central Ucayali, brook between Lake Cocha and Lake Yarina; MHNG 2407.98 (1 ♀, 35.3 mm SL) Pucallpa, Tapistica Alejandria; MHNG 2409.26 (1 ♀, 50.6 mm SL) Pucallpa, Masisea, Río Ucayali; MHNG 2409.27 (1 ♀, 41.4 mm SL) Pucallpa, Masisea, Río Ucayali; MHNG 2618.84 (1 ♂, 55.07 mm SL) Río Puntichao and Río Chicosa, two tributaries entering Ucayali River near Chicosa; MHNG 2708.059 (2 ♀, 37.4–38.6 mm SL) Yarina Cocha, an oxbow lake near Pucallpa; MUSM 32157 (3 ♀ + 2 ♂, 1 cs, 43.3–59.6 mm SL) Coronel Portillo, Pucallpa, Tapistica Alejandria; MUSM 32158 (2 ♀, 47.2–50.1 mm SL) Coronel Portillo, Pucallpa, Río Ucayali, Cocha Tacshitea; NRM 17987 (2 ♀, 64.4–64.6 mm SL) Río Ucayali dr., Yarinacocha, caño to Paca Cocha.

DIAGNOSIS: *Hypoptopoma thoracatum* is distinguished from all congeners by the presence of an elongated spot of black melanophores along the caudal-fin branched rays, not distinctly connected to the lanceolate plates at the base of the fin; spot extended over a larger number of lower-lobe rays than upper-lobe rays and along one-half to more than two-thirds of the ray length (figs. 17A, 24).

DESCRIPTION: Morphometric and meristic data presented in table 5. Body moderately robust. Dorsal profile of head and body straight from tip of snout to dorsal-fin origin, slightly elevated at predorsal plates; straight from dorsal-fin origin to anteriormost caudal-fin procurrent ray. Head moderately depressed and wide. Lateral process of lateral ethmoid bone visible dorsally. Snout slightly rounded in dorsal view; dorsally smoothly rounded, slightly concave anterior to naris. Posterior surface of bony pit of nasal organ gradually inclined. Body cross section between pectoral- and pelvic-fin origins horizontally ovoid, vertically ovoid to progressively rounded posterior to dorsal fin, progressively compressed posterior to adipose-fin base.

Eyes moderately large, positioned slightly closer to posterior tip of compound pterotic than to tip of snout. Ventral margin of orbit located close to ventral surface of head. Dorsal interorbital distance slightly shorter than ventral interorbital distance.

Total plates in lateral medial series 22–24 (23). Dorsal series 19–21 (20); middorsal series 3–4 (4); midventral series 13–14 (13), with 4–5 (4) plates anterior of first plate of ventral series; ventral series 19–21 (20).

Second plate of midventral series contacting a single plate of medial lateral series.

Abdomen covered by paired series of lateral sickle-shaped plates, with unequal number of plates between left and right series, 5–11 each; medial series of 5–13 (8) roughly squared plates; anterior azygous plate absent; occasionally, transversal series of more than three small plates posterior of coracoids, not aligned with main three longitudinal series. Single anal plate present. Thoracic plates absent. Preopercular canal absent. Posterolateral margin of canal-bearing plate and lateral margin of fourth infraorbital smooth; pore between canal-bearing ventral plate and fourth infraorbital absent.

Small odontodes evenly distributed on head. Odontodes ventral and dorsal to tip of snout not arranged in aligned series. No odontode-free discontinuity between ventral and dorsal odontodes; odontodes dorsal to tip of snout slightly larger than those on head. Lamina of trunk plates bearing longitudinal rows of odontodes, and becoming progressively smoother ontogenetically; distinct column of marginal odontodes on posterior plate border in mature adults.

Total vertebrae 27. Premaxillary teeth 19–34 (24); dentary teeth 14–28 (20). Maxillary barbels short, almost reaching to or slightly surpassing anterior margin of ventral canal-bearing plate in adults.

Dorsal-fin origin located slightly posterior of vertical through pelvic-fin origin. Depressed dorsal fin reaching to vertical through posterior half of anal-fin base. Pectoral fin reaching to vertical through midpoint of pelvic-fin base. Extension of serrae along pectoral spine margin, except for short basal segment; serrae of oblique type. Pelvic fin short, two longest branched rays slightly longer than spine. Depressed fin reaching to plate anterior to anal-fin spine. Caudal-fin margin forked; upper and lower lobes equal and not extremely elongate. Adipose fin present.

COLOR IN ALCOHOL: Ground color tan and pale ochre. Melanophores light to dark brown, clustered resulting in mottled appearance. Melanophores slightly more concentrated dorsally on head, narrow area among compound pterotic, cleithral process, and opercle, at base of dorsal fin, anterior surface of lip, and anterior half of branchiostegal membrane. Head uniformly tan dorsally, except for darker area over brain. Deep-lying melanophores arranged in narrow transverse bands posterior to dorsal-fin base, noncoincident with posterior margin of plates. Midlateral stripe situated mostly along medial series of trunk plates (fig. 24). Ventral surface of body mostly unpigmented, except for scattered melanophores on posterior portion of trunk, soft tissue along base of pectoral and anal fins, anterolateral margin of cleithrum and posterior tip of cleithral process, ventral canal-bearing plates, and lateral portions of lateral series of abdominal plates. Dorsal and anal fins with dark brown bands. Caudal-fin bars variable defined. Presence of an elongated spot of black melanophores along caudal-fin branched rays, not distinctly connected to lanceolate plates at base of fin; spot typically extending over larger number of lower-lobe rays than upper-lobe rays and along one-half to more than two-thirds of ray length (figs. 17A, 24). Tip of upper and lower lobes variably dark.

SEXUAL DIMORPHISM: Male urogenital papilla short and slender, covered by anterior flaplike anus. Males with patch of tightly arranged small odontodes oriented as a swirl, variably covering first to fourth plates of ventral series, lateral to urogenital papilla. Males with flaplike anus along posterior margin of pelvic spine variably developed; when present, short, weakly developed, restricted to basal one-third to half of spine. Female anus tubular, without separate urogenital papilla. In females, size and arrangement of odontodes on plates lateral to anus similar to adjacent plates, without distinct patch of differentially arranged odontodes. Female pelvic spine without flap of soft tissue on posterior surface.

TAXONOMIC REMARKS: The genus *Hypoptopoma* was established by Günther (1868a) for his new species *Hypoptopoma thoracatum* (fig. 2) on the basis of one specimen collected by Barlett at Xeberos (Peru, upper Amazon). He distinguished the new taxon from the loricariid *Plecostomus* [= *Hypostomus*] by the "peculiar formation of the head, depressed, spatulate, the eyes being on the lateral edges of the

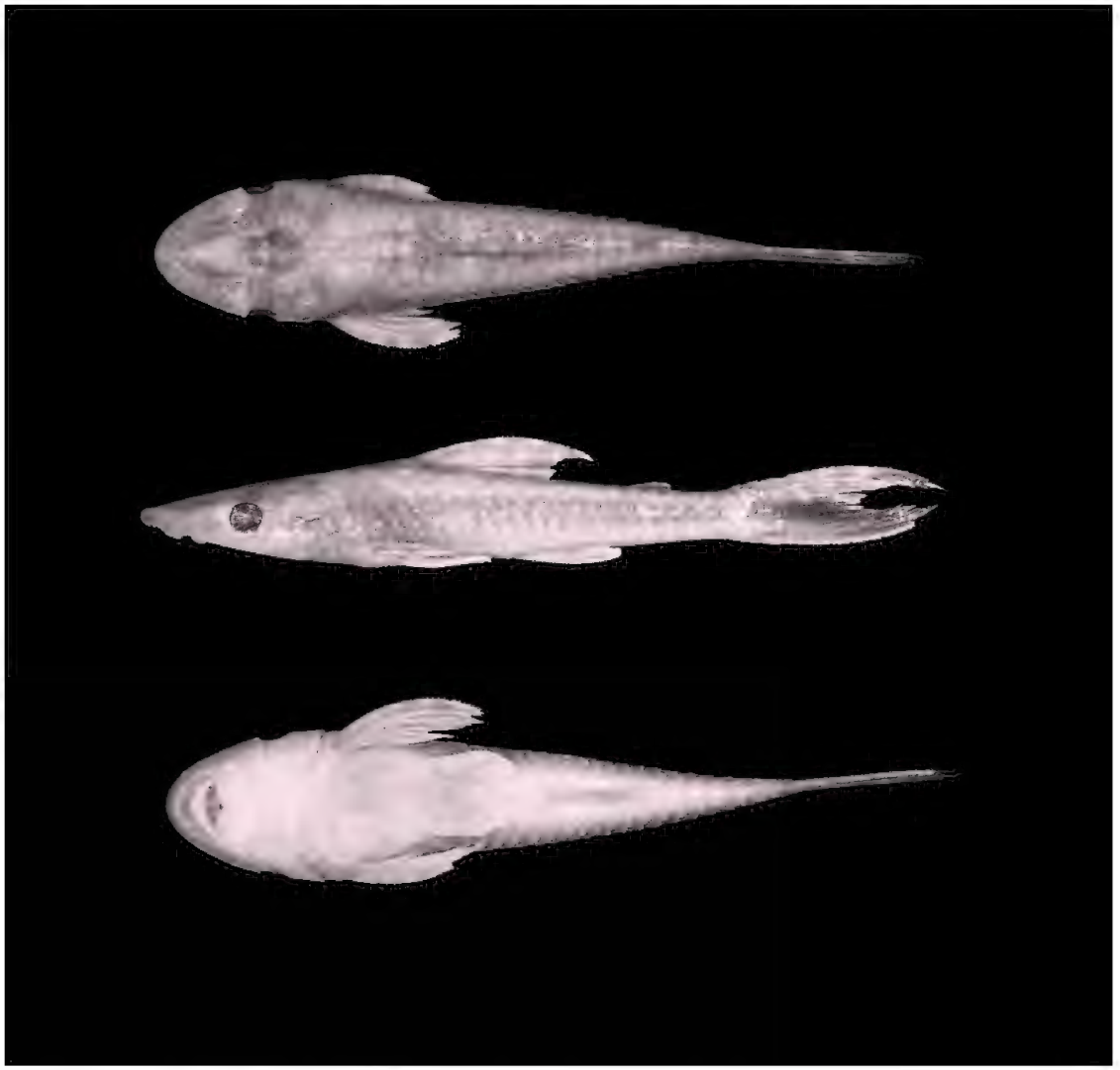

Fig. 24. *Hypoptopoma thoracatum*, SIUC 30062, 54.0 mm SL, female, in dorsal, lateral, and ventral views.

head." During 1868, Günther published two papers in which he provided a taxonomic account of the new genus and species. In the first publication, Günther (1868a) provided a brief diagnosis for the genus and the new species *H. thoracatum* that only specified counts for fin rays and lateral-line plates. A subsequent expanded description of *H. thoracatum* was published later during the same year (Günther, 1868b). Therefore, *H. thoracatum* is considered the type species of the genus. Regarding *Hypoptopoma bilobatum*, Cope (1870) established the new species on the basis of one specimen collected in 1869 by Hauxwell in Pebas, Ecuador (a region which is now part of Peru), but failed to provide a justification for the proposition of a new species distinguishable from *H. thoracatum* Günther 1868a, the only species described for the genus at the time. Ultimately, Eigenmann and Eigenmann (1889) placed Cope's species as junior synonym of *H. thoracatum*, a designation that has been maintained in the literature almost invariably since then, and confirmed herein.

Fig. 25. Drainage map of South America showing distribution of *H. thoracatum* (dots + circle). The open symbol designates the type locality; some symbols represent more than one locality record.

DISTRIBUTION: Ríos Caqueta, Mamoré, Purus, and Ucayali of Western Amazon (fig. 25).

Hypoptopoma brevirostratum, new species
Figure 26, table 6

HOLOTYPE: FMNH 105076 (♀, 34.0 mm SL) Colombia: Rio Amazonas, 1 mi. upstream from Leticia; collected by Navarro, Thomerson et al., 11 November 1973.

PARATYPES (collected with holotype): FMNH 117744 (14 ♀ + 4 ♂, 29.1–39.3 mm SL). AMNH 243577 (1 ♀ + 1 ♂, 33.2–34.0 mm SL).

NON-TYPES: **BRAZIL**, **Amazonas**: INPA 14317 (11 ♀ + 2 ♂, 2 cs, 24.1–32.1 mm SL)

Fig. 26. *Hypoptopoma brevirostratum*, holotype, FMNH 105076, 34.0 mm SL, female, in dorsal, lateral, and ventral views.

Rio Solimões, 1 km acima do Furo Paracuuba; INPA 14322 (1 ♀, 38.3 mm SL) Ihla Marchantaria. MZUSP 7015 (1 ♀, 28.2 mm SL) Rio Madeira, 25 km abaixo de Nova Olinda; MZUSP 36214 (1 ♀ + 1 ♂, 29.0–44.0 mm SL) Rio Japura, Manacabi, approximatly 50 km from Foz; MZUSP 36221 (4 ♀, 25.5–38.00 mm SL) Braço do Rio Solimões, Ihla Sorubim, acima do Coari; MZUSP 56820 (1 ♀; 30.6 mm SL) Rio Juruá, 10,2 km abaixo do Lago Pauapixuna. **Ecuador, Napo**: FMNH 101541 (1 ♀ + 3 ♂, 41.0–50.6 mm SL) Río Jivino, lower 4 km (mostly) to ca. 6 km upstream from mouth. **Peru, Loreto**: INHS 44126 (1 ♀, 48.8 mm SL) Río Napo and Quebrada Mazán, 33.3 km NE Iquitos; ANSP 187332 (1 ♀ + 1 ♂ + 2 juveniles, 29.6–49.0 mm SL) Río Itaya at bridge on Iquitos-Nauta highway, approx. 25 miles SSW of Iquitos; SIUC 27969 (1 ♂, 41.8 mm SL) Río Mazán.

TABLE 6
Morphometric and Meristic Data for *Hypoptopoma brevirostratum*
Holotype: FMNH 105076. Paratypes: FMNH 117744; AMNH 243577. Nontypes: FMNH 101541; INHS 44126; INPA 14317; SIUC 27969.

	Holotype	*N*	Range		Mean	sd
Standard length	34.1	28	24.2	50.6	33.3	7.22
PERCENT IN STANDARD LENGTH						
Predorsal length	41.6	28	41.6	46.1	43.9	0.92
Head length	31.4	28	30.1	34.8	32.7	1.27
Body depth	17.9	28	15.5	19.2	17.6	0.90
Dorsal-fin spine length	31.7	24	29.3	36.5	32.7	1.86
Trunk length	47.3	27	42.5	47.3	45.7	1.13
Pectoral-fin spine length	28.2	28	26.8	32.5	29.6	1.60
Abdominal length	15.6	28	15.0	18.9	16.8	1.12
Caudal-peduncle length	38.3	28	33.6	38.3	35.6	1.29
Caudal-peduncle depth	7.9	28	6.4	9.1	7.7	0.64
Caudal-fin base depth	9.5	10	9.1	10.5	9.7	0.48
Head depth	15.2	28	14.2	17.9	15.7	0.86
Snout length	15.7	28	15.5	17.9	16.6	0.65
Horizontal eye diameter	6.8	28	6.4	7.9	7.1	0.44
Least orbit-naris distance	2.8	28	2.8	4.1	3.3	0.30
Dorsal interobital distance	18.2	28	18.0	21.9	19.3	0.85
Ventral interobital distance	19.6	28	18.5	21.5	20.2	0.76
Cleithral width	25.1	28	23.7	27.0	25.7	0.84
Head width	22.6	28	10.6	25.2	22.6	2.50
Interpelvic distance	10.3	28	8.9	11.9	10.1	0.82
PERCENT OF HEAD LENGTH						
Body depth	17.9	28	15.5	19.2	17.6	0.90
Head depth	48.4	28	42.6	53.8	48.1	3.53
Snout length	49.9	28	47.6	55.1	51.0	2.03
Horizontal eye diameter	21.7	28	19.8	23.3	21.7	0.93
Least orbit-naris distance	9.1	28	8.4	13.0	10.0	1.11
Dorsal interobital distance	57.8	28	53.1	69.2	59.1	3.79
Ventral interobital distance	62.4	28	56.4	66.9	61.9	2.38
Cleithral width	79.9	28	72.1	85.4	78.9	3.96
Head width	71.8	28	34.4	79.5	69.2	7.62
Interpelvic distance	32.7	28	26.7	36.6	30.9	2.54
PERCENT OF CLEITHRAL WIDTH						
Snout	62.4	28	60.6	71.9	64.7	2.65
LATERAL SERIES OF PLATES						
Dorsal series	20	26	19	20	20	0.3
Middorsal series	3	26	3	4	3	0.5
Medial series	23	26	23	23	23	0.0
Midventral series	12	26	12	15	13	0.7
First midventral series plates	4	26	4	4	4	0.0
Ventral series	20	26	19	20	20	0.2
ABDOMINAL SERIES OF PLATES						
Right lateral series	5	18	3	7	5	1.4
Left lateral series	4	18	3	8	5	1.5
Medial lateral series	1	18	0	3	2	0.9
TEETH						
Premaxillary teeth	19	26	10	28	19	3.4
Dentary teeth	17	26	12	22	17	2.5

DIAGNOSIS: *Hypoptopoma brevirostratum* is distinguished from all congeners, with the exception of *H. muzuspi*, by having the preopercle constricted medially (vs. preopercle with no constriction); canal in preopercle present, semicircular, located posterior to the preopercle constriction (vs. canal absent from preopercle). *Hypoptopoma brevirostratum* is distinguished from *H. muzuspi* by its wider body (cleithral width 23.7–27.0 (25.7) vs. 19.1–23.5 (22.2)), a deeper caudal peduncle (caudal-peduncle depth 6.4–9.1 (7.7) vs. 5.2–6.7 (5.8)), and a larger eye (horizontal eye diameter 19.8–23.3 (21.7) vs. 13.6–20.7 (18.4)).

DESCRIPTION: Morphometric and meristic data presented in table 6. Body moderately wide and depressed; greatest depth at dorsal-fin origin. Dorsal profile of head and body, from tip of snout to dorsal-fin origin, smoothly convex to straight; straight posterior to dorsal-fin base. Head moderately depressed, almost as wide as cleithral width; lateral process of lateral ethmoid not visible dorsally. Snout rounded and short in dorsal view; dorsally slightly concave anterior to naris. Posterior surface of bony pit of nasal organ sharply inclined. Body cross section between pectoral- and pelvic-fin origins approximately ovoid horizontally, slightly rectangular posterior to dorsal fin, slightly compressed at level of two posteriormost lateral trunk plates.

Eyes large, positioned equally distant from posterior tip of compound pterotic and to tip of snout. Ventral margin of orbit located on ventral surface of head. Dorsal interorbital distance typically slightly greater than ventral interorbital distance.

Total plates in lateral medial series 23. Dorsal series 19–20 (20); middorsal series 3–4 (3); midventral series, 12–15 (13), with four plates anterior of first plate of ventral series; ventral series 19–20 (20). Second plate of midventral series contacting one plate of medial lateral series.

Abdomen covered by paired series of lateral sickle-shaped plates, with unequal number of plates between left and right series, 3–8; medial series of 1–3 (2) roughly squared plates; medial series occasionally absent, in which case paired series make contact along midline in fully developed individuals; abdominal shield fully developed in specimens greater than 25 mm SL. Single anal plate present. Thoracic plates absent. Canal in the preopercle present, semicircular; anteriormost pore opening between ventral canal-bearing plate and fourth infraorbital; posterolateral margin of canal-bearing plate and lateral margin of fourth infraorbital with notch for pore of semicircular canal poorly defined.

Small odontodes evenly distributed on head. Odontodes ventral and dorsal to tip of snout on anterior rostral plate not arranged in well-defined series. No odontode-free discontinuity between ventral and dorsal odontodes; odontodes dorsal to tip of snout small, slightly larger than those on dorsal surface of head. Odontodes on lamina of trunk plates roughly arranged in longitudinal rows; feeble column of marginal odontodes on posterior border of plates. No visible progressive smoothening of plates ontogenetically.

Total vertebrae 27. Premaxillary teeth 10–28 (19), dentary teeth 12–22 (18). Maxillary barbels short, not reaching to ventral canal-bearing plate in adults.

Dorsal-fin origin located at vertical through pelvic-fin origin. Depressed dorsal fin reaching to vertical through posterior half of anal-fin base. Pectoral fin almost reaching to vertical through tip of longest pelvic-fin ray. Extension of serrae along pectoral spine margin, except for short basal segment; serrae of oblique type. Pelvic fin short, unbranched rays slightly shorter than first branched. Depressed fin reaching to plate anterior to anal-fin spine. Caudal-fin margin slightly forked; upper and lower lobes equal. Adipose fin absent.

COLOR IN ALCOHOL: Ground color tan and pale ochre. Melanophores dark brown, irregularly distributed on trunk resulting in an overall marbled pattern. Melanophores on head not uniformly distributed. Melanophores slightly more concentrated between left and right nares and anterior to each naris, on anterior margin of opercle, cleithral posterior process, lateral rostral plates and anterior surface of lip. Narrow line of dark melanophores along margin of tip of snout. In dorsal view, melanophores arranged in ill-defined darker clusters (one on predorsal plate, two lighter clusters lateral to dorsal-fin

Fig. 27. Drainage map of South America showing distribution of *H. brevirostratum* (dots + circle), *H. muzuspi* (square), *H. spectabile* (triangles), and *H. sternoptychum* (stars). Open symbols designate type localities; some symbols represent more than one locality record.

base, two or three posterior to dorsal fin). Midlateral stripe fading toward dorsal surface of trunk and toward caudal fin. Ventral surface of body mostly unpigmented. Three to six dark blotches along dorsal-fin spine, weakly extended over branched rays. Basal triangular dark brown to black spot at base of caudal-fin lower lobe; 3–6 dark blotches along caudal-fin unbranched rays, weakly extended over branched rays.

SEXUAL DIMORPHISM: Male urogenital papilla completely covered by flaplike anus;

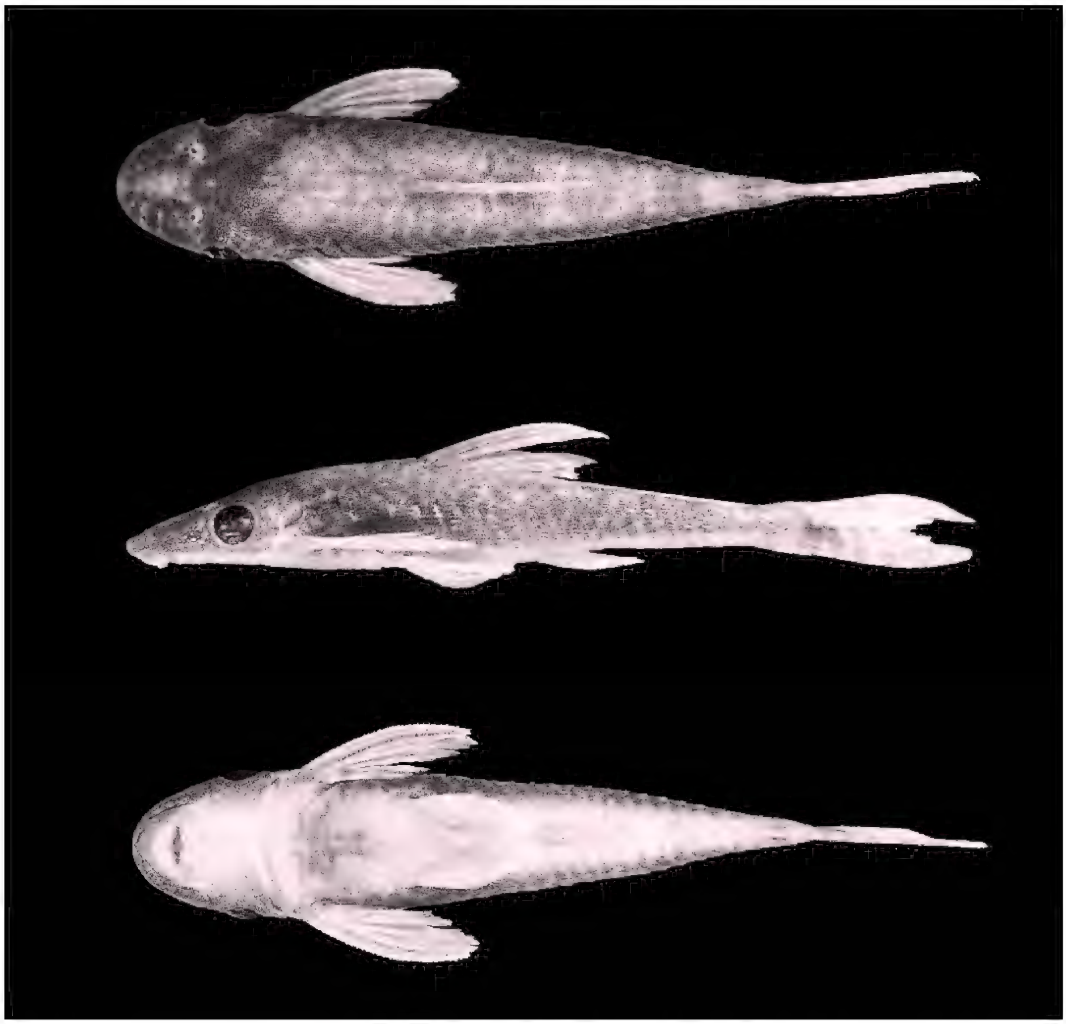

Fig. 28. *Hypoptopoma muzuspi*, holotype, MZUSP 52135, 36.3 mm SL male, in dorsal, lateral, and ventral views.

joined at base. Males with patch of tightly arranged small odontodes oriented as a swirl covering second, third, and fourth plates of ventral series, lateral to urogenital papilla. Males with soft-tissue flap along posterior margin of pelvic spine variably developed; when present, short, restricted to basal one-third to one-half of spine. Female anus tubular, without separate urogenital papilla. In females, size and arrangement of odontodes on plates lateral to anus similar to adjacent plates, without distinct patch of differentially arranged odontodes. Female pelvic spine without flap of soft tissue on posterior surface.

DISTRIBUTION: Tributaries of Río Amazonas between confluence of Ucayali-Marañon rivers and Manaus (fig. 27).

ETYMOLOGY: The specific epithet *brevirostratum* (Lt. *brevis*, meaning "short"; Lt. *rostrum*, meaning "snout")is a reference to the short head.

Hypoptopoma muzuspi, new species
Figure 28, table 7

HOLOTYPE: MZUSP 52135 (♂, 36.3 mm SL) Brazil: Tocantins State, Araguaçu, rio Agua Fria, fazenda Praia Alta 2, estrada Araguaçu/Barreira do Piqui, 27 km ao norte

TABLE 7
Morphometric and Meristic Data for *Hypoptopoma muzuspi*
Holotype: MZUSP 52135. Paratypes: MZUSP 95186; AMNH 243578.

	Holotype	*N*	Range		Mean	sd
Standard length	36.4	28	19.0	31.9	26.0	2.89
PERCENT OF STANDARD LENGTH						
Predorsal length	44.9	26	41.9	45.1	43.6	0.89
Head length	31.2	26	30.9	35.2	33.3	0.89
Body depth	16.1	26	13.8	16.7	14.7	0.64
Dorsal-fin spine length	29.4	26	27.0	30.5	28.6	0.83
Trunk length	47.0	26	42.4	47.5	45.5	1.46
Pectoral-fin spine length	25.7	26	22.3	26.9	24.5	1.08
Abdominal length	16.8	26	13.1	16.3	15.0	0.80
Caudal-peduncle length	34.8	26	34.1	38.0	36.0	1.07
Caudal-peduncle depth	5.9	26	5.2	6.7	5.8	0.33
Caudal-fin base depth	5.8	26	4.1	6.1	5.4	0.62
Head depth	14.8	26	12.4	15.5	13.3	0.76
Snout length	16.5	26	15.3	18.0	16.7	0.59
Horizontal eye diameter	5.8	26	5.2	7.0	6.2	0.40
Least orbit-naris distance	2.6	26	2.2	3.1	2.7	0.21
Dorsal interobital distance	17.1	26	16.4	18.0	17.3	0.48
Ventral interobital distance	18.8	26	17.6	22.1	19.2	0.85
Cleithral width	22.6	26	19.1	23.5	22.2	0.81
Head width	20.2	26	19.1	21.2	20.2	0.52
Interpelvic distance	9.4	26	8.2	10.0	8.9	0.44
PERCENT OF HEAD LENGTH						
Body depth	51.5	26	34.7	48.9	43.9	2.70
Head depth	47.4	26	29.9	45.5	39.7	3.20
Snout length	52.8	26	39.6	52.6	49.6	2.64
Horizontal eye diameter	18.5	26	13.6	20.7	18.4	1.48
Least orbit-naris distance	8.4	26	6.6	9.2	7.9	0.67
Dorsal interobital distance	54.8	26	41.5	55.7	51.4	2.71
Ventral interobital distance	60.3	26	46.1	66.3	57.2	3.64
Cleithral width	72.4	26	53.4	71.1	66.2	3.65
Head width	65.0	26	48.4	65.3	60.2	3.07
Interpelvic distance	30.1	26	20.5	30.1	26.4	1.82
PERCENT OF CLEITHRAL WIDTH						
Snout	72.9	26	68.8	90.2	75.1	3.59
LATERAL SERIES OF PLATES						
Dorsal series	20	13	19	20	19	0.5
Middorsal series	3	13	3	3	3	0.0
Medial series	23	13	22	23	23	0.3
Midventral series	13	13	13	14	13	0.3
First midventral series plates	4	13	4	4	4	0.0
Ventral series	19	13	19	19	19	0.0
ABDOMINAL SERIES OF PLATES						
Right lateral series	5	13	19	19	19	0.0
Left lateral series	4	8	4	7	5	1.2
Medial series	—	8	4	8	6	1.4
TEETH						
Premaxillary teeth	19	13	15	21	18	1.9
Dentary teeth	17	13	13	18	15	1.7

de Araguaçu; collected by Lima et al., 6 July 1997.

PARATYPES (collected with holotype): MZUSP 95186 (24 ♀, 2 cs, 19.0–31.0 mm SL). AMNH 243578 (5 ♀, 1 cs, 28.0–32.0 mm SL).

DIAGNOSIS: *Hypoptopoma muzuspi* is distinguished from all congeners by having the bifid neural spines of vertebra 10–12 expanded distally (vs. bifid neural spines progressively pointed distally). It can be further distinguished from all congeners, except H. *brevirostratum*, by the preopercle constricted medially (vs. preopercle without constriction) and canal in preopercle present, semicircular, and located posterior to the preopercle constriction. *Hypoptopoma muzuspi* can be readily distinguished from *H. brevirostratum* by its more elongated body and head (body depth 13.8–16.7 (14.7) vs. 15.5–19.2 (17.6); cleithral width 19.1–23.5 (22.2), vs. 23.7–27.0 (25.7); caudal-peduncle depth 5.2–6.7 (5.8) vs. 6.4–9.1 (7.7)), and caudal-fin pigmentation comprised of 7–10 bars of brown melanophores on unbranched and branched rays (vs. 3–6 dark blotches along unbranched rays, weakly extended over branched rays).

DESCRIPTION: Morphometric and meristic data presented in table 7. Body moderately elongate; greatest depth at dorsal-fin origin, trunk most shallow at origin of caudal-fin procurrent rays. Dorsal profile of head and body, from tip of snout to dorsal-fin origin, smoothly convex; straight posterior to dorsal-fin origin, smoothly tapering to caudal fin base. Head moderately depressed; lateral process of lateral ethmoid bone not visible dorsally. Snout rounded in dorsal view; smoothly concave anterior to naris. Posterior surface of bony pit of nasal organ sharply inclined. Trunk cross section between pectoral- and pelvic-fin origins horizontally ovoid, posterior to dorsal fin slightly rectangular, at level of two posteriormost trunk lateral plates slightly compressed.

Eyes moderately large, positioned slightly closer to posterior tip of compound pterotic than to tip of snout. Ventral margin of orbit located close to ventral surface of head. Dorsal interorbital distance shorter than ventral interorbital distance.

Total plates in lateral medial series 22–23 (23). Dorsal series plates 19–20 (19); middorsal series plates 3; midventral series plates 13–14 (13), with four plates anterior to first plate of ventral series; ventral series 19. Second plate of midventral series contacting a single plate of medial lateral series.

Abdomen covered by paired series of lateral sickle-shaped plates, with unequal number of plates between left and right sides, 4–8; medial series of 4–5 (5) roughly squared plates; anterior azygous plate absent; medial series occasionally absent, in which case paired series make contact along midline in fully developed individuals; abdominal shield fully developed in specimens greater ca. 30 mm SL. Single anal plate present. Thoracic plates absent. Canal in the preopercle present, semicircular; anteriormost pore located between ventral canal-bearing plate and fourth infraorbital; lateral margin of fourth infraorbital with notch for semicircular canal better defined than on posterolateral margin of canal-bearing plate.

Small odontodes evenly distributed on head. Odontodes on anterior rostral plate not arranged in well-defined series; no odontode-free discontinuity between ventral and dorsal odontode series; odontodes dorsal to tip of snout slightly larger than those on head. Odontodes on lamina of trunk plates arranged in longitudinal rows; progressive smoothing of plates with increased specimen size not observed; marginal odontodes on posterior border of trunk plates in specimens greater than 34 mm SL.

Total vertebrae 27. Premaxillary teeth 15–21 (18), dentary teeth 13–18 (15). Maxillary barbels short, not reaching ventral canal-bearing plate in adults.

Dorsal-fin origin located slightly posterior of vertical through pelvic-fin origin. Depressed dorsal fin reaching to vertical through posterior third of anal-fin length. Pectoral fin reaching to vertical through midpoint of pelvic-fin length. Pectoral fin reaching second half of pelvic-fin spine. Pectoral spine serrae extended along posterior margin of spine shaft, except for short basal segment; serrae oriented oblique to spine shaft. Pelvic fin short, longest branched rays slightly longer than spine; when depressed reaching to plate anterior to anal-fin spine. Caudal-fin posterior margin forked, upper and lower lobes not elongate. Adipose fin absent.

COLOR IN ALCOHOL: Ground color tan and pale ochre. Light to dark brown melanophores, clustered on trunk resulting in mottled appearance. Melanophores more densely concentrated on compound pterotic, supraoccipital, frontals, lateral rostral plates, at base of pectoral and anal fins, on anterior surface of lip, lateral half of branchiostegal membrane, and mesial portion of naris soft-tissue flap. Melanophores along dorsal midline between dorsal-fin base and caudal fin concentrated in irregular clusters, often defining darker outline on posterior margin of plates of dorsal series. Midlateral stripe situated along medial, midventral, and ventral series of plates, becomming progressively more pigmented between medial and ventral series. Ventral surface of body mostly unpigmented except for scattered melanophores on posterior portion of trunk, anterolateral to cleithral processes, on ventral canal-bearing plates and lateral portions of lateral abdominal plate series. Paired and unpaired fins with relatively numerous narrow, dark brown bars. Caudal-fin with 7–10 bands of brown melanophores on unbranched and branched rays. Series of lanceolate plates at caudal-fin base slightly darkened with black melanophores. Variably shaped dark brown to black spot over lower lobe of caudal-fin. Posteriormost plates of both dorsal and ventral series of lateral plates less pigmented, whitish.

SEXUAL DIMORPHISM: Male urogenital papilla covered by flaplike anus. Males with patch of more tightly arranged small odontodes from fourth to sixth plates of ventral series, lateral to urogenital papilla. Female anus tubular, without separate urogenital papilla. In females, size and arrangement of odontodes on plates lateral to anus similar to those on adjacent plates, without distinct patch of differentially arranged odontodes.

ETYMOLOGY: The specific epithet *muzuspi* is given in recognition of the Museu de Zoologia, Universidade de São Paulo, Brazil (MZUSP), as one of the leading institutional collections for ichthyology in South America. The name is treated as a noun in apposition to the generic name.

DISTRIBUTION: Rio Tocantins basin; known only from Rio Agua Fria, in the drainage of Rio Araguaia (main tributary of Rio Tocantins) (fig. 27).

Hypoptopoma spectabile (Eigenmann, 1914)
Figure 29, table 8

Otocinclus spectabilis Eigenmann, 1914: 229–230, figs. 2–3 (original description).—Eigenmann, 1916: 78–79 (holotype figured).—Eigenmann, 1922: 227 (list of freshwater fish species of Colombia).—Fowler, 1942 (list of fishes of Colombia).—Gosline, 1945: 100 (list of catfish species of South and Central America).

Nannoptopoma spectabilis Schaefer, 1996a: 915, figs. 1a–2 (redescription and placement in new genus *Nannoptopoma*).—Eschmeyer and Ferraris, 1998: 1583 (catalog of fishes).

Nannoptopoma spectabile Schaefer, 2003: 324 (list of hypoptopomatine fish species).—Ferraris, 2007: 272 (list of catfish species).

HOLOTYPE: CAS 33806, 22.5 mm SL, female, Quebrada Cramalote, Villavicencio, Dpto. Meta, Colombia; collected by M. González, 1914.

PARATYPES (collected with holotype): CAS 33807, 6 females and 2 males, 21.3–27.4 mm SL.

NON-TYPES: ANSP 136597 no data (5 ♀, 6 ♂, 20.9–24.5 mm SL). **COLOMBIA, Meta**: ANSP 134008 (4 unsexed, 21.4–23.1 mm SL) Quebrada Venturosa between La Balsa and Puerto López; ANSP 134009 (1 ♀ + 1 ♂, 23.6–24.6 mm SL) Río Negro, downstream of Villavicencio–Puerto López hwy.; ANSP 134010 (2 ♀, 21.9–23.1 mm SL) same data than ANSP 134008; ANSP 134011 (♀, 21.9 mm SL) same data than ANSP 134009; ANSP 133767 (7 unsexed, 1 cs, 21.0–24.6 mm SL) caño Emma, El Viento ranch, 33.5 km NE Puerto López. **ECUADOR, Napo-Pastaza**: FMNH 101545 (♂, 25.9 mm SL) Río Napo, 10.7 km upstream from bridge at Coca. **PERU, Amazonas**: LACM 41725-16 (3 unsexed, 24.9–25.9 mm SL) Río Santiago at La Poza; LACM 41726-18 (1 ♀ + 1 ♂, 24.3–26.6 mm SL) Río Santiago at La Poza; LACM 41729-36 (9 unsexed, 1 cs, 24.6–29.2 mm SL) Río Santiago at La Poza; LACM 41730-10 (1 ♂ + 1 ♀, 26.3–27.4 mm SL) Río Santiago at La Poza. **VENEZUELA, Barinas**: MCNG 6594 (7 unsexed, 21.9–23.9 mm SL) caño on the road between Puerta de Piedra and Santa Barbara. **Bolivar**: ANSP 139524 (1 unsexed, 18.4 mm SL) Quebrada Cuchivero, tributary of Río Matos. **Portuguesa**: CAS 64397 (2 unsexed, 19.2–19.8 mm SL) caño Maraca, km 60, Guanare to Guanarito Road.

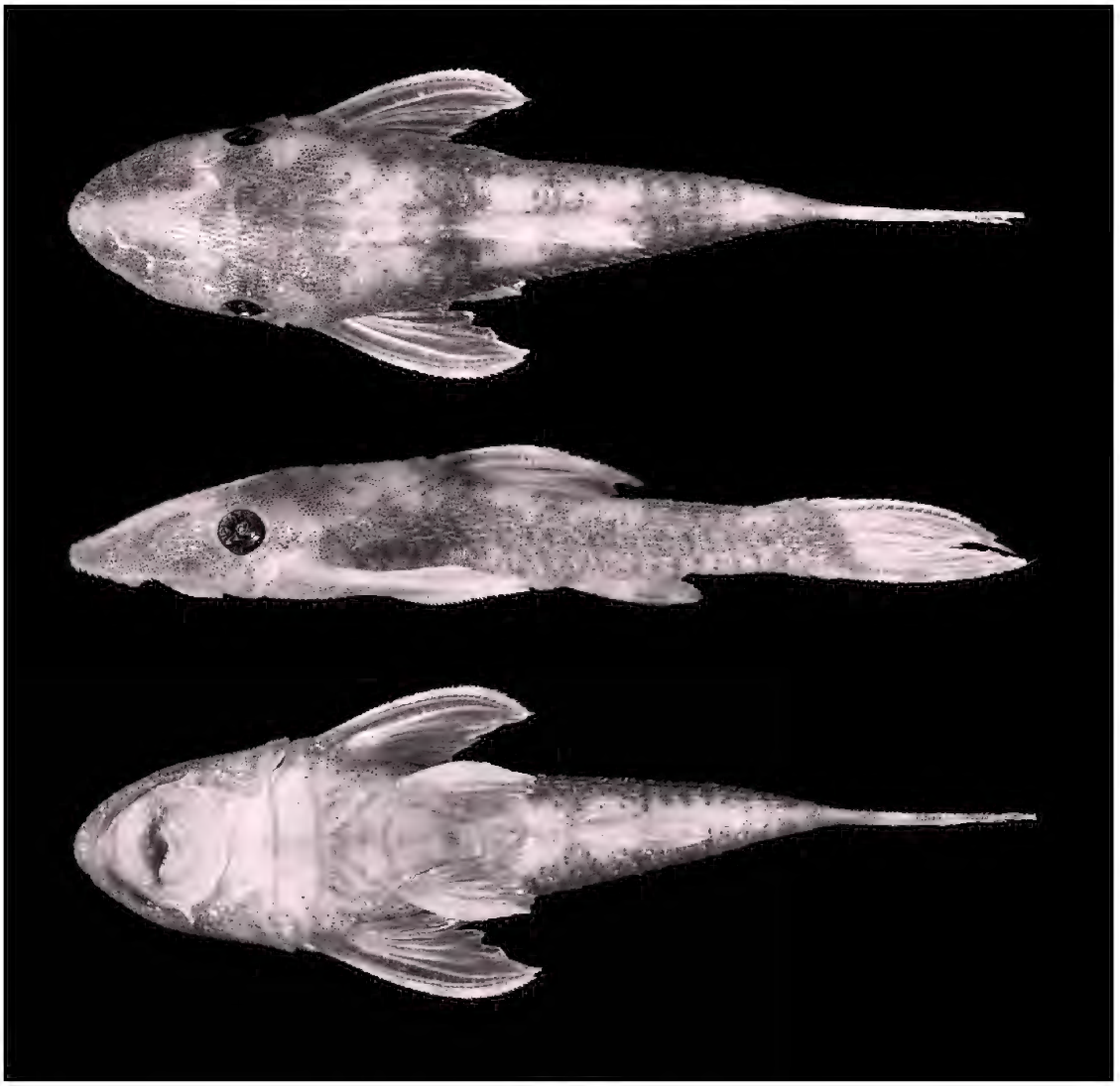

Fig. 29. *Hypoptopoma spectabile*, ANSP 136597, 23.4 mm SL male, in dorsal, lateral and ventral views.

DIAGNOSIS: *Hypoptopoma spectabile* is distinguished from all congeners, except *H. sternoptychum*, by the pattern of abdominal plates, consisting of a pair of slender plates posterior to the coracoids followed by a series of 1–3 unpaired medial abdominal plates (Schaefer, 1996a: fig. 1a) (vs. two or three series of abdominal plates), by having the posterior process of the coracoids strongly curved, with its distal tip pointing dorsally (vs. posterior process smoothly curved, with its distal tip pointing posterodorsally), and by the absence of basipterygium fenestrae (vs. presence of basipterygium fenestrae). *Hypoptopoma spectabile* can be distinguished from *H. sternoptychum* by the absence of thoracic plates, fewer total lateral plates (20–22 (20) vs. 21–22 (21)), fewer dentary teeth (20–31 (24) vs. 21–37 (30)), narrow dorsal interorbital distance (mean dorsal interorbital distance 58.5 vs. 63.5), pelvic fin placed more anteriorly (mean abdominal length 12.7 vs. 15.5), shorter pectoral fin; length not reaching anal-fin origin, (mean pectoral-fin spine length 29.8 vs. 39.3), and by the absence of marginal odontodes (vs. marginal odontodes present in adults longer of 35 mm SL).

TABLE 8
Morphometric and Meristic Data of *Hypoptopoma spectabile*
Holotype: CAS 33806.

		Paratypes and Nontypes				
	Holotype	*N*	Range		Mean	sd
Standard length	22.5	51	18.4	27.4		
PERCENT OF STANDARD LENGTH						
Head length	36.2	41			37.2	2.0
Body depth	17.6	41			19.7	1.2
Pectoral-fin spine length	25.1	41			29.8	2.1
Abdominal length	11.4	41			12.7	1.0
Cleithral width	22.8	41			24.2	1.3
PERCENT OF HEAD LENGTH						
Horizontal eye diameter	17.1				16.1	1.4
Dorsal interorbital distance	52.5				58.5	3.8
LATERAL SERIES OF PLATES						
Medial series	20	41	20	22	20	0.4
TEETH						
Premaxillary teeth	25	39	21	36	27	3.3
Dentary teeth	23	41	20	31	24	2.4

DESCRIPTION: Morphometric and meristic data presented in table 8. Body moderately robust; greatest body depth at dorsal-fin origin. Dorsal profile of head and body straight from tip of snout to supraoccipital, supraoccipital convex, nearly straight to dorsal-fin origin; slightly concave at dorsal-fin base; straight from posteriormost dorsal-fin ray to anteriormost procurrent caudal-fin ray. Ventral profile of head and body straight to slightly concave from tip of snout to anteriormost procurrent caudal-fin. Head depressed, almost as wide as cleithral width; lateral process of lateral ethmoid bone visible dorsally. Snout anterior margin parabolic in dorsal view; almost flat anterior to naris. Posterior surface of bony pit of nasal organ sharply inclined. Ventral surface flat from snout to anus, ovoid in cross section at anal base; caudal peduncle round in cross section.

Eyes moderate in size, positioned closer to posterior tip of compound pterotic than to tip of snout. Ventral margin of orbit located on lateral side of head. Dorsal interorbital distance shorter than ventral interorbital distance.

Total plates in medial series typically 20–22 (20). Dorsal series plates 18; middorsal series plates 4; midventral series plates 11–12, 3 plates anterior to first ventral series plate; ventral series plates 18. Second plate of midventral series contacting two plates of medial series.

Abdomen covered by one pair of slender plates posterior to coracoids, interdigitated at or near midline, followed by 1–2 medial unpaired rectangular to trapezoid-shaped plates. Single anal plate. Thoracic plates absent. Canal in preopercle present, semicircular; anteriormost pore located between ventral canal-bearing plate and fourth infraorbital, framed by notch at posterolateral margin of canal-bearing plate; notch on lateral margin of fourth infraorbital reduced.

Small odontodes evenly distributed on head; odontodes on anterior snout margin not arranged in well-defined series. No odontode-free discontinuity between ventral and dorsal odontode series; odontodes dorsal, ventral, and lateral to snout tip slightly larger than those on dorsal surface of head. Lamina of trunk plates with longitudinal rows of odontodes; marginal odontodes absent. Anterior margin of pectoral-fin spine and ventral surface of pelvic-fin spine with enlarged odontodes.

Total vertebrae 25. Premaxillary teeth 23–36 (29); dentary teeth 20–37 (30). Maxillary barbels short, reaching to anterior margin of ventral canal-bearing plate.

Dorsal-fin origin at vertical through middle of pelvic fin. Depressed dorsal fin surpassing vertical through end of anal-fin base. Depressed pectoral fin reaching to anus, not reaching to origin of anal fin. Pectoral spine serrae absent. Depressed pelvic fin reaching to anus. Caudal-fin margin moderately forked; upper and lower lobes equal. Adipose fin absent.

COLOR IN ALCOHOL: Ground color tan and pale ochre. Dorsal surface of head with clumped distribution of melanophores yielding mottled appearance, pigment concentrated in paired depression between tip of snout and nares. Sides of head and trunk with patchy distribution of melanophores, not arranged in distinct spots or bands; pigment slightly more concentrated between compound pterotic and dorsal cleithrum margin. Pigment arranged in series of three saddles between dorsal-fin origin and caudal fin; first saddle most intense and located at dorsal-fin origin, extending between nuchal plate and base of third branched dorsal-fin ray, and onto anterior dorsal-fin base; second saddle faint, comprised of scattered melanophores and located between base of last branched ray and posterior limit of dorsal fin when depressed; third saddle located midway between dorsal and caudal fins. Ventral surface of body mostly unpigmented, except for scattered melanophores on posterior portion of trunk and on anterior surface of lip. Paired and unpaired fins with few light dark brown bands. Dorsal fin with three light bands. Caudal fin with intense concentration of pigment at fin base; pigment extending slightly more posterior along length of ventralmost 3–4 caudal-fin branched rays, lanceolate plates at base of caudal fin light brown, continuous with basal pigmentation on caudal fin.

SEXUAL DIMORPHISM: Male urogenital papilla elongated. Patch of tightly arranged small odontodes on four paired plates between pelvic-fin origin and anus. Males with soft-tissue flap on dorsal proximal surface of first branched pelvic-fin ray. Female anus tubular, without separate urogenital papilla. In females, size and arrangement of odontodes on plates lateral to anus similar to adjacent plates, without distinct patch of differentially arranged odontodes.

DISTRIBUTION: Known from upland tributaries of the Río Amazonas in Colombia, Ecuador and Peru and tributaries of the upper Río Orinoco in Venezuela (fig. 27).

Hypoptopoma sternoptychum (Schaefer, 1996)
Figure 30, table 9

Nannoptopoma sternoptychum Schaefer, 1996a: 920, fig. 1b, 4 (original description).— Eschmeyer and Ferraris, 1998: 1610 (catalog of fishes).—Schaefer, 2003: 324 (list of hypoptopomatine fish species).—Bogotá-Gregory and Maldonado-Ocampo, 2006: 77 (list of fishes of the Amazon basin in Colombia).—Ferraris, 2007: 273 (list of catfish species).

HOLOTYPE: MUSM 4097, 33.2 mm SL, male (type locality: Quebrada Mariposa at Cusco-Amazonico Lodge, Puerto Maldonado, Tambopata, Dpto. Madre de Dios, Peru); collected by H. Ortega, 18 December 1989.

PARATYPES: **BOLIVIA**, **Beni**: USNM 305836 (unsexed, 27.4 mm SL) E.B.B. Campamento Trapiche Pozo, on hour by dirt road from la Pascana; USNM 305600 (4 unsexed, 25.1–32.3 mm SL) Río Matos below road crossing, 48 km E of San Borja; USNM 305610 (5 unsexed, 1 cs, 29.2–36.5 mm SL) Río Curiraba, 10 km NE of El Porvenir Biol. Station, 40 air km E of San Borja. **BRAZIL**, **Amazonas**: USNM 177720 (female, 23.1 mm SL) Rio Urubu. **COLOMBIA**, **Amazonas**: USNM 216851 (female, 33.4 mm SL) Leticia. **ECUADOR**, **Napo-Pastaza**: FMNH 101542 (male, 36.6 mm SL) Río Aguarico, 1 river km above to mouth of the Río Lagartacocha, beach on both banks; FMNH 101546 (female, 32.5 mm SL) Río Napo, mouth of the Río Tiputini near Tiputini military barracks. **PERU**, **Madre de Dios**: MUSM 7551 (male, 32.1 mm SL) (collected with holotype); Loreto, SU 36221 (2 females, 23.7–30.6 mm SL).

DIAGNOSIS: *Hypoptopoma sternoptychum* is distinguished from all congeners, except *H. spectabile*, by the pattern of abdominal plates, consisting of a pair of slender plates posterior to the coracoids followed by a series of 1–3 unpaired medial abdominal plates (Shaefer 1996a: fig. 1a) (vs. two or three series of abdominal plates), by having the posterior process of the coracoid strongly

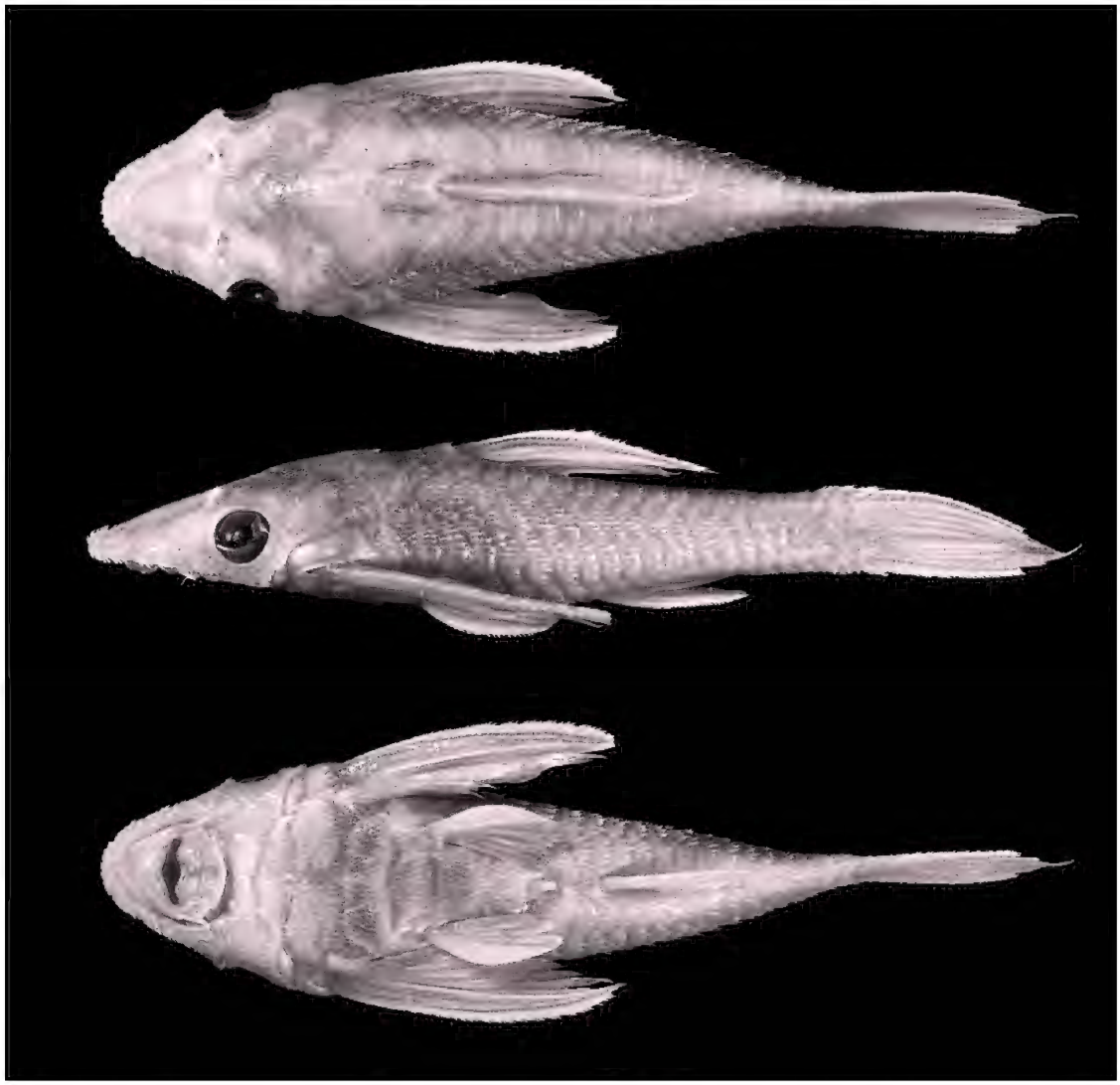

Fig. 30. *Hypoptopoma sternoptychum*, SU 36221, 30.6 mm SL female, in dorsal, lateral and ventral views.

curved, with its distal tip pointing dorsally (vs. posterior process smoothly curved, with its distal tip pointing posterodorsally), and by the absence of basipterygium fenestrae (vs. presence of basipterygium fenestrae). *Hypoptopoma sternoptychum* can be distinguished from *H. spectabile* by the presence of thoracic plates, greater number of total lateral plates (21–22 (21) vs. 20–22 (20)), greater number of dentary teeth (21–37 (30) vs. 20–31 (24)), greater dorsal interorbital distance (mean dorsal interorbital distance 63.5 vs. 58.5), pelvic fin placed more posteriorly (mean pectoral-pelvic distance 15.5 vs. 12.7), and longer pectoral fin, length reaching or surpassing the anal-fin origin (mean pectoral-fin spine length 39.3 vs. 29.8).

DESCRIPTION: Morphometric and meristic data presented in table 9. Body moderately robust; greatest body depth at dorsal-fin origin. Dorsal profile of head and body straight from tip of snout to supraoccipital, supraoccipital convex, small tuft of 3–5 enlarged odontodes at posterior supraoccipital tip; trunk profile nearly straight to dorsal-fin origin; slightly concave at dorsal-

TABLE 9
Morphometric and Meristic Data of *Hypoptopoma sternoptychum*
Holotype: MUSM 4097.

		Paratypes and Nontypes				
	Holotype	*N*	Range		Mean	sd
Standard length	33.2	16	23.1	36.6		
PERCENT OF STANDARD LENGTH						
Head length	35.5	16			37.9	1.7
Body depth	21.1	16			19.4	1.0
Pectoral-fin spine length	40.0	16			39.3	2.0
Abdominal length	17.0	16			15.5	1.1
PERCENT OF HEAD LENGTH						
Horizontal eye diameter	19.2	16			18.7	19.2
Dorsal interorbital distance	67.4	16			63.5	3.4
LATERAL SERIES OF PLATES						
Medial series	22	16	21	22	21	0.4
TEETH						
Premaxillary teeth	32	15	23	36	29	3.3
Dentary teeth	34	16	21	37	30	4.1

fin base; straight from posteriormost dorsal-fin ray to anteriormost procurrent caudal-fin ray. Ventral profile of head and body straight to slightly concave from tip of snout to anteriormost procurrent caudal-fin ray. Head depressed, almost as wide as cleithral width; lateral process of lateral ethmoid bone visible dorsally. Snout anterior margin parabolic in dorsal view, lateral margins nearly straight, snout tip rounded; rostrum depressed anterior to nares. Posterior surface of bony pit of nasal organ sharply inclined. Ventral surface flat from snout to anus, ovoid in cross section at anal base; caudal peduncle round in cross section.

Eyes moderate in size, positioned closer to posterior tip of compound pterotic than to tip of snout. Ventral margin of orbit located on lateral side of head; eyes visible from below. Dorsal interorbital distance shorter than ventral interorbital distance.

Total plates in medial series typically 21–22 (21). Dorsal series plates 19; middorsal series plates 4; midventral series plates 12, three plates anterior to first ventral series plate; ventral series plates 19. Second plate of midventral series contacting two plates of medial series.

Abdomen covered by one pair of slender plates posterior to coracoids, interdigitated at or near midline, followed by 2–3 unpaired medial rectangular to trapezoid-shaped plates. Single anal plate. Thoracic plates present, 1–2 pairs. Canal in preopercle present, semicircular; anteriormost pore located between ventral canal-bearing plate and fourth infraorbital, framed by notch on posterolateral margin of canal-bearing plate; notch on lateral margin of fourth infraorbital reduced.

Small odontodes evenly distributed on head. Odontodes on anterior snout margin not arranged in well-defined series, no odontode-free discontinuity between ventral and dorsal odontode series; odontodes dorsal, ventral and lateral to snout tip slightly larger than those on dorsal surface of head. Lamina of trunk plates with longitudinal rows of odontodes; marginal odontodes present in mature adults. Anterior margin of pectoral-fin spine and ventral surface of pelvic-fin spine with enlarged odontodes.

Total vertebrae 26. Premaxillary teeth 23–36 (29); dentary teeth 21–37 (30). Maxillary barbels short, reaching to anterior margin of ventral canal-bearing plate.

Dorsal-fin origin at vertical through middle of pelvic fin. Depressed dorsal fin surpassing vertical through end of anal-fin

base. Depressed pectoral fin surpassing origin of anal fin. Pectoral spine serrae absent. Depressed pelvic fin reaching to anus. Caudal-fin margin moderately forked; upper and lower lobes equal. Adipose fin absent.

COLOR IN ALCOHOL: Ground color tan and pale ochre. Dorsal surface of head with clumped distribution of melanophores, yielding mottled appearance. Pigmentation especially pronounced posterior to dorsal fin; pigment concentrated in paired depression between tip of snout and nares. Sides of head and trunk with patchy distribution of melanophores, arranged in distinct irregular blotches; pigment slightly more concentrated between compound pterotic and cleithrum dorsal margin. Pigment arranged in series of three saddles between dorsal-fin origin and caudal fin; first saddle most intense and located at dorsal-fin origin, extending between nuchal plate and base of third branched dorsal-fin ray, and onto anterior dorsal-fin base; second saddle faint, comprised of scattered melanophores and located between base of last branched rays and margin of fouth postdorsal plate; third saddle located midway between dorsal and caudal fins, occasionally separated from a fourth saddle by unpigmented area equal to one plate width. Ventral surface of body mostly unpigmented except for scattered melanophores on posterior portion of trunk and on anterior surface of lip. Paired and unpaired fins with few dark brown bands. Dorsal fin with three bands. Caudal fin with intense amorphous concentration of pigment at base. Lanceolate plates at base of caudal fin light brown.

SEXUAL DIMORPHISM: Male urogenital papilla elongated. Patch of tightly arranged small odontodes on four paired plates between pelvic-fin origin and anus. Males with soft-tissue flap on dorsal proximal surface of first branched pelvic-fin ray. Female anus tubular, without separate urogenital papilla. In females, size and arrangement of odontodes on plates lateral to anus similar to adjacent plates, without distinct patch of differentially arranged odontodes.

DISTRIBUTION: Known from tributaries from the upper Río Amazonas in Ecuador and Peru, and central Río Amazonas, including the upper Rio Madeira basin, in Bolivia and Peru (fig. 27).

Hypoptopoma bianale, new species
Figure 31, table 10

HOLOTYPE: FMNH 105077 (♀, 53.7 mm SL) Colombia: Amazonas, Amazon River at 2 to 3 miles upstream from Leticia; collected by Navarro et al., 13 November 1973.

PARATYPES (all material collected with holotype): FMNH 117745 (7 ♀ + 3 ♂, 2 cs, 37.2–47.9 mm SL); AMNH 243576 (1 ♀ + 1 ♂, 46.1–47.3 mm SL).

NON-TYPES: **PERU**, **Loreto**: MZUSP 36208 (1 ♀, 43.0 mm SL) Río Ucayali, Sgto. Lores; SIUC 28113 (1 ♀, 39.0 mm SL) Río Napo, confluence with Río Mazán, ca. 2–3 km N (town of) Mazán; SU 33272 (1 ♂, 42.6 mm SL) Río Ampiyacu. **Ucayali**: MHNG 2390.25 (1 ♀, 44.5 mm SL) Pucallpa, Río Ucayali, San Antonio; MZUSP 36206 (1 ♂, 43.2 mm SL) Pucallpa, Río Ucayali; MZUSP 36207 (1 ♀, 42.03 mm SL) Pucallpa, Río Ucayali, Laguna Yarinacocha. **BRAZIL**, **Amazonas**: MZUSP 27624 (1 ♀, 41.2 mm SL) Costa Japao, Baixao Rio Japurá, Mun. de Tefé; MZUSP 36211 (4 ♀, 41.0–51.8 mm SL) Rio Solimões, prox. I. Bururuá acima do boca do Jutaí.

DIAGNOSIS: *Hypoptopoma bianale* is distinguished from all congeners by presence of two medial anal plates (vs. single medial anal plate in all other species of *Hypoptopoma*) (fig. 9C).

DESCRIPTION: Morphometric and meristic data presented in table 10. Body robust, stocky, greatest body depth at dorsal-fin origin, least depth at caudal peduncle. Dorsal profile of head and body straight from tip of snout to posterior tip of supraoccipital, smoothly convex at level of predorsal plates. Dorsal profile of trunk straight from dorsal-fin origin to caudal procurrent rays. Ventral profile of head and abdomen straight to slightly convex from snout tip to caudal-fin procurrent rays (not apparent in lateral view of head profile). Head moderately depressed, slightly acute, smoothly concave anterior to naris. Posterior surface of bony pit of nasal organ gradually inclined. Lateral process of

Fig. 31. *Hypoptopoma bianale*, holotype, FMNH 105077, 53.7 mm SL female, in dorsal, lateral, and ventral views.

lateral ethmoid bone slightly visible in dorsal view of head. Trunk cross section ovoid to progressively compressed posterior to dorsal fin.

Eyes moderately large, positioned slightly closer to posterior tip of compound pterotic than to tip of snout. Ventral margin of orbit close to ventral margin of head. Dorsal interorbital distance roughly equal to ventral interorbital distance.

Total plates in medial series 22. Dorsal series plates 19; middorsal series plates 3–4 (4); midventral series plates 12–13 (13), three plates anterior to first ventral series plate; ventral series plates 19. Second plate of midventral series contacting two plates of medial series.

Abdomen covered by paired series of lateral sickle-shaped plates, with unequal number of plates between left and right series, 4–6; anterior azygous plate present; lateral series make contact along midline in fully developed individuals. Presence of two medial anal plates positioned along longitudinal axis of body, between pelvic fins laterally, abdominal plates anteriorly,

TABLE 10
Morphometric and Meristic Data of *Hypoptopoma bianale*
Holotype: FMNH 105177. Paratypes: FMNH 117745; AMNH 243576. Nontypes: MNHG 2390.25; MZUSP 27624, 36203, 36206, 36207, 36208, 36211; SU 33272.

		Paratypes and Nontypes				
	Holotype	*N*	Range		Mean	sd
Standard length	46.5	23	37.2	53.7	44.3	4.03
PERCENT OF STANDARD LENGTH						
Predorsal length	46.7	23	46.7	50.3	48.3	0.95
Head length	35.3	23	34.7	37.1	35.9	0.76
Body depth	20.4	23	18.5	23.8	20.3	1.27
Dorsal-fin spine length	33.5	18	30.2	36.9	34.4	1.75
Trunk length	42.8	23	34.6	42.4	39.4	2.69
Pectoral-fin spine length	31.3	23	27.1	42.1	31.0	2.71
Abdominal length	17.8	23	15.2	18.8	17.2	1.00
Caudal-peduncle length	32.4	23	29.3	33.2	31.4	1.09
Caudal-peduncle depth	11.4	23	11.0	12.8	11.7	0.55
Head depth	17.4	23	15.8	19.2	17.6	0.93
Snout length	19.3	23	17.6	20.2	19.3	0.63
Horizontal eye diameter	6.7	14	6.2	7.7	7.1	0.45
Least orbit-naris distance	3.9	14	3.2	4.7	4.2	0.41
Dorsal interorbital distance	21.2	23	20.6	22.8	21.4	0.56
Ventral interorbital distance	21.1	23	19.4	21.9	21.0	0.78
Cleithral width	27.6	23	25.3	28.8	27.4	0.79
Head width	24.6	23	23.3	28.3	25.2	1.41
Interpelvic distance	9.0	23	8.4	13.4	10.6	1.49
PERCENT OF HEAD LENGTH						
Body depth	57.7	23	51.2	67.5	56.6	3.72
Head depth	49.3	23	42.8	54.6	49.1	2.76
Snout length	54.7	23	49.1	56.5	53.8	1.71
Horizontal eye diameter	19.0	14	17.4	21.6	19.9	1.14
Least orbit-naris distance	11.0	14	9.0	13.2	11.6	1.14
Dorsal interorbital distance	60.1	23	56.9	63.2	59.7	1.75
Ventral interorbital distance	59.8	23	54.1	61.6	58.6	2.21
Cleithral width	78.1	23	68.9	80.9	76.4	2.84
Head width	78.3	23	59.1	94.3	69.9	8.21
Interpelvic distance	31.7	23	21.8	46.8	29.6	5.64
PERCENT OF CLEITHRAL WIDTH						
Snout	71.9	23	66.0	78.2	70.4	2.7
LATERAL SERIES OF PLATES						
Dorsal series	19	23	19	19	19	0.0
Middorsal series	4	23	3	4	4	0.3
Medial series	22	23	22	22	22	0.0
Midventral series	13	23	12	13	13	0.2
First midventral plates	3	23	3	3	3	0.0
Ventral series	19	23	19	19	19	0.0
ABDOMINAL SERIES OF PLATES						
Right lateral series	5	22	4	6	5	0.7
Left lateral series	5	22	4	6	5	0.5
TEETH						
Premaxillary teeth	30	22	21	29	25	2.7
Dentary teeth	24	22	20	27	23	2.0

and anus posteriorly; anterior plate larger than posterior plate (fig. 9C). Thoracic plates present, 4–5. Canal in preopercle present, semicircular; anteriormost pore located between ventral canal-bearing plate and fourth infraorbital, framed by notch at posterolateral margin of canal-bearing plate and lateral margin of fourth infraorbital.

Small odontodes evenly distributed on head. Odontodes on rostral margin of snout enlarged and arranged in irregular lines, without odontode-free discontinuity between dorsal and ventral margins. Lamina of trunk plates with odontodes arranged in longitudinal rows; plates progressively smoother in ontogeny; marginal odontodes present in mature adults. Anterior margin of pectoral-fin spine and ventral surface of pelvic-fin spine with enlarged odontodes.

Total vertebrae 26. Premaxillary teeth 21–29 (25), dentary teeth 20–27 (23). Maxillary barbels extending slightly beyond anterior margin of ventral canal-bearing plate.

Dorsal-fin origin located at vertical through pelvic-fin origin; depressed dorsal fin reaching almost to vertical through posterior tip of anal fin. Pectoral fin reaching to vertical through posterior tip of pelvic fin. Pectoral spine serrae along entire posterior margin, except for short basal segment; individual serrae oriented oblique to spine shaft. Pelvic fin short, unbranched and first branched rays equal in length; when depressed reaching to plate anterior to anal-fin spine. Caudal-fin margin concave. Adipose fin absent.

COLOR IN ALCOHOL: Overall body pigmentation relatively uniform, ground color tan to pale ochre. Melanophores variably light brown, slightly more concentrated along base of plates, dorsal portions of head, lateral border of compound pterotic, cleithral process, opercle, and base of dorsal fin. No lateral stripe on trunk. Ventral surface of body mostly unpigmented. Scattered dark melanophores present on anterior surface of lip. Fins with pale brown bands (dorsal fin 4–6; caudal fin 4–5). Triangular spot of dark brown melanophores at base of caudal-fin branched rays, mostly extended over basal plates and lower lobe, progressively widening toward lower marginal ray; caudal-fin bars mainly visible on marginal rays and outer most branched rays.

SEXUAL DIMORPHISM: Male urogenital papilla short, half-length of flaplike anus, which totally covers and joins base of papilla. Males with patch of tightly arranged small odontodes on second through fourth plates of ventral series, lateral to urogenital papilla. Female anus tubular, without separate urogenital papilla. In females, size and arrangement of odontodes on plates lateral to anus similar to adjacent plates, without distinct patch of differentially arranged odontodes.

DISTRIBUTION: Rio Solimões in Brazil and Río Ucayali in Peru (fig. 32).

ETYMOLOGY: The specific epithet *bianale* is a reference to the presence of two anal plates (Lt. *bi*, meaning "two"; Lt. *analis*, from *anal* (adaptation from modern Latin; *Oxford English Dictionary*: "Of or pertaining to the anus, or excretory opening").

Hypoptopoma inexspectatum (Holmberg, 1893)
Figure 33, table 11

Aristommata inexspectata Holmberg, 1893a: 96; 1893b: 354 (original description; Río Paraguay, al pie de Formosa).

Aristommata inexpectata.—Braga and Piacentino, 1994: 102 (catalog of type specimens at MACN).

Hypoptopoma guentheri Boulenger, 1895: 526 (original description; Descalvados, Mato Grosso, Brazil).—Boulenger, 1896: 31 (list of fishes from Río Paraguay; key to *Hypoptopoma* species).—Regan, 1904: 264 (list of loricariid species; key to *Hypoptopoma* species).—Fowler, 1954: 125 (list of freshwater fishes of Brazil).—Ringuelet and Arámburu, 1961: 52 (list of freshwater fishes of Argentina).—Isbrücker, 1980: 88 (list of loricariid species).—Isbrücker, 2002: 28 (list of loricariid species).

Hypoptopoma inexpectatum.—Berg, 1898: 11 (established synonymy between *Aristommata* and *Hypoptopoma*).—Miranda Ribeiro, 1911: 97–99 (list of fishes of Brazil; key to *Hypoptopoma* species).—Pearson, 1937: 112 (list of fishes of Bolivia).— López et al., 1987: 30 (list of freshwater fishes of Argentina).—García, 1992 (Argentina: occurrence in Rio Paraná, Misiones).—Isbrücker, 2002: 26, 28 (list of loricariid species).

Oxyropsis inexpectatus.—Eigenmann, 1910: 412 (list of freshwater fishes of South America).—Bertoni, 1914: 9 (list of fishes of Para-

Fig. 32. Drainage map of South America showing distribution of *H. bianale* (dots + circle), *H. inexspectatum* (squares), *H. steindachneri* (triangles), and *H. elongatum* (stars). Open symbols designate type localities; some symbols represent more than one locality record.

guay).—Bertoni, 1939: 53 (list of fishes of Paraguay).

Oxyropsis güntheri.—Eigenmann, 1910: 419 (list of freshwater fishes of South America).

Oxyropsis guentheri.—Pozzi, 1945: 263, 275 (list of freshwater fishes of Argentina).—Fowler, 1954: 110 (list of freshwater fishes of Brazil).

Oxyropsis inexpectata.—Pozzi, 1945: 263, 275 (list of freshwater fishes of Argentina).

Hypoptopoma inexspectata.—Ringuelet et al., 1967: 391 (annotated list of freshwater fish of Argentina).—Boeseman, 1974: 265 (list of nominal species of *Hypoptopoma*).— Braga and Azpelicueta, 1986: 87 (Argentina: occurrence

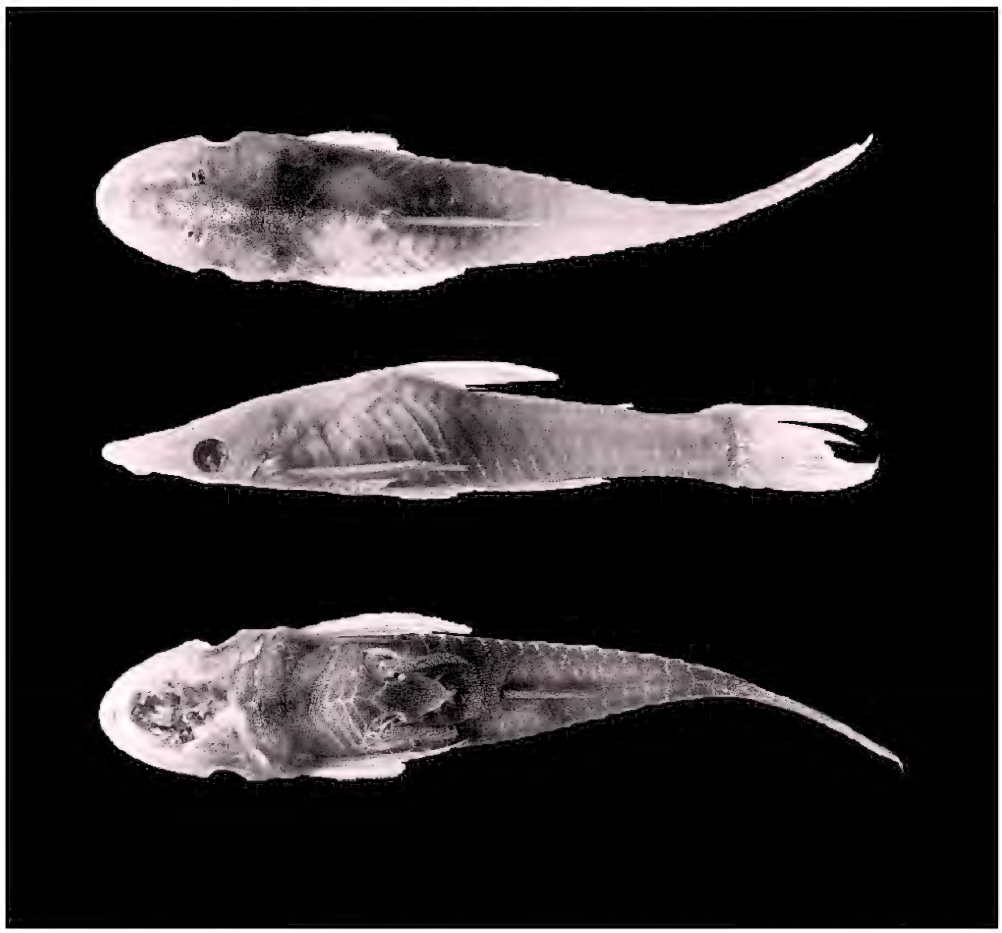

Fig. 33. *Hypoptopoma inexspectatum*, holotype, MACN 5164, 53.6 mm SL, in dorsal, lateral, and ventral views.

in Río Paraná, Misiones).— Aquino and Miquelarena, 1994: 211–212 (anatomy).— Aquino, 1997: 5, 8 (redescription, distribution).—Aquino, 1998: 232–237, 4 figs. (anatomy of myodome).—Aquino and Miquelarena, 2000 (2001): 1–18 (redescription; anatomy).— Liotta, 2006: 356 (geographic distribution of freshwater fish of Argentina).

Hypoptopoma inexpecta.—Gómez and Chébez, 1996: 62 (list of fishes of Misiones, Argentina; misspelling).

Hypoptopoma gulare not of Cope, 1878.—Ringuelet and Arámburu 1961: 52 (list of freshwater fishes of Argentina, Argentina: Rio Paraguay, misidentification).—Ringuelet et al., 1967: 390 (Argentina: Rio Paraguay, misidentification).

Hypoptopoma inexspectatum.—Isbrücker, 1980: 88 (list of loricariid species).—Weber et al., 1992: 11 (Paraguay: occurrence in Río Negro).— Eschemeyer and Ferraris, 1998: 773 (catalog of fishes).—Schaefer, 2003: 323 (list of hypoptopomatine species).—López et al., 2005: 8, 18, 28 (list of fishes of the Iguazú, Paraná, and Uruguay river basins in Argentina).—Veríssimo et al., 2005 (Brazil: occurrence in Rio Paraguay basin).—Ferraris, 2007: 250 (list of catfish species).

HOLOTYPE: MACN 5164 (53.6 mm SL) Argentina: Río Paraguay, near Formosa city; collected by Solari, March 1885.

OTHER MATERIAL EXAMINED: **ARGENTINA**, **Buenos Aires**: ILPLA 875 (1 ♂, 51.7 mm SL) Río Paraná drainage, Río Yaguarón, San Nicolás, Balneario Rio Municipal; MACN 6547 (1) Buenos Aires, Palermo, Lago. **Corrientes**: ILPLA 268 (1 ♀, 44.7 mm SL) Isla Toro; ILPLA 269 (20 ♀ + 20 ♂, 16 cs, 34.0–68.4 mm SL) Río Paraná,

TABLE 11
Morphometric and Meristic Data for *Hypoptopoma inexspectatum*
Holotype: MACN 5164. Nontypes: ILPLA 268, 269, 270, 875 (morphometric data only); NRM 22832 (meristic data only).

		Nontypes			
	Holotype	*N*	Range	Mean	sd
Standard Length	37.3	13	40.8 60.7	51.3	6.21
PERCENT OF STANDARD LENGTH					
Predorsal length	38.8	13	44.6 47.8	46.7	0.90
Head length	29	13	33.5 37.1	35.3	1.05
Body depth	10.6	13	15.2 20.7	18.7	1.40
Dorsal-fin spine length		10	0.0 32.3	24.5	8.97
Trunk length	51.8	13	40.6 45.4	42.3	1.26
Pectoral-fin spine length	21.5	12	27.9 30.9	29.4	1.10
Abdominal length	12.9	13	15.3 17.7	16.4	0.67
Caudal-peduncle length	42.5	13	29.9 32.2	31.2	0.88
Caudal-peduncle depth	2.9	13	8.4 10.0	9.4	0.47
Caudal-fin base depth					
Head depth	—	13	14.0 16.9	16.1	0.79
Snout length	—	13	17.2 19.6	18.7	0.57
Horizontal eye diameter	—	13	5.9 7.1	6.5	0.34
Least orbit-naris distance	—	13	3.0 4.1	3.6	0.36
Dorsal interorbital distance	—	13	17.4 19.9	18.6	0.70
Ventral interorbital distance	—	13	17.3 19.3	18.3	0.61
Cleithral width	—	13	22.8 24.6	23.6	0.64
Head width	—	13	19.9 22.8	21.4	0.84
Interpelvic distance	8.6	13	7.5 9.6	8.8	0.60
PERCENT OF HEAD LENGTH					
Body depth	36.4	11	42.7 58.0	51.8	4.72
Head depth	33.5	13	39.3 48.6	45.8	2.66
Snout length	50.2	13	51.3 55.0	53.1	1.42
Horizontal eye diameter	18.4	13	17.1 19.7	18.5	0.63
Least orbit-naris distance	5.6	13	8.3 11.6	10.3	1.08
Dorsal interorbital distance	49.1	13	48.3 55.5	52.6	2.29
Ventral interorbital distance	55.3	13	48.2 53.6	51.8	1.50
Cleithral width	64.1	13	63.9 70.4	66.9	2.20
Head width	55.9	13	57.5 63.0	60.6	1.68
Interpelvic distance	—	13	8.8 0.6	7.5	9.60
PERCENT OF CLEITHRAL WIDTH					
Snout	79.4	13	73.0 82.7	79.5	2.60
LATERAL SERIES OF PLATES					
Dorsal series	—	10	17 18	18	0.3
Middorsal series	—	10	3 3	3	0.0
Medial series		10	20 21	21	0.3
Midventral series	—	9	11 12	12	0.4
First midventral series	—	10	3 3	3	0.0
Ventral series	—	10	17 18	18	0.3
ABDOMINAL SERIES OF PLATES					
Right lateral series	—	10	4 7	5	1.0
Left lateral series	—	10	4 6	4	1.2
TEETH					
Premaxillary teeth	—	10	15 20	18	1.5
Dentary teeth	—	10	13 17	15	1.5

Tuyutí; ILPLA 270 (2 ♂42.8–60.8) Río Paraná; MACN 7014 (5) Río Santa Lucía; MZUSP 10262 to MZUSP 10273 (12, 15.7–55.2 mm SL) Paso de la Patria, Río Paraná. **Formosa**: MACN 3244 (3) Río Formosa. **Misiones**: FMNH 71344 (1 ♂, 0.5 mm SL) Río Paraná. **Santa Fe**: MACN 7013 (3) Helvecia, Arroyo Cigueña; MACN 7015 (+100) Helvecia; MFA-Z-VI.798 (n = 2, 35.5–36.9 mm SL) Dpto. Capital, Río Paraná drainage, riacho Santa Fe. **Bolivia**, **Santa Cruz**: FMNH 59593 (5 ♀ + 12 ♂, 46.6–62.9 mm SL) Puerto Suárez. **Brazil**, **Mato Grosso**: BMNH 1895.5.17.77-82 (paratypes of *Hypoptopoma guentheri*) (3 unsexed, 43.0–55.0 mm SL) Mato Grosso; FMNH 59617 (2 ♀ + 3 juveniles, 29.2–61.1 mm SL) Cáceres, Rio Paraguay; FMNH 59618 (2 juveniles, 35.0–39.7 mm SL) Campo Alegre, Rio Jaurú; FMNH 59619 (1 juvenile, 31.1 mm SL) Campo Alegre, Rio Jaurú; FMNH 69999 (1 ♀ + 1 ♂ + 1 juvenile, 40.1–61.7 mm SL) Descalvados, Rio Paraguay; FMNH 71329 (8 ♀ + 4 ♂ + 1 juvenile, 40.6–67.8 mm SL) Conceição, Rio Paraguay; FMNH 71330 (2 juveniles, 30.9–37.9 mm SL) Campo Alegre, Rio Jaurú, into Rio Paraguay; FMNH 71331 (7 ♀ + 2♂, 50.7–58.0 mm SL) Descalvados, Rio Paraguay; MNRJ 5829 (1) Jacaré, Rio Kolueme; MZUSP 44391 (26 unsexed, 30.6–52.8 mm SL) Rio Paraguay at Cáceres and surroundings; USNM 326344 (26 ♀, 37.9–60.9 mm SL) Rio Paraguay at Cáceres and surroundings. **Mato Grosso do Sul**: FMNH 108587 (4 ♀ + 8 ♂ + 2 juveniles) Rio Negro at road between Nhecolandia and BR 262; MNRJ 1083 (2 unsexed) Porto Esperança; MZUSP 28339 (3 ♀, 35.0–39.0 mm SL) Rio Pixaim, Transpantaneira highway; MZUSP 36183 (1 ♀, 35.8 mm SL) Rio Pequiri, mun. of Coxim; MZUSP 36210 (1 ♀, 35.8 mm SL) tributary of Rio Cuiba, mun. of Cuiba; MZUSP 36223 (62 ♀ + 1 ♂, 34.2–57.5 mm SL) Boca do Croara, Río Cuiba, mun. of B. de Melgaco; MZUSP 36344 (2 unsexed, 36.7–43.6 mm SL) Ladario, Codrasa, Corumba; MZUSP 38034 (1, 49.7 mm SL) Rio Paraguay, Morrinhos, mun. Corumbá. **Paraguay**, **Alto Paraguay**: FMNH 108109 (3 ♀ + 3 juveniles, 26.2–65.8 mm SL) Rio Paraguay, Estancia Voluntad at Puerto Voluntad; FMNH 108110 (2 ♀ + 7 juveniles, 28.1–50.3 mm SL) Riacho Vaqueiro, ca. 2 km above Fuerte Olympo, at base of Cerro Barrero; FMNH 108111 (1 ♀, 50.2 mm SL) Río Paraguay at left margin, above Estancia Cerrito; NRM 22832 (57 ♀, 31.3–59.5 mm SL) Río Paraguay at Estancia Doña Julia and halfway between estancia and village of Bahía Negra. **Amambay**: MHNG 2160.32 (3 ♂, 51.3–57.6 mm SL) arroyo Apa-mi (10 km Sud-Este de Bella Vista). **Central**: MHNG 2475.63 (4 ♀ + 2 ♂, 50.1–61.5 mm SL) San Antonio, Río Paraguay; MHNG 2515.9 (2 ♀ + 4 ♂, 61.4–67.9 mm SL) San Antonio, Río Paraguay; UMMZ 205878 (1 ♂ + 10 juveniles, 3 cs, 11.5–51.8 mm SL) E shore Río Paraguay, 1.0 km S of Puente Remanso bridge. **Concepción**: FMNH 108112 (1 juvenile, 37.2 mm SL) Río Apa, left margin, above San Carlos; MHNG 2353.24 (1 ♂, 54.8 mm SL) Laguna Negra, 15 km. Est. de Paso Bareto; MHNG 2531.70 (2 ♂, 58.5–63.1 mm SL) Riacho La Paz, a 6 km, North to Estancia Primavera. **Presidente Hayes**: FMNH 59621 (4 ♀, 47.3–59.9 mm SL) Villa Hayes; FMNH 77083 (1 ♀, 70.8 mm SL) Villa Hayes; MHNG 2231.65 (2 ♀, 45.3 mm SL) Río Negro, a 160 km route du Transchaco. **San Pedro**: MHNG 2353.26 (2 ♀, 63.5–68.2 mm SL) Río Jejuí Guazú at Jejuí.

Diagnosis: *Hypoptopoma inexspectatum* is distinguished from all congeners by having the odontodes on the snout margin, the rostral plate, and first and second infraorbitals arranged in regular series. Along the rostral margin, the dorsal and ventral series are separated by an odontode-free discontinuity approximately as wide as the base of individual odontodes. Along the first and second infraorbitals, the discontinuity becomes narrower, but forms a dividing line between ventral and dorsal odontode series (fig. 16). The odontode arrangement becomes more irregular posterolateral to the second infraorbital, and individual odontodes become roughly oriented with the trunk axis. In contrast, in all other species of *Hypoptopoma*, the ventral and dorsal odontodes on the rostrum are variably separated and/or covered by soft tissue, and odontodes are typically not clearly aligned in series.

Description: Morphometric and meristic data presented in table 11. Body moderately elongate; greatest body depth at dorsal-fin

Fig. 34. *Hypoptopoma inexspectatum*, ILPLA 875, 51.7 mm SL male, in dorsal, lateral, and ventral views.

origin. Dorsal profile of head and body straight to slightly convex from tip of snout to posterior tip of supraoccipital; straight from dorsal-fin origin to anteriormost procurrent caudal-fin ray; straight from tip of snout to anteriormost procurrent caudal-fin ray. Head moderately depressed, slightly narrower than cleithral width; lateral process of lateral ethmoid visible dorsally, short. Snout slightly spatulate in dorsal view (fig. 34A); slightly concave dorsally anterior to naris. Posterior surface of bony pit of nasal organ sharply inclined. Trunk cross section between pectoral- and pelvic-fin

origins slightly triangular, ovoid to progressively compressed posterior to dorsal fin.

Eyes relatively large, positioned slightly closer to posterior tip of compound pterotic than to tip of snout. Ventral margin of orbit located on ventral surface of head. Dorsal interorbital distance/ventral interorbital distance ratio changing from <1 to >1 during ontogeny.

Total plates in lateral medial series 20–22 (21). Dorsal series plates 17–18 (18); middorsal series plates 3; midventral series plates 11–12 (12), three plates anterior to first plate of ventral series; ventral series plates usually 17–18 (18). Second plate of midventral series contacting two plates of medial series.

Abdomen covered by paired series of lateral sickle-shaped plates, with unequal number of plates between left and right series, 4–7 each; anterior azygous plate present; medial plates, if present, not forming well-defined series (in 3 of 101 individuals examined). Single anal plate present. Thoracic plates present, 2–6. Canal in preopercle present, semicircular; anteriormost pore located between ventral canal-bearing plate and fourth infraorbital, framed by notch at posterolateral margin of canal-bearing plate and lateral margin of fourth infraorbital.

Small odontodes evenly distributed on head. Odontodes on rostral margin of snout, rostral plate, first and second infraorbitals arranged in regular series. Along rostral plate, dorsal and ventral series separated by odontode-free discontinuity approximately as wide as base of individual odontodes; along first and second infraorbitals, discontinuity becoming narrower but still clearly separating ventral and dorsal series. Lamina of trunk plates with longitudinal rows of odontodes and becoming progressively smoother ontogenetically; marginal odontodes present in mature adults.

Total vertebrae 25. Premaxillary teeth 15–20 (18); dentary teeth 17–17 (15). Maxillary barbels short, reaching slightly beyond anterior margin of ventral canal-bearing plate in adults.

Dorsal-fin origin located slightly posterior to vertical through pelvic-fin origin. Depressed dorsal fin reaching to vertical through posterior half of anal-fin base. Depressed pectoral fin reaching anus, not reaching to insertion of anal-fin spine. Extension of serrae along pectoral spine margin reduced ontogenetically from proximal two-thirds in smaller specimens to middle third in larger specimens; individual serrae oriented orthogonal to spine shaft. Pelvic fin short, unbranched and first branched rays of equal length. Depressed fin reaching to anus, but not reaching to insertion of anal-fin spine. Caudal-fin margin broadly concave; upper and lower lobes equal. Adipose fin variably present.

COLOR IN ALCOHOL: Ground color tan brown, lighter on ventral region of head and trunk. Darker longitudinal stripes anterior to naris. Dark to diffuse midlateral stripe along plates of medial series. Darker bands posterior to dorsal-fin base variably defined. All fins with brown bars, more pronounced along unbranched rays. Tips of branched rays distally hyaline. Basal darker spot at base of caudal-fin lower lobe.

SEXUAL DIMORPHISM: Male urogenital papilla present. Males with patch of tightly arranged small odontodes oriented as a swirl covering second, third, and fourth plates of ventral series, lateral to urogenital papilla. Female anus tubular, without separate urogenital papilla. In females, size and arrangement of odontodes on plates lateral to anus similar to adjacent plates, without distinct patch of differentially arranged odontodes.

DISTRIBUTION: Río Paraguay and Río Paraná drainage basin. There are no records for the upper Paraná upstream of Salto das Sete Quedas (Mato Grosso do Sul, Brazil) (fig. 32).

TAXONOMIC REMARKS: Holmberg (1893a) erected the genus *Aristommata* for his new species *A. inexspectata*, based on a single specimen from the Río Paraguay. While the synonymy of *Aristommata* and *Hypoptopoma* was subsequently recognized by Berg (1898), the taxonomic status of *H. inexspectata* remained unsettled. Although considered a valid species in several checklists and faunal studies, the specific name was also regarded at various times as a junior synonym of *H. joberti* (Berg, 1898), of *H. guentheri* (Fowler, 1915), or of *H. gulare* (Gosline, 1945). The first extensive monograph on loricariids (Regan, 1904) ignored *H. inexspectata*, and

Fig. 35. *Hypoptopoma elongatum*, holotype, INPA 7240, 95.4 mm SL, female, in dorsal, lateral, and ventral views.

more recently, Boeseman (1974) included it among the "obscure species" of the loricariid subfamily Hypoptopomatinae. The examination of type specimens and additional comparative material provided new character evidence to support the taxonomic status of *H. inexspectata* (Aquino, 1997; Aquino and Miquelarena, 2000).

Boulenger (1895) described the species *Hypoptopoma guentheri* based on "numerous specimens" from Descalvados (Mato Grosso, Brazil). Berg (1898) listed *H. guentheri* as a junior synonym of *H. inexspectata*, an opinion shared by Eigenmann (1910), Ringuelet et al. (1967), and Aquino (1997). Our examination of the syntype series and extensive collections of *Hypoptopoma* specimens from the Paraguay-Paraná system serve to confirm that action.

Hypoptopoma elongatum, new species
Figure 35, table 12

HOLOTYPE: INPA 7240 (♀, 95.4 mm SL) Brazil: Pará, Rio Tapajos, Itaituba; collected by L. Rapp Py-Daniel and J. Zuanon, 18 October 1991.

PARATYPES: INPA 29657 (32 ♀ + 26 ♂, 2 cs, 62.7–102.7 mm SL) (collected with holotype).

OTHER MATERIAL EXAMINED: **BRAZIL**, **Pará**: CAS 6748 (1 ♀, 93.2 mm SL) Santarem market; INPA 5405 (6 ♀, 93.0–96.2 mm SL) Rio Trombetas, Cach. Porteira a jusante da cachoeira; INPA 5406 (1 ♀,

TABLE 12
Morphometric and Meristic Data for *Hypoptopoma elongatum*
Holotype: INPA 7240. Paratype: INPA 29657. Nontype: MZUSP 38187.

		Paratypes and Nontypes				
	Holotype	*N*	Range		Mean	sd
Standard length	95.4	13	62.7	102.7	85.1	9.90
PERCENT OF STANDARD LENGTH						
Predorsal length	45.3	13	44.1	47.0	45.3	0.97
Head length	32.9	13	32.5	36.2	33.7	1.21
Body depth	18.2	13	16.4	18.2	17.6	0.56
Dorsal-fin spine length	27.4	13	25.8	29.5	27.8	1.10
Trunk length	46.6	13	43.6	47.8	45.9	1.43
Pectoral-fin spine length	27.4	13	26.5	29.8	27.8	1.00
Abdominal length	16.4	13	15.7	17.3	16.4	0.47
Caudal-peduncle length	35.4	13	32.3	36.3	34.4	1.21
Caudal-peduncle depth	8.8	13	7.9	8.8	8.4	0.30
Caudal-fin base depth	8.8	13	7.1	8.9	8.1	0.64
Head depth	15.4	13	15.0	16.1	15.5	0.35
Snout length	18.8	13	18.5	20.0	19.1	0.51
Horizontal eye diameter	5.3	13	5.1	5.8	5.4	0.17
Least orbit-naris distance	5.0	13	4.1	5.0	4.6	0.29
Dorsal interobital distance	18.5	13	17.3	19.8	18.2	0.67
Ventral interobital distance	18.2	13	16.5	18.2	17.3	0.55
Cleithral width	21.5	13	20.7	22.5	21.6	0.53
Head width	20.3	13	19.5	21.7	20.3	0.60
Interpelvic distance	6.6	13	6.6	8.1	7.2	0.51
PERCENT OF HEAD LENGTH						
Body depth	55.5	13	46.8	55.5	52.5	2.61
Head depth	46.8	13	41.7	48.8	46.1	2.01
Snout length	57.2	13	55.2	58.3	56.7	1.02
Horizontal eye diameter	16.0	13	15.4	16.8	16.0	0.43
Least orbit-naris distance	15.1	13	11.5	15.1	13.7	1.11
Dorsal interobital distance	56.2	13	49.4	58.1	54.2	2.28
Ventral interobital distance	55.3	13	47.1	55.3	51.5	2.40
Cleithral width	65.2	13	61.0	65.4	64.1	1.43
Head width	61.7	13	57.7	62.3	60.2	1.44
Interpelvic distance	20.1	13	19.8	24.4	21.2	1.40
PERCENT OF CLEITHRAL WIDTH						
Snout	89.6	13	88.2	2.1	85.6	93.77
LATERAL SERIES OF PLATES						
Dorsal series	20	10	20	20	20	0.0
Middorsal series	4	10	4	4	4	0.0
Medial series	23	10	23	23	23	0.0
Midventral series	13	10	12	13	13	0.5
First midventral series plates	3	10	3	3	3	0.0
Ventral series	13	10	20	20	20	0.0
ABDOMINAL SERIES OF PLATES						
Right lateral series	5	10	4	7	5	0.8
Left lateral series	5	10	4	6	5	0.8
TEETH						
Premaxillary teeth	20	10	16	23	21	2.4
Dentary teeth	16	10	14	22	18	2.6

101.4 mm SL) Rio Trombetas, Lago Tapagem; INPA 5570 (3 ♀, 88.4–104.2 mm SL) Rio Trombetas, R. Cumina, Lago Salgado; INPA 7130 (1 ♀ + 2 ♂, 90.6–94.1 mm SL) Rio Cupari, afluente do Rio Tapajos (próximo a boca); INPA 7131 (3 ♀ + 1 ♂, 88.8–94.3 mm SL) Rio Cupari, afluente do Rio Tapajos (próximo a boca); INPA 7213 (2 ♀, 88.2–9.2 mm SL) Rio Cupari, afluente do Rio Tapajos; MZUSP 34193 (8 ♀ + 3 ♂, 87.9–97.0 mm SL) Rio Tapajos, beira do rio, entre Itaituba e São Luis; MZUSP 36187 (2 ♀ + 2 ♂, 79.9–89.5 mm SL) Rio Tapajos, ihla confrontando Monte Cristo; MZUSP 36220 (1 ♀, 77.0 mm SL) Rio Tapajos, Igarape Jacare, margen dereita do Rio Tapajos, perto de Boim.

DIAGNOSIS: *Hypoptopoma elongatum* is distinguished from all congeners by having a nonpigmented band on the head positioned parallel to the ventral margin of the rostral and lateral snout plates, with the margin between pigmented and nonpigmented plates very well defined (fig. 35C) (vs. absence of a distinct pigmented band). *Hypoptopoma elongatum* can be further distinguished from congeners, except for *H. inexspectatum*, by having the ventral surface of the anterior rostral plate as wide as the ventral surface of the first lateral rostral plates (vs. ventral surface gradually widening from anterior rostral to lateral rostral plates). *Hypoptopoma elongatum* is readily distinguished from *H. inexspectatum* by having a greater number of plates along the trunk medial series (23 vs. 20–21 (21)), by having the snout appearing pointed in dorsal view due to a slight concavity between rostral plate and first infraorbital (fig. 35A) (vs. snout typically spatulate), and by having, if present, a distinct series of odontodes along dorsal and ventral rostral margin of snout restricted to the anterior rostral plate (vs. series of odontodes along dorsal and ventral rostral margin of snout extended laterally to include second and third infraorbitals).

DESCRIPTION: Morphometric and meristic data presented in table 12. Body robust; greatest body depth at dorsal-fin origin. Dorsal profile of head and body straight from snout tip to dorsal-fin origin, slightly elevated at posterior tip of supraoccipital; straight from dorsal-fin origin to anteriormost procurrent caudal-fin ray. Ventral profile of head and body straight to slightly concave from snout tip to anteriormost procurrent caudal-fin ray. Head moderately depressed, almost as wide as cleithral width; lateral process of lateral ethmoid bone visible dorsally. Anterior snout margin acute; slightly concave anterior to naris. Posterior surface of bony pit of nasal organ sharply inclined. Trunk cross section slightly triangular between pectoral- and pelvic-fin origins, ovoid to progressively round posterior to dorsal fin, caudal peduncle posterior to adipose-fin base progressively compressed.

Eyes relatively large, positioned closer to posterior tip of compound pterotic than to tip of snout. Ventral margin of orbit located on ventral side of head. Dorsal interorbital distance greater than ventral interorbital distance.

Total plates in medial series typically 23. Dorsal series plates 20; middorsal series plates 4; midventral series plates 12–13 (13), three plates anterior to first ventral series plate; ventral series plates 20. Second plate of midventral series contacting two plates of medial series.

Abdomen covered by paired series of lateral sickle-shaped plates, with unequal number of plates between left and right series, 4–7 each; anterior azygous plate usually present. Single anal plate. Thoracic plates present, 2–6. Preopercular canal in preopercle present, semicircular; anteriormost pore located between ventral canal-bearing plate and fourth infraorbital; framed by notch at posterolateral margin of canal-bearing plate and ventral margin of fourth infraorbital.

Small odontodes evenly distributed on head; odontodes on rostral margin not arranged in well-defined series, without odontode-free discontinuity. Odontodes on ventral surface of rostral plate variably enlarged. Lamina of trunk plates with odontodes arranged in longitudinal rows, becoming progressively smoother ontogenetically; marginal odontodes present in mature adults. Anterior margin of pectoral-fin spine and ventral surface of pelvic-fin spine with enlarged odontodes.

Total vertebrae 27. Premaxillary teeth 16–23 (21); dentary teeth 14–22 (18). Maxillary barbels short, only reaching to anterior margin of ventral canal-bearing plate.

Dorsal-fin origin located slightly posterior to vertical through pelvic-fin origin. Depressed dorsal fin reaching to or surpassing vertical through posterior half of anal-fin base. Depressed pectoral fin reaching to anus. Pectoral spine serrae typically along middle three-fifths of spine length, involving less of spine shaft with growth; individual serrae oriented oblique to spine shaft. Pelvic fin short, unbranched and first branched rays of equal length. Depressed pelvic fin reaching to anus, not reaching anal-fin origin. Caudal-fin margin markedly forked; upper and lower lobes equal. Adipose fin variably present; when present, small and membranous.

COLOR IN ALCOHOL: Ground color tan and pale ochre. Light to dark brown melanophores clustered on trunk and at base of plates, yielding mottled appearance. Melanophores slightly more concentrated on narrow area along compound pterotic, between cleithral process and opercle, and at base of both dorsal and pectoral fins. Well-defined nonpigmented band parallel to ventral surface of snout plates, including two plates lateral to barbel; margin between pigmented and nonpigmented plates distinct. Deep-lying melanophores arranged in series of blotches posterior to dorsal-fin base; butterfly-shaped blotch anterior to dorsal-fin origin, centered at anteriormost predorsal plate, anterior arms lateral to supraoccipital. Trunk lateral stripe involving medial plate series. Ventral surface of body mostly unpigmented except for scattered melanophores on posterior portion of trunk and anterior surface of lip. Paired and unpaired fins with few dark brown bands. Dorsal fin typically with faint bar at base followed by one dark bar roughly orthogonal to rays and closer to tip than to base of fin, with one or two additional faint bars intervening. Caudal-fin rays with melanophores arranged in parallel V-shaped pigmented bands, typically fainter on medial branched rays; anterior band located at base of branched rays, typically lighter than posterior band; posterior band located near posteror fin margin; unbranched rays and tip of median caudal-fin branched rays light. Lanceolate plates at base of caudal fin light brown, variably connected with basal faint vertical band.

SEXUAL DIMORPHISM: Male urogenital papilla well developed, pointed, joined at base to anterior flaplike anus. Patch of tightly arranged small odontodes on second, third, and fourth plates of ventral series, lateral to urogenital papilla. Males with soft-tissue flap along posterior margin of pelvic spine and along basal one-third to two-thirds of spine. Female anus tubular, without separate urogenital papilla. In females, size and arrangement of odontodes on plates lateral to anus similar to adjacent plates, without distinct patch of differentially arranged odontodes.

DISTRIBUTION: Lower Rio Tapajos and lower Rio Trombetas (fig. 32).

ETYMOLOGY: The specific epithet *elongatum* (Lt. *elongatus*, meaning "prolonged") is a reference to the elongated general shape of the body, particularly marked at the tip of snout, caudal peduncle, and caudal fin.

Hypoptopoma incognitum, new species
Figure 36, table 13

HOLOTYPE: AMNH 39759, 85.01 mm SL, female, Bolivia: Beni, Río Itenez, opposite to Costa Marques; collected by R.M. Bailey and R. Ramos, 1–3 September 1964.

PARATYPES (collected with holotype): AMNH 241976, 6 females and 13 males, 2 cs, 76.6–94.1 mm SL. UMMZ 204339, 8 females and 8 males, 3 cs, 79.56–95.03 mm SL.

OTHER MATERIAL EXAMINED: **BOLIVIA, Beni**: AMNH 40039 (1 ♂, 85.4 mm SL) Río Baures, above mouth 6 km SW Costa Marques, Brazil; AMNH 77403 (1 ♂, 72.1 mm SL) Río Mamoré, ca. 10 km west of San Pedro; AMNH 77467 (2 ♀ + 1 ♂, 43.5–57.3 mm SL) Río Mamoré, Puerto Siles; CAS 77140 (1 ♂, 56.7 mm SL) Cachuela Esperanza, first falls of the Beni; CBF 1323 (5 ♀, 53.1–78.9 mm SL) Ballivian, Espíritu, Arroyo Carnaval, Río Yacuma, Mamoré, Madeira; USNM 305596 (2 ♀, 47.2–49.2 mm SL) Río Matos/Apere/Mamoré; Prov. Ballivia, Río Matos below road x-ing, 48 km E San Borja. **Pando**: FMNH 107001 (2 ♀, 48.0–62.3 mm SL) 100 m de la boca del Nareuda en el Tahuamanu; FMNH 107002 (2 ♀, 36.4–39.1 mm SL) Río Nareuda, río arriba de la desembocadura en el Tahuamanu; FMNH

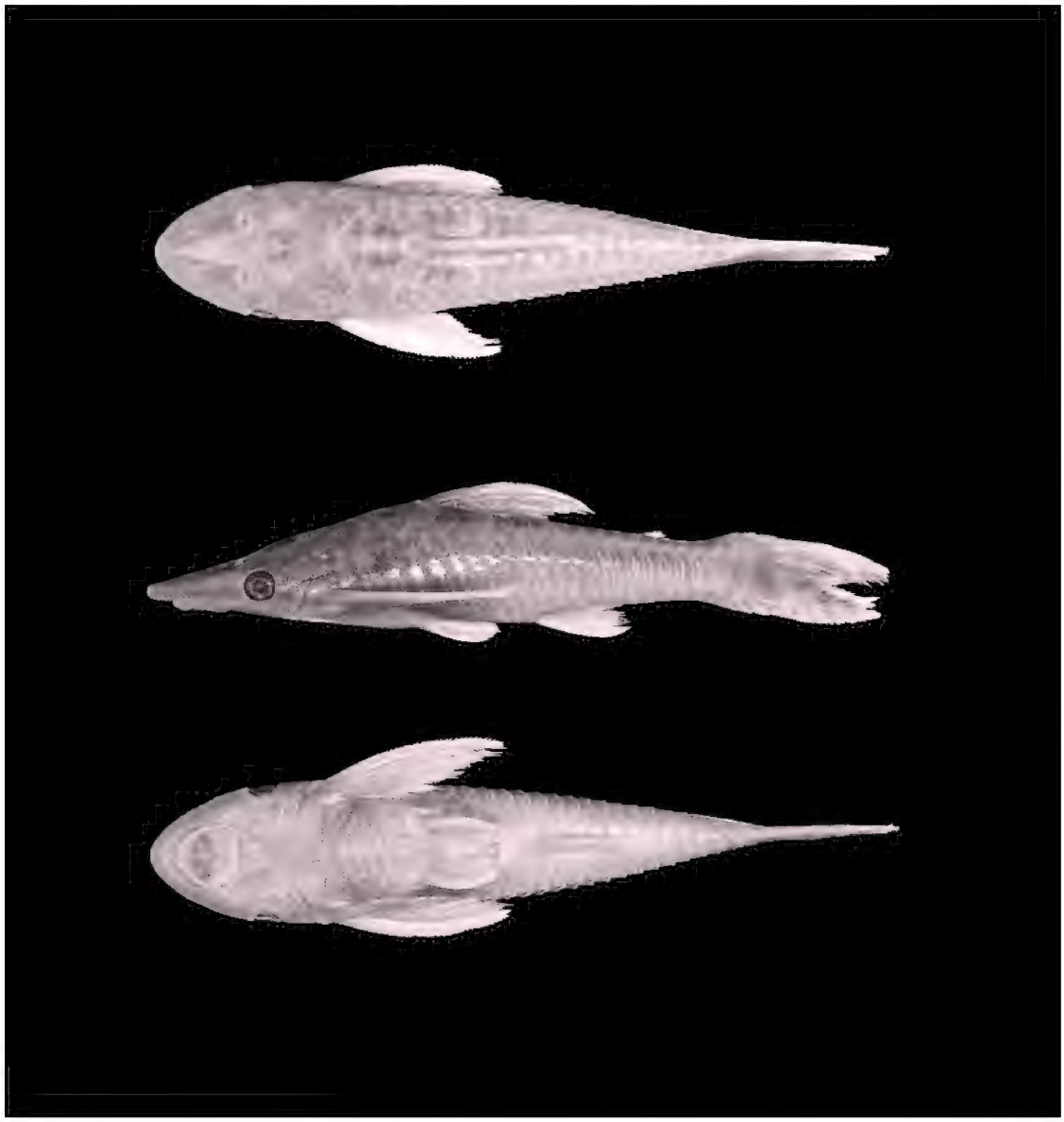

Fig. 36. *Hypoptopoma incognitum*, holotype, AMNH 39759, 85.01 mm SL, female, in dorsal, lateral, and ventral views.

107003 (7 ♀, 41.8–71.1 mm SL) Río Manuripi, +/− 12 km río arriba de Puerto Rico; FMNH 107004 (2 ♀ + 2 ♂, 54.5–71.5 mm SL) Río Manuripi, +/− 20 km río arriba de Puerto Rico; FMNH 107007 (1 ♀, 71.3 mm SL) Brazo del Manuripi, +/− 1 km río arriba del campamento; FMNH 107008 (8 ♀, 50.2–70.6 mm SL) Río Manuripi above camp; FMNH 107009 (3 ♀ + 2 ♂, 52.8–82.1 mm SL) Río Manuripi at playa, 5.78 km from camp, 9.23 from Puerto Rico; FMNH 107010 (2 ♀ + 2 ♂, 65.1–73.6 mm SL) Río Manuripi at playa outside, 6.76 km above camp and 9.78 above Puerto Rico; FMNH 107011 (1 ♀, 34.6 mm SL) Rio Manuripi at island 0.76 km above camp and 4.20 above Puerto Rico. **Santa Cruz**: CBF 2862 (1 ♀, 53.9 mm SL) Guarayos, Perseverancia, Río Negro cerca de Las Naranjas; CBF 10110 (1 ♀, 51.1 mm SL) Guarayos, Perseverancia,

TABLE 13
Morphometric Data for *Hypoptopoma incognitum*
Holotype: AMNH 39759. Paratype: AMNH 241976. Nontypes: CAS 6736, 6748, 56723; FMNH 117743; INPA 2798, 6039; MUSM 7520, 10521; MZUSP 4978; UMMZ 202339; USNM 177706, 177707, 308093.

		Paratypes and Nontypes				
	Holotype	*N*	Range		Mean	sd
Standard length	85.0	70	44.7	94.9	77.8	12.08
PERCENT OF STANDARD LENGTH						
Predorsal length	47.3	70	45.4	50.9	47.0	1.03
Head length	33.3	70	32.4	37.4	34.2	1.25
Body depth	21.2	70	17.4	22.9	20.7	1.06
Dorsal-fin spine length	28.1	64	26.0	33.7	29.9	1.60
Trunk length	42.1	70	40.6	46.4	43.6	1.29
Pectoral-fin spine length	31.0	70	27.2	35.9	30.8	1.66
Abdominal length	14.8	70	14.7	18.6	16.9	0.92
Caudal-peduncle length	25.1	70	26.0	36.0	32.0	1.73
Caudal-peduncle depth	9.7	70	8.8	11.0	10.1	0.51
Caudal-fin base depth	12.7	70	8.0	13.2	9.9	1.29
Head depth	17.2	70	14.8	20.1	17.4	0.85
Snout length	19.5	70	17.8	21.4	19.4	0.69
Horizontal eye diameter	5.1	70	4.9	7.0	5.7	0.45
Least orbit-naris distance	4.6	70	3.9	6.6	5.1	0.45
Dorsal interobital distance	19.9	70	19.5	23.2	20.8	0.89
Ventral interobital distance	18.8	70	18.3	22.4	20.0	0.82
Cleithral width	23.7	70	22.2	27.4	24.5	1.10
Head width	21.9	70	20.8	25.9	22.8	0.97
Interpelvic distance	7.2	70	6.2	9.2	7.8	0.73
PERCENT OF HEAD LENGTH						
Body depth	63.7	70	46.9	68.1	60.7	4.55
Head depth	51.5	70	39.7	59.5	50.9	3.54
Snout length	58.6	70	52.1	60.1	56.6	1.53
Horizontal eye diameter	15.2	70	14.7	19.0	16.6	0.91
Least orbit-naris distance	13.8	70	10.6	19.6	15.0	1.59
Dorsal interobital distance	59.8	70	52.9	67.4	60.9	2.90
Ventral interobital distance	56.5	70	53.3	64.2	58.4	2.51
Cleithral width	71.0	70	66.1	79.2	71.7	2.89
Head width	65.7	70	61.7	71.7	66.7	2.46
Interpelvic distance	21.7	70	18.7	31.9	22.9	2.39
PERCENT OF CLEITHRAL WIDTH						
Snout	82.5	70	70.2	84.6	79.0	3.19
LATERAL SERIES OF PLATES						
Dorsal series	18	10	19	19	19	0.0
Middorsal series	3	10	4	4	4	0.0
Medial series	24	10	21	22	22	0.3
Midventral series	12	10	12	14	13	1.0
First midventral series plates	3	10	3	3	3	0.0
Right ventral series	19	10	19	19	19	0.0
ABDOMINAL SERIES OF PLATES						
Right lateral series	7	10	4	8	6	1.1
TEETH						
Premaxillary teeth	19	10	18	23	21	1.6
Dentary teeth	14	10	17	20	18	1.1

Río Negro. **Brazil**, **Acre**: MZUSP 49782 (3 ♀ + 1 ♂, 45.5–46.9 mm SL) Rio Acre, entre Seringal Paraiso y Lago Amapa; MZUSP 49795 (1 ♀ + 1 ♂, 75.2–85.7 mm SL) Lago Amapa. **Amazonas**: CAS 56723 (1 ♀, 74.0 mm SL) Igarapé Chibareno, 30 km E of Manaus on south shore of Rio Negro, about 0.3 mi. S of its entrance into Rio Amazonas; INPA 127 (4, 51.3–70.4 mm SL) Lago Janauaca, Rio Solimões; INPA 807 (1 ♀, 84.0 mm SL) Flutuante do Tarumã Açu; INPA 2798 (9 ♀ + 4 ♂, 2 cs, 58.9–88.3 mm SL) Ihla da Marchantaria, Rio Solimões; INPA 2800 (1, 74.1 mm SL) Lago Janauaca, Rio Solimões; INPA 6035 (3 ♀, 82.0–85.6 mm SL) Rio Amazonas, Ihla do Careiro, Lago do Pedro; INPA 6082 (1 ♂, 78.8 mm SL) Rio Solimões, Boca do Paraná do Janauacá; INPA 6088 (1 juvenile, 58.8 mm SL) Río Madeira, Igarapé Aramaguara; INPA 14017 (1 ♂, 76.2 mm SL) Rio Solimões, Parana do Rei; MZUSP 6723 (1 ♀, 74.1 mm SL) Rio Negro, Manaus; MZUSP 7557 (1 ♀ + 1 ♂, 64.9–68.2 mm SL) Parana do Urucura, mun. de Urucura; MZUSP 7654 (1 ♀, 75.5 mm SL) Boca do lago José Açu, Parintins; MZUSP 6598 (1 ♀, 74.4 mm SL) Lago Manacupuru; MZUSP 27607 (1 ♀, 67.0 mm SL) Paraná de Capacete, Rio Solimões, mun. de Benjamin Constant; MZUSP 36198 (1 ♀, 90.0 mm SL) Lago Janauaca e arrededores, Rio Solimões; MZUSP 36227 (1 juvenile, 43.3 mm SL) Ihla Marchantaria, perto de Manaus; USNM 177706 (1 ♀, 62.3 mm SL) Amazonas, Rio Urubu; USNM 177707 (1 ♀, 65.95 mm SL) Amazonas, Rio Urubu; USNM 306963 (2 juveniles, 37.3–41.0 mm SL) ressaca da Ilha de Marchantaria; USNM 306991 (1 juvenile, 41.8 mm SL) ressaca da Ilha de Marchantaria; USNM 307056 (1 ♂, 62.24 mm SL) Amazonas, Paraná de Janauaca, entrada do Lago Castanho; USNM 308093 (1 ♂, 82.9 mm SL) Amazonas, entrada de Janauari, entre Furo de Paracuuba e Lago Terra Preta; USNM 308244 (1 ♂, 83.2 mm SL) near Manaus, entrance of lago Janauari, between furo (channel) de Paracuuba and lago Terra Preta; USNM 308303 (1 ♂, 79.0 mm SL) Amazonas, Lago Terra Preta, Janauari. **Goiás**: MZUSP 4881 (11, 39.2–71.0 mm SL) Rio Araguaia, Aruana. **Maranhão**: MNRJ 17720 (8) Rio Mearim em Arari; MNRJ 17725 (4) Rio Mearim; MNRJ 17726 (1) Lago Malhada Grande. **Mato Grosso**: MZUSP 36222 (1 juvenile, 47.6 mm SL) Río Araguaia, Santa Terezinha. **Pará**: CAS 6736 (1 ♀, 70.3 mm SL) Amazonas, Santarém market; CAS 6748 (1 ♀, 92.4 mm SL) Amazonas, Santarém market; FMNH 59622 (3 ♀, 47.0–55.6 mm SL) Santarém; FMNH 117743 (13 ♀ + 2 ♂, 41.6–72.3 mm) Santarém; INPA 558 (2) Rio Tocantins, Ig. Arapari, Breu Branco; INPA 6028 (1) Rio Tocantins, Breu Branco; INPA 6029 (1) Rio Tocantins, Poco do Paulo; INPA 6030 (1) Rio Tocantins, Breu Branco, Igarape Arapari; INPA 6031 (2) Rio Tocantins, Breu Branco, Igarape Canoal; INPA 6032 (1) Rio Tocantins, Breu Branco, Igarape Arapari; INPA 6033 (3) Rio Tocantins, Itupiranga; INPA 6036 (5) Rio Tocantins, a jusante da represa; INPA 6037 (1) Rio Tocantins, Breu Branco, Igarape Canoal; INPA 6039 (13) Rio Tocantins, Itupiranga; INPA 6053 (9) Rio Tocantins, Igarape Arapari, Breu Branco; INPA 6054 (1) Rio Tocantins, Icangui; INPA 6055 (2) Rio Tocantins, Capuerana; INPA 6057 (1) Rio Tocantins, Tucurui, Igarape Vallentim; INPA 6058 (1) Rio Tocantins, Itupiranga; INPA 6059 (1) Rio Tocantins, Breu Branco, Igarape Canoal; MHNG 2538 12 (1 ♀, 48.1 mm SL) Ig. Azul, Ilha do Cameta, face a Santarém; MHNG 2708.060 (1 ♂, 71.7 mm SL) Amazon river, side arm with lagos along right shore, about 10 km downriver of Santarém; MZUSP 5657 (6 juveniles, 19.1–39.8 mm SL) Lago Paru, Oriximiná; MZUSP 7850 (3 ♀, 63.5–69.7 mm SL) Parana Jacaré, Mun. Faro; MZUSP 8539 (1 ♀, 76.7 mm SL) Rio Tapajos, Santarém; MZUSP 34194 (1 ♀, 89.6 mm SL) Tocantins, Tucurui; MZUSP 36185 (1 ♀, 71.7 mm SL) Rio Arari, Cachoeira de Arari, Ilha de Marajo; MZUSP 36186 (2 ♀, 57.2–80.4 mm SL) Lagoa marginal do Rio Tocantins, perto de Baiao; MZUSP 36188 (1 ♀, 64.9 mm SL) Oriximiná. **Rondonia**: INPA 456 (16 ♀ + 9 ♂, 63.0–75.0 mm SL) Río Madeira, Varza de calama, Lago de Repartimento; INPA 2237 (1 ♀, 70.0 mm SL) Río Madeira, Calama Flechal. **Roraima**: INPA 49 (1 ♀, 86.1 mm SL) Paraná do Rio Branco. **Peru**, **Madre de Dios**: ANSP 144008 (1 ♀, 65.9 mm SL) NW of Puerto Maldonado, Lago Tupuhumaro, oxbow lake E bank of Madre de Dios, above junction with

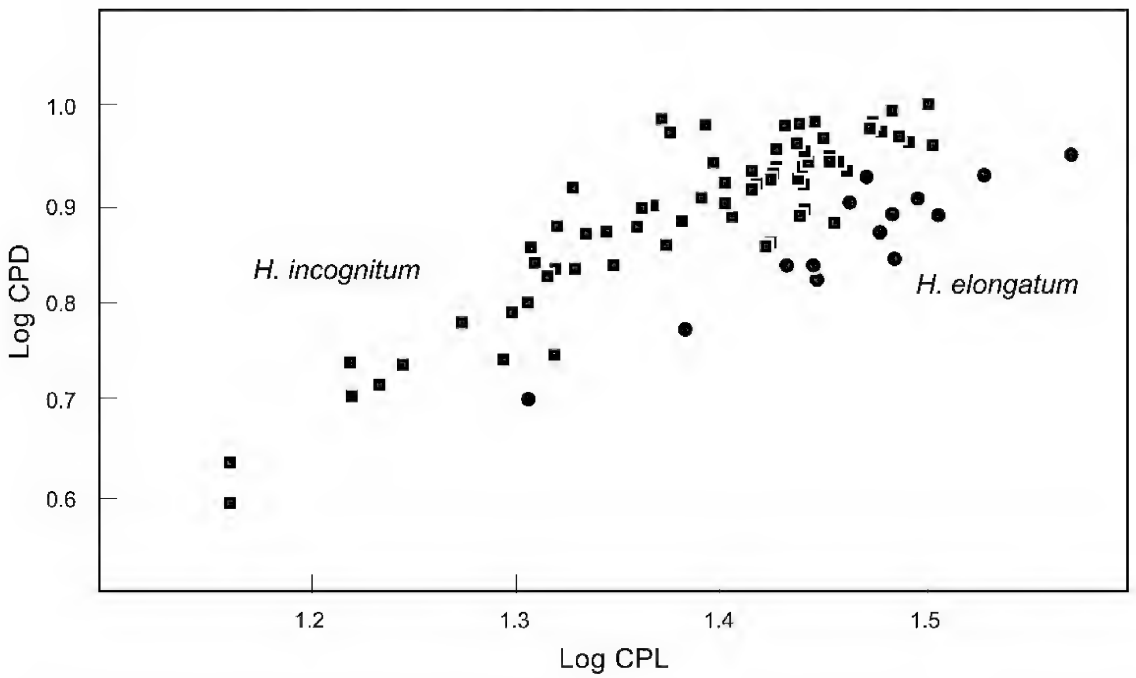

Fig. 37. Covariation between caudal-peduncle length and standard length for *H. elongatum* (dots) and *H. incognitum* (squares).

Río de las Piedras; MUSM 2474 (5 ♀, 40.6–66.6 mm SL) Manú, Parque Nacional, Pakitza, Cocha Salvador; MUSM 7520 (1 ♀ + 5 ♂, 33.2–65.8 mm SL) Tambopata, Río Madre de Dios, Lago Valencia; MUSM 7960 (1 ♀, 55.1 mm SL) Tambopata, Río Madre de Dios, Lago Valencia; MUSM 8123 (3 ♀, 60.2–65.2 mm SL) Tambopata, Candamo, Río Tambopata, Río Chuncho; USNM 263910 (3 ♀, 46.4–69.6 mm SL) Reserva Natural de Tambopata, Laguna Cococha, 5.1 km to E of explorers inn; USNM 264046 (2 juveniles, 35.9–44.5 mm SL) Reserva Natural de Tambopata, Laguna Chica, end opposite boat dock (farthest from trail leading to lodge); USNM 302696 (6 ♀ + 1 ♂, 2 cs, 40.3–68.1 mm SL) Prov. Manú, Coche Salvador, and oxbow lake off Río Manú about 1 hr. downriver from Pakitsa; USNM 327324 (3 ♀, 50.0–56.5 mm SL) Prov.Manú, Parque Nacional Manú, Cocha Salvador; USNM 327333 (1 ♀ + 1 ♂, 49.4–71.2 mm SL) Prov. Manú, Parque Nacional Manú, Cocha Nueva; USNM 327334 (2, 58.3–63.5 mm SL) Prov. Manú, Parque Nacional Manú, Río Manú, Cocha Juárez; USNM 327340 (1 ♀ + 1 ♂, 48.8–55.0 mm SL) Prov. Manú, Parque Nacional Manú, Cocha Nueva. **Ucayali**: MHNG 2407.97 (2 ♀, 68.8–76.0 mm SL) Bagazan, Río Ucayali, Pucallpa; MUSM 10476 (2 ♀, 44.6–47.6 mm SL) Purús, Río Purús, Cocha Zapote; MUSM 10521 (10 ♀ + 5 ♂, 44.7–77.1 mm SL) Purús, Río Purús, Cocha Bola de Oro; USNM 384194 (1 ♀, 44.8 mm SL) Río Purús.

DIAGNOSIS: *Hypoptopoma incognitum* is distinguished from all congeners, with the exception of *H. elongatum*, by the presence of a patch of odontodes on the anterolateral surface of the cleithrum at the opening to the branchial chamber. *Hypoptopoma incognitum* is distinguished from *H. elongatum* by having a shorter caudal peduncle (caudal-peduncle length 26.0–36.0 (32.0) vs. 32.3–36.3 (34.4); t-test, $p < 0.001$) (fig. 37); by a deeper, more robust caudal peduncle (caudal-peduncle depth 8.8–11.0 (10.1) vs. 7.9–8.8 (8.4); t-test, $p < 0.001$); by the round to slightly acute snout (vs. snout appearing pointed due to slight lateral inflexion between rostral plate and first infraorbital); by fewer plates along medial series (21–22 (22) vs. 23); by having caudal-fin lobes light brown (vs. caudal-fin lobes dark).

DESCRIPTION: Morphometric and meristic data presented in table 13. Body robust; greatest body depth at dorsal-fin origin. Dorsal profile of head and body straight from tip of snout to dorsal-fin origin, slightly elevated at posterior supraoccipital tip; straight from dorsal-fin origin to anteriormost procurrent caudal-fin ray. Ventral profile slightly convex from tip of snout to anteriormost procurrent caudal-fin ray. Head moderately depressed, almost as wide as cleithral width; lateral process of lateral ethmoid bone visible dorsally. Snout rounded to slightly acute in dorsal view; dorsally, slightly concave anterior to naris. Posterior surface of bony pit of nasal organ sharply inclined. Trunk cross section between pectoral- and pelvic-fin origin slightly triangular, ovoid to progressively rounded posterior to dorsal fin, progressively compressed posterior to adipose-fin base.

Eyes relatively large, positioned closer to posterior tip of compound pterotic than to tip of snout. Ventral margin of orbit located on ventral surface of head. Dorsal interorbital distance/ventral interorbital distance ratio changing from <1 to >1 during ontogeny.

Total plates in lateral medial series 21–22 (22). Dorsal series plates 19; middorsal series plates 4; midventral series plates 12–14 (13), three plates anterior to first ventral series plate; ventral series plates 19. Second plate of midventral series contacting two plates of medial series.

Abdomen covered by paired series of lateral sickle-shaped plates, with unequal number of plates between left and right sides, 4–8 each; anterior azygous plate usually present; medial abdominal plates, if present, not forming well-defined series. Single anal plate present. Thoracic plates present, 2–6 (4). Preopercular canal in preopercle present, semicircular; anteriormost pore opening between ventral canal-bearing plate and fourth infraorbital; framed by notch at posterolateral margin of canal-bearing plate and ventral margin of fourth infraorbital.

Small odontodes evenly distributed on head. Odontodes along anterior snout margin not arranged in well-defined series, without odontode-free discontinuity between ventrad and dorsad odontodes. Odontodes along dorsal snout margin small, slightly larger than those on dorsal surface of head. Lamina of trunk plates with odontodes arranged in longitudinal rows, becoming progressively smoother ontogenetically; marginal odontodes present in mature adults. Patch of odontodes on anterolateral surface of cleithrum, at opening to branchial chamber, visible upon retraction of branchiostegal membrane. Odontode patch variably developed, from few odontodes to elevated patch of closely arranged odontodes; expression of patch often bilaterally variable.

Total vertebrae 26. Premaxillary teeth 18–23 (21); dentary teeth 17–20 (18). Maxillary barbels short, extended slightly beyond anterior margin of ventral canal-bearing plate in adults.

Dorsal-fin origin located slightly posterior to vertical through pelvic-fin origin. Depressed pectoral fin reaching to anus; pectoral-fin spine with serrae along posterior margin, individual serrae oriented orthogonal to spine shaft. Extension of serrae along pectoral spine margin reduced ontogenetically from proximal two-thirds in smaller specimens to middle third in larger specimens. Pectoral fin reaching to vertical through midpoint between pelvic-fin tip and anal-fin origin. Pelvic fin short with unbranched and first branched rays equal in length. Depressed fin reaching beyond anus, not reaching to anal-fin origin. Caudal-fin margin concave to forked; upper and lower lobes equal. Adipose fin present or absent; when present, composed of bony spine shaft and membrane; when absent, small platelike scar visible.

COLOR IN ALCOHOL: Ground color tan and pale ochre. Melanophores light to dark brown on trunk; melanophores on head and trunk varying from uniformerly distributed to clustered in beanlike spots; melanophores slightly more concentrated along narrow area between compound pterotic, cleithral process, and anterior margin of opercle, at base of dorsal and pectoral fins, and on anterior surface of lip. Deep-lying melanophores arranged in series of blotches posterior to dorsal-fin base. Midlateral stripe situated mostly along medial plates series. Ventral surface of body mostly unpigmented except for scattered melanophores on posterior

portion of trunk, anterolateral margin of cleithra, cleithral process, canal-bearing plates, and lateral portions of lateral abdominal series. Paired, dorsal and anal fins with dark brown bands. Dorsal fin with dark triangular spot extended over base of anterior 3–4 branched rays. Series of lanceolate plates at caudal-fin base darkened by black melanophores. Basal triangular spot on caudal fin variably present, typically absent. Caudal fin pigmentation pattern typically composed of three broad bands, with distal tip of lobes light brown. Juveniles up to around 60 mm SL with slightly different caudal-fin pigmentation, having a small triangular spot at base of lower lobe, followed by darker broad bar and darker tips of dorsal and ventral lobes.

SEXUAL DIMORPHISM: Male urogenital papilla well developed, pointed, joined at base to anterior flaplike anus. Males with patch of tightly arranged small odontodes oriented as a swirl, variably covering first to fourth plates of ventral series, lateral to urogenital papilla. Female anus tubular, without separate urogenital papilla. In females, size and arrangement of odontodes on plates lateral to anus similar to adjacent plates, without distinct patch of differentially arranged odontodes.

COMPARISONS: The overall pattern of morphometric variation between *Hypoptopoma incognitum* and *H. elongatum* is summarized by the results of a sheared principal component analysis on 20 morphometric characters (fig. 38; table 14). The second and third components represent 35.1% and 1.6% of the variation of the morphometric data, respectively; the separation between species is complete along PC2. The analysis shows that the morphometric variance is expressed mostly by variables related to the elongation of the body (trunk and caudal peduncle length, caudal-peduncle depth, and snout length).

DISTRIBUTION: Broadest distribution among species of *Hypoptopoma* across the central and lower Rio Amazonas basin. It is found in the Rio Tocantins basin and is the only species known for northeastern coastal rivers (fig. 39).

ETYMOLOGY: The specific epithet *incognitum* (Lt. *incognitus*, meaning "unknown, strange") is a reference to the fact that specimens of the species have long been misidentified with other species of *Hypoptopoma*.

Hypoptopoma steindachneri Boulenger, 1895
Figure 40, table 15

Hypoptopoma steindachneri Boulenger, 1895: 526 (Type locality: Río Negro, Amazonas basin).—Boulenger, 1896: 31 (repeats Boulenger, 1895).—Regan, 1904: 264 (list of loricariid species; key to *Hypoptopoma* species).—Eigenmann, 1910: 412 (list of freshwater fishes of South America).—Miranda Ribeiro, 1911: 97–98, fig. 57a, b, c (list of fishes of Brazil; key to *Hypoptopoma* species).—Gosline, 1945: 98 (list of catfish species of South and Central America).—Fowler, 1954: 126–127, fig. 730 (list of freshwater fishes of Brazil).—Isbrücker, 1980: 88 (list of loricariid species).—Chang and Ortega, 1995: 4 (list of freshwater fishes of Peru).—Schaefer, 1996b: 1031–1033 (type designation).—Eschmeyer and Ferraris, 1998: 1604 (catalog of fishes); Isbrücker, 2002: 28 (list of loricariid species).—Schaefer, 2003: 323 (list of hypoptopomatine species).—Ferraris, 2007: 250 (list of catfish species).

Hypoptopoma (*Diapeltoplites*) *steindachneri*.—Fowler, 1915: 237 (assigned to subgenus *Diapeltoplites*).

Hypoptopoma thoracatum (not of Günther, 1868).—Steindachner, 1879: Taf. 6, fig. 1, 1a, 1b (Brazil: Rio Amazonas drainage in delta of Rio Negro).—Eigenmann and Eigenmann, 1889: 40 (list of catfish species of South America).—Eigenmann and Eigenmann, 1890: 398 (list of catfish species of South America).

HOLOTYPE: Specimen illustrated and described in Steindachner (1879: Taf. 6, fig. 1, 1a, 1b), by original designation of Boulenger 1895: 526. Stated type locality: Rio Amazonas drainage in the delta of the Rio Negro.

OTHER MATERIAL EXAMINED: **BRAZIL, Amazonas**: MNRJ 3672 (1 ♀, 84.9 mm SL) Rio Javari (tributary of Rio Solimões) at Benjamin Constant; MZUSP 36204 (1 ♂, 85.1 mm SL) San Antonio do Iça, Rio Solimões; MZUSP 36205 (1 ♀, 82.9 mm SL) Rio Solimões, Ihla Xibeco; MZUSP 36218 (1 ♀ + 1 ♂, 64.6–89.0 mm SL) Campina, Rio Purus. **COLOMBIA, Leticia**: USNM 190319 (1 ♀ + 1 ♂, 88.4–89.7 mm SL) Leticia. **PERU, Loreto**: ANSP 182723 (1 ♀, 64.4 mm SL) Río Itaya, ca. 100 minutes upstream from Puerto Belen, Iquitos, by canoe; CAS 133271 (1 ♂, 84.6 mm SL) Río Ampiyacu; INHS 39965 (5

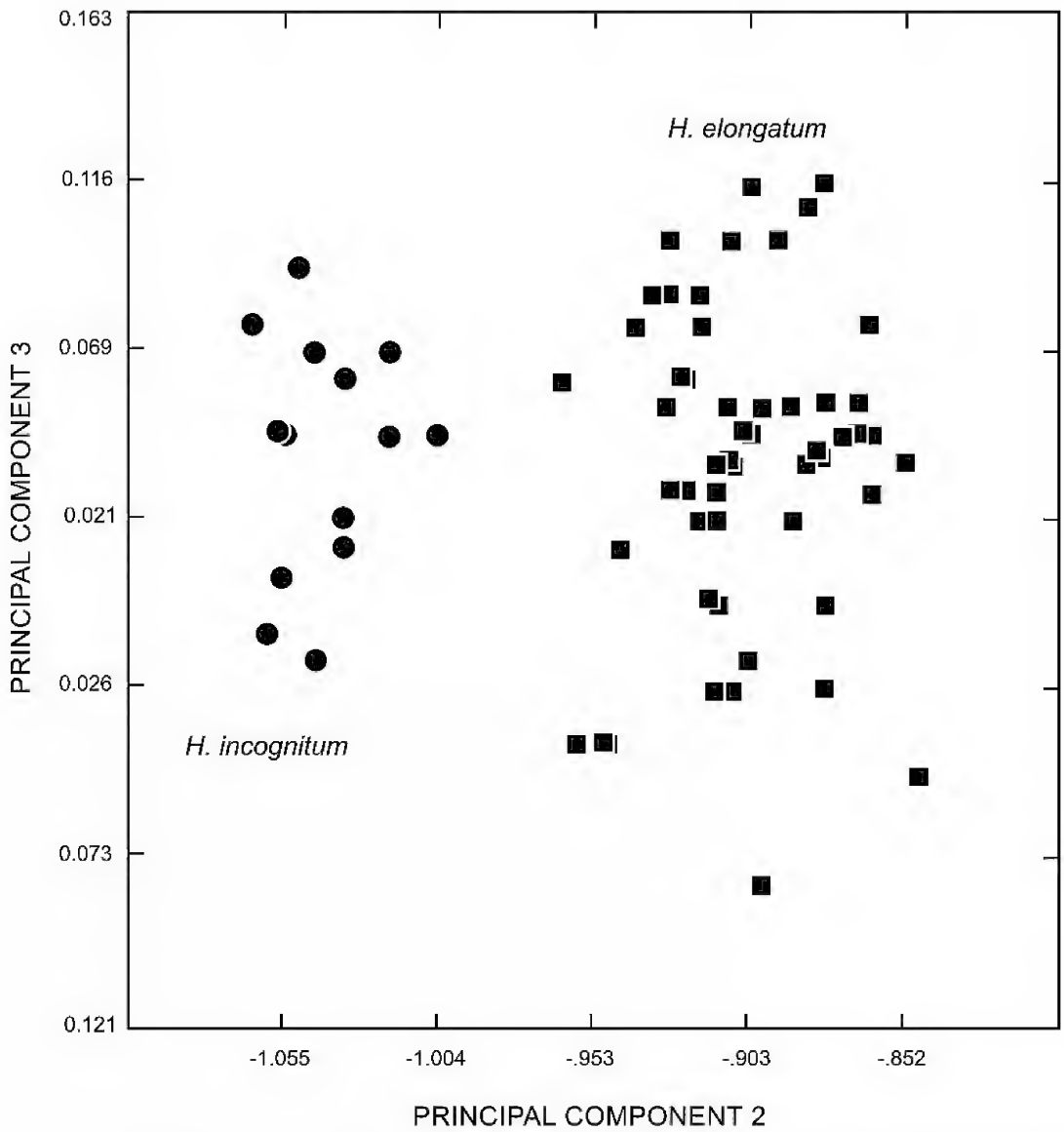

Fig. 38. Plot of scores along sheared second and third principal components from the morphometric analysis of body shape between *H. elongatum* (squares) and *H. incognitum* (circles).

♀ + 1 ♂, 62.0–98.2 mm SL) Río Itaya, ca. 4–5 km upstream from Iquitos, above and below mouth of Quebrada Mazana; INHS 40171 (1 ♀, 77.3 mm SL) Río Orosa, mouth of Tonche Caño, Madre Selva II field station, 69.4 mi E Iquitos; INHS 53744 (2 ♀, 70.7–88.8 mm SL) Río Nanay, 4.54 km W center of Iquitos; USNM 124826 (1 ♂, 86.3 mm SL) Ampiyacu river; SIUC 67365 (4 ♀ + 3 ♂, 73.1–93.6 mm SL) Río Itaya, upriver of Belen, approx. 4.5 km.

DIAGNOSIS: *Hypoptopoma steindachneri* is distinguished from all congeners by the presence of two or more paranasal plates between the pararostral plates and the second infraorbital (fig. 7C) (vs. a single paranasal plate in *H. gulare* (fig. 7B) and *H. machadoi*, or paranasal plates absent (fig. 7A) in all other *Hypoptopoma* species); by having a single plate between the canal-bearing plate and the first, second, and third infraorbitals (fig. 5B) (vs. two plates); by having the canal-

TABLE 14
Sheared Principal Components Loadings from the Morphometric Analysis of Head and Trunk of *Hypoptopoma elongatum* and *H. incognitum*

	PC2	PC3
Standard length	0.209052	0.166665
Predorsal length	0.201476	0.088970
Head length	0.175443	0.147908
Body depth	0.231603	−0.188937
Dorsal-fin spine length	0.126347	0.043166
Trunk length	0.265156	0.319042
Pectoral-fin spine length	0.299723	−0.130698
Abdominal length	0.161692	0.129852
Caudal peduncle length	0.361301	0.435230
Caudal-peduncle depth	0.242121	−0.241362
Caudal-fin base depth	0.208109	−0.600769
Head depth	0.215447	−0.067799
Snout length	0.338188	0.108948
Horizontal eye diameter	0.147757	0.111524
Least orbit-naris distance	0.096149	0.027950
Dorsal interobital distance	0.198984	−0.105903
Ventral interobital distance	0.154936	−0.097497
Cleithral width	0.187378	−0.079987
Head width	0.294834	−0.098622
Interpelvic distance	−0.135345	0.305641

bearing plate subdivided into a smaller plate along the anteromedial margin and the larger posterior portion that bears the canal (fig 5B) (vs. a single, undivided canal-bearing plate); by having the basipterygium constricted laterally (interpelvic distance 2.0–6.4 (5.1) vs. interpelvic distance > 6.5) (fig. 41B); by having the anterodorsal basipterygium lamina that forms the channel for the pelvic arrector muscles extended anteriorly beyond the lateral basipteryigium process (vs. anterodorsal basipterygium lamina not extended beyond the lateral basipterygium process); by having the tips of the caudal-fin rays darkly pigmented, forming a vertical band along the fin margin (vs. tips of the caudal-fin rays not uniformly dark, not forming a vertical band along posterior margin). *Hypoptopoma steindachneri* is further distinguished from all congeners, except for *H. brevirostratum*, by the presence in mature males of a membranous outgrowth between pelvic spine and first pelvic-fin branched ray (vs. membranous outgrowth absent).

DESCRIPTION: Morphometric and meristic data presented in table 15. Body robust; greatest body depth at dorsal-fin origin (fig. 42). Dorsal profile of head concave from tip of snout to frontals, convex from that point to dorsal-fin origin; roughly straight from dorsal-fin origin to anteriormost procurrent caudal-fin ray. Ventral profile smoothly convex from tip of snout to anteriormost caudal-fin procurrent ray. Head strongly depressed anterior to orbits, as wide as cleithral width; lateral process of lateral ethmoid bone visible dorsally. Snout rounded; flattened anterior to naris. Posterior surface of bony pit of nasal organ sharply inclined. Body cross section between pectoral- and pelvic-fin origins slightly triangular, round to progressively compressed posterior to dorsal fin.

Eyes relatively large, positioned slightly closer to posterior tip of compound pterotic than to tip of snout. Ventral margin of orbit located on ventral surface of head. Dorsal interorbital distance greater than ventral interorbital distance.

Total plates in lateral medial series typically 22. Dorsal series plates 19–20 (19); middorsal series plates 3–4 (4); midventral series plates 13–15 (15), three plates anterior to first ventral series plate; ventral series plates 19–20 (19). Second plate of midventral series contacting two plates of medial series.

Abdomen covered by paired series of lateral sickle-shaped plates, with unequal number of plates between left and right sides, 3–8 each; anterior azygous plate usually present. Single anal plate. Thoracic plates present, 2–6. Canal in preopercle present, semicircular; anterior pore located between ventral canal-bearing plate and fourth infraorbital, framed by notch at posterolateral margin of canal-bearing plate and ventral margin of fourth infraorbital, notch with greater contribution from fourth infraorbital.

Small odontodes evenly distributed on head. Odontodes on rostral margin of snout not arranged in well-defined series, without odontode-free discontinuity between ventrad and dorsad odontodes. Odontodes along dorsal rostral margin small, only slightly larger than those on head. Lamina of trunk plates with odontodes arranged in longitudinal rows, becoming progressively smoother ontogenetically; marginal odontodes well developed.

Total vertebrae 26. Premaxillary teeth 15–21 (19); dentary teeth 13–20 (16). Maxillary barbels short; in adults extending slightly

Fig. 39. Drainage map of South America and distribution of *H. incognitum* (dots), *H. gulare* (squares), and *H. machadoi* (triangles). Open symbols designate type localities; some symbols represent more than one locality record.

beyond anterior margin of ventral canal-bearing plate.

Dorsal-fin origin located slightly anterior to vertical through pelvic-fin origin; depressed dorsal fin reaching almost to vertical through posterior tip of anal fin. Pectoral fin variably reaching to anal-fin origin. Pectoral spine serrae orthogonal to spine shaft, typically entirely reduced. Pelvic fin short, unbranched and first branched rays of equal length, pelvic fin reaching to anus, not reaching anal-fin origin. Caudal-fin margin

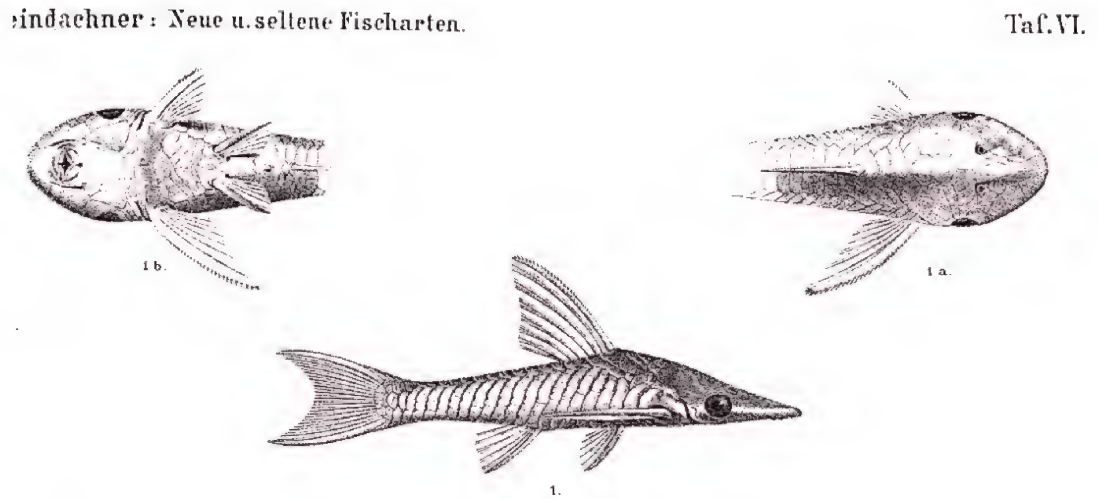

Fig. 40. *Hypoptopoma steindachneri*, holotype by original designation of Boulenger (1895), based on description and illustration appearing in Steindachner NMW 46272, 66.3 mm SL, in dorsal, lateral, and ventral views.

concave to forked; upper and lower lobes equal. Adipose fin variably present; when present, consisting of small plate with few small odontodes.

COLOR IN ALCOHOL: Ground color tan and pale ochre. Melanophores light to dark brown; arranged in clusters on trunk and at base of plates yielding mottled appearance. Pigmentation on head more uniformly distributed; melanophores slightly more concentrated on frontals, narrow area along anterior margin of opercle, narrow band along margin of snout slightly reflected ventrally. Deep-lying melanophores arranged in series of blotches posterior to dorsal-fin base and lateral stripe on body mostly along trunk medial series of plates. Ventral surface of body mostly unpigmented except for scattered melanophores on posterior portion of trunk region. Paired fins with faint bands. Unpaired fins with dark brown bands. Dorsal fin with dark triangular spot extended over base of branched rays. Basal plates of caudal fin with pigmented spot of black melanophores, contiguous to basal dark band, extended along one-fourth length of branched rays. Distal tips of unbranched and branched caudal-fin rays dark, forming continuous narrow band (fig. 17E).

SEXUAL DIMORPHISM: Male urogenital papilla pointed, variably joined to anterior flaplike anus. Males with patch of tightly arranged small odontodes oriented as a swirl, variably covering first to fourth plates of ventral series, lateral to urogenital papilla. Female anus tubular, without separate urogenital papilla. In females, size and arrangement of odontodes on plates lateral to anus similar to adjacent plates, without distinct patch of differentially arranged odontodes.

DISTRIBUTION: Known from tributaries of the lower Rio Ucayali and Rio Solimões basin (fig. 32).

TAXONOMIC REMARKS: The species herein designated as *Hypoptopoma steindachneri* is remarkable in possessing a large number of unique autapomorphic morphological characters serving to diagnose the species among congeners. Boulenger (1895) established *Hypoptopoma steindachneri* on the basis of the illustration of a single specimen that Steindachner (1879) had identified as *H. thoracatum*. Boulenger's *H. steindachneri* has been available since then, although without formal designation of a type specimen. Schaefer (1996b) subsequently argued that the specimen NMW 46272 should be regarded as the holotype of *H. steindachneri*. The specimen, labeled as *H. thoracatum*, had catalog date of entry of 1874 ("Brazil, Río Negro Mündg.") and showed similar values for a

TABLE 15
Morphometric and Meristic Data for *Hypoptopoma steindachneri*
Nontypes: CAS 133271; INHS 39965, 40171, 53744; SIUC 67365; USNM 124286, 190319.

	N	Range		Mean	sd
Standard length	19	62.0	98.2	85.4	9.11
PERCENT OF STANDARD LENGTH					
Predorsal length	19	45.1	48.8	46.6	0.90
Head length	19	33.0	38.6	35.0	1.60
Body depth	19	19.8	24.0	22.3	1.23
Dorsal-fin spine length	19	28.8	33.6	31.6	1.60
Trunk length	19	40.2	44.7	42.4	1.37
Pectoral-fin spine length	19	30.9	36.2	32.6	1.42
Abdominal length	19	16.1	19.1	17.7	0.85
Caudal-peduncle length	19	28.1	32.8	31.0	1.31
Caudal-peduncle depth	19	9.7	11.3	10.8	0.41
Caudal-fin base depth	19	10.2	11.7	10.8	0.50
Head depth	19	17.0	19.8	18.4	0.66
Snout length	19	19.6	22.7	20.9	0.84
Horizontal eye diameter	19	5.3	6.5	6.1	0.35
Least orbit-naris distance	19	6.2	7.6	7.1	0.33
Dorsal interobital distance	19	22.9	24.9	23.9	0.57
Ventral interobital distance	19	20.6	22.8	21.6	0.69
Cleithral width	19	25.9	27.9	27.0	0.60
Head width	19	25.4	28.0	26.3	0.80
Interpelvic distance	19	2.0	6.4	5.1	1.16
PERCENT OF HEAD LENGTH					
Body depth	19	51.3	71.4	63.8	5.93
Head depth	19	45.0	58.8	52.8	3.78
Snout length	19	58.4	62.5	59.8	1.10
Horizontal eye diameter	19	15.5	18.3	17.4	0.79
Least orbit-naris distance	19	18.0	22.3	20.2	1.52
Dorsal interobital distance	19	63.4	72.1	68.4	2.46
Ventral interobital distance	19	58.7	66.0	61.7	1.89
Cleithral width	19	72.4	80.9	77.3	2.18
Head width	19	71.0	79.6	75.3	1.96
Interpelvic distance	19	5.8	19.0	14.7	3.46
PERCENT OF CLEITHRAL WIDTH					
Snout	19	73	82	77	2.1
LATERAL SERIES OF PLATES					
Dorsal series	19	19	20	19	0.2
Middorsal series	19	3	4	4	0.2
Medial series	19	21	22	22	0.2
Midventral series	19	13	15	14	0.7
First midventral series plates	19	3	3	3	0.0
Ventral series	19	19	20	19	0.2
ABDOMINAL SERIES OF PLATES					
Right lateral series	19	4	8	6	1.0
Left lateral series	19	3	7	5	1.1
TEETH					
Premaxillary teeth	19	15	21	19	1.7
Dentary teeth	19	13	20	16	1.8

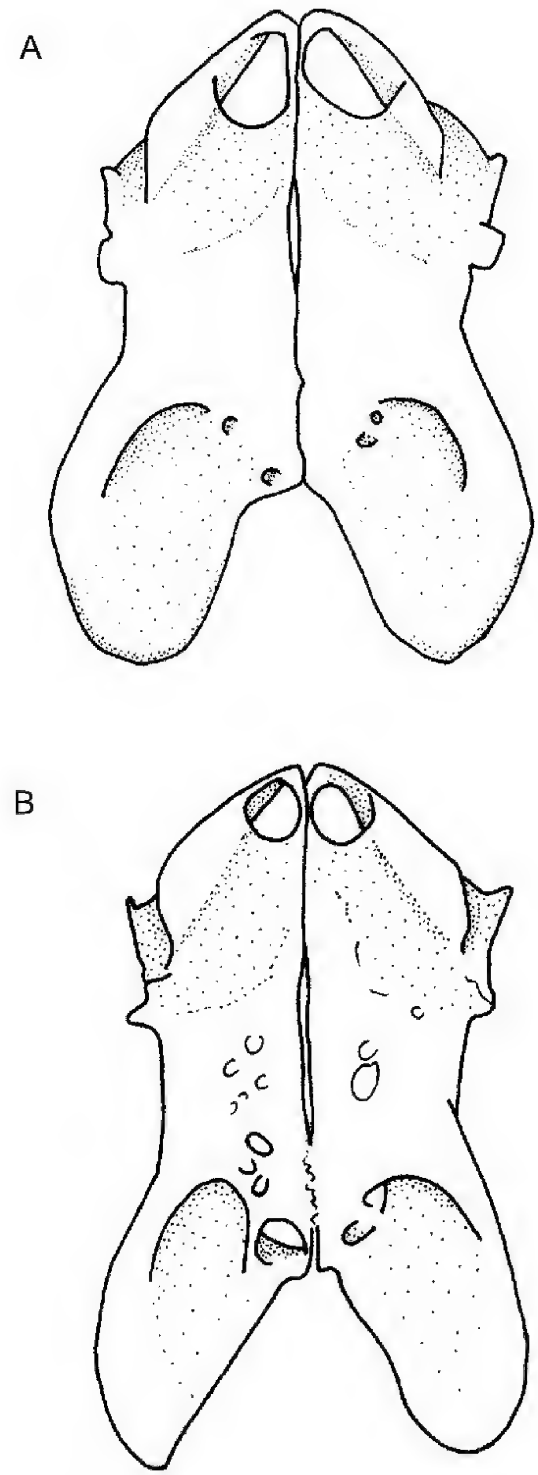

Fig. 41. Basipterygium, ventral view, anterior toward top. A, *H. incognitum*; B, *H. steindachneri*.

series of morphometric characters used in the Steindachner (1879) description. Schaefer (1996b) indicated that the differences in the pattern of plate distribution and the pectoral-fin length observed between the specimen illustrated by Steindachner (1879) and NMW 46272 were due to inaccuracy in the illustration. Subsequent examination of additional material has led us to the conclusion that those supposed discrepancies in plate-related characters and body robustness are rather consistent across material identified as *H. steindachneri* from throughout its geographic range. The following characters are shared by the specimen illustrated by Steindachner and 25 specimens (62.0–98.2 mm SL) we examined, but not shared by specimen NMW 46272: (1) presence of more than one paranasal plates; (2) paranasal plates separating second infraorbital bone from series of pararostral plates; (3) ventral canal-bearing plate subdivided; (4) one dermal plate laterally contacting first, second, and third infraorbital bones, and mesially contacting mostly the anteriormost subdivision of the ventral canal-bearing plate; (5) basipterygium laterally constricted, with interpelvic distance 4.5%–6.4% SL; body robust, which is reflected by the morphometric characters caudal-fin base depth (10.0% SL), cleithral width (27.2% SL), least orbit/naris distance (6.7% SL), and (9) adipose fin absent. Consequently, the designation of NMW 46272 as holotype of *H. steindachneri* is herein invalidated. Instead, we argue that the single specimen illustrated by Steindachner (1879) is the holotype by original designation of Boulenger (1895), as per application of ICZN art. 73.1.4 (ICZN, 1999), regardless of whether the holotype no longer exists.

COMPARISONS: Our observations confirmed *H. steindachneri* as a separate species from *H. gulare*. *Hypoptopoma steindachneri* is distinguished from *H. gulare*, in addition to the character presence of typically more than one paranasal plates between the second infraorbital and the nasal organ (vs. presence of a single paranasal plate), by having a wider head (head width 25.4–28.0 (26.3) vs. 22.4–24.2 (23.4); $t_{(14,247)}$, $p < 0.001$), longer least distance between orbit and naris (least orbit/nare distance 6.2–7.6 (7.1) vs. 4.7–6.0 (5.3);

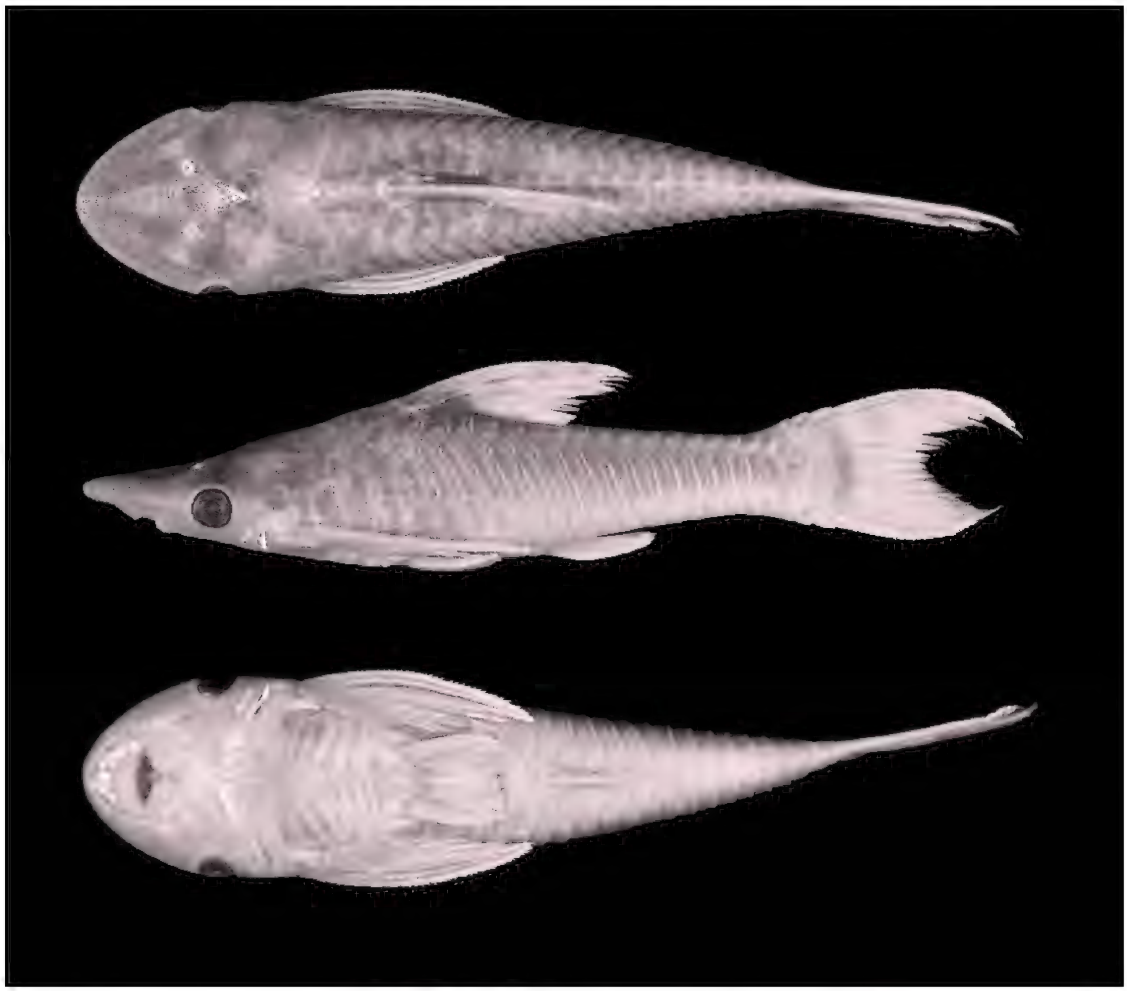

Fig. 42. *Hypoptopoma steindachneri*, SIUC 29198, 88.9 mm female, in dorsal, lateral, and ventral views.

$t_{(17,720)}$, $p < 0.001$), and deeper caudal peduncle (caudal-peduncle depth 9.7–11.3 (10.8) vs. 7.2–9.1 (8.3); $t_{(11.321)}$, $p < 0.001$); by having the second infraorbital entirely separated from the pararostral plates (fig. 7C) (vs. second infraorbital in contact with the pararostral plates); by having the canal-bearing plate typically subdivided (vs. ventral canal-bearing plate undivided); by having the tips of all caudal-fin branched rays typically pigmented (vs. middle caudal-fin branched rays distally light); and by the presence in males of a well-developed flap of soft tissue along the posterior surface of the pelvic spine (vs. absence in males of a flap of soft tissue along the posterior surface of the pelvic spine).

Hypoptopoma gulare Cope, 1878
Figure 43, table 16

Hypoptopoma gulare Cope, 1878: 678 (original description; Pebas, Peru).—Eigenmann and Eigenmann, 1889: 40 (list of catfish species of South America).—Eigenmann and Eigenmann, 1890: 390 (list of catfish species of South America).—Eigenmann and Eigenmann, 1891: 40 (list of catfish species of South America; key).—Regan, 1904: 265 (list of loricariid species; key to *Hypoptopoma* species).—Eigenmann, 1910: 412 (list of freshwater fishes of South America).— Fowler, 1915: 237 (proposed as holotype of subgenus *Diapeltoplites*).—Eigenmann and Allen, 1942: 200 (list of freshwater fishes of Western South America).—Gosline, 1945: 98 (list of catfish species of South and Central America).—Fowler, 1945: 99 (list of

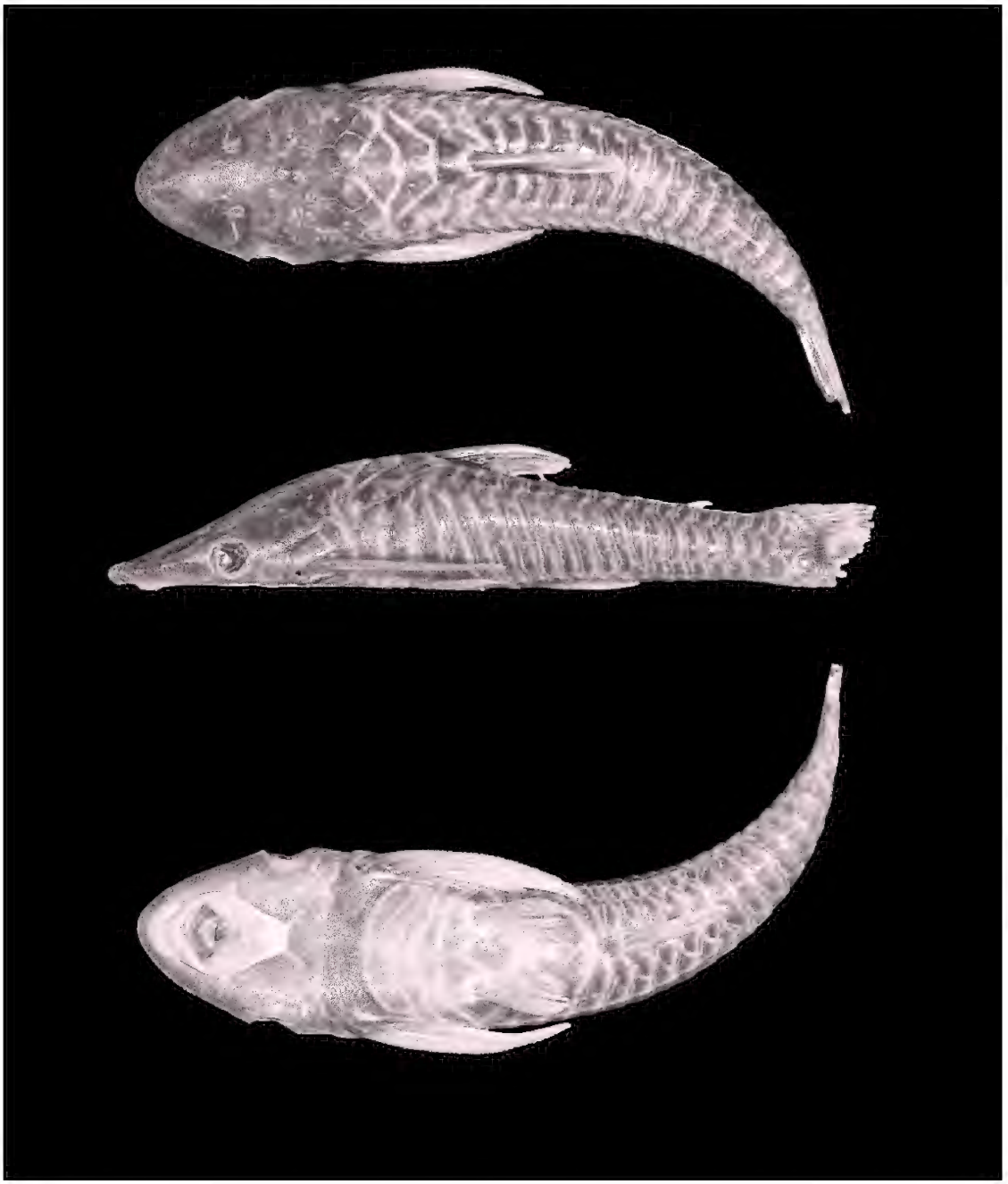

Fig. 43. *Hypoptopoma gulare*, holotype, ANSP 21477, 81.9 mm SL, male, in dorsal, lateral, and ventral views.

freshwater fishes of Peru).—Fowler, 1954: 125 (list of freshwater fishes of Brazil).—Ringuelet and Arámburu, 1961: 52 (Argentina: Rio Paraguay, misidentification).—Ringuelet et al., 1967: 390 (Argentina: Rio Paraguay, misidentification).—Terrazas Urquidi, 1970: 23 (list of fishes of Bolivia, misidentification).—Boeseman, 1974: 265 (list of nominal species of *Hypoptopoma*).— Isbrücker, 1980: 88 (list of loricariid species).—Böhlke, 1984: 122 (catalog of type specimens at ANSP).—Ortega and Vari, 1986: 17 (list of fishes of Peru; Carachama).—

TABLE 16
Morphometric and Meristic Data for *Hypoptopoma gulare*
Holotype: ANSP 21477. Nontypes: INHS 101387; MUSM 4183; NRM 57231; SIUC 26798.

		Nontypes			
	Holotype	*N*	Range	Mean	sd
Standard length	82.0	30	55.4 85.3	71.7	9.32
PERCENT OF STANDARD LENGTH					
Predorsal length	48.4	30	45.4 48.5	47.1	0.89
Head length	34.3	30	33.1 37.2	35.4	1.14
Body depth	20.0	30	17.0 20.8	19.1	1.02
Dorsal-fin spine length	—	26	25.0 29.7	27.5	1.42
Trunk length	43.9	30	39.8 46.2	43.1	1.43
Pectoral-fin spine length	27.7	30	27.1 31.4	29.4	1.14
Abdominal length	17.2	30	15.1 17.4	16.3	0.55
Caudal-peduncle length	33.5	30	30.4 33.5	32.2	0.67
Caudal-peduncle depth	8.7	30	7.2 9.1	8.3	0.51
Caudal-fin base depth	9.7	30	8.1 10.6	9.1	0.55
Head depth	17.4	30	15.8 18.2	16.9	0.59
Snout length	18.8	30	19.0 21.3	20.1	0.64
Horizontal eye diameter	5.8	30	5.3 6.4	5.9	0.27
Least orbit-naris distance	5.5	30	4.7 6.0	5.3	0.34
Dorsal interorbital distance	20.8	30	19.8 22.0	21.1	0.52
Ventral interorbital distance	19.9	30	19.2 21.5	20.3	0.54
Cleithral width	24.5	30	22.9 25.9	24.7	0.52
Head width	22.4	30	22.4 24.2	23.4	0.54
Interpelvic distance	7.1	30	6.3 8.8	7.6	0.70
PERCENT OF HEAD LENGTH					
Body depth	58.3	30	47.1 59.9	54.2	4.01
Head depth	50.6	30	43.1 52.2	47.9	2.31
Snout length	54.7	30	54.9 58.9	56.7	1.00
Horizontal eye diameter	17.0	30	15.2 18.2	16.6	0.67
Least orbit-naris distance	16.0	30	13.1 17.5	15.0	1.08
Dorsal interorbital distance	60.6	30	55.1 63.1	59.6	2.03
Ventral interorbital distance	57.9	30	53.5 60.5	57.4	1.84
Cleithral width	71.2	30	66.6 72.6	69.8	1.96
Head width	65.2	30	63.2 68.8	66.1	1.57
PERCENT OF CLEITHRAL WIDTH					
Snout	76.7	30	47.1 59.9	54.2	4.01
LATERAL SERIES OF PLATES					
Dorsal series	19	10	19 20	19	0.3
Middorsal series	4	10	4 4	4	0.0
Medial series	22	10	22 23	22	0.3
Midventral series	13	10	12 13	13	0.5
First midventral series plates	3	10	3 3	3	0.0
Ventral series	19	10	19 20	19	0.3
ABDOMINAL SERIES OF PLATES					
Lateral right series	4	10	4 8	5	1.3
Lateral left series	5	10	4 6	5	0.6
TEETH					
Premaxillary teeth	15	10	12 16	14	1.3
Dentary teeth	12	10	10 14	12	1.1

Eschmeyer and Ferraris, 1998: 691 (catalog of fishes).—Bistoni et al., 1992: 108 (Argentina: occurrence in Río Dulce, Córdoba; misidentification).—Isbrücker, 2002: 28 (list of loricariid species).—Schaefer, 2003: 323 (list of hypoptopomatine species).—Bogotá-Gregory and Maldonado-Ocampo, 2006: 76 (list of fishes of the Amazon basin in Colombia).—Ferraris, 2007: 250 (list of catfish species).

Otocinclus joberti Vaillant, 1880: 147 (original description; Calderon, upper Amazon, Brazil).

Hypoptopoma joberti Regan, 1904: 265 (placed *Otocinclus joberti* in genus *Hypoptopoma*; key).—Miranda Ribeiro, 1911: 99–101, fig. 59 (list of fishes of Brazil; key to *Hypoptopoma* species).—Miranda Ribeiro, 1912: 8 (Brazil: occurrence in Manaus; redescription).—Pearson, 1924: 24, pl. VIII, fig. 1 (Bolivia: occurrence in Rio Beni; pl. VIII, fig. 1).—Pearson, 1937: 112 (list of fishes of Bolivia).—Fowler, 1915: 237 (assigned to subgenus *Diapeltoplites*).—Fowler, 1940: 97 (fishes of Bolivia).—Fowler, 1945: 100 (list of freshwater fishes of Peru).—Eigenmann and Allen, 1942: 200 (Peru: occurrence in mouth of Río Pacaya, Lago Cashiboya).—Terrazas Urquidi, 1970: 23 (list of fishes in Río Beni).— Boeseman, 1974: 265 (list of nominal species of *Hypoptopoma*).—Schaefer, 2003: 323 (list of hypoptopomatine species).—Ferraris, 2007: 250 (list of catfish species).

Hypoptopoma (*Diapeltoplites*) *gulare*.—Fowler 1915: 237 (type of subgenus *Diapeltoplites*).

HOLOTYPE: ANSP 21477, 81.9 mm SL, ♂, Peru: Loreto, Peruvian Amazonia, Río Marañón; collected by J. Orton, 1877.

OTHER MATERIAL EXAMINED: **PERU, Amazonas**: LACM 36333-3 (1 ♀ + 1 ♂, 55.1–63.1 mm SL) Quebrada Caterpiza. **Loreto**: CAS 77138 (1 ♀, 76.7 mm SL) Ucayali, Lago Cashiboya, a cutoff lake of Río Ucayali above Contamana; CAS 77139 (1 ♀, 56.2 mm SL) Río Pacaya, at the mouth, Bretaña; FMNH 92883 (1 ♀, 78.3 mm SL) Yanamono creek and the small tributary behind Travelrama lodge; FMNH 92884 (1 ♀, 66.1 mm SL) swampy area in the interior of small island in the Río Amazonas; FMNH 108759 (19 ♀ + 10 ♂, 58.9–80.9 mm SL) Río Marañón dr., Caño Abico, tributary to Río Samiría, ca. 6–7 km from mouth in Río Marañón; FMNH 108760 (1 ♀, 33.6 mm SL) Río Marañón dr., Punto Caño ca. 7 km above mouth of Río Chambira in Río Marañón; INHS 40008 (1 ♀, 70.4 mm SL) Río Amazonas dr., Río Orosa, Caño Zapatilla, ca. 10 min. upstream by boat from Río Orosa, 76.4 mi E Iquitos; INHS 40216 (5 ♂, 75.7–87.0 mm SL) Río Itaya dr., Quebrada Mazama, ca. 1 km upstream from confluence with Río Itaya, S of Belem (Iquitos); INHS 44124 (2 ♀, 52.2–58.5 mm SL) Río Amazonas dr., Río Napo and Quebrada Mazán, 33.3 km NE Iquitos; INHS 52027 (1 ♀, 53.1 mm SL) Río Amazonas dr., Río Itaya, Moena caño near confluence with Ullpa caño and lower Ullpa caño, SE of Iquitos; INHS 53742 (2 ♀ + 1 ♂, 71.6–88.1 mm SL) Río Amazonas dr., Río Pampa Chica, 4.5 km W center of Iquitos; INHS 53845 (2 ♀ + 2 ♂, 76.7–105.0 mm SL) Río Amazonas dr., Río Napo, opposite Mazán, N channel Río Napo, N of Isla Milagro; INHS 101387 (63 ♀ + 47 ♂, 46.8–88.4 mm SL) Río Amazonas dr., Río Yamashi, Yamashi, 69.8 mi. E Iquitos; INHS 101390 (2 ♂, 68.5–81.0 mm SL) Río Amazonas dr., Río Orosa, mouth of Tonche Caño, Madre Selva II field station, 69.4 mi E Iquitos; MHNG 2390.25 (1 ♀, 44.5 mm SL) Río Ucayali, San Antonio; MUSM 2673 (12 ♀ + 2 ♂, 63.9–79.8 mm SL) Maynas, Iquitos, Cocha Aguajal; MUSM 7298 (1 ♀, 37.4 mm SL) Alto Amazonas, Río Pastaza, Lago Rimachi, Quebrada Chapuli; MZUSP 15308 (1 ♀, 86.2 mm SL) Río Corrientes; MZUSP 36206 (1 ♂, 43.2 mm SL) Río Ucayali; MZUSP 36208 (1 ♀, 43.0 mm SL) Río Ucayali, Sgto. Lores; SIUC 28113 (1 ♀, 39.0 mm SL) Río Napo, confluence with Río Mazán, ca. 2–3 km N town of Mazán; SU 33272 (1 ♂, 42.6 mm SL) Río Ampiyacu; NRM 17988 (2 ♀, 31.5–78.4 mm SL) Río Napo dr., Cayapoza, small laguna on left bank island; NRM 47513 (3 ♀, 45.7–48.7 mm SL) Río Samiria dr., caño Atún; NRM 57231 (13 ♀ + 4 ♂, 2 cs, 59.6–85.5 mm SL) Río Tahuayo dr., Caño Huayti; SIUC 26798 (1 ♀ + 1 ♂, 57.6–82.1 mm SL) Prov. Fernando Lores, Lago Aguajal, Lucero Pata (between Iquitos and Nauta); SIUC 29198 (2 ♂, 85.1–88.8 mm SL) Prov. Maynas, Río Itaya, upriver of Belén, approx. 4.5 km; SIUC 29363 (1 ♀, 51.5 mm SL) Río Napo, Mazán, 33.3 km from center of Iquitos; SIUC 29422 (2 ♀, 60.1–71.9 mm SL) Itaya dr., Ushpa caño, ca. 100 yrs. uptream from confluence with caño Moena; SIUC 29646 (1 ♀, 71.3 mm SL) Río Nanay,

Pampachica beach, 4.5 km from Iquitos center; SIUC 29664 (1 ♂, 76.9 mm SL) Río Napo, backwater playa behind Isla Milagro, 1.03 km from Mazán; SIUC 30062 (1 ♀, 60.2 mm SL) Prov. Maynas, Río Itaya and Quebrada Mazán, 11 km from Iquitos center; SIUC 67364 (2 ♀, 40.3–59.4 mm SL) Río Napo, confluence with Río Mazán, ca. 2–3 km N (town of) Mazán; SU 34253 (1 ♀, 89.6 mm SL) Río Ampiyacu near Pebas. **Ucayali**: FMNH 42963 (2 ♀, 63.5–77.9 mm SL) Yarinacocha, Río Ucayali dr., Pucallpa. MHNG 2618.88 (2 ♀, 60.2–72.6 mm SL) Pucallpa, Tapistica Alejandria; MHNG 2389–60 (1 ♀ + 1 ♂, 74.1–76.5 mm SL) Pucallpa, Río Ucayali, Romainecocha; MHNG 2389-62 (3 ♀, 56.6–72.9 mm SL) Pucallpa, Río Ucayali, Yarinacocha; MHNG 2618.86 (1 ♀, 70.0 mm SL) Pucallpa, San Antonio, Río Ucayali; MHNG 2618.87 (2 ♀, 68.8–76.0 mm SL) Pucallpa, Bagazán, Río Ucayali; MUSM 1845 (10 ♀ + 2 ♂, 57.28–77.10 mm SL) Pucallpa, Coronel Portillo, Tapistica Alejandria; MUSM 4183 (7 ♀ + 1 ♂, 55.7–80.0 mm SL) Pucallpa, Coronel Portillo, Río Ucayali, Cocha Tacshitea; MZUSP 36195 (21 ♀ + 3 ♂, 55.2–77.4 mm SL) Pucallpa, Río Ucayali; MZUSP 36196 (2 ♀, 52.9–61.0 mm SL) Pucallpa, Río Ucayali; MZUSP 36199 (4 ♀ + 8 ♂, 58.0–76.9 mm SL) Pucallpa, Cocha Romaine, Río Ucayali; MZUSP 36200 (1 ♂, 70.7 mm SL) Pucallpa, Laguna Yarinacocha; MZUSP 36201 (1 ♂, 69.4 mm SL) Laguna Yarinacocha, Río Ucayali, close to Pucallpa; MZUSP 36202 (1 unsexed, 55.1 mm SL) Pucallpa, Río Ucayali; MZUSP 36207 (1 ♀, 42.03 mm SL) Laguna Yarinacocha, Río Ucayali; MZUSP 36229 (2 ♀, 54.5–59.6 mm SL) Utuquinia, Río Ucayali; USNM 284866 (10 ♀, 48.9–60.8 mm SL) Coronel Portillo, Yarinacocha, side caño. **Brazil, Acre**: MZUSP 50368 (1 ♀, 70.0 mm SL) Lago do Breu, Ponto 7, Rio Jurúa. **Amazonas**: INPA 2420 (17 ♀ + 9 ♂, 62.2–85.6 mm SL) Paraná Jaraná, Río Japurá; INPA 2489 (1 ♀, 78.8 mm SL) Lago do Reis; MNHN A-1966 (73.7 mm SL) (holotype of *Otocinclus joberti* Vaillant 1880) Calderon; MZUSP 36209 (6 ♀ + 6 ♂, 55.1–72.9 mm SL) Lago Supiá, in front of Codajás. **Colombia, Amazonas**: NRM 16561 (1 ♀ + 2 ♂, 77.9–82.5 mm SL) Leticia, lagos de Leticia.

Diagnosis: *Hypoptopoma gulare* is distinguished from all congeners, with the exception of *H. machadoi*, by the presence of a single paranasal plate separating the lateral process of the lateral ethmoid from the second infraorbital and the nasal organ (fig. 7B). In contrast, in all other species of *Hypoptopoma*, except *H. steindachneri*, the paranasal plates are absent and the lateral process of the lateral ethmoid contacts the second infraorbital (fig. 7A). In *H. steindachneri*, there are two or more paranasal plates. *Hypoptopoma gulare* is distinguished from *H. machadoi* by a slender caudal peduncle (caudal-peduncle depth 7.2–9.1 (8.3) vs. 9.0–12.0 (10.3); $t_{(16.298)}$, $p < 0.001$); by fewer premaxillary (12–16 (14) vs. 16–25 (20); $t_{(12,675)}$, $p < 0.001$) and dentary teeth (10–14 (12) vs. 14–21 (17); $t_{(12,068)}$, $p < 0.001$); by lanceolate plates at the base of the caudal fin with dark spot, asymmetrically shaped and slightly more extended over lower-lobe branched rays, followed by two V-shaped bars pointing forward, with the anterior bar variably developed on the upper lobe but always connected at its angle with the basal spot (vs. the lanceolate plates at the base of the caudal fin with a light brown spot, symmetrically shaped and shortly extended over the branched rays, typically followed by three vertical bands variably defined, with the anterior band not continuous in the middle with the basal spot); by dorsal fin with dark brown, roughly triangular spot extended over base of anterior 3–4 branched rays, followed typically by 2–3 bars (vs. dorsal fin without triangular spot at base; dorsal fin typically with 4–7 bars).

Description: Morphometric and meristic data presented in table 16. Body robust; greatest body depth at dorsal-fin origin. Dorsal profile of head and body straight from tip of snout to dorsal-fin origin, slightly angled dorsally at posterior tip of supraoccipital; straight from dorsal-fin origin to anteriormost procurrent caudal-fin ray. Ventral profile straight from tip of snout to anteriormost procurrent caudal-fin ray. Head moderately depressed, almost as wide as cleithral width; lateral process of lateral ethmoid visible dorsally. Snout rounded to slightly acute in dorsal view; slightly concave dorsally anterior to naris. Posterior surface of

bony pit of nasal organ sharply inclined. Trunk cross section between pectoral- and pelvic-fin origins slightly triangular, ovoid to progressively rounded posterior to dorsal fin, progressively compressed posterior to adipose-fin base.

Eyes relatively large, positioned closer to posterior tip of compound pterotic than to tip of snout. Ventral margin of orbit located on ventral surface of head. Dorsal interorbital distance/ventral interorbital distance ratio changing from <1 to >1 during ontogeny.

Total plates in medial series 22–23 (22). Dorsal series plates 19–20 (19); middorsal series plates 4; midventral series plates 12–13 (13), three plates anterior to first ventral series plate; ventral series plates 19–20 (19). Second plate of midventral series contacting two plates of medial series.

Abdomen covered by paired series of lateral sickle-shaped plates, with unequal number of plates between left and right sides, 4–8 each; anterior azygous plate usually present; medial abdominal plates, if present (22% of 132 individuals examined), not forming well-defined series. Single anal plate present. Thoracic plates present, 2–6. Preopercular canal present and semicircular; anteriormost pore opening between ventral canal-bearing plate and fourth infraorbital; posterolateral margin of canal-bearing plate and lateral margin of fourth infraorbital smooth, framed by notch at posterolateral margin of canal-bearing plate and ventral margin of fourth infraorbital.

Small odontodes evenly distributed on head. Odontodes along snout margin not arranged in well-defined series, without odontode-free discontinuity between ventrad and dorsad odontodes. Odontodes on dorsal snout margin small, slightly larger than those on dorsal surface of head. Lamina of trunk plates with odontodes arranged in longitudinal rows, becoming progressively smoother ontogenetically; marginal odontodes present in mature adults.

Total vertebrae 26. Premaxillary teeth 12–16 (10); dentary teeth 10–14 (10). Maxillary barbels short, reaching slightly beyond anterior margin of canal-bearing plate in adults.

Dorsal-fin origin located slightly posterior to vertical through pelvic-fin origin. Depressed dorsal fin reaching to vertical through midpoint of anal-fin base. Pectoral fin reaching to vertical through midpoint between pelvic-fin tip and anal-fin origin. Pectoral spine serrae present, oriented orthogonal to spine shaft. Extension of serrae along pectoral spine margin reduced ontogenetically from proximal two-thirds in smaller specimens to middle third in larger specimens. Pelvic fin short, unbranched and first branched rays of equal length. Depressed fin reaching anus, not reaching anal-fin origin. Caudal-fin margin concave to forked; upper and lower lobes equal. Adipose fin present.

COLOR IN ALCOHOL: Ground color tan and pale ochre. Melanophores light to dark brown on trunk and particularly clustered at base of plates, resulting in mottled appearance; melanophores on head more uniformly distributed; melanophores slightly more concentrated along narrow area among compound pterotic, cleithral process, and opercle, at base of dorsal and pectoral fins, and on anterior surface of lip. Deep-lying melanophores arranged in series of blotches posterior of dorsal-fin base. Midlateral stripe situated mostly along medial series of trunk plates. Ventral surface of body mostly unpigmented except for scattered melanophores on posterior portion of trunk, anterolateral margin of cleithra and posterior tip of cleithral processes, ventral canal-bearing plates, and lateral portions of lateral abdominal series. Paired dorsal and anal fins with dark brown bars, roughly orthogonal to rays. Dorsal fin with dark brown, roughly triangular spot extended over base of anterior 3–4 branched rays. Series of lanceolate plates at base of caudal fin darkened by black melanophores. Basal triangular dark spot over caudal-fin lower lobe determined by lower-lobe arm of most anterior V-shaped bar variably merging with spot at lanceolate plates. Upper-lobe arm of same bar light brown to absent, clearly separated from spot at lanceolate plates. One or two following, nearly complete V-shaped bars pointing forward and 1–3 incomplete bars along posterior half of upper and lower lobes; tip of branched rays usually light (fig. 17D).

SEXUAL DIMORPHISM: Males with urogenital papilla well developed, pointed; joined at base to anterior flaplike anus. Males with

patch of tightly arranged small odontodes oriented as a swirl, variably covering from first to fourth plates of ventral series, lateral to urogenital papilla and narrow band along posterior border of anal plate. Female anus tubular, without separate urogenital papilla. In females, size and arrangement of odontodes on plates lateral to anus similar to adjacent plates, without distinct patch of differentially arranged odontodes.

DISTRIBUTION: Upper Amazon River in Brazil; lower and upper Río Ucayali (fig. 39).

TAXONOMIC REMARKS: Cope (1878) described *Hypoptopoma gulare* based on a single specimen collected in 1877 near Pebas by Orton. Cope compared the new species with *H. bilobatum* Cope (1870) and distinguished *H. gulare* by having a more robust body, a lower number of lateral plates, presence of thoracic plates, and the absence of a medial series of abdominal plates. Vaillant (1880) described the new species *Otocinclus joberti* based on the examination of a single specimen collected by Jobert in Calderón (Rio Amazonas, Manaus region). The genus *Otocinclus* had been established by Cope (1871) (for a historical review, see Schaefer, 1997). Vaillant failed to recognize the similarity between his specimen and previously described *Hypoptopoma* species (*H. thoracatum* in 1868, *H. bilobatum* in 1870, and *H. gulare* in 1878). Berg (1898) properly reassigned Vaillant's species to the genus *Hypoptopoma*. Gosline (1945) proposed *H. joberti* as a junior synonym of *H. gulare*, an opinion shared by Fowler (1954); however, neither of these authors provided argumentation for that nomenclatural act. Our examination of the type specimens and additional comparative material confirm the synonymy of *H. joberti* and *H. gulare*.

Hypoptopoma machadoi, new species
Figure 44, table 17

HOLOTYPE: MBUCV V-35362 (♀, 46.2 mm SL) Venezuela: San Fernando de Apure, swamps on south bank of Río Apure, ca. 3 km west of Fisheries Station; collected by Apure Fisheries Station technicians, 21 January 1983.

PARATYPES: AMNH 77794, 23 females, 42.1–53.7 mm SL (collected with holotype).

OTHER MATERIAL EXAMINED: **COLOMBIA, Meta**: ANSP 128569 (1 ♂, 48.3 mm SL) Hacienda Mozambique, N. shore at main house; ANSP 128955 (9 ♀ + 3 ♂, 45.8–61.7 mm SL) Río Negro, just downstream from where it passes under the main Villavicencio, Puerto López highway at La Balsa (W side of river); ANSP 128956 (6 ♀ + 3 ♂, 50.4–69.3 mm SL) Río Negrito midway between La Argelia and La Balsa (Plancha 267 – Río Guayuriba); ANSP 128960 (16 ♀ + 2 ♂, 47.5–66.5 mm SL) Río Negro, just downstream from where it passes under the main Villavicencio, Puerto López highway at La Balsa; ANSP 131666 (5 ♀ + 1 ♂, 45.6–61.9 mm SL) Río Negrito downstream bridge at La Balsa; ANSP 134438 (18 ♀ + 3 ♂, 2 cs, 39.8–53.2 mm SL) tributary caño La Raya (first caño N de La Siberia); ANSP 139463 (3 juveniles, 25.5–31.0 mm SL) canal y laguna Aerotas, S. side of Río Metica, entrance on Metica, ca. 2 km. SW (upstream) of entrance to Lake Mozambique; FMNH 84005 (1 ♂ + 2 juveniles, 24.3–51.3 mm SL) Caño Venturosa, at 1 km N Puerto López. **VENEZUELA, Amazonas**: MCNG 6306 (4 ♀, 43.7–59.7 mm SL). **Anzoátegui**: ANSP 166734 (2 ♀, 54.9–57.8 mm SL) Río Orinoco basin, Soledad, L. Terecaya. **Apure**: ANSP 130028 (1 ♀, 41.7 mm SL) Camaguán swamp, on W side of Hwy to San Fernando de Apure, about 2 km N of Camaguán; ANSP 130040 (12 ♀, 1 cs; 38.2–50.5 mm SL) S bank and backwater areas pm downstream side of bridge at San Fernando de Apure; ANSP 165843 (4 ♀ + 3 ♂, 53.6–69.0 mm SL) Río Cunaviche, ca. 20 km SW of Cunaviche on San Fernando de Apure–Puerto Paez Hwy; ANSP 165844 (1 ♀, 38.8 mm SL) Río Matiyure, at Achaguas; ANSP 166433 (2 ♀, 31.4–44.9 mm SL) Caño Caicara, 10–12 km W of Montecal; CAS 64271 (3 ♀, 44.0–58.1 mm SL) pool just S of Bruzual alongside dyke that parallels highway behind bull run; CAS 64283 (59 ♀ + 4 ♂, 35.6–62.2 mm SL) Caño first creek S of Bruzual at red steel bridge; FMNH 85814 (35 ♀ + 3 ♂, 33.9–53.4 mm SL) River 24 km S Biruaca on road to San Juan de Apayara; FMNH 85826 (10 ♀ + 1 ♂, 31.2–47.2 mm SL) Río Aruaca, 32.5 Km S Biruaca; INHS 29809 (13 ♀, 40.7–53.2 mm SL) tributary caño Setento, 10 km. S Bruzual; INHS 30098 (34 ♀, 27.9–45.4 mm SL) Caño Guaritico (=

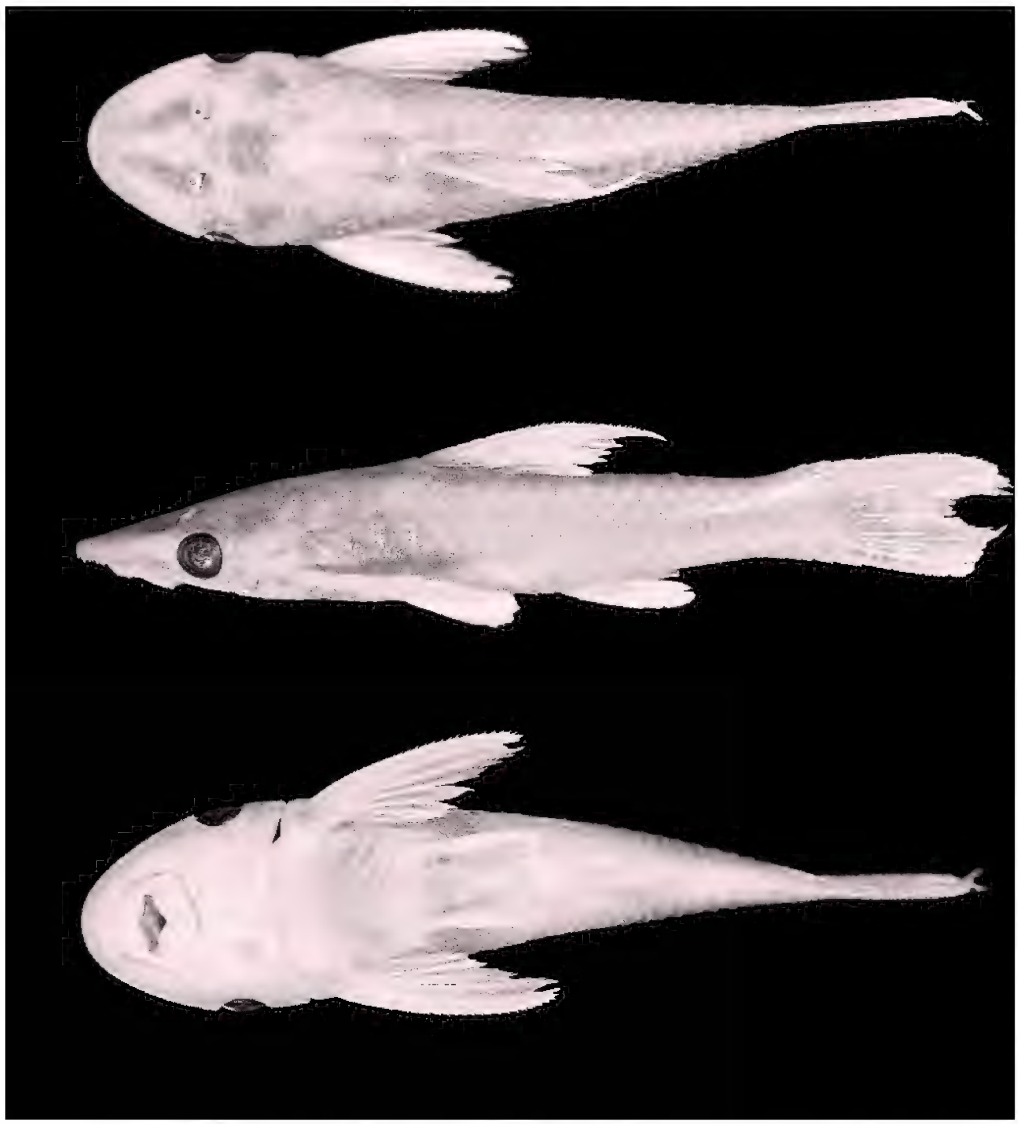

Fig. 44. *Hypoptopoma machadoi*, paratype, AMNH 77794, 46.2 mm SL female, in dorsal, lateral, and ventral views.

caño Maporal) (Río Apure drainage), 58 km SSW Bruzual; MCNG 6104 (7 ♀, 37.1–44.3 mm SL); MCNG 9369 (8 ♀ + 4 ♂, 42.5–49.3 mm SL); MZUSP 27973 (51 ♀, 32.3–51.0 mm SL) caño 1 km ao sul passagem de balsa, na altura da estrada de San Fernando de Apure; USNM 257971 (2 ♀, 43.3–44.2 mm SL) Río Apure West of town center; USNM 257972 (68 ♀ + 1 ♂, 35.1–49.7 mm SL) Caño Caicará, where crossed by bridge on road from Montecal; USNM 257975 (2 ♀, 46.8–50.6 mm SL) Río Apure ca. 2 km East of bridge at San Fernando de Apure; USNM 260193 (52 ♀ + 2 ♂, 32.7–66.1 mm SL) side channel of Río Apure ca. 5 km West of San Fernando de Apure. **Barinas**: FMNH 105985 (2 ♀, 36.7–42.9 mm SL) Río Suripa ca. 10 min. by boat above confluence with Río Carapo; FMNH 105986 (1 ♀, 62.5 mm SL) Río Anaro ca. 10 min. from mouth in Río Suripa, small island and collected small arms of river; FMNH 105987 (27 ♀ + 4 juveniles, 30.7–49.2 mm SL) Caño La Indiecita near mouth

TABLE 17
Morphometric and Meristic Data for *Hypoptopoma machadoi*
Holotype: MBUCV V-35362. Paratype: AMMH 77794. Nontypes: ANSP 165843; CAS 64283; FMNH 85814, 85826; LACM 43204-4; MCNG 9369.

	Holotype	*N*	Range		Mean	sd
Standard length	48.1	74	38.5	69.6	54.3	8.02
PERCENT OF STANDARD LENGTH						
Predorsal length	48.0	74	45.7	50.8	47.8	1.20
Head length	35.6	74	32.7	39.8	35.9	1.60
Body depth	18.3	74	18.0	22.2	20.1	0.84
Dorsal-fin spine length	32.6	71	27.3	35.4	31.4	1.58
Trunk length	37.6	74	36.4	46.0	42.1	1.70
Pectoral-fin spine length	30.1	73	28.1	33.7	31.1	1.25
Abdominal length	15.1	74	14.1	18.3	16.7	0.92
Caudal-peduncle length	28.4	74	27.3	34.4	31.1	1.30
Caudal-peduncle depth	10.2	74	9.0	12.0	10.3	0.59
Caudal-fin base depth	11.8	69	7.8	13.9	9.5	1.48
Head depth	15.9	74	16.2	19.4	17.7	0.74
Snout length	19.4	74	18.2	22.0	19.8	0.90
Horizontal eye diameter	6.2	74	5.8	7.8	6.5	0.39
Least orbit-naris distance	4.9	73	4.5	6.5	5.3	0.43
Dorsal interobital distance	22.9	74	20.2	24.4	21.8	1.05
Ventral interobital distance	22.3	74	19.5	23.5	21.2	1.08
Cleithral width	26.1	74	24.3	27.9	26.1	0.82
Head width	25.1	74	22.3	27.2	24.7	1.16
Interpelvic distance	6.9	74	4.5	9.0	7.5	0.78
PERCENT OF HEAD LENGTH						
Body depth	51.3	74	48.2	63.7	56.2	3.63
Head depth	44.7	74	41.6	54.9	49.5	2.97
Snout length	54.6	74	52.0	58.0	55.4	1.14
Horizontal eye diameter	17.4	74	15.7	21.3	18.3	0.96
Least orbit-naris distance	13.7	74	12.5	19.1	14.7	1.31
Dorsal interobital distance	64.4	74	55.7	65.8	60.9	2.12
Ventral interobital distance	62.5	74	54.6	64.5	59.3	1.87
Cleithral width	73.2	74	67.9	77.5	72.8	2.32
Head width	70.6	74	65.2	73.9	69.0	1.62
Interpelvic distance	19.5	74	11.5	25.9	21.1	2.18
PERCENT OF CLEITHRAL WIDTH						
Snout	74.5	74	71.3	82.3	76.1	2.37
LATERAL SERIES OF PLATES						
Dorsal series	19	45	18	19	19	0.2
Middorsal series	4	45	3	4	4	0.1
Medial series	23	45	21	22	22	0.1
Midventral series	12	45	12	13	13	0.3
First midventral series plates	3	45	3	3	3	0.0
Ventral series	7	45	18	19	19	0.1
ABDOMINAL SERIES OF PLATES						
Right lateral series	7	44	3	10	6	1.2
Left lateral series	6	44	4	8	6	0.9
TEETH						
Premaxillary teeth	19	46	16	25	20	1.9
Dentary teeth	17	45	14	21	17	1.4

in Río Suripa ca. 35 min. up river from boat launch in Hato Mercedes; FMNH 105988 (3 ♀, 42.7–48.1 mm SL) Caño Socopo ca. 3.5 hours upstream from boat launch of Hato Mercedes in Río Suripa.; FMNH 108762 (1 ♀, 48.3 mm SL) Río Orinoco drainage, Caño Caigua ca. 20 min. by boat from boat launch at Hato Las Mercedes; INHS 28696 (20 ♀, 47.1–56.0 mm SL) Río Santo Domingo (Río Apure drainage) in Torunos, hacienda La Isla; MCNG 21329 (7 ♀, 42.2–53.3 mm SL); MCNG 26277 (6 ♀ + 1 ♂, 41.9–55.9 mm SL). **Bolívar**: ANSP 135631 (11 ♀ + 7 ♂, 42.1–63.1 mm SL) Caño Chuapo ca. 20 min. downstream from Jabillal (opposite bank) on Río Caura; ANSP 135678 (20 ♀ + 1 ♂, 36.8–57.1 mm SL) mouth of caño Chuapo ca. 20 min. downstream from Javillal (opposite bank) on Río Caura; ANSP 139521 (1 ♀, 39.9 mm SL) Quebrada Cuchivero (Cuchiverito), tributary of Río Mato (right bank); ANSP 139620 (12 ♀ + 1 ♂, 40.0–61.2 mm SL) Sandbar along Río Mato; ANSP 160863 (1 ♀, 42.2 mm SL) Río Cuchivero at Cuchivero ferry crossing; FMNH 97050 (1 ♀, 40.8 mm SL) Río Orinoco, cove West end of islote Fejardo, 182 naut. mi. upstream from sea buoy; FMNH 108767 (1 ♀, 43.4 mm SL) Río Orinoco basin, S bank of Río Orinoco at mouth of Río Orocopiche, in mouth and along Orinoco; FMNH 108768 (4 ♀, 38.2–55.0 m SL) Río Orinoco basin, Río Orinoco just above bridge at Ciudad Bolívar; MCNG 6658 (3 ♀ + 1 ♂, 47.4–70.8 mm SL); SU 48664 (9 ♀ + 1 ♂, 40.6–48.9 mm SL) Río Orinoco at Caicará; USNM 265696 (1 ♀, 41.5 mm SL) Río Orinoco, Cove, Islote de Fajardo, 182 naut. mi. upstream from sea buoy; USNM 265963 (1 ♀, 47.6 mm SL) small caño connecting with Río Orinoco immediately South of El Burro. **Cojedes**: MCNG 13770 (1 ♀ + 6 juveniles, 20.6–45.0 mm SL). **Delta Amacuro**: AMNH 47955 (6 ♀, 38.6–48.0 mm SL) lagoon at caño Araguaíto, ca. Km 130, Río Orinoco; ANSP 152860 (9 ♀, 1 cs, 36.7–47.1 mm SL) ca. Km. 65, small caño near mouth of caño Fiscal, Río Orinoco; FMNH 97051 (1 ♀, 36.3 mm SL) backwater caño Araguao, 112 naut. mi. upstream from sea buoy; FMNH 97052 (4 ♀, 44.4–49.7 mm SL) Río Orinoco, cave on sand bar near E end of Isla Portuguesa, 117 naut. mi. upstream from sea buoy; FMNH 97066 (14 ♀, 37.9–53.5 mm SL) Río Orinoco, first small caño on W side of caño Paloma 100 m above its mouth, 92 naut. mi. upstream from sea buoy; FMNH 108765 (1 ♀, 43.4 mm SL) Río Orinoco at plays on North side; FMNH 108766 (2 ♀, 44.7–48.3 mm SL) Río Santa Clara at first tributary on East side ca. 0.5 hour above mouth; LACM 43016-2 (1 ♀, 48.2 mm SL) N bank – beach across from Los Castillos; 160 NM upstream from sea buoy; LACM 43151-16 (69 ♀ + 1 ♂, 32.9–54.1 mm SL) Río Orinoco, inlet; 82 NM upstream from sea buoy; LACM 43204-4 (30 ♀ + 3 ♂, 35.2–66.8 mm SL) Río Orinoco, shallow lagoon on N side of river, W of caño Araguarito; LACM 43297-2 (15 ♀ + 1 juvenile, 25.3–46.5 mm SL) Teda, caño Paloma system; USNM 265682 (1 ♀, 44.3 mm SL) Río Orinoco, first small caño on W side of caño Paloma 100 m above its mouth, 92 naut. mi. upstream of sea buoy; USNM 265708 (5 ♀, 38.3–50.6 mm SL) Río Orinoco, small caño near mouth of caño Socoroco, 111 naut. mi. upstream from sea buoy. **Guárico**: ANSP 166732 (19 ♀, 38.9–48.8 mm SL) Río Orinoco basin, Cabruta, Laguna Larga II; ANSP 166733 (1 ♀ + 1 ♂, 37.4–62.7 mm SL) Río Orinoco basin, Cabruta, Laguna Larga II; FMNH 85807 (1 ♀, 39.9 mm SL) pond by river at 8 km E of Camaguán on road to Uvenito; INHS 62063 (43 ♀,33.9–47.1 mm SL) caño (Río Guariquito–Río Orinoco drainage) 100 air km E San Fernando; MCNG 15072 (10 ♀, 37.8–48.7 mm SL); USNM 257969 (7 ♀, 32.8–43.4 mm SL) Caño Falcon ca. 5 km north of RPV 83-4; Río Portuguesa drainage basin; USNM 257973 (16 ♀, 36.2–48.3 mm SL) Caño to West of highway from Calabozo to San Fernando about 35 km South of Fundo Masaguaral, Caño Falcon; USNM 257976 (1 ♀, 45.6 mm SL) Río Guárico at Flores, Moradas ranch ca. 3–4 km East of road from Calabozo to San Fernando. **Monagas**: CAS 58157 (5 ♀, 47.0–54.8 mm SL) Río Orinoco, small caño 0.75 miles upstream from mouth of caño Guarguapo, near Barrancas; LACM 43382-29 (7 ♀, 43.0–54.9 mm SL) Río Orinoco, secondary caño about 500 m from its mouth in caño Guarguapo; LACM 43423-4 (31 ♀ + 1 ♂, 35.1–50.7 mm SL) Río Orinoco, S shore of Isla Noina, 51–52 NM

from sea buoy; USNM 163172 (1 ♀, 53.0 mm SL) Caicará, Río Guarapiche; USNM 265718 (17 ♀, 3 cs, 36.3–48.3 mm SL) Río Orinoco, 161 naut. mi. upstream from sea buoy, laguna Tapatapa on Isla Tapatapa near downstream end of caño de Limón. **Portuguesa**: MCNG 1179 (4 ♀ + 3 ♂, 39.0–55.5 mm SL); TNHC 12513 (6, 43.6–53.3 mm SL) Caño Maraca at Urriolas ranch, 35 km SE Guanaré; TNHC 12766 (10 ♀, 35.6–39.8 mm SL) Caño Maraca at Urriolas ranch, 35 km SE Guanaré; USNM 348681 (12 ♀, 38.2–57.8 mm SL) Guanaré-Guanarito, road at road km 60; caño Igues–Río Portuguesa (Caño Maraca).

DIAGNOSIS: *Hypoptopoma machadoi* is distinguished from all congeners, with the exception of *H. gulare*, by the presence of a single paranasal plate separating the lateral process of the lateral ethmoid from the second infraorbital and the nasal organ (fig. 7B). In contrast, in all other species of *Hypoptopoma*, except *H. steindachneri*, the paranasal plates are absent and the lateral process of the lateral ethmoid contacts the second infraorbital (fig. 7A). In *H. steindachneri*, there are two or more paranasal plates (fig. 7C).

Hypoptopoma machadoi is distinguished from *H. gulare* by its deeper caudal peduncle (caudal-peduncle depth 9.0–12.0 (10.2) vs. 7.2–9.1 (8.7); $t_{(16.298)}$, $p < 0.001$); by its greater number of premaxillary (16–25 (20) vs. 12–16 (14); $t_{(16.298)}$, $p < 0.001$) and dentary teeth (14–21 (17) vs. 10–14 (12); $t_{(12,068)}$, $p < 0.001$); by having lanceolate plates at caudal-fin base with light brown spot, symmetrically shaped, shortly extended over branched rays; spot followed by three vertical bands variably defined, with anterior band not continuous along midline with the basal spot (vs. lanceolate plates at caudal-fin base with dark spot, asymmetrically shaped, slightly more extended over lower-lobe branched rays; this spot is followed by two V-shaped bars, anterior bar variably developed on the upper lobe but always connected with basal spot) (fig. 17B); and by having the dorsal fin with typically three bars, without triangular spot at base (vs. dorsal fin with roughly triangular dark brown spot extended over base of anterior 3–4 branched rays, followed typically by 3–4 bars) (fig. 17G).

Hypoptopoma machadoi is distinguished from *H. steindachneri* by having a single paranasal plate (vs. presence of two or more paranasal plates) (fig. 7B–C), second infraorbital in contact with nasal and pararostral plates (vs. second infraorbital entirely separated from nasal and pararostral plates), and ventral canal-bearing plate undivided (vs. canal-bearing plate typically subdivided) (fig. 5A–B).

DESCRIPTION: Morphometric and meristic data presented in table 17. Body robust; greatest body depth at dorsal-fin origin. Dorsal profile of head and body straight from tip of snout to dorsal-fin origin, slightly angled dorsally at posterior tip of supraoccipital; straight from dorsal-fin origin to anteriormost procurrent caudal-fin ray. Head moderately depressed, almost as wide as cleithral width; lateral process of lateral ethmoid bone visible dorsally. Snout rounded in dorsal view; dorsally, slightly concave anterior to naris. Posterior surface of bony pit of nasal organ sharply inclined. Trunk cross section between pectoral-fin and pelvic-fin origins slightly triangular, ovoid to progressively rounded posterior to dorsal fin, progressively compressed posterior to adipose-fin base.

Eyes relatively large, positioned closer to posterior tip of compound pterotic than to tip of snout. Ventral margin of orbit located on ventral surface of head. Dorsal interorbital distance/ventral interorbital distance ratio changing from <1 to >1 during ontogeny.

Total plates in lateral medial series typically 21–22 (22). Dorsal series plates 18–19 (19); middorsal series plates 3–4 (4); midventral series plates 12–13 (13), three plates anterior to first ventral series plate; ventral series plates 18–19 (19). Second plate of midventral series contacting two plates of medial series.

Abdomen covered by paired series of lateral sickle-shaped plates, with unequal number of plates between left and right series, 3–10 each; anterior azygous plate usually present; medial series of plates, if present (47% of 316 individuals examined), not forming well-defined series. Single anal plate present. Thoracic plates present, 2–6. Preopercular canal present, semicircular;

anteriormost pore located between ventral canal-bearing plate and fourth infraorbital; posterolateral margin of canal-bearing plate and lateral margin of fourth infraorbital variably developed, framed by notch at posterolateral margin of canal-bearing plate and ventral margin of fourth infraorbital.

Small odontodes evenly distributed on head. Odontodes along rostral margin of snout not arranged in well-defined series, without odontode-free discontinuity between ventrad and dorsad odontodes. Odontodes dorsal to tip of snout small, slightly larger than those on dorsal surface of head. Lamina of trunk plates with odontodes arranged in longitudinal rows, becoming progressively smoother ontogenetically; marginal odontodes present in mature adults.

Total vertebrae 26. Premaxillary teeth 16–25 (20); dentary teeth 14–21 (17). Maxillary barbels short; in adults, slightly surpassing anterior margin of ventral canal-bearing plate.

Dorsal-fin origin located slightly posterior to vertical through pelvic-fin origin. Depressed dorsal fin reaching to vertical through distal half of anal-fin base. Pectoral fin reaching to vertical through midpoint between anus and anal-fin origin. Pectoral spine with serrae along posterior margin, individual serrae oriented orthogonal to spine shaft. Extension of serrae along pectoral spine margin reduced ontogenetically from proximal two-thirds in smaller specimens to middle third in larger specimens. Depressed pelvic fin not reaching to anal-fin origin; unbranched and first branched rays of equal length. Caudal-fin margin concave; upper and lower lobes equal. Adipose fin present.

COLOR IN ALCOHOL: Ground color tan and light brown. Melanophores light to dark brown, clustered on trunk and at base of plates, yielding mottled appearance. Pigmentation slightly more concentrated dorsally on head, along narrow area betweeen compound pterotic, cleithral process and opercle, at base of dorsal and pectoral fins, and on anterior surface of lip. Deep-lying melanophores arranged as series of blotches posterior to dorsal-fin base. Midlateral stripe mostly along trunk medial series of plates. Ventral surface of body mostly unpigmented except for scattered melanophores on posterior portion of trunk, anterolateral margin of cleithra and posterior tip of cleithral process, lateral border of canal-bearing plates, and lateral portions of lateral abdominal series. Paired dorsal and anal fins with dark brown bars, aligned roughly orthogonal to the rays. Basal dark spot on anterior dorsal-fin branched rays typically not developed; if present, spot poorly defined. Lanceolate plates at base of caudal fin with light brown spot, symmetrically shaped and shortly extended over branched rays, followed by typically three vertical bands variably defined, with anterior one not continuous in the middle with basal spot; tips of lobes variably pigmented (fig. 17G).

SEXUAL DIMORPHISM: Males with genital papilla small, not clearly separated from tubelike anal papilla. Males without patch (or patch poorly developed) of tightly arranged small odontodes oriented as a swirl on plates lateral to anal region. Female anus tubular, without separate urogenital papilla. In females, size and arrangement of odontodes on plates lateral to anus similar to adjacent plates, without distinct patch of differentially arranged odontodes.

DISTRIBUTION: Known for the Rio Orinoco basin in Venezuela, including the Rio Meta drainage in Colombia (fig. 39).

REMARKS: Specimens collected in the Río Meta drainage and in localities along the southern tributaries of the Río Orinoco are slightly more slender and with fewer caudal-fin bars than specimens that originated in localities from northern tributaries to the Río Orinoco.

ETYMOLOGY: The specific epithet *machadoi* is a patronymic honoring Antonio Machado-Allison, in recognition of his lifelong dedication and contributions to Neotropical ichthyology.

PHYLOGENETIC ANALYSIS

Character Descriptions and Coding

Dermal Plates

0. **Trunk plates with column of slightly enlarged and flattened odontodes arranged along posterior plate margin**—all *Hypoptopoma* species except *H. spectabile*.

In loricariids, the exposed surface of the trunk plates bears odontodes of uniform size and regular distribution. Those odontodes that may extend beyond the posterior plate margin are of the same form and size as those distributed on the plate surface (fig. 6B). In the derived condition, the odontodes arranged along the posterior plate margin are conspicuous, larger than the typical odontode, and slightly flattened relative to the typical conical shape. Further, the marginal odontodes are not aligned with the odontodes of the longitudinal rows covering the exposed surface of the plates (fig. 6A).

1. **Second plate of midventral lateral plate series associated dorsally with two plates of medial series**—*bianale*, *elongatum*, *gulare*, *incognitum*, *inexspectatum*, *machadoi*, *spectabile*, *steindachneri*, *sternoptychum*.

Loricariids generally have the dermal plates arranged in five serially homologous rows along the trunk, which can be identified on the basis of positional relationship to one another and to the trunk lateral-line canal and nerve (Schaefer, 1997). The plesiomorphic state in loricariids is having a one-to-one relationship between midventral and medial plates along the entire series (fig. 8A). In the derived condition, two medial plates of the medial series are arranged in tandem with the second midventral plate (fig. 8B).

The arrangement of plates in the derived condition may have arisen as the consequence of either the addition of one medial-series plate and its associated laterosensory canal, or by the loss of one midventral series plate. In the plesiomorphic 1:1 condition, the medial plate contacting the second midventral plate is associated with the ventral tip of the connecting bone on its mesial surface. In the derived condition, the connecting bone association involves the anterior of the two medial-series plates.

2. **Reduced number of midventral series plates between cleithrum posterior process and first plate of ventral series**—*bianale*, *elongatum*, *gulare*, *inexspectatum*, *incognitum*, *machadoi*, *spectabile*, *steindachneri*, *sternoptychum*.

Species of *Oxyropsis*, like most Hypoptopomatinae, have four midventral lateral trunk plates between the posterior process of the cleithrum and the first plate of the ventral lateral trunk series (fig. 8A). In the derived condition, the number of plates is reduced to three (state 1) (fig. 8B).

3. **Transverse shield of plates on head between cleithra and paired canal-bearing plates**– *bianale*, *elongatum*, *gulare*, *incognitum*, *inexspectatum*, *machadoi*, *steindachneri*, *sternoptychum*.

The plesiomorphic condition among loricariids is having an unplated area on the ventral surface of the head between the anterior margin of the paired cleithra and the paired ventral canal-bearing plates (fig. 9A). In the derived condition, that area is covered by a transverse shield of 4–6 plates (thoracic plates) that contacts the margin of the cleithra and the canal-bearing plate (state 1) (fig. 9B–C). The shield formed by the thoracic plates can be clearly distinguished from the bones of the pectoral girdle and the abdominal plates.

4. **Medial series of abdominal plates in fully mature adults reduced or absent**—*bianale*, *elongatum*, *gulare*, *incognitum*, *inexspectatum*, *steindachneri* (state 1); *spectabile*, *sternoptychum* (state 2). Character nonadditive.

The plesiomorphic condition for Hypoptopomatini is having the abdominal plates arranged in three series, with the medial series composed of three or more individual plates (fig. 9A). In the derived condition, the medial series is reduced to presence of a single plate, positioned anteriorly at the posterior margin of the coracoids (state 1) (fig. 9B–C), or absent, with the paired lateral plates in contact along the midline for their entire length (state 2) (Schaefer, 1996a: fig. 1). This character applies only for fully mature adult specimens. The abdominal plates (along with both the prenostril and thoracic plates) are the last to form in ontogeny, and therefore the character cannot be evaluated for immature specimens.

5. **Distinct patch of odontodes on anterolateral aspect of cleithrum, at entrance to branchial cavity**—*elongatum*, *incognitum*.

The plesiomorphic condition among loricariids is having the region anterior to the cleithrum at the opening to the branchial cavity smooth, unplated, and without odontodes. In the derived condition, the anterolateral aspect of the cleithrum bears a patch of odontodes, which is visible upon retraction

of the branchiostegal membrane. The size of the odontodes and the extent of the patch vary in ontogeny, ranging from just a few small odontodes to a platformlike patch of large odontodes.

6. **Paranasal plates present**—*gulare*, *machadoi* (state 1); *steindachneri* (state 2). Character nonadditive.

Among the Hypoptopomatini, the lateral process of the lateral ethmoid makes direct contact with the second infraorbital and there are no paranasal plates (fig. 7A). In the derived condition, a single plate (state 1) (fig. 7B) or two plates (rarely more than two) (state 2) (fig. 7C) are present between the lateral process of the lateral ethmoid and the second infraorbital plate. These paranasal plates are neither part of the infraorbital series or the series of plates anterior to nasal parallel to the mesethmoid. Though consistently present, there is no uniformity in shape and size of the interposing plates. Like other plates anterior to the nares, these plates are not fully developed until late in ontogeny.

7. **Canal-bearing plate and fourth infraorbital located ventrally on head**—*carinatum*, *bianale*, *elongatum*, *gulare*, *incognitum*, *inexspectatum*, *machadoi*, *steindachneri*.

In the plesiomorphic condition shared by *Oxyropsis* and some *Hypoptopoma* species, the canal-bearing plate is partially ventral, presenting a narrow band along the lateral margin in contact with the fourth infraorbital occupying a ventrolateral position on the head; the fourth infraorbital is lateral. In the derived state, the canal-bearing plate plus the fourth infraorbital are entirely ventral.

8. **Canal-bearing plate posterior margin pointed**—*bianale*, *brevirostrata*, *elongatum*, *gulare*, *incognitum*, *inexspectatum*, *machadoi*, *spectabile*, *steindachneri*.

The plesiomorphic condition in loricariids and most Hypoptopomatinae is a canal-bearing plate with the posterior margin rounded and located in tandem with the opercle (fig. 13A). The derived condition is a canal-bearing plate with a pointed, digitlike posterior tip, located like a wedge between the fourth infraorbital and the opercle (fig. 13B).

9. **Canal-bearing plate notch present**—*bianale*, *brevirostratum*, *elongatum*, *gulare*, *incognitum*, *inexspectatum*, *machadoi*, *muzuspi*, *spectabile*, *steindachneri*, *sternoptychum*.

In loricariids with a ventrally expanded canal plate, the dorsal margin of the canal plate at the entrance of the branch of the mandibular canal into the preopercle is straight and simple (Schaefer, 1998) (fig. 13A). In the derived condition, the dorsal margin of the canal-bearing plate presents a notch for the anteriormost exit pore of the semicircular canal in the preopercle (fig. 13B–C).

10. **Preoperculo-mandibular laterosenory canal passage through fifth infraorbital**—*bianale*, *brevirostratum*, *elongatum*, *gulare*, *incognitum*, *inexspectatum*, *machadoi*, *muzuspi*, *spectabile*, *steindachneri*, *sternoptychum*.

In *Oxyropsis*, most Hypoptopomatini, and loricariids generally, the pathway of the preoperculo-mandibular canal from the compound pterotic to the preopercle is either direct or indirect via a small intermediate plate (Schaefer, 1987: figs. 4, 5A). In the derived state, the preoperculo-mandibular canal exits the compound pterotic to enter the fifth infraorbital, forming a separate canal immediately posterior to the infraorbital canal (figs. 13B–C).

Opercular Series

11. **Preopercle extended posteriorly**—*bianale*, *brevirostratum*, *elongatum*, *gulare*, *incognitum*, *inexspectatum*, *machadoi*, *muzuspi*, *spectabile*, *steindachneri*, *sternoptychum*.

The presence of a robust preopercle is plesiomorphic for loricariids and other Hypoptopomatinae (Schaefer, 1998: character 19). In *Oxyropsis* and some *Hypoptopoma* species, the preopercle is reduced, having its posterior ramus typically not reaching the hyomandibula adductor crest (fig. 14A). In the derived state, the preopercle is extended posteriorly and its posterior ramus reaches the opercle at a position proximal to the articular condyle (fig. 14B–C).

12. **Preopercle constricted**—*brevirostratum*, *muzuspi*.

The form of the preopercle in *Oxyrospsis* and most Hypoptopomatini is either smoothly tapering or broadening toward the posterior ramus, without a constriction in the middle (fig. 14B). In the derived condition,

the preopercle is constricted in breadth in its middle portion (fig. 14C).

13. **Canal in preopercle**—*bianale*, *brevirostratum*, *elongatum*, *gulare*, *incognitum*, *inexspectatum*, *machadoi*, *muzuspi*, *spectabile*, *steindachneri*, *sternoptychum*.

The loricariid plesiomorphic condition is presence of the preoperculo-mandibular laterosensory canal in the preopercle bone; however, the canal is absent in *Oxyropsis* and some hypoptopomatines (fig. 14A), and therefore represents the plesiomorphic condition at this level in Hypoptopomatinae phylogeny. In the derived condition, the preopercle bears a laterosensory canal (fig. 14B–C).

Neurocranium

14. **Strongly curved ventral ridge on anterior process of lateral ethmoid**—*Oxyropsis* (*acutirostra*, *carinata*); *baileyi*, *brevirostratum*, *guianense*, *muzuspi*, *psilogaster*, *thoracatum*.

The presence of a straight ridge on the ventral surface of the anterior process of the lateral ethmoid is plesiomorphic among Hypoptopomatinae and other loricariids. This ventral ridge extends parallel to the dorsal margin of the metapterygoid with which it connects contiguously via connective tissue. In the derived condition, the ventral ridge is strongly curved and is positioned roughly orthogonal to the dorsal margin of the metapterygoid, with which it connects via connective tissue only at the "crossing" point of ventral ridge and dorsal margin.

15. **Posteroventral origin of obliquus eye muscles**—*bianale*, *elongatum*, *gulare*, *incognitum*, *inexspectatum*, *machadoi*, *steindachneri*.

In loricariids generally, the obliquus eye muscles originate within the snout region from a tendinous sheet of tissue attached to the lateral ethmoid, anterior to entry of the optic nerve in the orbit cavity. The obliqui run along a short myodomelike cavity of the lateral ethmoid mesial to the olfactory cavity (Aquino, 1998: fig. 4). In the derived condition, the obliqui originate from the posteroventral border of the lateral process of the lateral ethmoid (Aquino, 1998: fig. 5).

16. **Frontal and sphenotic excluded from dorsal rim of orbit in adults**—*elongatum*, *gulare*, *incognitum*, *inexspectatum*, *machadoi*, *steindachneri*.

In the loricariids generally, the frontal and the sphenotic form part of the dorsal rim of the orbit. In the derived condition, expressed only in mature specimens, the frontal and the sphenotic are excluded of the orbit rim. During ontogeny, and with increasing size of the head and corresponding depression and ventral rotation of the orbits, we observe a decreasing contribution of the frontal, and in later developmental statges, the sphenotic to the dorsal margin of the orbit (fig. 12A–D). In the adult condition, the dorsal rim of the orbit is formed only by the preorbital plate and the fifth infraorbital.

Mandibular arch and jaw suspensorium

17. **Metapterygoid channel shallow, its depth, less than 50% of its length**—*bianale*, *elongatum*, *gulare*, *incognitum*, *inexspectatum*, *machadoi*, *spectabile*, *steindachneri*, *sternoptychum*.

The plesiomorphic condition for the Hypoptopomatinae is a metapterygoid channel as deep as about 50% of its length, similar to the morphology found in most other loricariids (Schaefer, 1991; 1998: character 13). In the derived condition, the channel is shallow, and its depth is clearly less than 50% of its length.

18. **Metapterygoid channel short, not extended beyond vertical through point slightly beyond middle of dorsal margin of metapterygoid**—*bianale*, *elongatum*, *gulare*, *incognitum*, *inexspectatum*, *machadoi*, *spectabile*, *steindachneri*, *sternoptychum*.

The plesiomorphic condition for the Hypoptopomatinae and other loricariids is having the metapterygoid channel occupy more than half of the dorsal margin of the metapterygoid, typically occupying the entire length of the margin. In the derived condition, the metapterygoid channel is short, not extended beyond a vertical through a point slightly beyond the middle of the dorsal margin.

19. **Hyomandibula with reduced fenestra**—*bianale*, *elongatum*, *gulare*, *incognitum*, *inexspectatum*, *machadoi*, *spectabile*, *steindachneri*, *sternoptychum*.

The plesiomorphic condition for the Hypoptopomatinae and other loricariids is having the surface of the hyomandibula unfenestrated (fig. 14B). In *Oxyropsis* and

some *Hypoptopoma* species, the lamina of the hyomandibula bears one or more large fenestrae between the adductor crest and the ridge proximal to the hyomandibula-metapterygoid cartilage (fig. 14A, C). In the derived condition, the fenestrae, when present, are small.

Axial skeleton

20. **Number of bifid hemal spines reduced to two**—*spectabile*, *sternoptychum*.

Oxyropsis and most *Hypoptopoma* have a single bifid hemal spine on the abdominal vertebrae, posterior to the first anal-fin proximal radial. In the derived condition, there are two bifid hemal spines associated with the abdominal vertebrae.

21. **Ossified pleural ribs absent**—*Oxyropsis acutirostra*; *bianale*, *elongatum*, *gulare*, *incognitum*, *inexspectatum*, *machadoi*, *steindachneri*.

Presence of ribs is plesiomorphic for loricariids. Among Hypoptopomatinae, Schaefer (1997) reported the presence of three pairs of thin, hairlike ossified pleural ribs associated with connective tissue of vertebrae 10–12. In *Oxyropsis* (except *O. acutirostra*) and most *Hypoptopoma*, ossified pleural ribs are present and associated with the connective tissues of vertebrae 9–13. In the derived condition, ossified ribs are absent, although thick ribbonlike bands of connective tissue are observed between the anteroventral area of each centrum and the body wall.

Median and Paired Fins

22. **Pectoral spine serrae orthogonal type**—*bianale*, *elongatum*, *gulare*, *incognitum*, *inexspectatum*, *machadoi*, *steindachneri* (state 1); *sternoptychum* and *spectabile* (state 2). Character nonadditive.

Oxyropsis shares with some *Hypoptopoma* species the oblique orientation of the serrae on the posterior margin of the pectoral-fin spine. Individual serrae are oriented at an oblique angle relative to the pectoral spine axis, the tips of the individual serrae are acute; the serrae extends from the near distal tip to the base of the spine, except for a short proximal region, and the serrae are well developed throughout ontogeny. In the derived condition, individual serrae are arranged orthogonal to the spine axis, tips of the individual serrae are slightly blunt, the serrae are most prominent along the middle region of the spine shaft, and the serrae are poorly developed or absent in the largest specimens of those species with the longest average standard length (i.e., *H. steindachneri*). Spine serrae are absent in *H. sternoptychum* and *H. spectabile*.

23. **Second and third radials of pectoral fin sutured along longest axis**—*bianale*, *elongatum*, *gulare*, *incognitum*, *inexspectatum*, *machadoi*, *steindachneri*.

The plesiomorphic condition among the Hypoptopomatinae and other loricariids is separation of the second and the third pectoral radials. In the derived condition the second and third radials of the pectoral fin are joined and in direct contact along their longest axis; the suture line between the radials is variably visible.

24. **Basipterygium marginal foramina absent**—*spectabile*, *sternoptychum*.

The plesiomorphic condition among the Hypoptopomatinae and other loricariids is a basipterygium perforated with marginal foramina (fig. 41A–B). In the derived condition, the surface of the basipterigium is continuous, without marginal foramina.

Pigmentation

25. **Elongated dark spot along middle caudal-fin branched rays**—*guianense*, *psilogaster* (state 1); *thoracatum* (state 2).

Among members of the tribe Hypoptopomatini, the plesiomorphic condition is having caudal fin with "concentrated pigment anteriorly, representing a continuation of the midlateral trunk pigmentation, and a rectangular posteroventral extension occupying the midventral anterior third to half of the caudal fin and [few] bands" (Schaefer, 1997: 108). In the derived condition, the caudal fin presents an elongated spot along the branched rays of its medial sector. The elongated spot can be extended over equal number of upper- and lower-lobe branched rays (state 1) (fig. 17B–C), or it can be slightly more extended over a larger number of lower-lobe branched rays than upper-lobe branched rays (state 2) (fig. 17A). Unlike other species of *Hypoptopoma*, the three species having the derived condition lack

TABLE 18
Data Matrix of Character States Assigned to Species of *Hypoptopoma* and *Oxyropsis* (outgroup) and Used as Input to the Phylogenetic Analysis

Taxon	Character State
Outgroup	
acutirostra	00000000000000100000010000
carinata	00000001000000000000000000
wrightiana	00000000000000100000000000
Ingroup	
baileyi	10000000000000100000000000
guianense	10000000000000100000000001
psilogaster	10000000000000100000000001
thoracatum	10000000000000100000000002
brevirostratum	10000000111111100000000000
muzuspi	10000000011111100000000000
spectabile	01102000111101000111102010
sternoptychum	11112000111101000111102010
bianale	11111001111101010111011100
inexspectatum	11111001111101011111011100
steindachneri	11111021111101011111011100
elongatum	11111101111101011111011100
incognitum	11111101111101011111011100
gulare	11111101111101011111011100
machadoi	11111011111101011111011100

the dark rectangular spot at the anteroventral portion of the fin, although they present 1–6 roughly vertical bands variably marked.

Topology and Character Support

Hypoptopoma is a member of the tribe Hypoptopomatini, one of the two main clades recovered in Schaefer's (1990) analysis of relationships within the family Hypoptopomatinae (Hypoptopomatini and Otothyrini). The addition of new Hypoptopomatini taxa in subsequent analyses did not modify that preliminary two-clade hypothesis (Schaefer, 1996a, 1997; Schaefer and Provenzano, 1998). However, the addition of new species of the tribe Otothyrini sensu Schaefer (1998) in more recent analyses (Gauger and Buckup, 2005; Chiachio et al., 2008) recovered the clade Otothyrini as paraphyletic. The Hypoptopomatini was recovered as monophyletic in all analyses.

In this section, we present an analysis of the phylogenetic relationships among the 15 species of *Hypoptopoma* based on a matrix of 26 morphological characters (table 18). Four equally parsimonious trees were recovered, overall length 38 steps, with consistency index of 0.78 and a retention index of 0.94. The strict consensus of these trees is provided in figure 45. We interpret and discuss the character-state changes based on accelerated ("fast") transformation optimization.

In adddition to the derived expansion of the nuchal plate (described under the generic diagnosis, above), monophyly of the genus *Hypoptopoma* (fig. 45, node 1) is supported by one character: presence of marginal odontodes (0.1). Presence of marginal odontodes was recognized by Schaefer (1998: 41) as a synapomorphy of *Hypoptopoma* plus *Nannoptopoma*. In the present analysis, this character is reversed in *H. spectabile*, the only species of *Hypoptopoma* to lack the marginal odontodes. The absence of marginal odontodes in *H. spectabile* is perhaps not surprising, given the tendancy among individuals of *Hypoptopoma* to express marginal odontodes relatively late in ontogeny. *Hypoptopoma spectabile* is peculiar among congeners in expressing a number of adult features (e.g., well-developed plates) and autapomorphic

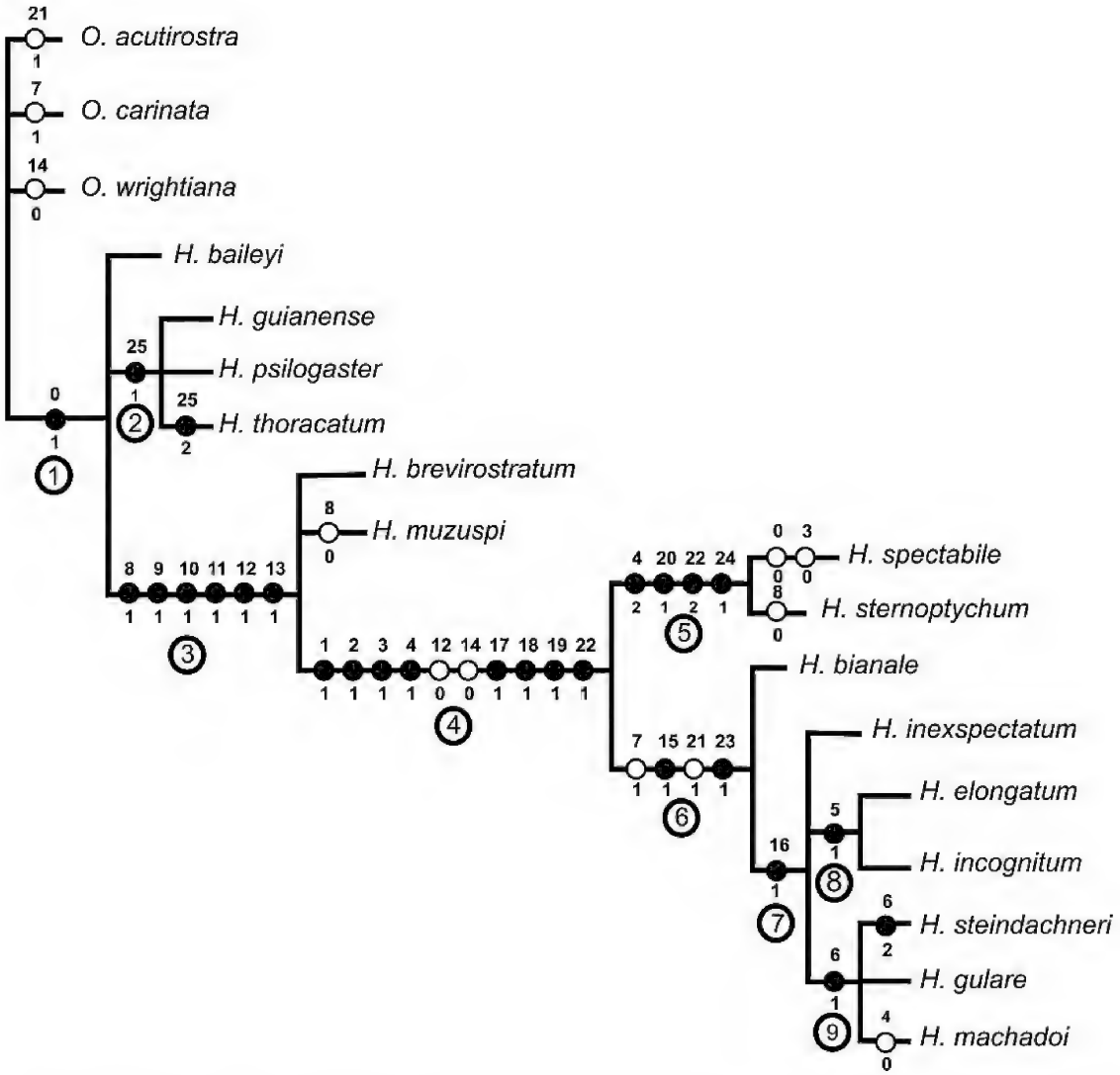

Fig. 45. Interrelationships among *Hypoptopoma* species. Most parsimonious cladogram (length 41 steps, CI = 0.85, RI = 0.95); bars mapped onto the map represents either unequely derived (solid bars) or homoplastic state changes (open bars), numbered in the text.

conditions in specimens of relatively small size, compared to other species of *Hypoptopoma*.

The basal node (fig. 45, node 1) is represented by an unresolved trichotomy between *Hypoptopoma baileyi*, a clade (node 2) comprised of *H. guiananse*, *H. psilogaster*, and *H. thoracatum*, plus a clade (node 3) composed of all other species. The former clade of three species (fig. 45, node 2) shares a single synapomorphy in the form of the caudal-fin pigmentation pattern (25.1). The latter clade (fig. 45, node 3) represents a large assemblage of species diagnosed by six synapomorphies, all but two (8, 12) uniquely derived and unreversed on the tree topology. Notable apomorphies at this level of the cladogram include the passage of the preoperculo-mandibular canal through the fifth infraorbital bone (10.1) and the presence of a canal in the preopercle (13.1).

The clade at node 4 is strongly supported by 10 synapomorphies and all but four (3, 4, 12, 14) represent unreversed character-state

changes. These species share the presence of tandem medial-series plates associated with the second midventral plate (1.1), reduced number of midventral series plates (2.1), metapterygoid channel shallow (17.1) and short (18.1), and presence of orthogonal pectoral-spine serrae (22.1); serrae were subsequently lost (22.2) in *H. spectabile and H. sternoptychum*), among other specializations.

In our more inclusive taxon sampling involving the species of both genera, we recovered the two species of *Nannoptopoma* nested within *Hypoptopoma*, most closely related to a subset of *Hypoptopoma* species (fig. 45, clade 6). A similar finding was reported by Chiachio et al. (2008) in a phylogenetic analysis of the Hypoptopomatinae and Neoplecostomatinae based on a molecular dataset. In their analysis, *Oxyropsis* and *Acestridium* clustered together and formed the sister group of *Hypoptopoma* + *Nannoptopoma*, the latter nested within the clade formed by the five species of *Hypoptopma* included in that analysis. The most conservative course of action that would retain the older generic name *Hypoptopoma* as monophyletic and valid would require synonymy of the genus *Nannoptopoma* with *Hypoptopoma*, and is clearly preferable to any alternative taxonomic rearrangement requiring the proliferation of new generic-level taxa. A sister-group relationship between the two former *Nannoptopoma* species was supported in this analysis by four synapomorphies (fig. 45, node 5).

A derived condition for the configuration of bones of the skull roof (16.1) diagnosis a clade (node 7) comprised of six species (*H. elongatum*, *H. gulare*, *H. incognitum*, *H. inexspectatum*, *H. machadoi*, *H. steindachneri*). In these species, the frontal and sphenotic bones are excluded from the orbit, a likely result of the progressively increasing depression of the head and tendancy toward large adult size exhibited by members of this clade. The shift in the position of the eyes from laterodorsal to lateral correlates with the degree in lateral development of the preorbital region. The lateral position of the eyes in *Hypoptopoma* and its sister group *Oxyropsis* is such that the eyes can be observed in a ventral view of the head. The most extreme lateral shift is observed in the clade at node 6, which is supported by a number of uniquely derived characters related to the preorbit and orbit region: the decreasing contribution of the frontal and sphenotic to the dorsal rim of the orbit, which is complete in adults; the ventral location of both the canal-bearing plate and the fourth infraorbital; and the posteroventral origin of obliquus eye muscles.

Within clade 7, our analysis recovered a sister-group relationship between *H. elongatum* and *H. incognitum*, supported by a single synapomorphy (5.1—presence of an odontode patch on the cleithrum at the brachial opening). Three species (*H. steindachneri*, *H. gulare*, and *H. machadoi*) were recovered in an unresolved trichotomy (node 9) that was supported by the presence of paranasal plates (6.1).

This phylogenetic analysis of *Hypoptopoma* represents the first-ever complete species-level phylogeny for the genus, and the only hypothesis of phylogenetic relationships for the group based on morphology. The species-level phylogeny of *Hypoptopoma* compliments several other studies on the systematics of members of the tribe Hypoptoptopomatini, which stands as the only higher-level taxon within the Loricariidae for which species-level phylogenies of all genera are available.

Biogeographical Implications

Given the wide-ranging geographic distribution of the genus, our species-level phylogeny is potentially informative in attempts to interperet historical events associated with the diversification of the Neotropical ichthyofauna. In this section, we briefly consider some of the biogeographical implications of the species-level phylogeny for *Hypoptopoma* and compare patterns of area relationships revealed by the phylogeny of *Hypoptopoma* species to patterns suggested by other Neotropical fishes.

Species of *Hypoptopoma* occur in four of the eight areas of endemism proposed by Vari (1988) for the cis-Andean South American ichthyofauna: Amazon, Orinoco, Guianas, and Paraguay/de la Plata. Members of the genus have not been recorded from the

trans-Andean rivers of the Pacific slope, the upper Paraná basin, the Rio San Francisco basin, nor the Atlantic coastal rivers between Uruguay and southern Brazil. *Oxyropsis*, the sister group of *Hypoptopoma*, includes two species distributed in western and central Amazonia (*O. wrightiana*: lower Marañon, lower Ucayali, and Solimões; *O. carinata*: Solimões and rios Negro and Urubu near Manaus), plus one species (*O. acutirostra*) in the Rio Negro/Rio Orinoco basin (Aquino and Schaefer, 2002). The combined distribution of the species of *Oxyropsis* and *Hypoptopoma* suggests an ancestral distribution that included the drainages of the Amazon, Negro, and Orinoco basins. Species of *Hypoptopoma* are absent from the river drainages of the Pacific slope, suggesting that the origin of the group occurred in lowland Amazonia after the rise of the eastern Andean Cordillera (12 Ma) (Lundberg et al., 1998; Sivansundar et al., 2001; Montoya-Burgos, 2003; Turner et al., 2004). An Amazonian ancestral distribution for *Hypoptopoma* is congruent with the phylogenetic hypothesis of the Hypoptopomatinae advanced by Chiachio et al. (2008), who recovered an Amazonian range for the Hypoptopomatinae stem lineage (= Hypoptopomatini sensu Schaefer, 1998) and a Brazilian east coastal and Upper Paraná range for the Neoplecostominae + Otothyrinae stem lineage. The phylogenetic analysis of Chiachio et al. (2008) included five species of *Hypoptopoma* and their results are only partially congruent with our findings, due in part to disparity in taxonomic coverage. Areas of agreement involve finding *H. thoracatum* (their *H. bilobatum*) placed in a relatively basal position in the cladogram, and a representative of the former *Nannoptopoma* (their taxon unidentified to species) nested among species of *Hypoptopoma*.

Of the 15 species of *Hypoptopoma* recognized herein, only three species (*H. spectabile*, *H. sternoptychum*, *H. incognitum*) have distributions that span multiple (geographically adjacent) major drainage basins. Both *H. spectabile* and *H. sternoptychum* occur in the Amazon and Orinoco basins, while *H. incognitum* is distributed in both the Amazon and Tocantins basins. All other species are restricted to a single major river basin. Eight species occur only in the Amazon basin and, from these, five species (*H. bianale*, *H. brevirostratum*, *H. gulare*, *H. thoracatum*, and *H. steindachneri*) have a moderately widespread geographic distribution in the river systems of central and western Amazonia (lower Ucayali, Japura/Caquetá, Napo, and Solimões). The remaining three Amazonian species have a more restricted geographic distribution: *H. baileyi* occurs only in the upper Rio Madeira, *H. psilogaster* occurs only in western Amazonia (Napo, Marañón), and *H. elongatum* is found only in the Rio Tapajos. Finally, four species each occur in single drainage basins outside the Amazon basin: *H. guianense* (Guianas), *H. machadoi* (Orinoco), *H. muzuspi* (Tocantins), and *H. inexspectatum* (Paraná/Paraguay).

Phylogenetic relationships among the species of *Hypoptopoma* (fig. 45) suggest the occurrence of four separate, independent cases of divergence of species in areas peripheral to the Amazon basin (*H. guianense*, *H. inexspectatum*, *H. machadoi*, and *H. muzuspi*). Each case involves a narrowly distributed species endemic to a region on the outside periphery of the Amazon basin sister to a species (or clade of multiple species) more widely distributed in the Amazon basin. We discuss each of these cases in turn.

The restricted occurrence of *H. guianense* in the Essequibo and Nickerie river basins is congruent with the high degree of endemism in the ichthyofauna of the Guiana Shield (Vari and Ferraris, 2009). Our phylogenetic analysis resolved *H. guianense* as more closely related to *H. psilogaster* and *H. thoracatum* (fig. 45), two species distributed in central and western Amazonia, than to *H. machadoi* from the Orinoco basin, the only other species sharing a distribution to the north of the Amazon basin. The freshwaters of the Guiana Shield have had a long history of isolation and complicated hydrogeological history that accounts for its species level richness (Vari and Ferraris, 2009). Cardoso and Montoya-Burgos (2009) presented evidence for a relationship between Amazon and Guiana clades within the loricariid *Pseudancistrus*. A similar pattern of biogeographic relationship was recovered by Hubert and Renno (2006) for Characiformes, *Hy-*

postomus (Montoya-Burgos, 2003: clade D2 in fig. 3), and *Potamorrhaphis* (Lovejoy and Araújo, 2001).

Hypoptopoma muzuspi occurs only in the upper Rio Tocantins; its relationships lie with species distributed widely in the central and western Amazon basin. A historical connection involving the Tocantins and Amazon was recoverd by Montoya-Burgos (2003: fig. 3) for some species (his clade D1) of *Hypostomus*, but incongruent with his clade D3, in which species from the Tocantins are more closely related to species from the São Francisco, Paraguay/Paraná, and Uruguay river systems than to species of the upper and middle Amazonas. Among *Otocinclus* species, *O. macrospilus*, an upper Amazonas species, is sister group of *O. hoppei*, from the Tocantins—although the latter species is also reported for the Amazonas, Paraguay and southeastern Brazil (Schaefer, 1997).

Hypoptopoma inexspectatum has not been recorded in drainages outside the Rio Paraguay basin or the lower Rio Paraná (Aquino and Miquelarena, 2000; Nion et al., 2002). In our cladogram, *H. inexspectatum* forms an unresolved trichotomy with species distributed in the Amazon and Orinoco basins. Other examples of an area relationship between the Amazon and Paraná/Paraguay include the callichthyid *Lepthoplosternum* and the characids *Xenubrycon* and *Brachychalcinus* (Reis, 1998: fig. 11). These three genera have species in the Paraguay basin that are more closely related to species from the upper Rio Madeira (Amazon) than to species in other areas.

Hypoptopoma machadoi is the only species of *Hypoptopoma* to occur exclusively in the Orinoco river basin. Its relationships lie within an unresolved clade of species distributed in central and western Amazonia. A history of hydrogeographical connection between these two basins is well documented (Hoorn et al., 1995), as is the pattern of area relationships based on phylogenetic information on Neotropical fishes (e.g., *Hypostomus* in Montoya-Burgos, 2003; *Pygocentrus* in Winemiller et al., 2008; *Cichla* in Willis et al., 2007). The present connection between the upper Orinoco and the Rio Negro via the Casiquiare provides a physical conduit for faunal exchange, but appears to operate in a restricted fashion, with dispersal of fishes limited by their physiological tolerance of the gradient in physicochemical properties of the two rivers systems (Toumisto, 2007; Winemiller at al., 2008; Vari and Ferraris, 2009).

In the only other species-level phylogenetic analysis of hypoptopomatine fishes, Schaefer (1997) presented patterns of area relationships based on the phylogenetic relationships among species of *Otocinclus*, and summarized that pattern as representative of successive vicariance and speciation events in non-Amazonian regions of endemism in southeastern Brazil, followed by dispersal and speciation within in the Amazon, Orinoco, and Paraná/Paraguay basins. This pattern is largely incongruent with our findings, and those of Chiachio et al. (2008), based on the relationships of species of *Hypoptopoma*. For *Otocinclus*, the *affinis* clade (southeastern Brazil) forms the sister group of all other *Otocinclus* species (Amazon basin, Orinoco, upper Paraguay, Sao Francisco). For *Hypoptopoma*, *H. baileyi* (western Amazon) and an unresolved clade comprised of *H. guianense* (Guianas), *H. psilogaster* (western Amazon), and *H. thoracatum* (central and western Amazon) form the sister group to all other *Hypoptopoma*. Both *Hypoptopoma* (*H. inexspectatum*) and *Otocinclus* (*O. flexilis*, *O. affinis*) include species endemic to the Paraguay/de la Plata system sensu Vari (1988). Although *O. flexilis* and *O. affinis* are widely distributed across the Paraguay/de la Plata area (Aquino, 1994; Schaefer, 1997), *H. inexspectatum* is restricted to the Río Paraguay and lower portion of the Río Paraná. Lopez and Miquelarena (2005) listed about 50 species endemic to the Parano-Platense region (e.g., the loricariine *Ixinandria steimbachi*, the characids *Hyphessobrycon igneus* and *Bryconamericus eigenmanni*). Historical events promoting species endemism in the Paraná/Paraguay system have been suggested to involve establishment of the divide (Michicola Arch) between the Amazon and Paraguay basins, estimated to have taken place between 11.8 and 10.0 Mya (Lundberg et al., 1998: fig. 2). Using a molecular-clock approach, Montoya-Burgos (2003) dated the divergence among Paraguay and Amazon species of *Hypostomus* at 11.4–10.5 Ma, a range of

dates consistent with the paleogeographical estimate.

ACKNOWLEDGMENTS

We thank the following colleagues and institutions for loan, exchange, information, and other courtesies: M. Sabaj Pérez and B. Saul (ANSP); D. Catania and T. Iwamoto (CAS); S. Barrera (CBF); B. Chernoff and M.A. Rogers (FMNH); H. López, A. Miquelarena, and L. Protogino (ILPLA/MLP); M. Retzer (INHS), L. Rapp Py-Daniels (INPA); J. Seigel and R. Feeney (LACM); L. Braga (MACN); F. Provenzano (MBUCV); J. Liotta and B. Giacossa (MCN "Rvdo. P. Antonio Scasso"); C. Weber and S. Fisch-Muller (MHNG); P. Buckup (MNRJ); H. Ortega (MUSM); J. Lima de Figueiredo and O. Oyakawa (MZUSP); S.O. Kullander (NRM); M. van Oijen (RMNH); E. Mikschi (NMW); B. Burr (SIUC); R. Vari and S. Jewett (USNM); and A. Zarske (ZSM). A.E.A. thanks L. Braga, P. Buckup, J. Lima de Figueiredo, S. Jewett, L. Rapp Py-Daniel, M.A. Rogers, and R. Vari for courtesies extended during visits to their respective institutions, and to S. Buck for her help during visit to São Paulo. Barbara Brown and her team at the AMNH have assisted in all phases of the project. We thank H. Ahmed and F. Thompson (NSF-ITEST interns at the AMNH) for their assistance. Part of this research was supported by grants to A.E.A. from CONICET (Argentina) and from the Starr Fellowship and Axelrod Funds of the American Museum of Natural History. Additional support was provided by NSF award DEB-0314849 to S.A.S.

REFERENCES

Aquino, A.E. 1994. Biosistemática de los Hypoptopomatinae (Pisces, Siluriformes, Loricariidae) de la Argentina. Ph.D. dissertation, Universidad Nacional de La Plata (no. 612), iii + 118 pp.

Aquino, A.E. 1996. Redescripción de *Otocinclus flexilis* Cope, 1894 (Siluriformes, Loricariidae, Hypoptopomatinae) con un nuevo sinónimo. Iheringia Série Zoologia, (81): 13–22.

Aquino, A.E. 1997. Las especies de Hypoptopomatinae (Pisces, Siluriformes, Loricariidae) en la Argentina. Revista de Ictiología 5 (1–2): 5–21.

Aquino, A.E. 1998. Topography of the extrinsic eye-muscles in four hypoptopomine species (Siluriformes: Loricariidae), with comments on myodomes in catfishes. Ichthyological Exploration of Freshwaters 8 (3): 231–238.

Aquino, A.E., and A.M. Miquelarena. 1994. Osteología de *Hypoptopoma inexpectata* Holmberg, 1893 (Siluriformes, Loricariidae, Hypoptopomatinae). Tankay 1: 211–212.

Aquino, A.E., and A.M. Miquelarena. 2000 (2001). Redescription of *Hypoptopoma inexspectata*, with notes on its anatomy (Siluriformes: Loricariidae). Physis Sección B 58: 134–135.

Aquino, A.E., and S.A. Schaefer. 2002. Revision of *Oxyropsis* Eigenmann and Eigenmann, 1889 (Siluriformes, Loricariidae). Copeia 2002 (2): 374–390.

Armbruster, J.W. 2003. The species of the *Hypostomus cochliodon* group (Siluriformes: Loricariidae). Zootaxa 249: 1–60.

Armbruster, J.W. 2004. Phylogenetic relationships of the suckermouth armoured catfishes (Loricariidae) with emphasis on the Hypostominae and the Ancistrinae. Zoological Journal of the Linnean Society 141: 1–80.

Armbruster, J.W. 2008. The genus *Peckoltia* with the description of two new species and a reanalysis of the phylogeny of the genera of the Hypostominae (Siluriformes: Loricariidae). Zootaxa 1822: 1–76.

Berg, C. 1898. Comunicaciones ictiológicas. Comunicaciones del Museo Nacional de Buenos Aires 1 (1): 9–13.

Bertoni, A.de W. 1914. Peces. *In* Fauna Paraguaya. Catálogos sistemáticos de los vertebrados del Paraguay. Peces, batracios, reptiles, aves y mamíferos conocidos hasta 1913: 5–13. Asunción, Paraguay: M. Brossa.

Bertoni, A.W. 1939. Catálogos sistemáticos de los vertebrados del Paraguay. Revista de la Sociedad Científica del Paraguay 4 (4): 1–60, Peces: 50–58.

Beurlen, K. 1970. Geologie von Brasilien. Berlin: Gebrüder Borntraeger.

Bhatti, H.K. 1938. The integument and dermal skeleton of Siluroidei. Transactions of the Zoological Society of London 24: 1–102.

Bistoni, M.A., J.G. Haro, and M. Gutiérrez. 1992. Ictiofauna del río Dulce en la provincia de Córdoba (Argentina) (Pisces, Osteichthyes). Iheringia Série Zoologia 72: 105–111.

Boeseman, M. 1974. On two Surinam species of Hypoptopomatinae, both new to science (Loricariidae, Siluriformes, Ostariophysi). Proceedings of the Koninklijke Nederlandse Akademie van Wetenschappen Serie C Biological and Medical Sciences 77: 251–271.

Bogotá-Gregory, J.D., and J.A. Maldonado-Ocampo. 2006. Peces de la zona hidrografica de la Amazonia, Colombia. Biota Colombiana 7 (1): 55–94.

Böhlke, E.B. 1984. Catalog of type specimens in the ichthyological collection of the Academy of Natural Sciences of Philadelphia. Special Publication 14, Academy of Natural Sciences of Philadelphia. viii + 246 pp.

Boulenger, G.A. 1895. [Abstract of a report on a large collection of fishes formed by Dr. C. Ternetz at various localities in Mato Grosso and Paraguay, with descriptions of new species.]. Transactions of the Zoological Society of London 34: 523–529.

Boulenger, G.A. 1896. On a collection of fishes from the Rio Paraguay. Transactions of the Zoological Society of London 14: 25–39, pls. 3–18.

Braga, L., and M.M. Azpelicueta. 1986. Adiciones a la ictiofauna argentina en la Provincia de Misiones. Historia Natural (Corrientes) 6 (10): 85–89.

Braga, L., and G.L.M. Piacentino. 1994. Lista de los tipos de peces actuales depositados en el Museo Argentino de Ciencias Naturales "Bernardino Rivadavia." Revista del Museo Argentino de Ciencias Naturales "Bernardino Rivadavia" 16: 97–108.

Buckup, P.A. 1981. *Microlepidogaster taimensis* sp. n., novo Hypoptopomatinae de Estação Ecológica do Taim, Rio Grande do Sul, Brasil (Ostariophysi, Loricariidae). Iheringia Série Zoologia 60: 19–31.

Cardoso, Y.P., and J.I. Montoya-Burgos. 2009. Unexpected diversity in the catfish *Pseudancistrus brevispinis* reveals dispersal routes in a Neotropical center of endemism: the Guyanas region. Molecular Ecology 18: 947–964.

Chang, F., and H. Ortega. 1995. Additions and corrections to the list of freshwater fishes of Peru. Publicaciones del Museo de Historia Natural (Universidad Nacional Mayor de San Marcos) Serie A Zoología 50: 1–11.

Chiachio, M.C., C. Oliveira, and J.I. Montoya-Burgos. 2008. Molecular systematics and historical biogeography of the armored Neotropical catfishes Hypoptopomatinae and Neoplecostomatinae (Siluriformes: Loricariidae). Molecular Phylogenetics and Evolution 49: 606–617.

Cope, E.D. 1870. Contribution to the ichthyology of the Marañon. Proceedings of the American Philosophical Society 11: 559–570.

Cope, E.D. 1871. [Professor Cope demonstrated some anatomical points of importance in the classification of some of the siluroids of the Amazon....] Proceedings of the American Philosophical Society 1871: 112.

Cope, E.D. 1878. Synopsis of the fishes of the Peruvian Amazon, obtained by Professor Orton during his expeditions of 1873 and 1877. Proceedings of the American Philosophical Society 17 (101): 673–701.

Eigenmann, C.H. 1910. Catalog of the fresh-water fishes of tropical and south temperate America. *In* Reports of the Princeton University expeditions to Patagonia 1896–1899. Zoology 3 (2): 375–511.

Eigenmann, C.H. 1914. On new species of fishes from Colombia, Ecuador, and Brazil. Indiana University 2: 231–234.

Eigenmann, C.H. 1916. New and rare fishes from South American riers. Annals of the Carnegie Museum 10 (1–2): 77–86 (pls. 13–16).

Eigenmann, C.H. 1922. The fishes of western South America, part I. The fresh-water of northwestern South America, including Colombia, Panama, and the Pacific slopes of Ecuador and Peru, together with an appendix upon the fishes of the Rio Meta in Colombia. Memoirs of the Carnegie Museum 9 (1): 1–346 (pls. 1–38).

Eigenmann, C.H., and W.R. Allen. 1942. Fishes of western South America. I. The intercordilleran and Amazonian lowlands of Peru. II. The high pampas of Peru, Bolivia, and northern Chile. With a revision of the Peruvian Gymnotidae, and of the genus Orestias. Lexington: University of Kentucky.

Eigenmann, C.H., and R.S. Eigenmann. 1889. Preliminary notes on South American Nematognathi. II. Proceedings of the California Academy of Sciences (series 2) 28–56.

Eigenmann, C.H., and R.S. Eigenmann. 1890. A revision of the South American Nematognathi or cat-fishes. Occasional Papers of the California Academy of Sciences 1: 1–508.

Eigenmann, C.H., and R.S. Eigenmann. 1891. A catalog of the fresh-water fishes of South America. Proceedings of the United States National Museum 14: 1–81.

Eschmeyer, W.N. and C.J. Ferraris (editors). 1998. Catalog of fishes. San Francisco: California Academy of Sciences.

Ferraris, C.J., Jr. 2007. Checklist of catfishes, recent and fossil (Osteichthyes: Siluriformes), and catalog of siluriform primary types. Zootaxa 1418: 1–300.

Ferraris, C.J., Jr, and R.E. Reis. 2005. Neotropical catfish diversity: an historical perspective. Neotropical Ichthyology 3: 1–2.

Ferraris, C.J., Jr, and R.P. Vari. 1992. Catalog of type specimens of Recent fishes in the National Museum of Natural History, Smithsonian Institution, 4: Gonorynchiformes, Gymnotiformes, and Siluriformes (Teleostei: Ostario-

physi). Smithsonian Contributions to Zoology 535: 1–52.

Ferreira, K.M., and A.C. Ribeiro. 2007. *Corumbataia britskii* (Siluriformes: Loricariidae: Hypoptopomatinae) a new species from the upper Rio Paraná basin, Mato Grosso do Sul, central Brazil. Zootaxa 1386: 59–68.

Fowler, H.W. 1915. Notes on nematognathous fishes. Proceedings of the Academy of Natural Sciences of Philadelphia 67: 203–243.

Fowler, H.W. 1939. A collection of fishes obtained by Mr. William C. Morrow in the Ucayali river basin. Proceedings of the Academy of Natural Sciences of Philadelphia 91: 219–289.

Fowler, H.W. 1940. Zoological results of the second Bolivian expedition for the Academy of Natural Sciences of Philadelphia, 1936–1937. Part I.—The fishes. Proceedings of the Academy of Natural Sciences of Philadelphia 43–103.

Fowler, H.W. 1942. Lista de los peces de Colombia. Revista de la Academia Colombiana de Ciencias Exactas, Físicas y Naturales 5 (17): 128–138.

Fowler, H.W. 1945. Los Peces de Peru. Catálogo sistemático de los peces que habitan en aguas peruanas. Lima, Peru: Museo de Historia Natural "Javier Prado.".

Fowler, H.W. 1954. Os peixes de água doce do Brasil. Arquivos de Zoologia do Estado de São Paulo 9: 1–400.

Garavello, J.C. 1977. Systematics and geographical distribution of the genus *Parotocinclus* Eigenmann and Eigenmann, 1889 (Ostariophysi, Loricariidae). Arquivos de Zoologia do Estado de São Paulo 24 (4): 1–37.

García, J.O. 1992. Lista de peces de la cuenca del Alto Paraná Misionero. Programa de Estudios Limnológicos Regionales, UNAM, Serie Informes Técnicos 1 (1): 1–15.

Gauger, M.F.W., and P.A. Buckup. 2005. Two new species of Hypoptopomatinae from the Rio Paraíba do Sul basin, with comments on the monophyly of *Parotocinclus* and Otothyrini (Siluriformes: Loricariidae). Neotropical Ichthyology 3 (4): 509–518.

Goloboff, P.A., J.S. Farris, and K. C Nixon. 2008. TNT, a free program for phylogenetic analysis. Cladistics 24: 774–786.

Gómez, S.E., and J.C. Chebez. 1996. Peces de la provincia de Misiones. *In* J.C. Chebez (editor), Fauna Misionera. Catálogo sistemático y zoogeográfico de los vertebrados de la Provincia de Misiones (Argentina): 38–70 + 315–316. Buenos Aires, Argentina: Ed. L.O.L.A.

Gosline, W.A. 1945. Catálogo dos Nematognatos de agua-doce da America do Sul y Central. Boletim do Museu Nacional (Rio de Janeiro) Nova Série Zoologia 33: 1–138.

Günther, A. 1868a. Diagnoses of some new freshwater fishes from Surinam and Brazil, in the collection of the British Museum. Annals and Magazine of Natural History (Series 4) 1 (6): 475–481.

Günther, A. 1868b. Descriptions of freshwater fishes from Surinam and Brazil. Proceedings of the Zoological Society of London 1868 (pt. 2): 229–247, pls. 20–22.

Holmberg, E.L. 1893a. Nombres vulgares de peces argentinos con sus equivalencias científicas. Revista del Jardín Zoológico de Buenos Aires 1 (entrega 3): 85–96.

Holmberg, E.L. 1893b. Dos peces argentinos: *Aristommata inexpectata* y *Liposarcus ambrosetti*. Revista del Jardín Zoológico de Buenos Aires 1 (entrega 12): 353–354.

Hoorn, C., J. Guerrero, G.A. Sarmiento, and M.A. Lorente. 1995. Andean tectonics as a cause for changing drainage patterns in Miocene northern South-America. Geology 23: 237–240.

Hubert, N., and J.-F. Renno. 2006. Historical biogeography of South American freshwater fishes. Journal of Biogeography 33: 1414–1436.

Humphries, J.M., et al. 1981. Multivariate discrimination by shape in relation to size. Systematic Zoology 30: 291–308.

ICZN. 1999. International code of zoological nomenclature. 4th ed. London: International Trust for Zoological Nomenclature.

Isbrücker, I.J.H. 1980. Classification and catalog of the mailed Loricariidae (Pisces, Siluriformes). Verslagen en Technische Gegevens, Universiteit van Amsterdam 22: 1–181.

Isbrücker, I.J.H. 2002. Nomenklator der Gattungen und Arten der Harnischwelse, Familie Loricariidae Rafinesque, 1815 (Teleostei, Ostariophysi). Datz-Sonderheft Harnischwelse 2: 25–32.

Jordan, D.S. 1920. The genera of the fishes. Part 4. From 1881–1920, thirty-nine years, with the accepted type of each. Stanford University Publications in Biological Sciences 1: 411–576.

Liotta, J. 2006. Distribución geográfica de los peces de aguas continentales de la República Argentina. ProBiota/Serie Documentos 3: 1–654.

López, H.L., R.C. Menni, and A.M. Miquelarena. 1987. Lista de los peces de agua dulce de la Argentina. Biología Acuática 12: 1–50.

López, H.L., and A.M. Miquelarena. 2005. Peces continentales de la Argentina. *In* J. Llorente Bousquets and J.J. Morrone (editors), Regionalización biogeográfica en Iberoamérica y tópicos afines: 509–550. Mexico, D.F.: Las Prensas de Ciencias, Facultad de Ciencias, UNAM.

López, H.L., A.M. Miquelarena, and J. Ponte Gómez. 2005. Biodiversidad y distribución de la

ictiofauna mesopotámica. *In* F.G. Aceñolaza (editor), Temas de la biodiversidad del litoral fluvial argentino II. Miscelánea 14. Tucumán: INSUGEO.

Lovejoy, N.R., and M.L.G. de Araújo. 2001. Molecular systematics, biogeography and population structure of Neotropical freshwater needlefishes of the genus *Potamorrhaphis*. Molecular Ecology 9 (3): 259–268.

Lundberg, J.G., and Baskin. 1969. The caudal skeleton of the catfishes, order Siluriformes. American Museum Novitates 2398: 1–49.

Lundberg, J.G., et al. 1998. The state for Neotropical fish diversification: a history of tropical South American rivers. *In* L.R. Malabarba, R.E. Reis, R.P. Vari, Z.M.S. Lucena, and C.A.S. Lucena (editors), Phylogeny and classification of neotropical fishes: 13–48. Porto Alegre, Brazil: EDIPUCRS.

Machado Allison, A., et al. 2000. Ictiofauna de la Cuenca del Río Cuyuní en Venezuela. Interciencia 25 (1): 12–21.

Malabarba, L.R., R.E. Reis, R.P. Vari, Z.M.S. Lucena, and C.A.S. Lucena (editors). 1998. Phylogeny and classification of neotropical fishes. Porto Alegre, Brazil: EDIPUCRS.

Miranda Ribeiro, A. de. 1911. Fauna brasiliense. Peixes. Eleutherobranquios. Aspirophoros. Arquivos do Museu Nacional Rio de Janeiro 16: 1–504.

Miranda Ribeiro, A. de. 1912. Loricariidae, Callichthyidae, Doradidae e Trichomycteridae. *In* Commissão de Linhas Telegraphicas Estrategicas de Matto-Grosso ao Amazonas. Annexo no. 5: 1–31, 1 pl.

Mojica, J.I. 1999. Lista preliminar de las especies dulceacuícolas de Colombia. Revista de la Academia Colombiana de Ciencias 23 (Suplemento especial): 547–566.

Mojica, J.I., et al. 2005. Peces de la Cuenca del Río Amazonas en Colombia: Región de Leticia. Biota Colombiana 6 (2): 191–210.

Montoya-Burgos, J.I. 2003. Historical biogeography of the catfish genus *Hypostomus* (Siluriformes: Loricariidae), with implications on the diversification of Neotropical ichthyofauna. Molecular Ecology 12: 1855–1867.

Nijssen, H., L. van Tuijl, and I.J.H. Isbrücker. 1982. A catalogue of the type-specimens of Recent fishes in the Institute of Taxonomic Zoology (Zoölogisch Museum), University of Amsterdam, Netherlands. Verslagen en Technische Gegevens, Universiteit van Amsterdam 33: 1–173.

Nion, H., C. Ríos, and P. Meneses. 2002. Peces del Uruguay. Lista sistemática y nombres comunes. Montevideo, Uruguay: Dinara-Infopesca.

Nixon, K.C. 2002. WinClada, ver. 1.00.08. Ithaca, NY, Distributed by the author.

Ortega, H., and R.P. Vari. 1986. Annotated checklist of the freshwater fishes of Peru. Smithsonian Contributions to Zoology 437: iii + 25 p.

Pearson, N.E. 1924. The fishes of the eastern slope of the Andes. I. The fishes of the Rio Beni basin, Bolivia, collected by the Mulford Expedition. Indiana University Studies 11 (64): 1–83.

Pearson, N.E. 1937. The fishes of the Beni-Mamoré and Paraguay Basins, and a discussion of the origins of the Paraguayan fauna. Proceedings of the California Academy of Sciences (Ser. 4) 23 (7): 99–114.

Pozzi, D.J. 1945. Sistemática y distribución de los peces de agua dulce de la República Argentina. Anales de la Sociedad Argentina de Estudios Geográficos, GAEA 7 (2): 239–292.

Regan, G.T. 1904. A monograph of the fishes of the family Loricariidae. Proceedings of the Zoological Society of London 18: 191–350.

Reis, R.E. 1998. Systematics, biogeography, and the fossil record of the Callichthyidae: a review of the available data. *In* L.R. Malabarba, R.E. Reis, R.P. Vari, Z.M.S. Lucena, and C.A.S. Lucena (editors), Phylogeny and classification of neotropical fishes: 351–362. Porto Alegre, Brazil: EDIPUCRS.

Reis, R.E., and P. Lehman A. 2009. Two new species of *Acestridium* Haseman, 1911 (Loricariidae: Hypoptopomatinae) from the Rio Madeira Basin, Brazil. Copeia 2009 (3): 446–452.

Ringuelet, R.A., and R.H. Arámburu. 1961. Peces argentinos de agua dulce. Agro 3 (4): 1–98.

Ringuelet, R.A., R.H. Arámburu, and A. Alonso de Arámburu. 1967. Los peces argentinos de agua dulce. La Plata, Argentina: Comisión de Investigaciones Científicas de la Provincia de Buenos Aires.

Schaefer, S.A. 1987. Osteology of *Hypostomus plecostomus* (Linnaeus), with a phylogenetic analysis of the loricariid subfamilies (Pisces: Siluroidei). Natural History Museum of Los Angeles County Contributions in Science 394: 1–31.

Schaefer, S.A. 1990. Anatomy and relationships of the scoloplacid catfishes. Proceedings of the Academy of Natural Sciences of Philadelphia 142: 167–210.

Schaefer, S.A. 1991. Phylogenetic analysis of the loricariid subfamily Hypoptopomatinae (Pisces: Siluroidei: Loricariidae), with comments on generic diagnoses and geographic distribution. Zoological Journal of the Linnean Society 102: 1–41.

Schaefer, S.A. 1996a. *Nannoptopoma*, a new genus of loricariid catfishes (Siluriformes: Loricarii-

dae) from the Amazon and Orinoco River Basins. Copeia 1996 (4): 913–926.

Schaefer, S.A. 1996b. Type designations for some Steindachner loricariid material (Siluriformes: Loricariidae) in the Natural History Museum, Vienna. Copeia 1996 (4): 1031–1035.

Schaefer, S.A. 1997. The Neotropical cascudinhos: systematics and biogeography of the *Otocinclus* catfishes (Siluriformes: Loricariidae). Proceedings of the Academy of Natural Sciences of Philadelphia 148: 1–120.

Schaefer, S.A. 1998. Conflict and resolution: impact of new taxa on phylogenetic studies of the Neotropical Cascudinhos (Siluroidei: Loricariidae). *In* L.R. Malabarba, R.E. Reis, R.P. Vari, Z.M.S. Lucena, and C.A.S. Lucena (editors), Phylogeny and classification of neotropical fishes: 351–362. Porto Alegre, Brazil: EDIPUCRS.

Schaefer, S.A. 2003. Subfamily Hypoptopomatinae (armored catfishes). *In* R.E. Reis, S.O. Kulander, and C.J. Ferraris (editors), Check list of freshwater fishes of South and Central America: 321–329. Porto Alegre, Brazil: EDIPUCRS.

Schaefer, S.A., and F. Provenzano R. 1998. *Niobichthys ferrarisi*, a new genus and species of armored catfish from southern Venezuela (Siluriformes: Loricariidae). Ichthyological Explorations of Freshwaters 8 (3): 221–230.

Schaefer, S.A., and D.J. Stewart. 2003. Systematics of the *Panaque dentex* species group (Siluriformes: Loricariidae), wood-eating armored catfishes from tropical South America. Ichthyological Exploration of Freshwaters 4: 309–342.

Sivansundar, A., E. Bermingham, and G. Orti. 2001. Population structure and biogeography of migratory freshwater fishes (Prochilodus: Characiformes) in major South American rivers. Molecular Ecology 10: 407–417.

Steindachner, F. 1879. Über einige neue und seltene Fischarten aus den zoologischen Museen zu Wien, Stuttgart und Warschau. Denkschriften der Mathematisch-Naturwissenschaftlichen Classe der Kaiserlichen Akademie der Wissenschaften 41 (1): 1–52, pls. 1–9.

Steindachner, F. 1882. Ichthyologische Beitäge (XII). Anzeiger der Akademie der Wissenshaften in Wien 142–143.

Taylor, W.R., and G.C. Van Dyke. 1985. Revised procedures for staining and clearing small fishes and other vertebrates for bone and cartilage study. Cybium 9: 107–119.

Terrazas Urquidi, W. 1970. Lista de peces bolivianos. Academia Nacional de Ciencias de Bolivia Publicación 24: 1–65.

Tuomisto, H. 2007. Interpreting the biogeography of South America. Journal of Biogeography 34: 1294–1295.

Turner, T.F., M.V. McPhee, P. Campbell, and K.O. Winemiller. 2004. Phylogeography and intraspecific genetic variation of prochilodontid fishes endemic to rivers of northern South America. Journal of Fish Biology 64: 186–201.

Vaillant, L.M. 1880. Note sur le genre *Otocinclus* et description d'une espèce nouvelle. Bulletin des Sciences par la Société Philomatique de Paris 4 (ser. 7): 145–148.

Vari, R.P. 1988. The Curimatidae, a lowland Neotropical fish family (Pisces: Characiformes); distribution, endemism, and phylogenetic biogeography. *In* W.R. Heyer and P.E. Vanzolini (editors), Neotropical distribution patterns: proceedings of a 1987 workshop: 313–348. Rio de Janeiro, Brazil: Academia Brasileira de Ciencias.

Vari, R.P., and Ferraris, C.J., Jr. 2009. Fishes of the Guiana Shield. *In* R.P. Vari, C.J. Ferraris, Jr, A. Radosavljevic, and V.A. Funk (editors), Checklist of the freshwater fishes of the Guiana Shield: 9–18. Bulletin of the Biological Society of Washington 17: i–vii, 1–95.

Vari, R.P., C.J. Ferraris, Jr, A. Radosavljevic, and V.A. Funk (editors). 2009. Checklist of the freshwater fishes of the Guiana Shield. Bulletin of the Biological Society of Washington 17: i–vii, 1–95.

Veríssimo, S., C. Simone Pavanelli, H.A. Britski, and M.M. Monaco Moreira. 2005. Fish, Manso Reservoir region of influence, Rio Paraguai basin, Mato Grosso State, Brazil. Check List 1 (1): 1–9.

Weber, C. 1992. Révision du genre *Pterygoplichthys* sensu lato (Pisces, Siluriformes, Loricariidae). Revue Francaise d'Aquariologie Herpétologie 19: 1–36.

Weber, C., S. Muller, and V. Mahnert. 1992. Harnischwelse Paraguays. Datz Sonderheft. Harnishwelse. Verlag Eugen Ulmer, Stuttgart, Sept. 1992: 10–13.

Willis, S.C., M.S. Nunes, C.G. Montaña, I.P. Farias, and N.R. Lovejoy. 2007. Systematics, biogeography, and evolution of the Neotropical peacock basses *Cichla* (Perciformes: Cichlidae). Molecular Phylogenetics and Evolution 44: 291–307.

Winemiller, K.O., H. López-Fernández, D.C. Taphorn, L.G. Nico, and A. Barbarino Duque. 2008. Fish assemblages of the Casiquiare River, a corridor and zoogeographical filter for dispersal between the Orinoco and Amazon basins. Journal of Biogeography 35: 1551–1563.

APPENDIX

Comparative material examined by species, country, catalog number, and number of specimens in parenthesis. Cleared and stained material indicated as "cs." Abbreviations for museum repositories indicated in Methods section.

CALLICHTHYIDAE

Brochis brtskii. Brazil: AMNH 98088 (1 cs)
Callichthys callichthys. Guyana: AMNH 17617 (1 cs)
Corydoras paleatus. Argentina: AMNH 12349 (1 cs)
Hoplosternum punctatum. Panama: AMNH 11580 (4 cs)

LORICARIIDAE

HYPOPTOPOMATINAE sensu Schaefer, 1998

Hypoptopomatini sensu Schaefer, 1998

Acestridium dichrorum. Venezuela: USNM 269948 (10)
Acestridium discus. Venezuela: ANSP 161494 (1 cs)
Niobichthys ferrarisi. Venezuela: AMNH 74452 (2 cs); MBUCV 14903 (1 cs)
Otocinclus sp. (aquarium material) AMNH 22310
Otocinclus affinis. (aquarium material) AMNH 22310 (8 cs).
Otocinclus flexilis. Argentina: ILPLA 207 (4 cs); ILPLA 208 (2 cs). Brasil: MZUSP 9622 (1).
Otocinclus mariae. Bolivia: MZUSP 27826 (2)
Otocinclus vittatus. Bolivia: AMNH 39815 (1 cs). Argentina: ILPLA 249 (1 cs); ILPLA 254 (4 cs); ILPLA 261 (4 cs).
Oxyropsis wrightiana. Brazil: INPA 61 (10); INPA 14324 (1); MCZ 8055 (holotype); MZUSP 36213 (15); MZUSP 36215 (1); MZUSP 36230 (11); USNM 364994 (5). Colombia: CAS 150561 (2); CAS 150585 (1); FMNH 105078 (1); USNM 190320 (3). Peru: CAS 136222 (1); FMNH 70313 (2); FMNH 108761 (1); MHNG 2538.10 (1); MHNG 2618.85 (3); MUSM 10404 (1); NRM 15204 (1); NRM 15207 (1); NRM 16563 (4); NRM 17990 (6); NRM 17991 (4); NRM 17993 (32, 2 cs); NRM 17997 (1); NRM 17999 (1); NRM 18001 (19); NRM 47514 (1 cs); NRM 47515 (1 cs); NRM 47512 (17); SIUC 27740 (1); SIUC 37819 (1); SIUC 39994 (1); SU 36220 (1).
Oxyropsis carinata. Brazil: INPA 14316 (1); INPA 2390 (25, 2 cs); INPA 3218 (1); INPA 7304 (28); MZUSP 23297 (3); MZUSP 35777 (1); MZUSP 43650 (1); USNM 177721 (1). Peru: NMW 46267 (holotype).
Oxyropsis acutirostris. Brazil: INPA 16 (4); INPA 586 (2); INPA 6593 (2); INPA 14324 (2); MCZ 59695 (3); MZUSP 7318 (2); MZUSP 31398 (1); MZUSP 35090 (6); MZUSP 35091 (2); MZUSP 35093 (1); MZUSP 36228 (1). Colombia: FMNH 105089 (5). Venezuela: ANSP 160643 (1); ANSP 162354 (2; ANSP 164280 (7, 1 cs); FMNH 105989 (1); FMNH 105990 (1); MCNG 26629 (5, 1 cs).

Otothyrini sensu Schaefer, 1998

Corumbataia cuestae. Brazil: MZUSP 47968 (24)
Epactionotus gracilis. Brazil: USNM 285878 (1 cs)
Eurycheilichthys limulus. Brazil: ANSP 168965 (1 cs)
Hisonotus laevior. Brazil: USNM 326112 (8)
Hisonotus maculipinnis. Argentina: ILPLA 234 (2 cs); ILPLA 235 (4 cs). Paraguay: UMMZ 206297 (2 cs); UMMZ 206880 (2 cs)
Hisonotus nigricauda. Paraguay: USNM 181550 (27)
Hisonotus paraibensis. Brazil: MZUSP 44556 (121)
Hisonotus ringueleti. Brazil: ANSP 177878 (1); FMNH 108806 (4); ILPLA 886 (1); ILPLA 883 (95, 3 cs); MLP 9536 (4); MZUSP 62788 (3); USNM 362665 (4)
Microlepidogaster perforatus. Brazil: ANSP 174718 (1 cs)
Otothyris lophophanes. Brazil: MNRJ 17324 (1); MZUSP 8718 to 8728 (11, 1 cs)
Otothyris travassosi. Brazil: ANSP 174151 (1 cs); MNRJ 17330 (1)
Pareiorhina rudolphi. Brazil: MNRJ 13560 (52)
Pareiorhaphis alipionis. Brazil: MNRJ 14179 (34)
Paratocinclus britskii. Venezuela: ANSP 168172 (1 cs)
Paratocinclus cf. *doceanatus*. Brazil: MZUSP 51791 (3)
Paratocinclus maculicauda. Brazil: ANSP 168971 (1 cs)
Paratocinclus maculicauda. Brazil: MZUSP 36568 (1)
Pseudotocinclus sp. Brazil: USNM 292194 (1)
Pseudotocinclus tietensis. Brasil: MZUSP 28762
Pseudotothyris sp. Brazil: MZUSP 24812 (59); MZUSP 38129 (3 cs)
Pseudotothyris sp. Brazil: USNM 297971 (1 cs)
Pseudotothyris obtusa. Brazil: MZUSP 28997 (12)
Schizolecis sp. Brazil: MZUSP 24072 (6); MZUSP 24805 (7); MZUSP 42133 (6)
Schizolecis guentheri. Brazil: MZUSP 49934 (18)

HYPOSTOMINAE

Ancistrini

Ancistrus sp. Bolivia: AMNH 77416 (2 cs). Brazil: MZUSP 23796 (3)
Ancistrus montanus. Bolivia: AMNH 40129 (2 cs)
Chaetostoma sp. (uncat. aquarium specimen)
Exastilithoxus sp. Venezuela: AMNH 74457 (6)
Hemiancistrus sp. Venezuela: AMNH 91017 (9, 1 cs)

Hypostomini

Hypostomus sp. Brazil: MZUSP 52512 (1)
Hypostomus popoi. Bolivia: AMNH 52672 (1 cs)
Hypostomus punctatus. (aquarium material) AMNH 18852 (3, 1 cs)

LORICARIINAE

Crossoloricaria sp. Colombia: USNM 081922
Dasyloricaria filamentosa. Colombia: USNM 175296
Loricaria cf. cataphracta. Bolivia: AMNH 40081 (1 cs)
Farlowella oxyrhyncha. Bolivia: AMNH 39883 (1 cs)
Farlowella vittata. Venezuela: USNM 348675 (10)
Harttia sp. Surinam: USNM 226184 (2)
Hemiodontichthys acipenserinus. Peru: USNM 263882 (7)
Loricariichthys sp. Venezuela: AMNH 77791 (1 cs)
Pseudohemiodon sp. Peru: MZUSP 26786 (1)
Pseudoloricaria laeviuscula. Brazil: MZUSP 35083 (3)
Rineloricaria isocuspis. Brazil: MZUSP 37729 (4)
Rineloricaria caracasensis. Venezuela: AMNH 74464 (1 cs); AMNH 74469 (1 cs)

Spatuloricaria evansi. Brazil: AMNH 12611 (1 cs)
Sturisoma barbatum. (lab-reared material) FMNH 96972 (3 cs)
Sturisoma lira. Brazil: AMNH 12610 (16)

NEOPLECOSTOMATINAE
Neoplecostomus sp. Brazil: USNM 320302 (1)
Neoplecostomus microps. Brazil: USNM 300906 (1)
Neoplecostomus paranensi. Brazil: AMNH 93230 (1 cs)